ANTONIO HENRIQUE DA FONTOURA KLEIN

Faculdade de Ciências do Mar e do Ambiente

UNIVERSIDADE DO ALGARVE

MORPHODYNAMICS OF HEADLAND-BAY BEACHES:

EXAMPLES FROM THE COAST OF SANTA CATARINA STATE, BRAZIL.

Dissertação apresentada à Universidade do Algarve para obtenção do grau de Doutor de Ciências do Mar, especialidade de Geologia Marinha.

FARO

2004

DEDICATORY

To the girls of my life Marlei and Maylla

To my parents "Antonio Klein" (in memoriam) and Zeli da Fontoura Klein

ACKNOWLEDGEMENT

I believe and agree with my Italian friend Paolo Ciavola. He wrote in the introduction of his Ph.D. thesis that "***modern environmental science is teamwork, particularly in oceanography***". During the time of this thesis I had a opportunity to be a under graduation advisor in the Oceanography program of the UNIVALI-CTTMAR, from João Thadeu de Menezes, Lindino Benedett Filho, Graziela Miot da Silva, Narbal Adriani Jr, José Renato Derntl, and Gustavo Dafferner. It was a great experience, working with very good young students. I learned a lot science and human relationship with them. The papers published and submitted from this thesis were in collaboration with this teamwork. They help me to obtain, organize and analyze the thousands of beach profiles and beach sediment samples and analyze the plan shape of beaches. The student Ariel Vargas and Prof. Andre Raabe, MSc., from Computer Science program helped me with the development of MEPBAY software. It was a great interdisciplinary collaboration. Due the Internet facilities it was possible to promote good discussions and collaboration with Prof. John Hsu (Tawain) that also has helped me to understand the Parabolic Beach Model. After brainstorms in Faro, Portugal, and by Internet with my advisors Prof. João Alveirinho Dias and Dr. Oscar Ferreira the ideas of this thesis were coming along. Today, as a result form the internet and globalisation, there is no distance between the people and certainly benefited from that.

I would like acknowledging the following institutions and persons to help me understand this simple rules and finish my Ph.D.:

- CNPq for providing fellowships (Reference Number 201003-97.0 – "Ação Induzida" program and Reference Number 61.0083/96-1 – "RHAE program") between July of 1998 and July of 1999;

- DAAD for providing fellowships (Reference Number 201003-97.0 – to learn German and English during my time in Bremen between March and July of 1998;

- Prof. Alberto Figueiredo for stimulating me to do the Ph.D. out side of Brazil;

- Fundação Banco do Brasil (Banco do Brasil Foundation), City Hall of Balneário Camboriú and PADCT III for funding the research;

- Prof. Fernando Luiz Diehl (Director of the UNIVALI/ CTTMar), especially for help me during the time of "*storms*" that occurred during this work; to give me his "support" as a friend and to give me a opportunity and facilities to do my field research and to do my PhD out side of Brazil;

- Prof. José Roberto Provesi (Rector from UNIVALI), Prof. João L. B. de Carvalho (Director of the UNIVALI/ CTTMar), Maria Inês F. dos Santos (Oceanography program coordinator) and Rafael Medeiros Sperb (Environmental Engineering program coordinator) to give me the facilities to do my field research and go abroad to do my Ph.D.

- Prof. João Alveirinho Dias and Dr. Oscar Ferreira from "Universidade do Algarve-FCMA/CIACOMAR for their supervision and opportunity to undertake my Ph.D. degree at Universidade do Algarve, and for believe in my work. They had opened the door of my future.

- Special thanks are due to the fieldworkers who provided the beach profiles, to make this project possible: Prof. Norberto Olmiro Horn Filho (UFSC), Prof. Fernando Luiz Diehl (UNIVALI-CTTMar), Prof. José Gustavo Natorf de Abreu (UNIVALI-CTTMar), Prof. João Thadeu de Menezes (UNIVALI-CTTMar), Prof. Maria Inês Freitas dos Santos (UNIVALI/ CTTMar), Prof. Delamar Schumacher (UNIVALI/ CTTMar) and the following former Oceanographic students: Armand Amim Hanna, Alex Grecchi, Fabricio Stevo da Silva, Andre Lima dos Santos, Lindino Benedett Filho, Graziela Miot

da Silva, Jose Renato Derntl, and Gustavo Daffener; and Eduardo da Silva, Marcos Berribili and Gentil Silvester for the laboratory work;

- Mr. Fernando Toro for the English review in chaper 4. Marco Antonio Ferreira and Nilberto Lafin are also acknowledged for the pictures and computer related help.

- For my colleagues of CTTMar-UNIVALI that helped the girls of my life, during my time in Germany, specially Guto and Nane. Tio Guto, you were more than a friend to my young daughter.

- I would like also to acknowledge Prof. Charles Finkl (USA), for the english review and helpful discussions and critical readings of the initial manuscript of my papers and thesis. With his commentary every time I had learned about the Science and the Life. For Prof. John Hsu (Taiwan) for the good discussions and help in the initial manuscript and to share with me his experience with his Parabolic Beach Model. For Prof. Henk Jan Verhagen (Holland) for his help with his Engineering point of view during the review of the initial manuscript. He pointed out his ideas in a very clear manner. To Prof. Andrew Short (Australia) for discussions and lessons about the beach morphodynamic models. To Prof. Prof. Ian Eliot (Australia), Prof. Karl Nordstrom (USA) and Prof. Nancy Jackson (USA) for discussions about protected beaches. Finally to Prof. Gerard Masselink , Prof. Paolo Ciavola , Prof. Duncan Fitgerald, Prof. Willian Cleary, Dr. Eduardo Siegle for the review and helpful discussions and critical readings of the initial manuscripts and papers. Duncan and Bill, I will not forget our discussion in a gas station in a rain day near Florianopolis in the BR101 highway.

I would like also to dedicate my thesis to the people that help me in my long trip until here. This trip began with Prof. Maria da Graça Baungartem and Prof. Lauro Júlio Calliari, from FURG. They introduced to good science during my undergraduation and master of science times. Special thanks goes to Lauro for helping me in the beginning of

my carrier opening doors to my works. I will never forget the Calliari Foundation. To Fernando Diehl to show me how to be a professional in the last 10 years. To José and Lena David and José and Ligia Ramos to receive me in their heart like a Kid. To my parents Zeli and Antonio Klein for showing me the way to be a good person and do not exited for me to finish my undergraduate course. To Charlie Finkl for believing in my work and giving good counseling. To Oscar for his help, understateding of my temperament, during my stay in Faro. To Alveirinho Dias for believing in my work. Alveirinho showed me the right direction of the life not as a advisor but as a friend during our dinner talks in Faro, Itajaí and Recife. Many thanks to Prof. Angulo, Prof. Tessler, Prof. Toldo for ask me about the end of this thesis. Finally, Marlei and Maylla thank you for your patience with me and for helping me during this big trip.

After five (5) years, at the end of this work I hope that I had helped at least to improve the Natural Science.

Itajaí, 23 June 2004

SHORT RESUME OF THE AUTHOR

Name: **Antonio Henrique da Fontoura Klein**

Born: **Pelotas, Brazil, 01/29/1966**

Present Appointment:

2002 Associate Editor from Journal of Coastal Research – An international Forum for the Littoral Sciences. Published by The Coastal Education and Research Foundation [CERF]. West Palm Beach, FL. USA.

13 February 1994, Lecturer in Geology Oceanography (sedimentology, morphology of oceans, coastal morphology and geology, wave and tides, coastal engineering and coastal process) at University of Vale do Itajai, Itajaí, Brazil.

Previous Appointments:

1991-1992 Research Fellow from CNPq, University of Rio Grande, Rio Grande, Brazil.

1992 – 1995 Academic Fellow from CNPq, University of Rio Grande do Sul, Porto Alegre, Brazil.

1998 – 1999 Academic Fellow from CNPq (Process Number 201003-97.0 – "Ação Induzida" program.

1998 Academic Fellow from DAAD (German course).

Academic Qualifications:

1990 BSc in Oceanography, University of Rio Grande, Rio Grande, Brazil.

1996 MSc in Geosciences, Marine Geology specialization, University of Rio Grande do Sul, Porto Alegre, Brazil.

2003 Name included in the book Who's Who in Science and Engineering 2003-2004, published by Marquis Who's Who

Awards

2003 Award Young Research – Institutional Category – CNPq/GERDAU, Brazil.

2000 Award ADVB – Universidade Cidadã - for the extension project – Beach safety and management in Santa Catarina coastline, Brazil.

2001 Award – Social Tecnologia from "Fundação Banco do Brasil" and "UNESCO" - for the extension project – Beach safety and management in Santa Catarina coastline, Brazil.

Academic Production

1990 – 2004: 167 contributions between chapter of books, papers in journals with editoral bording, papers in proceedings, abstracts, articles in newspapers, folders, softwares and videos.

ABSTRACT

The overall goal of this study is to contribute to increased understanding of headland-bay beach morphodynamics, *i.e* to elucidate the interaction between hydrodynamic processes, beach morphology and sedimentology at Large Scale Coastal Behaviour in the coastline of Santa Catarina, between Laguna and São Francisco, an east coast swell environment with headland and bay geomorphologies.

In order to investigate morphodynamic processes, beach planforms for 90 beaches on the Santa Catarina coast were analyzed by utilizing maps and aerial photography at different scales. An intensive field investigation of morphologic and sedimentological changes was conducted on 28 beaches in central-north Santa Catarina coast from May 1994 to March 1996, where morphological and sedimentological changes were related to spatial variations in wave/tidal and sedimentary provenance conditions. Field investigations were additionally conducted on three beaches in an effort to determine alongshore sediment mobility at headland-bay beaches. In this case, temporal morphological changes were correlated with wave information (wave height, period and direction obtained from visual beach observations and wave forecast models).

The parabolic bay shape equation fits the geometrical shape of headland bay beach, in static equilibrium, with the input of wave direction and the wave diffraction point, *i.e* it is not purely geometrical and the physical insight of wave action exist. Occasionally, it may be difficult to define the diffraction point (*i.e.* the upcoast control point) from aerial photographs, especially when the tip is hidden (submerged) or with extensive shallow regions in the lee of the headland. The determination of the wave crest line, assumed to be in the same orientation as the tangent downcoast, is another issue affecting the accuracy of the prediction. A possibility of the use of a second

(inner) control point, is recognized in this work to fit bay shape stability. This is a result of progressive wave diffraction in an irregular headland. It should be emphasized that the parabolic model is an efficient tool for determining the planform assumed by the salients and tombolos, when the angle β is variable.

For a coast with headland bays, the alongshore range in beach geomorphology is a function of headland distance, shape of the bay, wave obliquity, indentation ratio, grain size distribution and nearshore slope. The beaches are classified as: (1) exposed, (2) semi-exposed or (3) sheltered. In the exposed beach, the indentation ratio is small and waves approach the coast parallel to the shoreline. Exposed beaches can be divided into three types: (a) reflective; (b) intermediate; and, (c) dissipative. In semi-exposed beaches the indentation ratio is longer and the wave obliquity is usually greater than 40°. A three-dimensional beach morphodynamics is presented and it is a function of wave breaker height and grain size and relative tidal range. When $H_b << H_o$, the diffraction zone may be in reflective condition with coarse grain or dissipative/low tide terrace to sand-mud flat condition with fine grains. Usually, in the central position ($Hb \geq Ho$) the beach is dissipative without bar or low tidal terrace (fine sand), but reflective with medium sand. When the indentation ratio is larger and with fine sediment input from rivers, beach and mud flat with mud ridges (RTR is larger - eg. Tijucas) are possible. Only diffracted waves or locally-generated waves influence sheltered beaches. Normally, waves approach the beach with angle greater than 50°. RTR is larger (>2). Again, they can be divided into: (a) reflective mode with medium to coarse sand with convex to linear profile and (b) dissipative mode non-barred or low tide terrace (fine sediment) with concave to linear profile. Short-term beach rotation processes were evident in the exposed reflective beach at Taquaras/Taquarinhas, and on the exposed dissipative northern sector of Balneário Camboriu. The process probably

occurs on other headland bay beaches along our coastline, in response to waves from varying angles of incidence.

The analyses of sediment distribution patterns show that three-grain size types are identified in the study area. Type 1 represents sediments that have a mean (Mz) grain size between 2.0 ∅ and 3.5 ∅ (0.1 to 0.2 mm, fine to very fine sand). Type 2 is characterized by medium grain size (1∅ to 2∅ and 0.2 mm – 0.5 mm). Type 3 is characterized by grain sizes between 0.0 ∅ and 1.0 ∅ (0.5 to 1.0 mm, coarse sand). There are distinct grain sizes located on adjacent beaches, indicating that circulation patterns are restricted to each beach, and that there are no sediment exchanges among different cells or different headland-bay beaches. Dissipative beaches are composed of fine sediments (Type 1) if compared to reflective beaches, which are composed by coarse grain sizes (Type 3). Intermediate beaches comprise all grain sizes. There is no clearly relationship between average wave height and mean grain size (Mz), indicating the importance of sediment provenance to characterize the distribution patterns of sediments in the study area. Dissipative beaches show greater grain size stability over time due to the low declivity of the beachface slope, which makes them more resistant to coastal processes. Reflective and intermediary exposed beaches are more dynamic.

This work contributed toward the increase of knowledge on beach morphology and sedimentology for headland bay coasts, but there is still much work to be done. The beach models presented herein are thus a first approximation. Studies in other areas with the same geographical/geomorphological characteristics are necessary to provide more information and data to support model validation.

RESUMO

O objetivo principal deste estudo é contribuir para o aumento do entendimento da morfodinâmica de praias de enseada, isto é, elucidar a interação entre processos hidrodinâmicos, morfologia e sedimentologia praial em meso e macro escala. A área de estudo compreende as praias do estado de Santa Catarina, entre Laguna e São Francisco, as quais se encontram em uma zona costeira que recebe ondulações provenientes de leste e apresenta uma geomorfologia composta de promontórios e baias.

Para a definir a forma em planta, 90 praias foram analisadas utilizando-se de mapas e fotografia aéreas em diferentes escalas. Um programa intensivo de levantamento de campo das mudanças morfológicas e sedimentológicas foi conduzido em 28 praias no litoral centro-norte de Santa Catarina, entre Maio de 1994 e Março de 1996. As mudanças morfológicas e sedimentológicas foram relacionadas com variações espaciais nas condições das ondas/marés, bem como proveniência dos sedimentos. Adicionalmente, foram conduzidos levantamentos morfológicos em três praias (Praia Brava, Balneário Camboriú e Taquaras/Taquarinhas) para determinar-se o transporte de sedimento ao longo da costa em praias de enseada. Neste caso, as variações morfológicas foram relacionadas com observações visuais e previsões de ondas.

A equação parabólica que define a geometria em planta de praias de enseada, em equilíbrio estático, a partir da definição da direção da onda e ponto de difração, não é puramente geométrica, apresentando um fundamento físico ao relacionar-se a ação das ondas. Ocasionalmente, torna-se difícil definir o ponto de difração a partir de fotografias aéreas, especialmente quando o ponto está submerso e/ou tem-se uma região rasa junto ao promontório. Neste trabalho, também foi reconhecida a validade do uso de um segundo ponto de controle (difração) para definição da forma em planta da praia. Este é resultado do processo progressivo de difração da onda em um promontório

totalmente irregular. Enfatiza-se neste trabalho que o modelo parabólico é uma eficiente ferramenta para determinar a forma em planta assumida por uma saliência ou tombolo, quando o ângulo β é variável.

Para uma zona costeira com presença de promontórios e baias, a variação da morfologia das praias é função da distância entre os promontórios, forma da enseada, direção de incidência das ondas, razão de endentação, distribuição do tamanho de grão e declividade da antepraia. Desta forma, as praias são classificadas como: (1) expostas; (2) semi-expostas; e (3) protegidas. Em praias expostas, a razão de endentação é pequena e as ondas aproximam-se aproximadamente paralelas à linha de costa. Estas ainda podem ser divididas em três tipos: (a) reflectivas; (b) intermediárias; e, (c) dissipativas. Em Praias semi-expostas a razão de endentação é maior e a obliqüidade da onda é normalmente maior que 40°. Neste tipo de praia a tri-dimensionalidade esta presente e é uma função da altura de quebra da onda, tamanho de grão e variação relativa da maré. Quando Hb<<Ho, uma zona de difração com sedimentos grosseiros, resulta em uma praia do tipo reflectiva, quando com sedimentos finos resulta em praias do tipo dissipativas/terraço de baixo mar ou planícies de maré arenosas-lamosas. Normalmente, na porção central (Hb>Ho) a praia é do tipo dissipativa sem bancos ou terraço de baixo mar (areia fina), mas será do tipo reflectiva quando da presença de areias médias. Quando a razão de endentação é grande e ocorre uma entrada de sedimentos finos a partir de rios, cristas de praias e planos de maré com cristas de lamas são encontrados. Praias protegidas são influenciadas pela ação das ondas difratadas ou ondas geradas localmente. Normalmente, as ondas se aproximam com um ângulo maior que 50°. O RTR é maior que dois (>2). Estas ainda podem ser divididas em: (a) Reflectivas, as que apresentam forma convexa a linear e são compostas por areia média a grossa; (b) Dissipativas sem bancos ou terraço de baixo mar (sedimentos finos), com

perfil côncavo a linear. Processo de rotação praias foram evidenciados em praias reflectivas expostas(e.x. Taquaras/Taquarinhas), bem como no setor exposto de praias dissipativas semi-expostas (ex. Balneário Camboriú). Este processo provavelmente é encontrado em outras praias de enseada do estado de Santa Catarina em resposta as mudanças do regime das ondas.

Três tipos de tamanho de grão foram identificados na área de estudo: Tipo 1, sedimentos que tem tamanho médio (Mz) entre 2,0 ∅ e 3,5 ∅ (0,1 a 0,2 mm, areia fina a muito fina); Tipo 2, areias do tamanho médio (1∅ a 2∅ ; ou 0,2 mm – 0,5 mm); Tipo 3, tamanho de grão entre 0 ∅ e 1 ∅ (0,5 a 1,0 mm, areia grossa). Os resultados mostram que existem diferentes tipos de tamanhos de grãos em praias adjacentes, indicando que o padrão de circulação ou transporte de sedimentos é restrito a cada praia de enseada, não existindo trocas de sedimentos entre estas. Praias dissipativas são compostas de sedimentos finos (Tipo 1) quando comparadas as reflectivas, que são compostas por areia grossa (Tipo 3). As praias intermediárias apresentam todos os tamanhos de grão. Não foi encontrada uma relação clara entre a altura média da onda na zona de surfe e o tamanho médio de grão (Mz), indicando a importância da fonte/proveniência dos sedimentos para caracterizar o padrão dos sedimentos na área de estudo. Análises temporais dos sedimentos da face da praia, evidenciaram que praias dissipativas apresentam uma grande estabilidade no tamanho do grão. Ao contrário, praias expostas reflectivas e intermediárias mostraram uma maior variação do tamanho de grão.

Este trabalho contribuiu para um aumento do conhecimento da morfologia e sedimentologia de praias de enseada, entretanto ainda existe um vasto campo de trabalho para ser realizado. O modelo aqui apresentado é uma primeira aproximação e, portanto mais estudos devem ser conduzidos em regiões com características geográficas similares a fim de fornecer mais informações e validação deste.

Table of Contents

Figure List

Chapter 1

Chapter 2

Chapter 3

Chapter 5

Chapter 6

Table List

Chapter 6

Signals List

a	maximum indentation
B	length of obstacle
B*	bar parameter
cal yr BP	before present
C_l	embayment width between headlands
$C_{0,1,2}$	constants relate to reference angle β
d	particle diameter
F	subaerial dimensionless beach shape
h_{max}	maximum height of the profile.
H_b	wave break height
H_s	significant wave height
H_{smax}	maximum significant wave height
H_{max}	maximum wave height
J	length of salients
K_1	diurnal lunar constituent
k	surf zone slope
L	subaerial beach width

M_2	main semi-diurnal lunar constituent
Mz	graphic mean
O_1	diurnal lunar constituent
r_1, r_2	consecutive radii from the center of a logarithmic spiral
R_β	control line length or headland spacing
R_n	length of the line at 'n' point of the bay periphery in static equilibrium
R_1	length between diffraction point and apex of salients.
RTR	relative tidal range (spring tidal range/ wave break height)
S	distance between obstacle and root of salients
S_1	embayment shoreline length
S_2	semi-diurnal lunar constituent
tanβ	beach face or nearshore slope
T	wave period
T_p	peak period
T_{pmax}	maximum peak period
T_i	storm wave period
TR	spring tidal range
V	subaerial beach volume
Y	(y axis – vertical axis)

y	alongshore dimension
X	x axis and distance from obstacle to apex of salients
X_s	surf zone width
x	cross-shore dimension
χ_s	surf zone and nearshore length
W_s	sediment fall or settling velocity
β	reference wave obliquity to the headland alignment
Δt	time dependence
Ω	omega or Dean´s parameter or dimensionless fall velocity
Ω_t	empirical dimensionless fall velocity
δ'	nondimensional embayment scaling parameter
λ_r	distance between rip-currents
θ	logarithmic spiral angle apart on the curve, which has a constant outer tangent α
θ_c	angle at maximum indentation

θ_n	angle equivalent to R_n
θ_p	Wave direction
θ_{rang}	Wave direction range
ϕ	phi
τ_I	inclusive graphic standard deviations

CHAPTER ONE

INTRODUCTION

Morphodynamics of Headland-Bay Beaches: A Review

1.1. GENERAL CONSIDERATIONS

A sandy shoreline bounded by rocky outcrops or headlands, natural or man-made, where its shoreline assumes some form of curvature is the definition used for the term *headland embayed beaches* or *headland bay beaches*. These kind of beaches have received various names in the past, such as: zeta curved bays (Halligan, 1906, Zenkovich, 1967; Carter, 1988; Silvester *et al.*, 1980), half-heart shaped bays (Silvester, 1960), logarithmic spiral beaches (Krumbein, 1944; Yasso, 1965; LeBlond, 1972), crenulate shaped bays (Silvester and Ho, 1972; Finkelstein, 1982), curved or hooked beaches (Rea and Komar, 1975), pocket beaches (Silvester *et al.*, 1980; Komar, 1996,1998; Uda *et al.*, 2002), bay-head beaches (Bird, 1996), bayed beaches (Tan and Chiew, 1994), headland bay beaches (Yasso, 1965; LeBlond, 1979; Wong, 1981; Phillips, 1985; Moreno and Kraus, 1999), headland embayed beaches, structurally controlled beaches (Short and Masselink, 1999) or topographically-bound beaches (Short, 2002). In most cases, theses beaches are asymmetric in shape, characterized by a curved shadow zone, a gently curved middle transitional zone, and distally as a relatively straight tangential end downcoast (Silvester and Hsu, 1993, 1997; Short and Masselink, 1999). They may be in the form of salients or tombolos behind offshore islands or man-made structures. In some rare cases, they may even appear as a short and straight beach sheltered behind groins or headlands.

Inman and Nordstrom (1971) estimated that almost 50% of the world's coast consists of hilly or mountainous coastline. However, more recently Emery and Kuhn (1982) have shown that cliffs (*i.e.* steep slopes bordering ocean coasts) occur along *circa* 80 % of the world's coastline, and are found in all latitudes, as shown in Figure

1.1. This is an indication of the prevalence of beaches between headlands around the world (Short and Masselink, 1999).

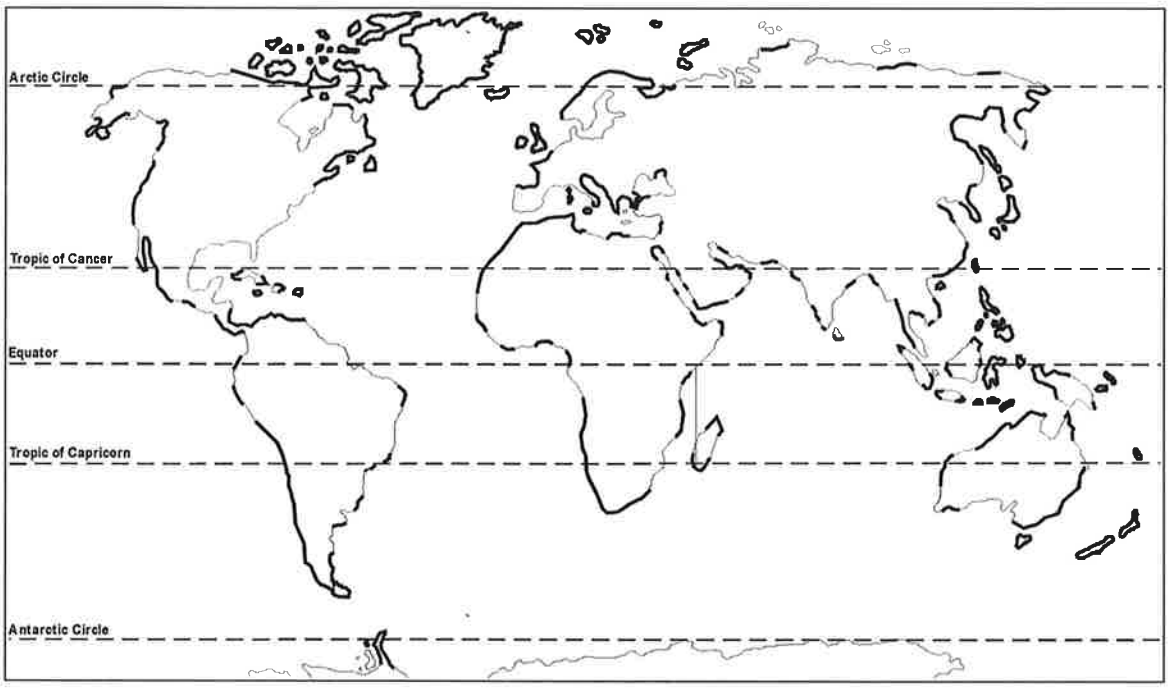

Figure 1.1. Distribution of worldwide rocky coasts (after Emery and Kuhn, 1982).

As indicated by Short and Masselink (1999), the length and spacing of these beaches depends entirely on pre-existing bedrock topography that has been partially drowned by the Quaternary sealevel transgression and regression with flooded valleys partially filled with sediment, while the valley sides and spurs remain as headlands and rock coast.

The purpose of this Chapter is to provide the framework for this thesis. Initial considerations outline morphodynamic approaches and time-scales and equilibrium definitions, which are followed in this PhD dissertation, as presented by Wright and Thom (1977), Bird (1996) and Komar (1998), respectively. Subsequently, there follows a summary of previous work performed on headland bay beaches. This section is an introduction to previous research relevant to this study, but does not represents a

comprehensive literature review. Finally, the aims and structure of the dissertation are presented.

1.2. THE MORPHODYNAMIC AND SCALE APPROACH

The term *morphodynamics* was introduced in the coastal literature by Wright and Thom (1977), in an effort to describe " *the mutual adjustment of topography and fluid dynamics involving sediment transport* ". On beaches, this implies that the surface topography of the beach will adjust to accommodate fluid motions produced by waves, tides and other currents, which in turn will influence the wave and tide processes (Short, 1999). Cowell and Thom (1994) state "*the essential properties of coastal morphodynamic process are attributable to the feedback loop between topography and the fluid dynamics that drive sediment transport producing morphological change*" (Figure 1.2). These authors also discuss the "*chicken-and-egg*" nature of mutual interactions between coastal topography and processes, as articulated formally by Wright and Thom (1977), which involves changes to coastal landforms over a broad range of temporal and spatial scales. Scales at which morphodynamic processes operate were grouped into four classes as presented in Figure 1.3.: (a) instantaneous, (b) event, (c) engineering, and (d) geological.

Larson and Kraus (1995) suggested that beach profile change, in a engineering point of view could be classified as: *microscale*, changes from sub-wave period to several wave periods over lengths of millimeters to centimeters; *mesoscale*, net sediment transport rates over many wave periods are evaluated for distances of meters to a kilometer; *macroscale*, seasonal changes and a space scale of kilometers; and

megascale, decade to century changes over coastal sub-reaches and reaches, *e.g.* over a littoral cell.

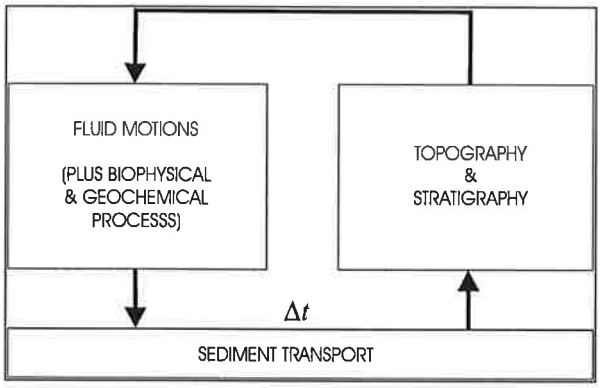

Figure 1.2. Primary components involved in coastal morphodynamics. The feedback loop between form and process is responsible for fundamental complexity in coastal evolution. Time dependence, Δt, is inherent in morphodynamic evolution of beaches and coasts (after Cowell and Thom, 1994).

In headland bay beaches, as indicated initially by Rodriguez (1995), there is a maximum relation between the alongshore (y) and cross-shore (x) dimensions. When $y >>> x$ the beach will be rectilinear. As a scalar term, the dimensions of x are in the order of 10^2-10^3 m while y dimensions are in the order of magnitude of 2 to 3 times x in a headland bay beach system. In general terms, the magnitude order of the planform is 10^3m. The presence of rhythmic planforms on the beachface (*e.g.* cusps) or punctual elements that change the form exchanging the wave propagation are in the order of 10^1m to 10^2m and this is at least one order of magnitude less than the beach planform. In this condition, these beachface features for equilibrium planforms analysis will not be considered in this dissertation.

The morphodynamic approach, as presented by Wright and Thom (1977), is extensively applied to a range of beach environments and widely followed by researches

around the world, especially by the Australian Beach School. The morphodynamic approach was frequently cited in a comprehensive literature review in the "*Handbook of Beach and Shoreface Morfodynamics*", edited by Andrew D. Short (Short, 1999). In this study, the Sedimentology and Geomorphological paradigms of beach morphodynamics will be used, *i.e* the beach morphology and sedimentology change is a result of the dynamics and sediment transport patterns. A Large Scale Coastal Behaviour (year to decades), *i.e.* Macro to Megascale (Geological and Engineering) to analyze the beach stability, changes and evolution is considered in this study.

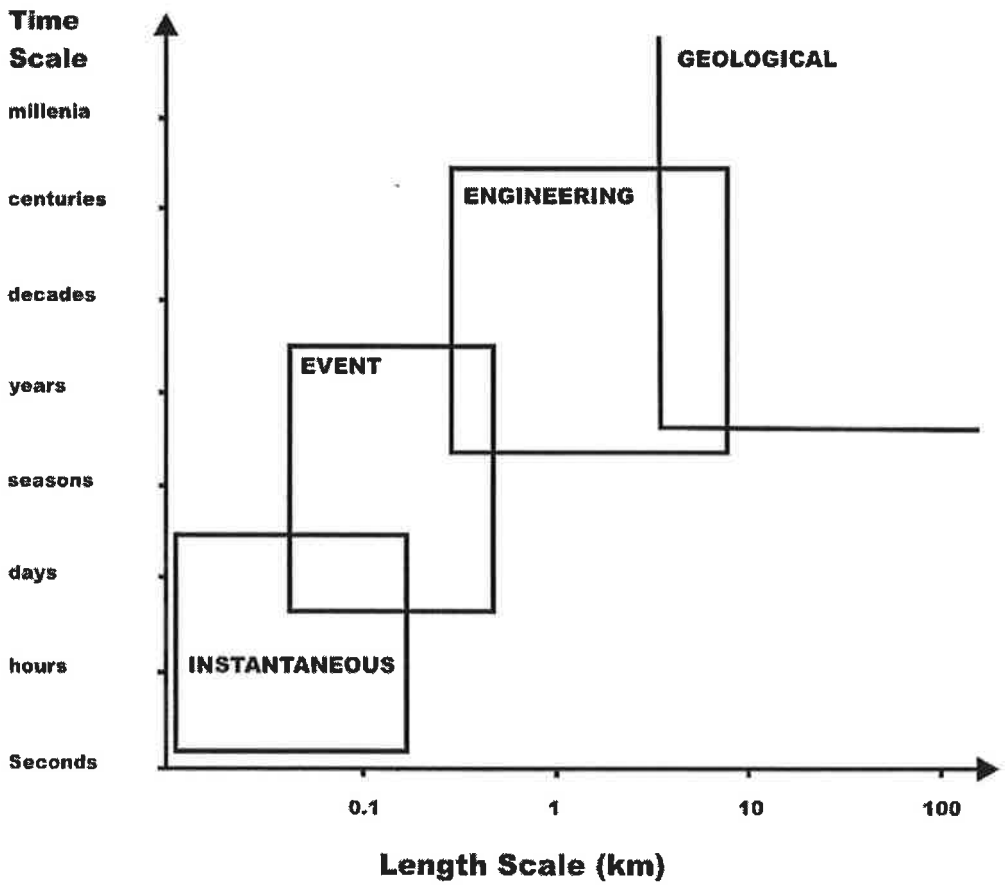

Figure 1.3. Definition of spatial and temporal scales involved in coastal evolution with typical classes of sedimentary features (after Cowell and Thom, 1994).

1.3. EQUILIBRIUM PLANFORM DEFINITION

To give a definition of equilibrium is a difficult task and is very complex, some times resulting in controversy between researchers, since it involves different variables that are continuously adjusting the geomorphology to the changing hydrodynamic conditions at different time and spatial scale. It is a "*relative*" definition, relative to the time and scale that the researchers define. In this dissertation, in terms of beach planform stability, headland-bay beaches may be classified as being in *static equilibrium* or *dynamic equilibrium* as proposed by the "*parabolic model*" of Silvester and Hsu (1993, 1997), Bird (1996) and Hsu *et al.* (2000).

Bird (1996) describes beaches in *static equilibrium* as swash-dominated beaches (with swash alignments), having been build parallel to incoming wave crests with little or no longshore sediment movement. On the other hand *dynamic equilibrium* as drift-dominated beaches (with drift alignments), they are parallel to the line of maximum longshore sediment flow, generated by obliquely incident waves. Bird (1996) complement, in general, beaches with swash alignments are smoothers in outline than those drift alignments, which are typically sinuous. In other words, after Silvester and Hsu (1993, 1997) *static equilibrium* or *stable* is reached when the predominant waves are seen to be breaking simultaneously around the whole bay periphery. At this stage littoral drift is almost non-existent, and the curved beach is stable without long-term erosion or deposition, except during storm periods. For bays in *dynamic equilibrium* or *unstable*, balance in sediment budget is the key factor in maintaining the shoreline in its existing position. However, shorelines in dynamic equilibrium can retreat as sediment supply reduces from upcoast or from a river within the embayment, and recede towards the limit defined by the static equilibrium, if supply diminishes completely (Figure 1.4).

The planform equilibrium curvature is in balance with the sediment supply and the capability of the waves to redistribute that sediment alongshore and the time element for such an equilibrium shoreline is long term – years and decades (Komar, 1998). Superimposed to this Large Scale Coastal Behaviour (LSCB) equilibrium is the continuously geomorphic adjustment to the changing hydrodynamic conditions (*e.g.* shoreline and consequently bar growth, migration and degeneration) as described above (Small Scale Coastal Behaviour, SSCB).

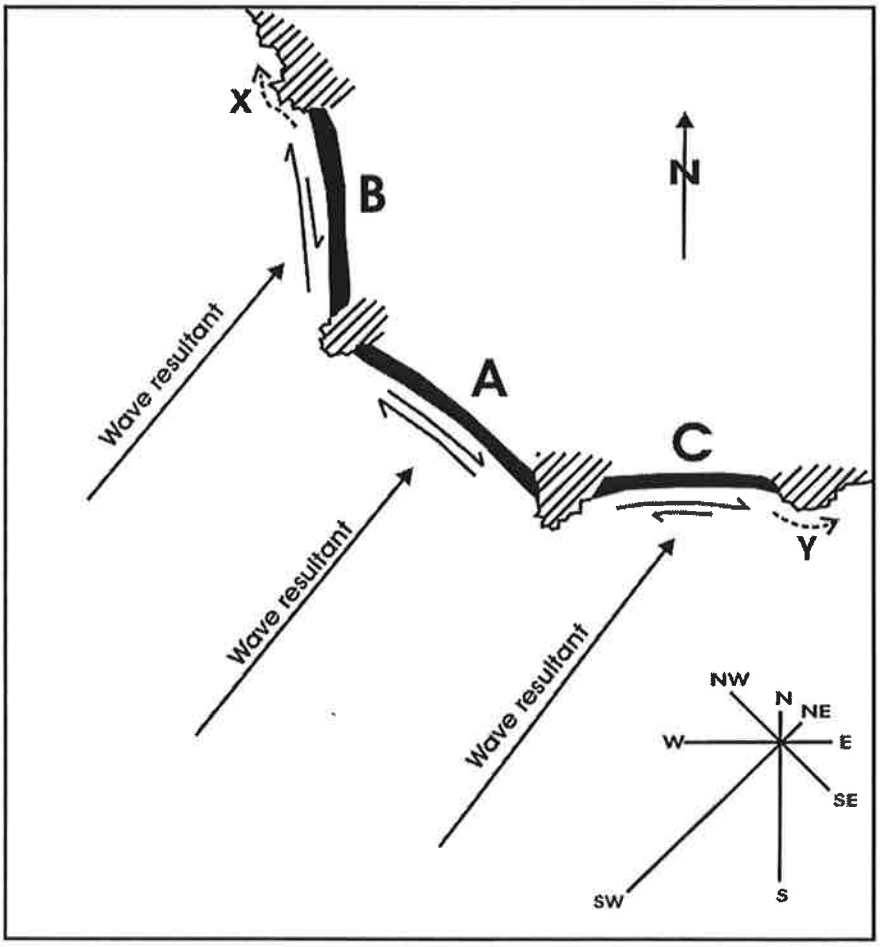

Figure 1.4. The influence of aspect on longshore drift at headland bay beaches. On beach A, with an orthogonal wave resultant, there is no net drifting; on beach B and C drifting can be important. Losses are likely around headlands at X and Y (modified from Bird, 1996).

1.4. HEADLAND BAY BEACHES – PREVIOUS WORK

1.4.1. Morphological Studies on Headland Bay Beaches

To define the **shoreline planform** of headland bay beaches, a number of numerical models have been developed in the past, such as those of Rea and Komar (1975) and Le Blond (1979), who make use of the fact that wave crests in the bay at a state of equilibrium are parallel to the shoreline or bottom contours. However, the numerical models could not simulate the time evolution of the beaches as the incident waves refract and diffract in the lee of the headlands. In order to define the **shoreline planform,** other studies proposed several mathematical functions to curve-fit the shoreline of a headland-bay beach through analysis of field data supplemented with results of modeling studies. Among them, the three major expressions are the logarithmic spiral (Krumbein, 1944; Yasso, 1965), the parabolic bay shape (Hsu and Evans, 1989; Silvester and Hsu 1993, 1997), and the hyperbolic-tangent shape (Moreno and Kraus, 1999; Martino *et al.* 2003). These empirical equations have different coordinate systems, origins, and controlling parameters related to wave direction and bay geometry. Wave heights and periods were not included in the formulations. As presented by Moreno and Kraus (1999) the parabolic bay shape equation and the hyperbolic-tangent shape equation define very well the planform shape of beaches. However, the parabolic bay shape equation is unique, since it considers the wave direction approach and diffraction. The logarithmic spiral does not consider the diffraction process/point and the hyperbolic-tangent is only a geometrical equation. Additionally, their shortcoming is originated from the data base of mixed bay beaches leading to the derivation of these equations using any curved beaches, but not only data

in static equilibrium (Hsu *et al. in preparation*). According to Silvester and Hsu (1993, 1997) and Hsu *et al.* (2000), as defined in terms of beach stability, a headland bay beach may be classified in two states as *static equilibrium* or *stable* and *dynamic equilibrium* or *unstable.* The amount of sediment input and output (sediment budget) and the change in the wave direction control and define the beach planform state as postlude in section 1.3.2. According to Komar (1998, p 424) the most elementary shoreline is where there is no long-term net transport of sediment. For this author, this condition is closely approached by a headland-bay beach where little or no additional sediment is being supplied to the beach and essentially no losses occur. Under this simplest condition, the shape of the beach depends on the wave refraction and diffraction, yielding an arcuate shape typical of these beaches with bounding headlands. According to Tan and Chiew (1994) and John Hsu (*personal communication*) the influence of the magnitude of waves (height and period) and tidal water-level fluctuation appears to be secondary.

Superimposed to planform shape a continuous **beach rotation process** adjusting to changing hydrodynamic conditions in a Small Scale Coastal Behaviour (SSCB) occurs. Although the medium-term average shoreline configuration reflects the net-zero longshore transport as a result of wave diffraction and refraction, individual wave trains could produce an oblique-wave approach and a temporary longshore transport. Beach rotation process is a common phenomena that occurs in headland bay beaches, according to Short *et al.* (1995) and Short and Masselink (1999). This phenomena, was also addressed by Bird (1996) in his review about beach compartments. This process refers to a shift in alongshore sediment transport between extremities of headland bay beaches, being attributed to periodic or medium term changes in wave climate, especially in wave direction. Beach rotation can occur over a range of time scales that

involve great variation and movement of the coastline (in the order of 10^2m), without gain or loss of sediment in the system. However, this process was only well understood for an intermediate beach stage by Short *et al.* (1995; 2000). These authors, analyzing twenty years of data, discovered a rotation cycle between 3 and 8 years. The rate of change is related to the wave period and magnitude of the wave directional change.

Headland bay beach experience both longshore drift and consequently beach rotation process. In this condition **headland sand bypassing *occurs*,** *i.e* periodically sediment can escape around the headland, as a result of downdrift accumulation of sediment (Short and Masselink, 1999) and the development of megarips (Short, 2002). This can be a function of headland size and water depth in front of the headland, as well as of the amount of sediment entrainment in the littoral cell.

Beach dimensions and its exchange can be defined in two-dimensional space as described above (as a profile or in planform analysis) and in three-dimensional space (also profile and planform analysis) (Short, 1999). **Beach Profile** variations are due to wave shoaling and breaking. Short (1999) reports that at the low energy end of the spectrum, beaches are narrow and shallow, rip-dominated beaches are produced by moderate to high waves, and wide multi-barred systems at the high energy end (Figure 1.5). On the other hand, the three-dimensional beach variation begins with wave refraction and attenuation/diffraction across the nearshore zone producing longshore change in wave height and direction, leading to variations in beach planform (shoreline) and consequentely in beach profile (beach type) at different scales. Figure 1.5 shows the scale of three-dimensional variations in beach morphodynamics.

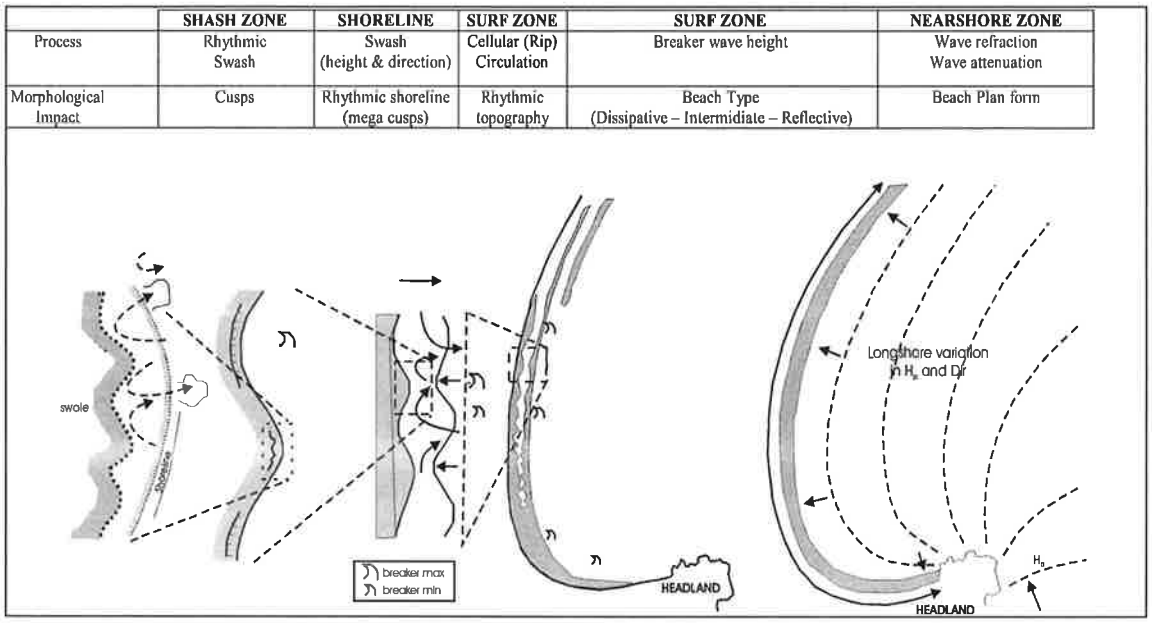

Figure 1.5. Scale of three-dimensional variation in bayed beach morphodynamics (After Short, 1999).

1.4.2. Sedimentological Studies on Headland Bay Beaches

Textural variation of sandy beaches, both alongshore and cross-shore, and spatial distribution patterns have been widely studied around the world (*e.g.* Pettijohn and Ridge, 1932; Krumbein, 1944; King, 1972; Bascom, 1951, Nordstrom, 1977, 1981; Bryant, 1982; Short, 1983; Short, 1984a; Short, 1984b; Short, 1986; Short, 1994; Short and Ni 1997, between others). Many researchers report that wave height (wave energy) is the most important parameter that determines grain size distribution patterns alongshore - gradings (*e.g.* Krumbein, 1944; Bascom, 1951). However, Martins *et al.* (1970) and Nordstrom (1977, 1981), after studying exposed and sheltered beaches, suggested that sedimentary provenance is the most important factor that defines sand grain size. Recently, Calliari (1994), Short and Ni (1997), Short (1999), Miot da Silva *et. al* (2000) and Miot da Silva *et. al.* (2003) concurs with Nordstrom's (1977, 1981)

observations by reporting that the sedimentary provenance defines grain size distributions on beaches.

Type and distribution of beach sediments have been extensively studied worldwide, but the connection between wave/current processes, morphology and alongshore grain size variation, were firstly reported by Sonu (1973). The beach morphodynamic types as proposed today by Short (1979) and Wright *et al.* (1979) and behavior of grain size characteristics linkage were well reported by Bryant (1982).

Bryant (1982) showed that the different gradings are a result of the different processes in the foreshore of reflective and dissipative beaches and reported that grain size may not always be a good indicator of wave energy, as proposed by Nordstrom (1977). Short (1979), Wright *et al.* (1979), Bryant (1982), Wright and Short (1984), Short (1983; 1984a; 1984b; 1986; 1994; 1999), and Short and Ni (1997) reported an inverse relationship between wave height and grain size, because fine and very fine sands are found on dissipative beaches with high wave heights (high energy) and coarse sands occurs on reflective beaches with low wave heights (low energy).

However, despite the number of studies of the phenomena responsible for alongshore and crosshore beach sediment distribution patterns, only a few studies concentrated on the explanation of beach foreshore sediment distribution on and between headland bay beaches (*e.g.* Bascom 1951; Bryant, 1982; Carter, 1988).

1.4.3. Wave and Current Processes at Headland Bay Beaches

Field experiments to define the influence of wave refraction and attenuation/diffraction on headland bay beaches were not performed or at least are not expressed on the scientific literature. On the other hand, numerous studies and field

experiments focusing on rip currents, circulation and sediment transport patterns were conducted by Andrew Short and co-workers over the last 20 years (*e.g.* Short, 1985; Huntley and Short, 1992; Short and Hogan, 1994, Short 1999; Short and Brander, 1999; Brander, 1999a,b; Brander and Short, 2000). These authors posit various hypothesis to account for rip density on headland bay beaches. They employed infragravity wave theory to define the number of rips on headland bay beaches. Recently, Brander and Short (2000) and Brander (1999a,b) presented results, which showed the dynamic behavior and sediment transport of megarip-currents and rip-currents during events of high and low wave energy. Short and Brander (1999) reported that the number of rip currents decrease with high waves, but at the same the size of rip-currents and spacing increase. During storm conditions (H_b > 2.5 m) there is a predominance of megarip-currents. Short and Brander (1999) defined a relationship between the wave climate and the possible number of rip-currents per length of beach (Km). According to these authors, for moderate east coast swell environment, such as Southern Brazil, the suggested number of rip-currents per length of beach (Km) is 5.

1.4.4. Beach Stages Studies on Headland Bay Beaches

As presented by Larson and Kraus (1989,1994), quantitative studies of three-dimensional morphology began early with studies of Hom-ma and Sonu (1962) and Sonu (1973), Birkemeier (1984), Lippman and Holman (1990), Liang and Seymour (1991). However, seminal work defining the three-dimensional beach stage changes at headland bay beaches was conducted by Short (1979). He reported that all beaches experience a spectrum of beach morphodynamic states (10 beach stages) and the range and frequency of excitation within the spectrum depends primarily on breaker wave

power and beach gradient in time and in space (alongshore). Wright and Short (1984) and recently Short (1999) suggest subsequently, that the dimensional fall velocity parameter ($\Omega = \frac{H_b}{W_s.T}$) can be applied to different beach sectors to define a longshore beach morphodynamic stage variation. Masselink (1993) suggested the existence of a tidal effect to sheltered beaches at estuaries/bays as well as in a microtidal environment. Wave and tidal influence can be defined by the relative tidal range parameter (RTR = spring tidal range/wave break height (Masselink, 1993).

Recently Short and Masselink (1999), in their review of headland bay beaches, presented a new parameter, the nondimensional embayment scaling parameter, which represents the degree of impact of end effects or embaymentisation (δ'). When deepwater waves enter an embayment of a given width (C_l) between headlands, the wave energy is redistributed along the embayment shoreline (S_l), according to the formulation:

$$\delta' = S_l^2 / (k\, C_l\, H_b) \qquad (1.1)$$

Where k is the surf zone slope, H_b is wave break, and S_l is the embayment shoreline length. Cellular circulation occurs when δ' is less than 8, transitional circulation for δ' occurs between 8 and 20, and normal circulation takes place where δ' is greater than 20 (Figure 1.6). These authors also suggest the use of Ω and δ′ to define the morphodynamics of headland bay beaches. The nondimensional embayment scaling parameter, however, only considers parallel wave approach to the embayment.

The beach response when the modal wave approach the coast with a certain obliquity was not discussed. Short (1979) reported that the most obvious effect of waves arriving obliquely to the shore is to skew the morphology in the direction of net

longhore current. He also pointed out, that the skewing does not contradict the presented beach model, rather it introduces a longshore bias to morphology and net longshore flow. In section 1.4.1 the consequence of small and medium scale of opposite change in the wave direction, which result in the beach rotation process is described, *i.e* it is possible to find Short's (1979) erosion and deposition sequence alongshore of the same beach.

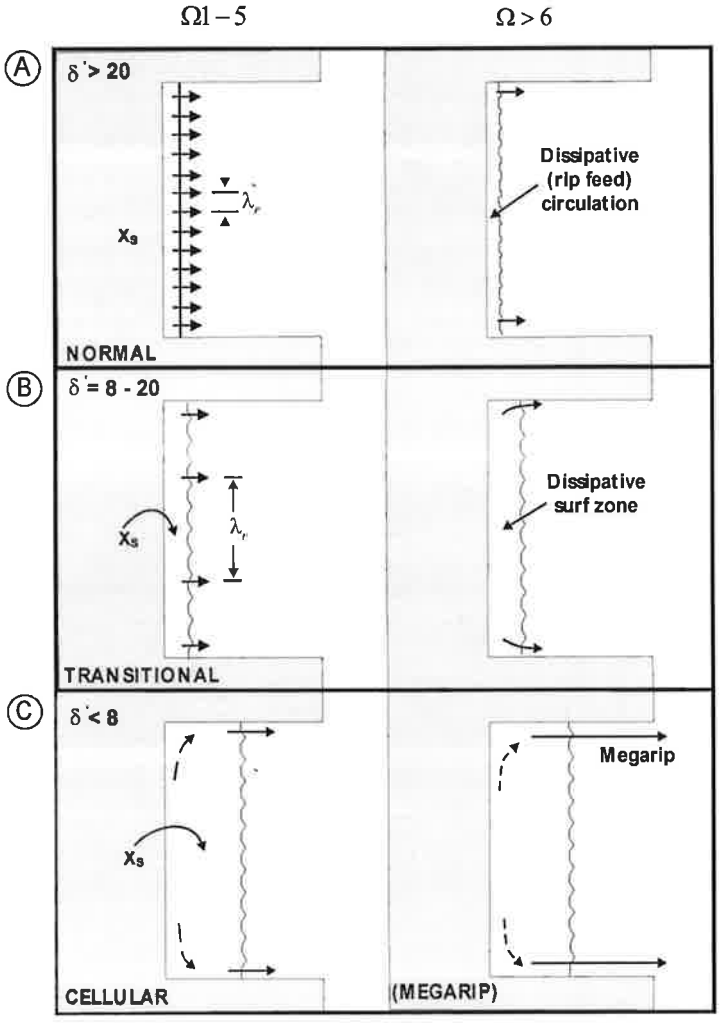

Figure 1.6. Schematic illustration of the impact of embaymentisation on surf zone circulation basead on δ' and Ω (after Short and Masselink, 1999). (A) Normal circulations with end effects; (B) transitional circulations; and (C) cellular circulations ($\delta' < 8$, $\Omega < 6$ and $\Omega > 6$). X_s is the surf zone width and λ_r is the distance between rip-currents.

1.4.5. Summary

Following an introduction to previous research relevant to this study, that does not represents a comprehensive literature review, a number of general conclusions can be drawn:

1) Headland bay beaches are found in all latitudes, as a sandy shoreline bounded by rocky outcrops or headlands, natural or man-made, where its shoreline assumes some equilibrium form of curvature as a consequence of balance with the sediment supply and the capacity of the waves to redistribute that sediment alongshore, and the time element for such an equilibrium shoreline is medium term – years and decades.
2) Headland-bay beaches planform, as reported in the literature, are better described by the parabolic bay shape empirical equation that uses polar coordinate systems, origins, and controlling parameters related to wave direction (diffraction/attenuation) and bay geometry.
3) Beach rotation process is a common phenomena that occurs in headland bay beaches as a result of a shift in alongshore sediment transport between its extremities, being attributed to periodic or medium term changes in the wave direction. However, this process was only well understood for an intermediate beach stage.
4) The type and alongshore distribution of beach foreshore sediment is a consequence of sedimentary provenance of the study area. The grain size is not a good indicator or is inconsistently related to wave energy. Nevertheless, it can be a good indicator of sediment transport and

dispersion. Studies about sediment exchange between headland bay beach in the literature are more from the geomorphologic point of view.

5) Process studies at headland bay beaches concentrated on rip current circulation and sediment transport.

6) Field experiments (instruments) to define the wave refraction and attenuation/diffraction and their influence on headland bay beaches have not been performed, or at least are not reported in the scientific literature. However, from the geomorphologic point of view, wave refraction and attenuation/diffraction across the nearshore zone leads to variations in beach planform (shoreline) and beach type in headland-bay beaches, as a result of longshore change in wave height and direction.

7) Cross-shore sediment transport results from variations in spatial-temporal scales of wave shoaling and breaking (*i.e* the wave climate). At the low end of the energy spectrum, beaches are narrow and shallow. Rip-dominated beaches are produced by moderate to high waves whereas wide multi-barred systems occur at the high energy end. This concept was applied punctually to define the variation of beach types alongshore in headland bay beaches.

1.5. AIMS AND STRUCTURE OF THE THESIS

The overall goal of this study is to contribute to increase the understanding of headland-bay beach morphodynamics, *i.e* to elucidate the interaction between hydrodynamic processes, beach morphology and sedimentology in east coast swell environments with headland and bay geomorphologies at event, historical, and geological scales. Although a large percentage of the world's coastline is characterized

by headlands, mountains and hills (between 50% and 80% - depending on the source), structural controls of headlands on beach morphodynamics have received little attention in the literature and consequently not much is known about headland-bay beach parameterization.

According to Short (1999), global studies of oceanic sandy beaches require many variables to better understand processes and morphodynamic behaviours. Short (1999) suggests five major parameters: tidal range, wave height, wave period, grain size and beach length/embaymentisation which are incorporated into seven equations that can be used to describe the major features of beach systems. These equations include, among others, those for beach type, beach slope, number of bars, and the embaymentisation parameter. Additional studies along different sandy coasts, especially those with headland and bay geomorphologies, are needed to develop a global (universal) model, as indicated by Short and Masselink (1999) due to wide ranges of wave and tidal conditions.

The main contribution of this Ph.D. thesis to existing knowledge of beach morphology and sedimentology is to ascertain differences and similarities in structurally controlled beaches. The following goals are specifically set forth:

1) Analyze the planform of headland-bay beaches using the empirical parabolic model;

2) Identify the beach morphodynamics and sequence profile for a bay-headland coast and suggest a parameterization of the effect of headland size, oblique wave approach and alongshore wave variation and sediment on beach morphodynamics.

3) Investigate the small-scale beach rotation phenomena in different headland-bay beach types (reflective, intermediate and dissipative).

4) Investigate the beach grain size distribution in and between headland-bay beaches.

These four goals are discussed in subsequent chapters following different (geomorphologic and geological) approaches. In order to investigate the morphodynamic processes that occur at different scales (small and medium), beach planforms for 90 beaches on the Santa Catarina coast were analyzed through the use of maps and aerial photographs at different scales. An intensive filed investigation of morphologic and sedimentological changes was conducted on 28 beaches in central-north Santa Catarina coast from May 1994 to March 1996, where morphological and sedimentological changes were related to spatial variations in wave/tidal conditions and sediment source. Field investigations were additionally conducted on three beaches in an effort to determine alongshore sediment mobility at headland-bay beaches. In this case, temporal morphological changes were related to wave climate (beach observations and forecasting). The environmental setting of the study are is described in Chapter 2. Methods and results are exposed in Chapters 3, 4, 5 and 6. Chapter 3 presents beachplan form analyses. Chapter 4 discusses the beach morphologies and profile sequences. Chapter 5 summarizes beach rotation phenomena at different beach stages while Chapter 6 reports sediment distribution in and between headland bay beaches as a consequence of sedimentary provenance. A final synthesis of this study on headland-bay beach morphodynamics is brought together in Chapter 7. Appendices contain the MEPBAY computational model and the collected beach planform data.

CHAPTER TWO

Physical Setting of the Santa Catarina Coast

2.1. PHYSICAL SETTING OF THE SANTA CATARINA COAST

In this chapter a review of the physical setting of the Santa Catarina coast is presented. Considerations about geology and geomorphology, climate, drainage basins, waves, surf zone currents, sediment transport, and tides are discussed. The headland bay beach planforms studied include beaches between Santa Marta Cape and São Francisco Island and studies of beach morphodynamics include beaches located between Tijucas bay and Itapocu river (Figure 2.1).

2.1.1. Geology and Geomorphology

From the landward western side to the eastern side of the Santa Catarina State merges the Serra Geral Mountains (plateau) with igneous rocks, Paraná Basin with sedimentary rocks, Crystalline Basement composed by magmatic and metamorphic rocks; and in the seaward margins with the continental shelf, the Coastal Plain (Sheibe, 1986; Figure 2.2).

The igneous rocks of Serra Geral Mountains are a result of a spill succession during Jurassic and Cretaceous period, circa 130 millions years before present (Mesozoic era), that covers approximately 50 % of Santa Catarina state surface (Sheibe, 1986). Paleozoic and Mesozoic rocks from Paraná Basin are composed by sandstones, conglomerates, mudstone (siltites), arcose and filites, frequently associated with extrusive volcanic rocks (Sheibe, 1986). The crystalline basement rocks comprehend seaward alignments (littoral mountains and hills), that form rock cliffs and headlands (Sheibe, 1986). In the northeast region the basement is composed by granulites; in the southeast by gneiss and migmatites; in the central-east by schist and filites; and by granites rocks from east to south (Càruso *et al.*, 1997).

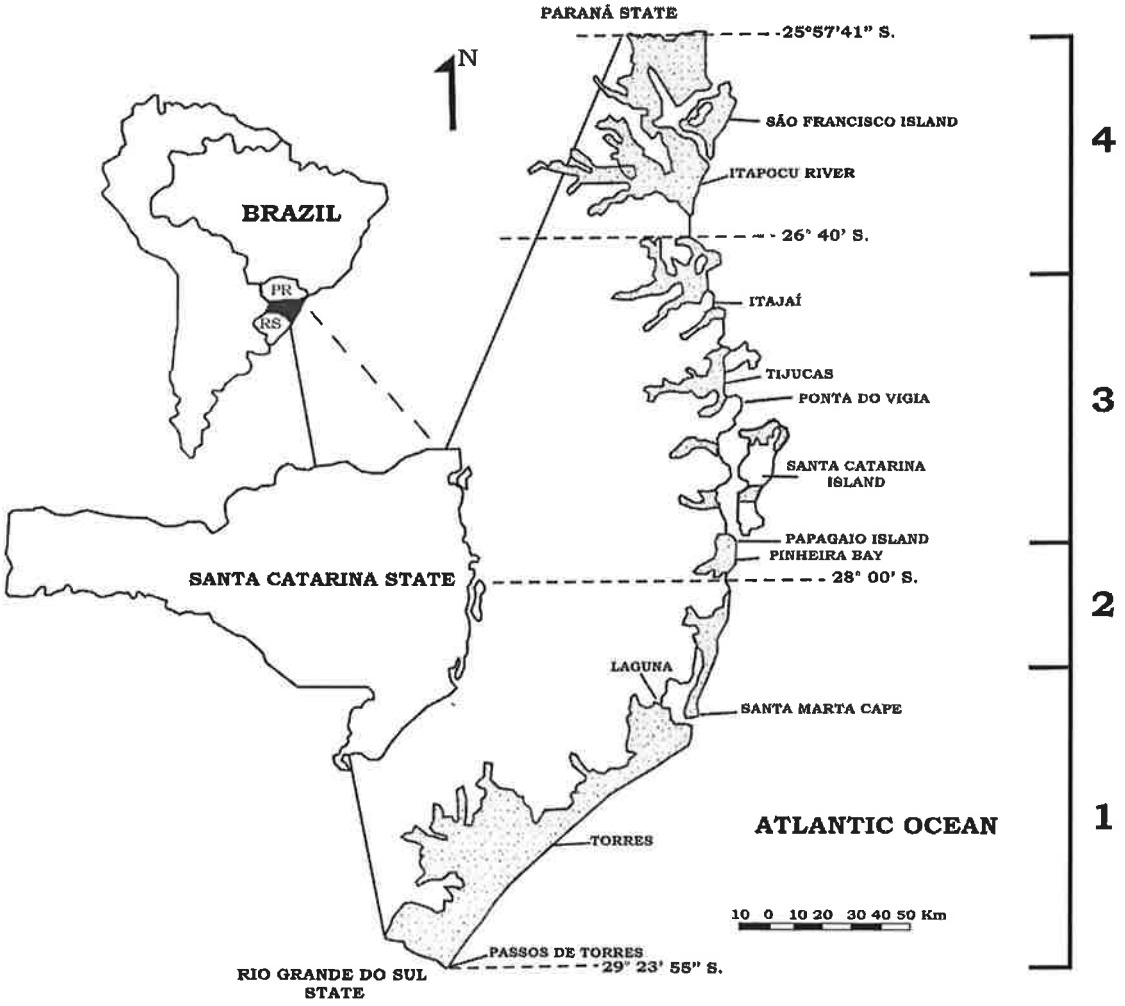

Figure 2.1. Santa Catarina coast showing its four main sectors (Duncan Fitzgerald and Willian Cleary, personal communication). Hachured areas represent the Quaternary deposits according Horn Filho *et al.* (1994).

The Santa Catarina coastline has been compressed by tectonics movements after the Gondwana rupture. From Imbituba northwards, relatively recent tectonic movements are responsible for the headlands and islands, *e.g.* Santa Catarina island (Sheibe, 1986).

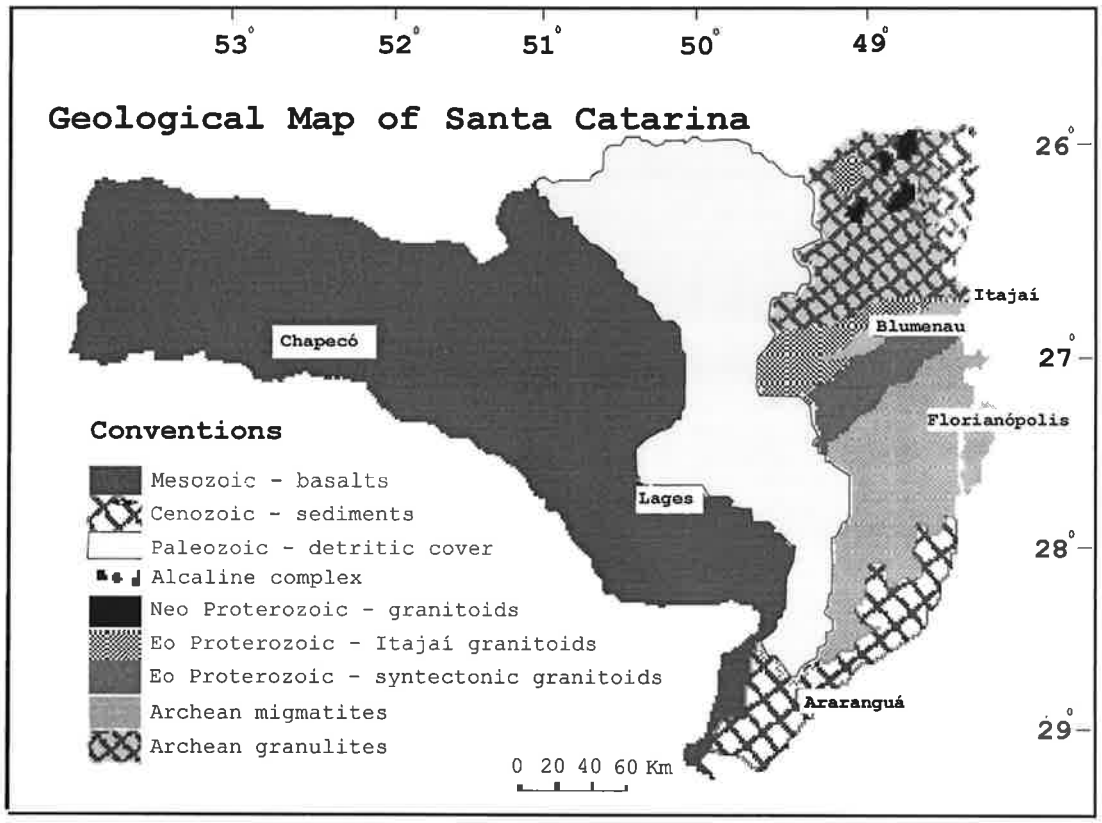

Figure 2.2. Geological map of Santa Catarina State shows age of major lithologies and rock units (modified from Scheibe, 1986)

The Santa Catarina coast of southeastern Brazil can be divided into four coastal segments based on their gross morphology (see Figure 2.1- Duncan Fitzgerald and William Cleary, *personal communication*). These sections, from south to north, include the following:

1. **Barrier Coast** (Passos de Torres northward to Santa Marta Cape): This is a straight section of coastline that is characterized by prograding foredune ridges backed by lagoons, coastal ponds, and lowlands. There are several small tidal inlets that are connected to freshwater drainage or saltwater lagoons. This type of barrier coast extends southward along Rio Grande do Sul although the lagoonal environment is much better developed to the south. The narrowing of

the lagoon northward along the barrier coasts corresponds to the appearance of bedrock outcrops close to the coast.

2. **Headland-Cuspate Barrier Coast** (Santa Marta Cape northward to Papagaios Island): Small bedrock headlands separated by cuspate barriers characterize this coastal segment. Many of the barriers form parabolic-shaped shorelines. Lagoons of variable size back the barriers and are connected to the ocean by small tidal inlets. Active dune systems occur along this entire section of coast. The northernmost bay along the coastal segment, Pinheira Bay, is cuspate in shape and backed by a large number of closely spaced arcuate foredune ridges.
3. **Rugged Bedrock Headland-Strand Plain Coast** (Papagaios Island northward to Ponta do Vigia): This section of coast, which includes Santa Catarina Island, is dominated by large bedrock headlands, reentrants, and bays. Between many of the small and large headlands, prograded foredune ridges, beach ridges and chenier plains have contributed to smoothing the irregular coast. An interesting contrast exists where river discharge forms deltas in protected settings, whereas cheniers or beach ridges characterize areas exposed to open-ocean waves.
4. **Strand Plain-Estuarine Coast** (Ponto do Vigia to São Francisco Island). This coast reflects a regime of abundant sediment supply in which foredune ridges plains formed between large estuarine systems. This type of coast continues along Paraná and into São Paulo. The slightly irregular nature of the shoreline is due to widely spaced bedrock promontories. On a smaller scale narrow barrier spits, tidal inlets, and small rivers characterize this region.

One characteristic common to all of these compartments is that portions of the coast within each segment have experienced extensive sedimentation resulting in progradation and straightening of the shoreline. These depositional regions represent

periods of abundant sediment supply and/or a fall in sea level. Progradation of the Santa Catarina coast encompasses elevation changes of up to 20 m above present sea level spanning development during the past 120,000 years. It has been shown by several researchers that the central and southern Brazilian coast was transgressed during the early Holocene reaching a maximum highstand (of 3.5 to 4.5 m above present mean sea level, MSL) approximately 5,600 cal yr BP (*e.g.* Martin *et al.*, 1979; 1984; Suguio *et al.*, 1980; Dominguez *et al.*, 1990; Angulo and Lessa, 1997; Martin *et al.*, 2003). Evidence for the highstand of sea level is based on radiocarbon dating of peats, shells, and coral, and thermo-luminesence dating of sand, respectively. The highstand also correlates with a change in estuarine foramineferal assemblages due to a decrease in oxygen level. Martin *et al.* (2003) suggested that during the falling sea level following the highstand, there have been two high-frequency oscillations encompassing 2 to 3 m of sea-level change. However, Angulo and Lessa (1997) are contrary to this high-frequency oscillation, or drops, in the Brazilian sea-level curve. Recently, pollen and diatom data coupled with radiocarbon dates have shown that relative sea level was about 2.0 m above present level around 3,300 cal yr BP (Ybert *et al.*, 2003). Whereas the existence of highstand at other low latitude sites is well documented (Pirazzoli, 1991; 1996) the cause for the higher than present sea level and its subsequent fall to present levels is not well understood. The mechanism may be related to glacio and hydro-isostatic adjustments following deglaciation or tectonic flexure due to sediment loading of the continental shelf (Bittencourt *et al.*, 1999).

The processes of regional coastal progradation during the Late Quaternary and the source of the sediment are poorly understood/documented in Santa Catarina coast. The sand deposited along the coast may have been reworked onshore from the inner continental shelf and/or it may have been discharged from local rivers and distributed

alongshore. The sediment comprising the present inner shelf and barrier systems along the southern half of the Santa Catarina consists of fine and very fine sand. The fine-grained nature of the sand and strong persistent onshore winds have produced magnificent parabolic, barchan, and linear dune systems along much of the southern coastal region (Bigarella, 1975). Extensive Pleistocene dune and lagoonal sediments also cover a wide swath of coast extending up to 6 km inland from and intermingling with the Holocene deposits along the Santa Catarina coast (Bigarella, 1972; Gianini, 1993). The dominant characteristic of this coast is its pronounced sediment abundance, however the timing of deposition is unknown. The high sedimentation interval has been associated with a regressing sea.

2.1.2. Drainage System

Surface drainage in Santa Catarina falls into two major systems: the Paraná-Uruguay drainage basin and the Atlantic drainage basin. Paraná-Uruguai basin drains to the Atlantic Ocean through the Prata Estuary (*i.e.* the border between Argentina and Uruguay). Atlantic drainage is separated by the Iguaçu drainage catchment to the north by the Serra do Mar mountains and by the Uruguay drainage catchment to the south by the Serra Geral mountains.

The Atlantic drainage area comprises about of 35,300 km^2, representing 37% of total state area (Santa Catarina - GAPLAN, 1986; Santa Catarina - SEDUMA, 1997; see Table 2.1. and Figure 2.3) and consisting of several fluvial basins.

The main basin of the Atlantic drainage is the Itajaí-Açu, with the existence of several smaller river basins with more than 1,000 km^2: Tubarão, Araranguá, Itapocu, Tijucas and Mampituba, in decreasing order. The drainage area of these rivers together

with the Itajaí-açu drainage represents of about 86% of all Atlantic drainage basin area (Santa Catarina - GAPLAN, 1986; Santa Catarina - SEDUMA, 1997).

Table 2.1. Physical characteristics of Atlantic drainage basins (After Santa Catarina – SEDUMA, 1997).

Basin	Drainage Area (Km^2)	Drainage density (Km/Km^2)	Discharge (m^3/s) Average	Minimal	Maximum
Cubatão	472	-	(*) 17.7	(*) 3.8	(*) 360.0
Itapocu	2,930	1.59	25.0	10.0	100.0
Itajaí-Açu	15,000	1.61	205.0	50.0	1,120.0
Tijucas	2,420	1.68	(*) 40.5	5.0	60.0
Cubatão do Sul	738	-	12.0	5.0	40.0
Biguaçu	382	1.52	-	(**) 2.3	-
Madre	305	1.90	-	(**) 1.3	-
D'Una	-	-	-	-	-
Tubarão	5,640	1.45	50.0	20.0	330.0
Araranguá	3.020	1.95	40.0	15.0	270.0
Urussanga	580	1.83	-	(**) 2.1	-
Mampituba	1,224	1.52	-	(88) 2.3	-

(-) No data ; (*) Data from DNAEE; (**) Discharge with 7 dry days and 10 year of recurrence.

The seasonal discharge regime is highly variable, changing from year to year and is mainly related to the path and frequency of cold fronts that transit southern Brazil (*e.g.* Klein, 1997; see section 2.1.3). Mean monthly rainfall is highest during the winter and spring (June to October), but a second peak often occurs in summer. In the Southwestern Atlantic, distinct interannual variations in precipitation and consequently discharge, with either a high amount of rainfall or dry periods, seem to be a consequence of the effect of the El Niño-Southern Oscillation (ENSO) (Nobre *et al.*, 1986; Gan, 1992) and La Niña-Northern Oscilation (LNNO) as pointed out in section 2.1.3. This phenomena influences directly the amount of continental freshwater runoff to coastal and marine ecosystems in the southern region of Brazil (Klein, 1997). Consequently, there are sometimes catastrophic floods in Santa Catarina State, especially on the Ararangua River (south) and Itajaí Valley (north). In summer,

precipitation occasionally surpasses 100 mm/day (flash floods) resulting in coastal flooding. This is catastrophic in urban areas due to the low soil infiltration capability (*e.g.* Balneário Camboriú and Florianópolis).

Figure 2.3. Santa Catarina's Atlantic drainage basins. Dotted lines mark drainage basin boundaries (after Santa Catarina – SEDUMA, 1997).

2.1.3. Climate

The interaction among three large air masses formed by three semi-permanent anti-cyclones (high pressure systems), the Atlantic, the Pacific and the Polar anti-cyclones, govern the climate and the atmospheric circulation (wind) in southern Brazil (Nobre *et al.*, 1986). The dynamics of this interaction is dominated by the movement of the following systems: high pressure systems originated from low latitudes, tropical anti-cyclones distinguished from the polar mass and migrated towards the continent or the south American coastline, and finally, the extratropical cyclones, associated with the passage of cold fronts (Nobre *et al.*, 1986; Klein, 1997; Figure 2.4). Northeasterly

winds are predominant and are later substituted by southwesterly winds, associated with the arrival of cold fronts (Nobre *et al.*, 1986).

According to Taljaard (1972), active cold fronts advance northward and in weakened form occasionally reach 20° S over the interior as well as over the east coast. The fronts are preceded by broad convergence zones and disturbed weather. When anti-cyclones pass eastward over the sea, rain belts of a warm front character occasionally develop on land along the leading edge of returning tropical air.

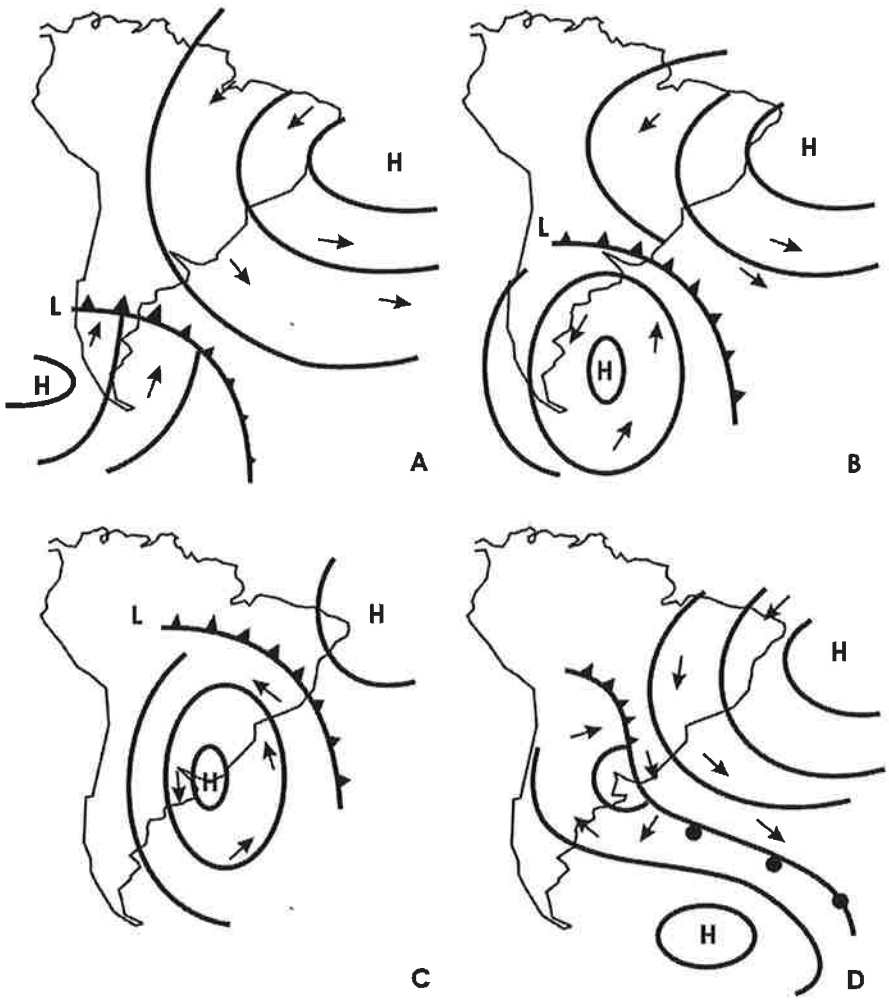

Figure 2.4. Atmospheric circulation in southern of Brazil and the modifications as a result of cold front propagation (after DHN, 1994): (A) Normal circulation; (B) origin of cold front (frontogenesis); (C) northern cold front passage; and (D) extratropical cyclones, associated with the passage of cold fronts (ciclo genesis). H = High pressure, L = Low pressure.

In the Southwestern Atlantic, distinct interannual variations in precipitation and consequently discharge, with either a high amount of rainfall or dry periods, seem to be a consequence of the effect of the El Niño-Southern Oscillation (ENSO) cycle and as well as La Niña Northern Oscillation (LNNO) on the global climate (Nobre *et al.*, 1986; Gan, 1992), but the processes involved are still not well understood (Klein, 1997). Nobre *et al.* (1996) and CPTEC/INPE (2001) reported that during the ENSO, cold front displacement over the continent (Uruguay and southern Brazil) is blocked. Consequently, a cold front can be stationary for weeks resulting in floods in Santa Catarina State, mainly in the winter season. However, the effect of LNNO is contrary to ENSO, i.e. there is a decrease in precipitation in southern Brazil, between September and February, as a consequence of the increase of displacement velocity of cold fronts (CPTEC/INPE 2001).

As a result of this atmospheric circulation pattern and the latitude position, the climate along the Santa Catarina coast is subtropical, wet, mesothermic, with small or no water deficit (Santa Catarina - GAPLAN, 1986). In general, from south to north there is an increase in average temperature from 18.9 °C to 20.3 °C and in precipitation from 1,219 mm to 1,875 mm. The potential evapotranspiration also increases from south to north, but relatively not as much as the precipitation. Results for the water budget between precipitation and potential evapotranspiration show the same trend as precipitation, but it increases almost three times from south to north of Santa Catarina coast, from 0.333 to 0.921 mm (Santa Catarina - GAPLAN, 1986).

2.1.4. Wave Climate

In Santa Catarina there are different sources of wave data: 1) Long time boat observation, published in Ocean Waves Statistics (Hogben and Lumb, 1967) and Global

Waves Statistics (Hogben *et al.*, 1986); 2) JICA (1990), eleven months (December, 1988, to October, 1989) non directional wave records at Enseada de Itapocorói, Piçarras beach, at 10 m deep; 3) three months wave record (height and period) in front of Balneário Camboriú by UNIVALI-CDTN (João Carvalho *personal communication*); 4) Wave records (directions, periods and heights) between February and May, 1996, in the shoreface (18 m deep) in front of São Francisco Island, northern Santa Catarina (Alves, 1996); 5) one year wave-gauging buoy data obtained at 80 m deep, in front of Santa Catarina Island (about 35 km from the coast) by the Coastal Information Program Maritime, Hydraulics Laboratory of Federal University of Santa Catarina (Melo *et al.*, 2003; Araujo *et al.*, 2003); INPH (2000), two weeks wave record inside of Balneário Camboriú Bay; 6) visual observation on the coast from the sea sentinels project (Melo, 1993); and 7) Daily wave forecast models recorded from Internet sites (www.atlasul.inpe.br and www.fnmoc.navy.mil).

In distinct beaches of Santa Catarina Island, visual observations were punctually conducted by Cruz (1993, Ingleses beach); Abreu de Castilho (1995; Armação beach), Santos (1995; Joaquina beach); Leal (1999; Moçambique-Barra da Lagoa beach), Diehl (1997; Daniela beach) and Torronteguy (2002; Joaquina and Morro das Pedras beaches). Daily visual observation (wave height and direction) is also available in the CameraSurf site (http://www.uol.com.br/camerasurf) for Joaquina beach. The Safety and Management Project has a database with eight years visual wave observations during the beach accidents in the summer (Klein *et al.*, *in press*).

Alves (1996) reported four see states in the Santa Catarina's wave climate during the period he observed (February to May, 1996), that are classified according to the associated meteorological conditions:

1) **East-northeast wind seas** correspond to approximately 10% of the observed wave climate regimes and were mainly observed during summer. Peak periods varied from 3 to 8 s, while significant wave height ranged from 0.5 to 1.5 m (Figures 2.5 a and b). Their generation is associated with the intensification of northeasterly winds at the boundary of the semi-permanent South Atlantic high-pressure system (Figure 2.6a).

2) **South-Southeast wind seas** correspond to approximately 10% of the observed wave climate regimes and are the most severe sea state in terms of significant wave height, typical values ranging from 1 to 3.5 m. Peak periods varied between 4 and 8 s (Figures 2.5 g, h, i and j). They are generated by winds associated with low-pressure systems carried along the coast by cold fronts (Figure 2.6 b).

3) **Easterly waves** are waves grouped under the same pattern, that arrive from east and southeast and dominate the local wave climate (approximately 50% of all observations, Figure 2.5 c,d,e and f). Peak periods and significant wave height varied between 6 to 11 s and 0.5 to 1.5 m, respectively.

4) **South-Southeast swell** represented approximately 25 % of the observations and are long peak periods not connected to local winds, ranging from 7 to 16 s. They are the most energetic swell waves with significant wave heights varying between 1 and 2 m (Figure 2.5). These waves are associated with storms that propagate along the South American east coast and deviate into the Atlantic Ocean within the 20°S and 40°S latitude band at distance in excess of 1000 Km from the coast (figure 2.6c). According to Melo and Alves (1993), long travelled swells are also generated by storms that migrate

northwards along the Patagonia coast (Argentina), deviating to the Atlantic Ocean at latitudes greater than 40°S, located more than 4000 Km away from the coast.

Recently, Araujo *et al.* (2003) provided a statistical identification of distinct sea states and the seasonal variability using a one-year waverider time series off Santa Catarina Island (at 80 m depths) (January 2002 to January 2003). The results show a frequent bimodal sea-swell configuration (31% of 2 peaked spectra for the whole year) with a significant seasonal variation (43% in summer and 24% in winter). Sea and swell presented the following characteristics: (1) a well-defined 12s swell from the South with increasing significant heights from summer to winter, ranging from 1.25 m to 2 m; and (2) a 8s sea with an average significant height of 1.25 m from the East. Araujo *et al.* (2003) also reported that during autumn and winter swell conditions prevail over local seas and that in the summer there is a balance between these two states while in spring seas prevails over swells.

In summary, all authors cited above, that did visual observation and instrumented records of waves, as well as reported in the Ocean Waves Statistics (Hogben and Lumb, 1967), agree that the most energetic waves (swell) come from the south-southeast direction, and are generate during the cold front displacement over the sea.

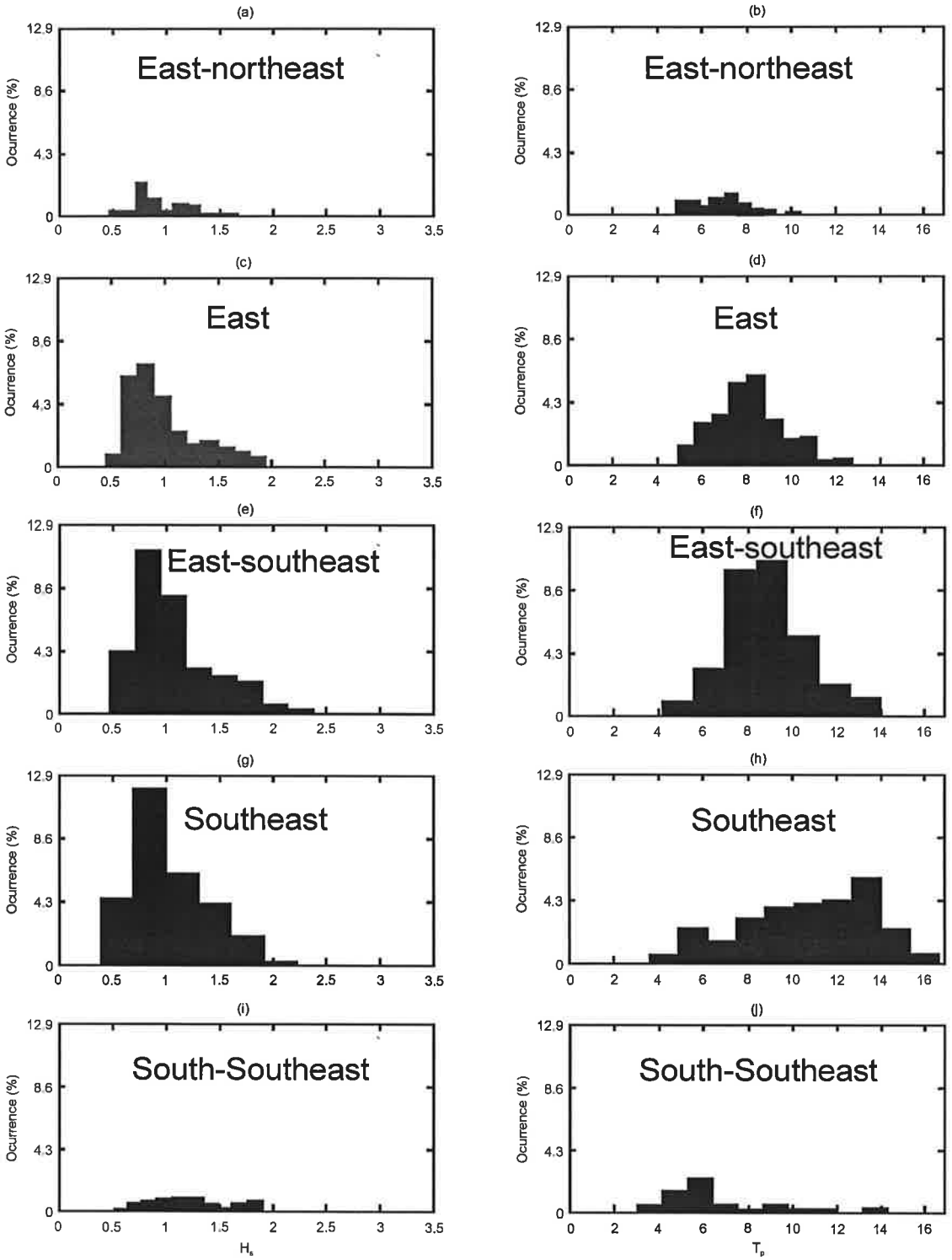

Figure 2.5. Santa Catarina significante wave heights (Hs) and peak periods (Tp) after Alves (1996). Hs is in meter, Tp is in second. Data obtained in front of São Francisco Island at 18 m deep. (a) and (b) – East-northeast direction; (c) and (d) – East-southeast direction; (e) and (f) – South-east direction; and (g) and (h) – South-southeast direction.

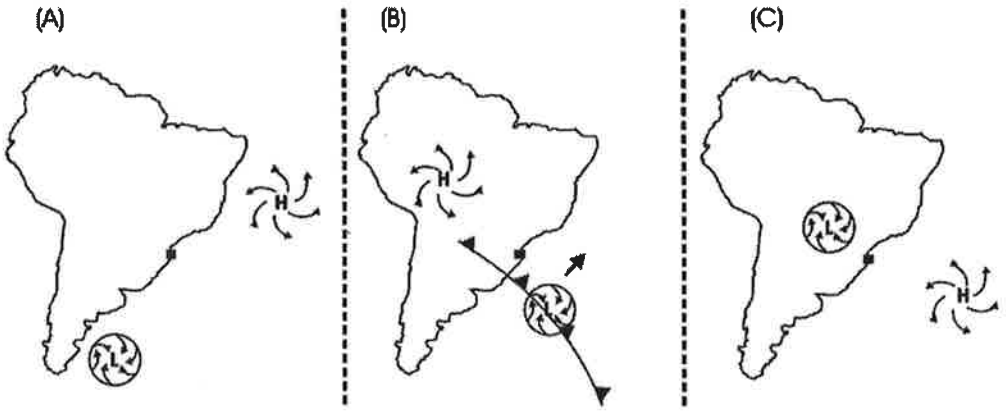

Figure 2.6. Interaction among large air masses formed by Atlantic semi-permanent anti-cyclones (high pressure) and the extratropical cyclones, associated with the passage of cold fronts (low pressure) that are responsible by the origin of the wave climate in Santa Catarina (according to Alves, 1996). (a) Northeast, (b) Southeast and (c) Easterly. H = high pressure, L = low pressure.

2.1.5. Surf Zone Currents and Sediment Transport

Studies about rip currents are very rare for Santa Catarina's beaches. Hoefel and Klein (1998a,b) reported the position of rip currents in three distinct beaches (Balneário Camboriú, Brava and Atalaia beaches) as a beach hazard. Klein *et al.* (*in press*) reported the number and the position of rip currents for Brava Beach (Summer, 2002) and Atalaia beach (Summer, 2003) as well as a beach hazard. Dafferner *et al.* (2002) reported for Brava beach a rip current average velocity of 0.35 m/s during low wave energy conditions (H_b< 1.0 m) experiment, using a floating body. They also reported that the number of rip current by Km is 5.

Longshore currents studies are also punctual in distinct beaches of Santa Catarina Island (e.g. Cruz, 1993, 1998; Abreu de Castilho, 1995; Santos, 1995; Leal, 1999), and were carried out with the use of floating objects. These authors reported velocities between 0.04 m/s and 1.01 m/s and most of data were collected during E-NE waves, resulting in a Southern current. However, the morphology of inlets and headland bay beaches are in agreement with wave climate and show that waves that

came from south-southeast are responsible for net littoral drift (to north) as reported by Muehe (1998).

2.1.6. Tides

The Santa Catarina coast is under a microtidal regime, according to Hayes (1979) classification. The tide is mixed, mainly semi-diurnal, presenting the form number $[(M_2 + S_2)/(O_1 + K_1)]$ varying from 0.77 to 0.32, and the mean spring tide height changing from 0.46 m to 1.06 m at Imbituba and Enseada, respectively. This variation can be explained because there is an amphidromic point for the main semi-diurnal lunar constituent M_2 close to Rio Grande City, *i.e.* 350 km southward from the southern board of Santa Catarina state, inducing a tidal height increase and a form number decrease from this point northwards (Garcia, 1996; Schettini, *in preparation;* see Figure 2.7).

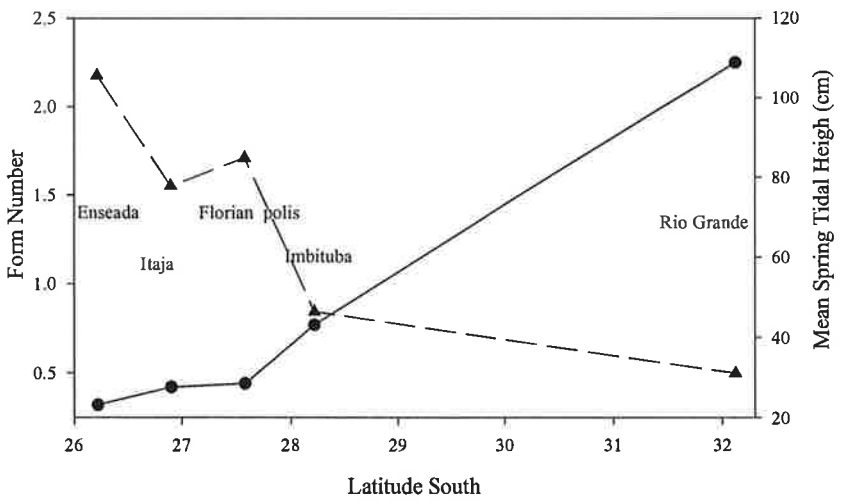

Figure 2.7. Form number $[(M_2 + S_2)/(O_1 + K_1)]$ and Mean Spring Tidal Height along Rio Grande do Sul and Santa Catarina Coast line (after Schettini, *in preparation*).

The meteorological influence on the sea level in southern Brazil is very important as mentioned by Schettini *et al.* (1996) and Carvalho *et al.* (1996). Truccolo

(1998) and Truccolo *et al.* (2002), in five months studies (July to December, 1996) of sea level, wind and atmospheric pressure hourly records at São Francisco Island, reported that storm surges could raise sea level to about one meter above the astronomical tide as a consequence of cold front displacement northward. Truccolo *et al.* (2002) also reported that: there is a time-lag between both atmospheric forcing and sea level changes; the maximum response of the coastal sea level was induced by local 12° N winds, which are long-shoreline oriented; the response of the sea level presented a 10 hour lag to the wind stress; the cross-shore wind effect was negligible, and the isostatic effect of the atmospheric pressure was not observed.

2.2. Summary

In summary, it is important to consider that there is a requirement of studies about sedimentary provenience and dispersion (*e.g.* mineralogy, geochemistry), the importance of solid river discharge (*i.e.* exportation of coarse and fine sediment to the coast, and the influence of dams and river sand mining in the total solid discharge), and the amount of littoral drift. Initial studies about waves and tidal behaviour were conducted, as well as about consequence of the effect of the El Niño-Southern Oscillation (ENSO) cycle of precipitation. Studies about the sedimentology of continental shelf were conducted in large-scale. Most of the studies are concentrated in the description of the climate (not the dynamic), geology and geomorphology of the rocks and costal plain system, respectively. Coastal plain and continental shelf stratigraphic is practically absent, but the coastal dunes stratigraphy was well studied, as well as the beach morphodynamic in Santa Catarina Island. In outline, there is a lack of basic environment information.

CHAPTER THREE

Planform of the Headland-Bay Beaches

Unless referred to otherwise, the contents of this thesis are the results of original research carried out by the author.

Some of the results have been published in:

KLEIN, A.H.F., ADRIANI JR, N., and MENEZES, J.T., 2002. Shoreline salients and tombolos on the Santa Catarina coast (Brazil): Description and analysis of the morphological relationships. *Journal of Coastal Research*, SI (36), 425-440.

KLEIN, A.H.F., BENEDET FILHO, L., and HSU, J.R.C., 2003. Stability of headland-bay beaches in Santa Catarina: a case study. *Journal of Coastal Research*, SI (35), 151-166.

KLEIN, A.H.F., VARGAS, A., RAABE, A.L.A., and HSU, J.R.C, 2003. Visual assessment of bayed beach stability using computer software. *Computer and Geosciences*, 29, 1249-1257.

3.1. INTRODUCTION

Santa Catarina state in southern of Brazil has countless headland-bay beaches, that are produced by the interaction between headlands and persistent swell heading onshore from the southern Atlantic Ocean, and locally generated winds (east and southeast swell). Headland-bay beaches may be fully exposed to waves, partially sheltered or fully protected by rocky headlands (Klein and Menezes, 2001; see Chapter 4). Due to this graceful curvature between stable anchor points, there are esthetically beautiful and often very stable beaches compared to rectilinear sand shores. Due to their beauty and stability, headland-bay beaches are recreation sites but vulnerable targets for development.

This chapter presents the results of a case study, where many headland-bay beaches were analyzed. The stability of the existing beaches is assessed by comparing their planforms with the prediction given by the parabolic bay shape equation (Hsu and Evans, 1989). The application of parabolic equation to define the existence of tombolos and salients is also presented. Finally, an example of parabolic equation application to man-made structure is presented, and an alternative and rough checking based on indentation ratio is examined.

3.2. PARABOLIC BAY SHAPE EQUATION

Distinct mathematical functions have been proposed since 1944 to curve-fitting the bay periphery of headland-bay beaches. These equations are *logarithmic spiral* (Krumbein, 1944; Yasso, 1965), *parabolic bay shape* (Hsu and Evans, 1989; Silvester and Hsu 1993, 1997), and *hyperbolic-tangent* (Moreno and Kraus, 1999; Martino *et al.*, 2003). These empirical equations have different coordinate systems, origins, and

controlling parameters related to wave direction and bay geometry (Klein *et al.*, 2003; Hsu *et al.*, *in preparation*). Wave heights and periods were found to be insignificant and are not included in the formulations (Hsu and Evans, 1989).

Hsu and Evans (1989) developed a second-order polynomial equation, *i.e.* a parabolic equation, from fitting the planform of 27 mixed cases of prototype and model bays believed to be in *static equilibrium*:

$$\frac{R_n}{R_\beta} = C_o + C_1\left(\frac{\beta}{\theta_n}\right) + C_2\left(\frac{\beta}{\theta_n}\right)^2 \tag{3.1}$$

Where R_β is *control line length* and β is reference *wave obliquity* or that between the incident wave crest (assumed linear) and the *control line*, joining the upcoast *diffraction point* (X_o, Y_o) to a point on the near straight downcoast beach (*end point*- X_1, Y_1 - Figure 3.1). This is how it is determined from maps, vertical aerial photograph and satellite images (*e.g.* IKONOS) for verification or sketches design. The *control line* length R_β is also angled β to the tangent at the downcoast beach end. The radius R_n to any point on the bay periphery in static equilibrium is angle θ_n from the same wave crest line radiating out from the point of wave diffraction upcoast (Hsu and Evans, 1989).

The three C constants, generated by regression analysis to fit the peripheries of the 27 prototypes and model bays, differ with reference angle β (Hsu and Evans, 1989). Numerically, these coefficients may be expressed by forth-order polynomials as follows:

$$C_o = 0.0707 - 0.0047\beta + 0.000349\beta^2 - 0.00000875\beta^3 + 0.00000004765\beta^4 \tag{3.2}$$

$$C_1 = 0.9536 + 0.0078\beta - 0.00004879\beta^2 + 0.0000182\beta^3 - 0.000001281\beta^4 \tag{3.3}$$

$$C_2 = 0.0214 - 0.0078\beta + 0.0003004\beta^2 - 0.00001183\beta^3 + 0.0000000\beta^4 \qquad (3.4)$$

These C values are bounded within 2.5 and –1.0 for the usual range of angle β from 10° to 80° applicable in most field conditions (Silvester and Hsu, 1993, 1997). Values of non-dimensional ratios R_n/R_β versus increments of 2° of β from 20° to 80° have been tabulated for manual application by Silvester and Hsu (1993, 1997; Table 3.1).

For a bay beach with a given set of β and R_β, locations for pairs of R_n and θ_n can be marked on the existing waterline, and a curve sketched for the static bay shape prediction. The nearness of the existing beach planform to the static equilibrium shape can then be verified. If the predicted curve is landward of the existing beach, the headland bay beach is said to be in *dynamic equilibrium*, or it may be *unstable*, because the shoreline may degrade or protrude as sand supply decreases or increases. For headland-bay beaches in static equilibrium, the wave orthogonal at the downcoast limit of the bay is assumed to be perpendicular to the downcoast tangent and the first wave crest line starting at the point of wave diffraction (see Figure 3.1). Under this condition, it may be assumed that:

- No further sediment is being added or eroded from the bay, under the persistent swell condition;
- Waves break simultaneously around the bay periphery;
- Littoral drift or longshore currents are almost non-existent.

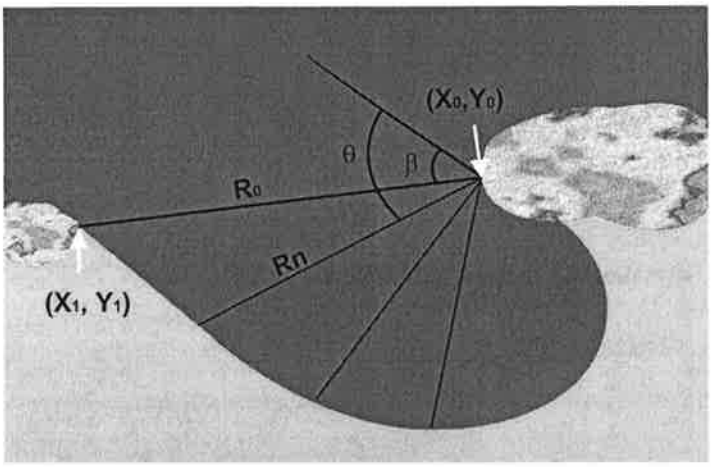

Figure 3.1. Definition sketch of the parabolic model given by Hsu and Evans (1989). R_β is *control line* length; β is wave oblique; R_n is radius to any point on the bay periphery in static equilibrium with a angle θ_n.

Table 3.1. Radii ratios R/R_β for a range of β and θ (see definition plan, Figure 3.1.) (after Silvester and Hsu, 1993, 1997).

	Coefficients for Eq 1.			Values of R_n/R_β for θ_n =							
β	C_0	C_1	C_2	30	45	60	75	90	120	150	180
20	0.054	1.040	-0.094	0.705	0.497	0.390	0.324	0.280	0.225	0.191	0.168
22	0.054	1.053	-0.109	0.768	0.543	0.426	0.354	0.305	0.244	0.206	0.181
24	0.054	1.069	-0.125	0.829	0.588	0.461	0.383	0.330	0.263	0.222	0.194
26	0.052	1.088	-0.144	0.887	0.633	0.497	0.412	0.355	0.281	0.237	0.207
28	0.050	1.110	-0.164	0.944	0.677	0.532	0.442	0.379	0.300	0.251	0.219
30	0.046	1.136	-0.186	1.000	0.721	0.568	0.471	0.404	0.319	0.266	0.230
32	0.041	1.166	-0.210		0.763	0.603	0.500	0.429	0.337	0.280	0.242
34	0.034	1.199	-0.237		0.805	0.638	0.529	0.453	0.355	0.294	0.252
36	0.026	1.236	-0.265		0.845	0.672	0.558	0.478	0.373	0.307	0.262
38	0.015	1.277	-0.296		0.883	0.706	0.586	0.502	0.390	0.320	0.272
40	0.003	1.322	-0.328		0.919	0.739	0.615	0.526	0.407	0.332	0.281
42	-0.011	1.370	-0.362		0.953	0.771	0.643	0.550	0.424	0.344	0.289
44	-0.027	1.422	-0.398		0.983	0.802	0.670	0.573	0.441	0.356	0.297
46	-0.045	1.478	-0.435			0.832	0.698	0.596	0.457	0.367	0.304
48	-0.066	1.537	-0.473			0.861	0.724	0.619	0.473	0.378	0.311
50	-0.088	1.598	-0.512			0.888	0.750	0.642	0.489	0.388	0.317
52	-0.112	1.662	-0.552			0.914	0.775	0.664	0.505	0.398	0.322
54	-0.138	1.729	-0.592			0.938	0.800	0.686	0.520	0.408	0.327
56	-0.166	1.797	-0.632			0.960	0.823	0.707	0.535	0.417	0.332
58	-0.196	1.866	-0.671			0.981	0.846	0.728	0.549	0.425	0.336
60	-0.227	1.936	-0.710			1.000	0.867	0.748	0.563	0.434	0.339
62	-0.260	2.006	-0.746				0.888	0.768	0.577	0.441	0.342
64	-0.295	2.076	-0.781				0.908	0.787	0.590	0.449	0.345
66	-0.331	2.145	-0.813				0.927	0.805	0.603	0.456	0.346
68	-0.368	2.212	-0.842				0.945	0.823	0.615	0.462	0.348
70	-0.405	2.276	-0.867				0.963	0.840	0.627	0.468	0.349
72	-0.444	2.336	-0.888				0.981	0.857	0.638	0.473	0.349
74	-0.483	2.393	-0.903				1.000	0.874	0.649	0.478	0.348
76	-0.522	2.444	-0.912					0.891	0.660	0.482	0.347
78	-0.561	2.489	-0.915					0.909	0.670	0.486	0.346
80	-0.600	2.526	-0.910					0.927	0.680	0.489	0.343

3.2.1. Why Use Parabolic Bay Shape Equation?

Krumbein (1944) and Yassos (1965) introduced the *logarithmic spiral equation* ($r_2 = r_1 \exp(\theta \cot \alpha)$ to fitting bay periphery of Half-Moon Bay, California, United States and four natural headland-bay beaches on the east and west coasts of US, respectively. The r_1 and r_2 states the relationship between two consecutive radii from the center of a logarithmic spiral at angle θ apart on the curve, which has a constant outer tangent α (see Figure 3.2).

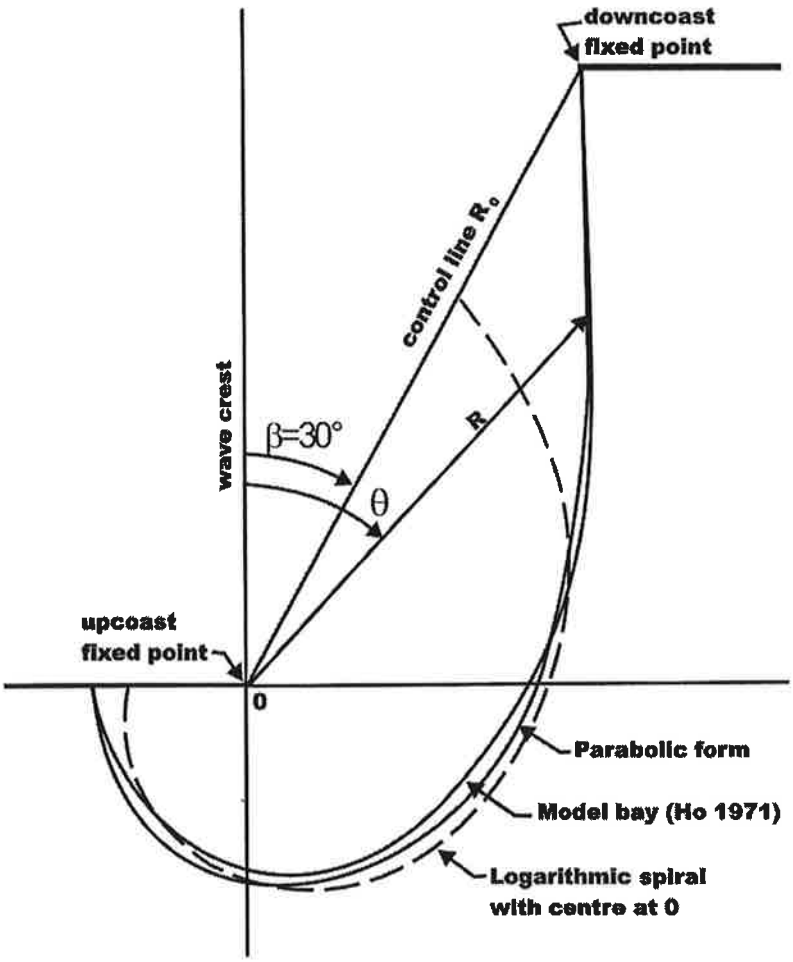

Figure 3.2. Comparison of parabolic and log-spiral equations for β=30° (Hsu and Silvester, 1996; Silvester and Hsu, 1997 - pg 223).

Hsu *et al.* (*in preparation*) in their review reported that: (1) in the four cases presented by Yasso (1965), there are offsets between the center of the spiral and the point of wave diffraction ranged from 0.3 to 2000 m; (2) despite the failure of the logarithmic spiral to mach the relatively straight section of the curved periphery and even the curved part of the bay, if the point of diffraction was used as the center of the spiral, the equation can fit the curved part of the bay in Silvester's work (Silvester, 1970); and (3) since these publications, many coastal researches have misconception in referring all curved beaches as spiral beaches.

The *hyperbolic-tangent shape equation* ($y = \pm a \tanh^m(bx)$) was presented recently by Moreno and Kraus (1999) and Martino *et al.* (2003) fitting 46 beaches in Spain and north America. A relative coordinate system should be established such that the x-axis is parallel to the general trend of the shoreline with the y-axis point onshore. The relative origin of coordinates should be placed at a point where the local tangent to the beach is perpendicular to the general trend of the shoreline (Figure 3.3).

Hsu *et al* (*in preparation*) reported that: (1) this equation fits the geometrical shape of any bay beach, regardless whether it may be in static or dynamic equilibrium, without the input of wave direction and the wave diffraction point, *i.e* it is purely geometrical and without the physical insight of wave action; (2) consequently it would not be possible to predict the environmental impact as the diffraction point changes from its original location by for example the introduction of a man-made structure to the beach; (3) Moreno and Kraus (1999) agree that both equations give similar result to fit bay periphery, but they do not consider the wave action around the bay, and this is a misinterpretation of the basic concepts behind the development of the parabolic equation that was originally developed for bay beaches in static equilibrium, but not for

all the beaches on the earth; and (4) Martino *et al.* (2003) committed a mistake when adopting a incorrect procedure to apply the parabolic equation to compare with the hyperbolic equation. These authors used the diffraction point in the middle of the ocean or in the middle of the shoreline which was never the case proposed by Hsu and Evans (1989).

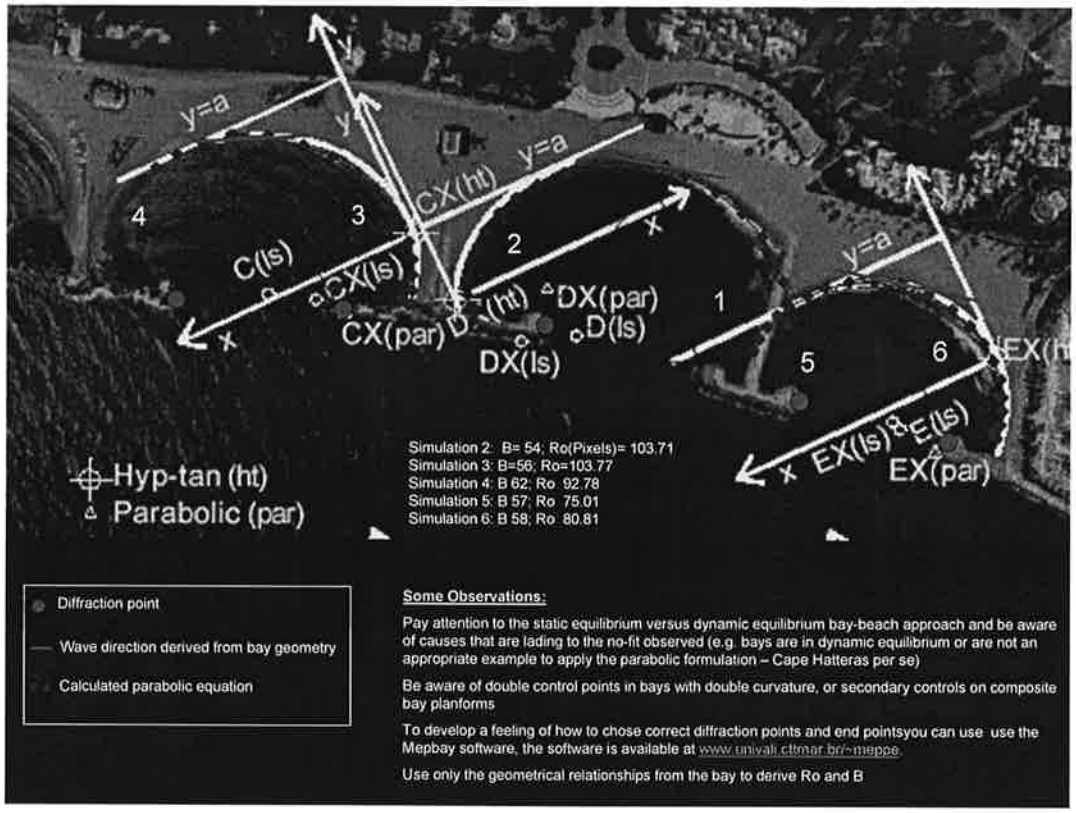

Figure 3.3. Comparison of parabolic and hyperbolic-tangent equations applied to example of Martino *et al.* (2003; after Hsu et al., *in preparation*).

For the parabolic equation, the physical location at the point of wave diffraction is used as the center of the coordinates system (see Figure 3.2). Consequently, the effect of relocating the point of diffraction, by various engineering means, can be assessed. Despite these two methods, *logarithmic spiral and hyperbolic-tangent*, may fit the

periphery of any bay, their stability cannot be determined. Since parabolic bay shape equation inception in 1989 (Hsu and Evans, 1989), it has taken more than a decade for the equation to gain positive recognition by the coastal community (Hsu *et al., in preparation*), and this was culminated with the Silvester and Hsu's books (Silvester and Hsu ,1993, 1997) that have produced necessary verification on parabolic bay shape equation and, with four scientific papers on this theme being delivered at an international conference and journals in 1999/2001 (Hardaway and Gunn, 1999; Gonzales and Medina, 1999, 2001; Moreno and Kraus, 1999; and Weesakul, 1999) A range of other applications of headland control can be found in the literature (Hsu and Silvester, 1990; Hsu *et al.*, 1993; Silvester and Hsu, 1993, 1997; Tan and Chiew, 1994; Hsu and Silvester, 1996; Hsu *et al.*, 2000; Smith *et al.*, 2000; Oliveira *et al.*, 2000; Dean and Maurmeyer, 1977; Dean and Dalrymple, 2002; Papps and Priestley, 2003; Klein *et al.*, 2003a,b). The parabolic bay shape equation has been cited in the books of Carter (1988), Komar (1976, 1998), van Rijn (1998), Short (1999). Recently it has been recommended in the *Coastal Engineering Manual* (CERC, 2002) for project management and coastal process.

Some technicality arose while applying the parabolic bay shape equation, for example, on the location of both the upcoast and downcoast control points, and the downcoast tangent. Occasionally, it may be difficult to define the diffraction point (*i.e*, the upcoast control point) from an aerial photograph, especially when the tip of diffraction point is hidden (submerged) or with extensive shallow region in the lee of the compared headland. The determination of the wave crest line, defined to be in the same orientation as the tangent at downcoast, is another issue affecting the accuracy of the prediction. With some experience, a smooth waterline can be drawn from the

irregular shoreline, caused by the existence of an offshore shoal or irregularity in bottom bathymetry. The definition of downcoast point (end point) was well discussed and solved by Tan and Chiew (1994) and Gonzales and Medina (1999). However, in general way when increasing or decreasing R_β, decreasing or increasing β, consequently there is a compensation in the ratios R_n/R_β and β/θ_n. Therefore, this equation is preferred over the log-spiral and hyperbolic-tangent mentioned above.

3.3. PARABOLIC EQUATION APPLIED TO FIT TOMBOLOS AND SALIENTS

Hsu and Silvester (1990) modified the parabolic model to analyse areas close to obstacles (*e.g.* offshore rock outcrops, islands and offshore breakwaters), with accumulated sediments on the coastline, in the form of salient or tombolos. These features are similar to that found on planform of bay beaches, in terms of the static equilibrium. That is to say, if the wave crests reach the obstacle in a parallel way, β change between 30° and 40° (see Figure 3.4).

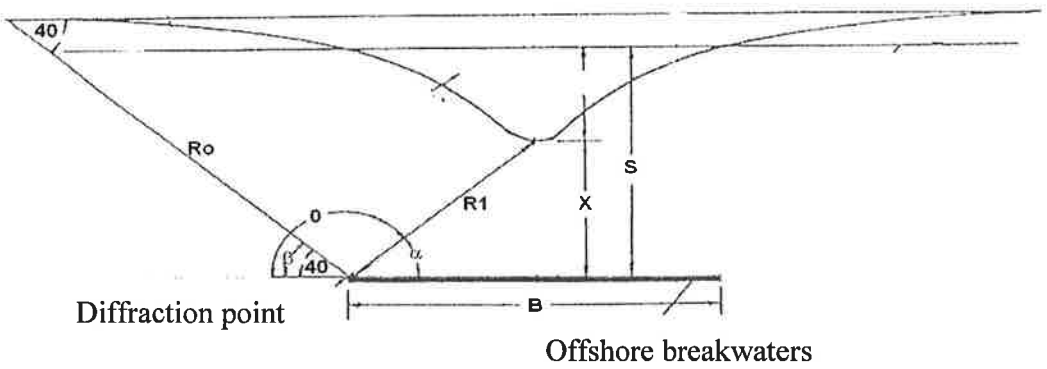

Figure 3.4. Definition of variables for the Hsu and Silvester (1990) model, based on polar coordinates. B = length of obstacle; X = distance from obstacle to apex of salients, J = length of salients; S = distance between obstacle and root of salients (S = X+J); β = α = wave obliquity (30° - 40°); R_β = control line length; R_1= length between diffraction point and apex of salients.

3.4. INDENTATION RATIO

Silvester and co-workers (*e.g.* Silvester, 1970, 1974; Silvester and Ho, 1972) had advanced the application of the reference wave obliquity angle β and the identation ratio (a/R_β) of the bay beach. Everts (1983) has attempted indentation ratio rather than shoreline shape to investigate shoreline denudation over time once littoral drift has been intercepted. Silvester and Hsu (1993, 1997) have also indicated that: "Sometimes it is not essential to derive the actual static equilibrium shape to prove instability of an existing b ayed c oast. A n a lternative m ethod that is swifter to apply could be what is termed the *indentation ratio*." As seen in Figure 3.5, the greatest indentation (a) is measured normal from the *control line* to the point of largest retreat of the shoreline. This is obtained by drawing a tangent parallel to the control line, which is asymptotic to the downcoast beach. Although the indentation ratio (a/R_β) can be used as a secondary check for the stability of the bay, scattering was found in displaying a/R_β versus reference wave obliquity β (Silvester and Hsu, 1993). In Figure 3.5, the dashed line indicates static equilibrium conditions (Silvester and Hsu, 1993, 1997).

3.5. SAMPLING AND ANALYSES

A total of ninety (90) headland-bay beaches including fitting of beaches in the lee of offshore islands, as well as man-made beaches, were chosen for this study. Each headland bay beach was analyzed using the parabolic bay shape equation of Hsu and Evans (1989), from which its stability was classified into one of the categories of *static equilibrium*, *close to static equilibrium* and *dynamic equilibrium*. The indentation ratio (a/R_β) for all bays was also determined.

The study area covers the coastline of Santa Catarina state between 26°30' S and 28°40' S, From São Francisco Island to Santa Marta Cape (Figure 3.6.). To facilitate the analysis, the study area, *i.e* the sector defined in Figure 2.1 is divided into three areas: (1) northern area between São Francisco Island and Tijucas Bay; (2) central sector is represented by Florianópolis Island; and (3) southern area, from Pinheira Bay to Santa Marta Cape.

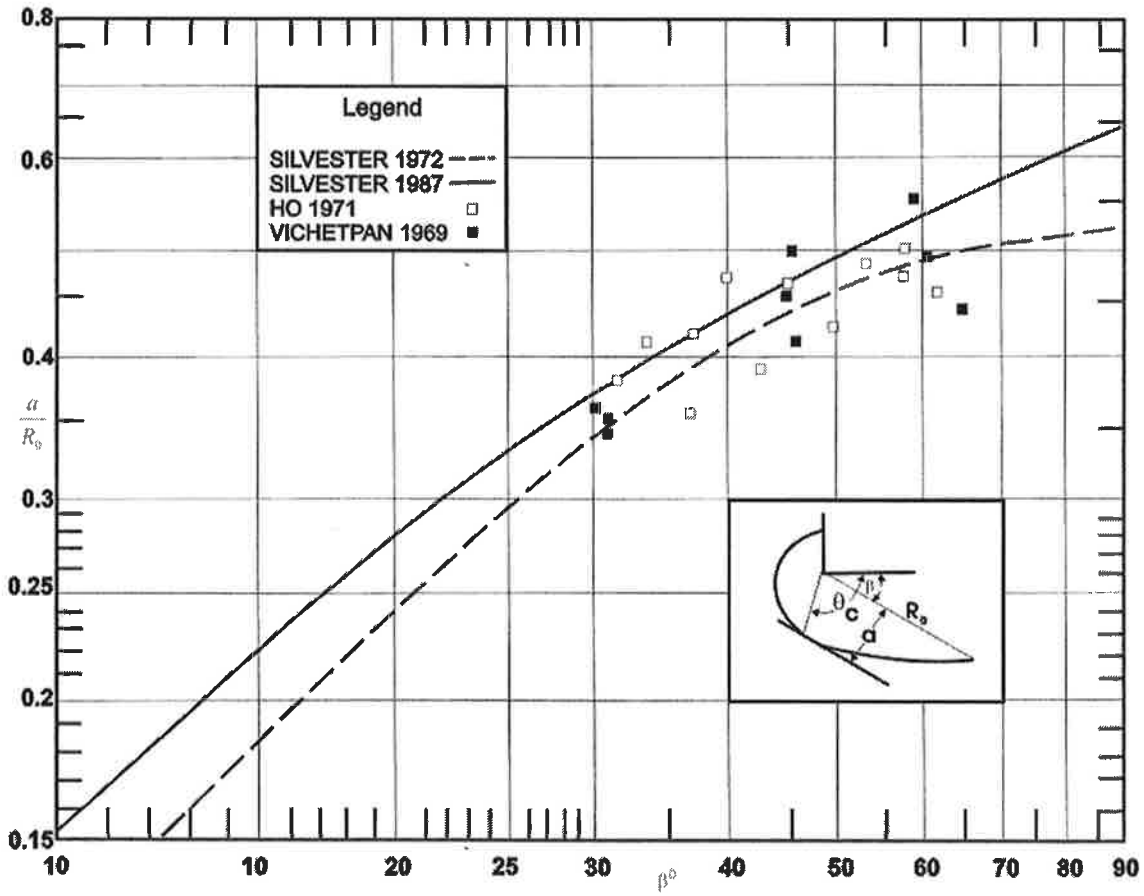

Figure 3.5. Relationship between indentation ration and (a/R_β) and the wave obliquity (β). The dashed line indicates static equilibrium conditions after Silvester and Hsu (1993, 1997). Definition of maximum indentation a and angle θ_c at maximum indentation (after Silvester and Hsu, 1993, pg 230).

3.5.1. Sampling of Headland Bay Data

Geomorphic parameters of the bay beaches in Santa Catarina were extracted from aerial photographs, maps, or nautical charts. Working procedure included: (1) the *control line* with length R_β is obtained by joining the point of diffraction (the upcoast control point) and a point on the downcoast limit of the bay, usually at the beginning of the straight section; (2) a straight-line tangent to the downcoast shoreline was drawn from this point downcoast; (3) the reference angle β is determined by the angle between the control line and the downcoast tangent, which is assumed to be parallel to the first wave crest line meeting the point of diffraction; (4) the radii R_n for a range of θ_n could be calculated or simply read from Table 3.1., once the two basic parameters of R_β and β are available; (5), finally, a curve representing the bay shape in static equilibrium was sketched and compared on the aerial photographs or maps, and its stability assessed by the difference; (6), additionally, the maximum indentation (a) is obtained as proposed in Figure 3.5. To facilitate the application of parabolic equation, MEPBAY software was developed (see Appendix I).

To determine beach stability, the following rules are applicable as proposed by Hsu and Evans (1989) and Silvester and Hsu (1993, 1997). For example, if the sketched curve is landward of the existing waterline, the headland bay beach under consideration is in *dynamic equilibrium*. The beach may be considered as *unstable*, implying the shoreline will recede when sediment supply is reduced (by river dam or littoral drift). It may even erode back to the planform predicted by the static bay shape equation, should sediment supply cease altogether. On the other hand, if the existing headland bay shape coincides with model predictions, the bay is in *static equilibrium* or *stable.* When the former curve is in the close proximity of the latter, it is classified as *close to static*

equilibrium. The approach is more qualitative (*perception and background*) than quantitative.

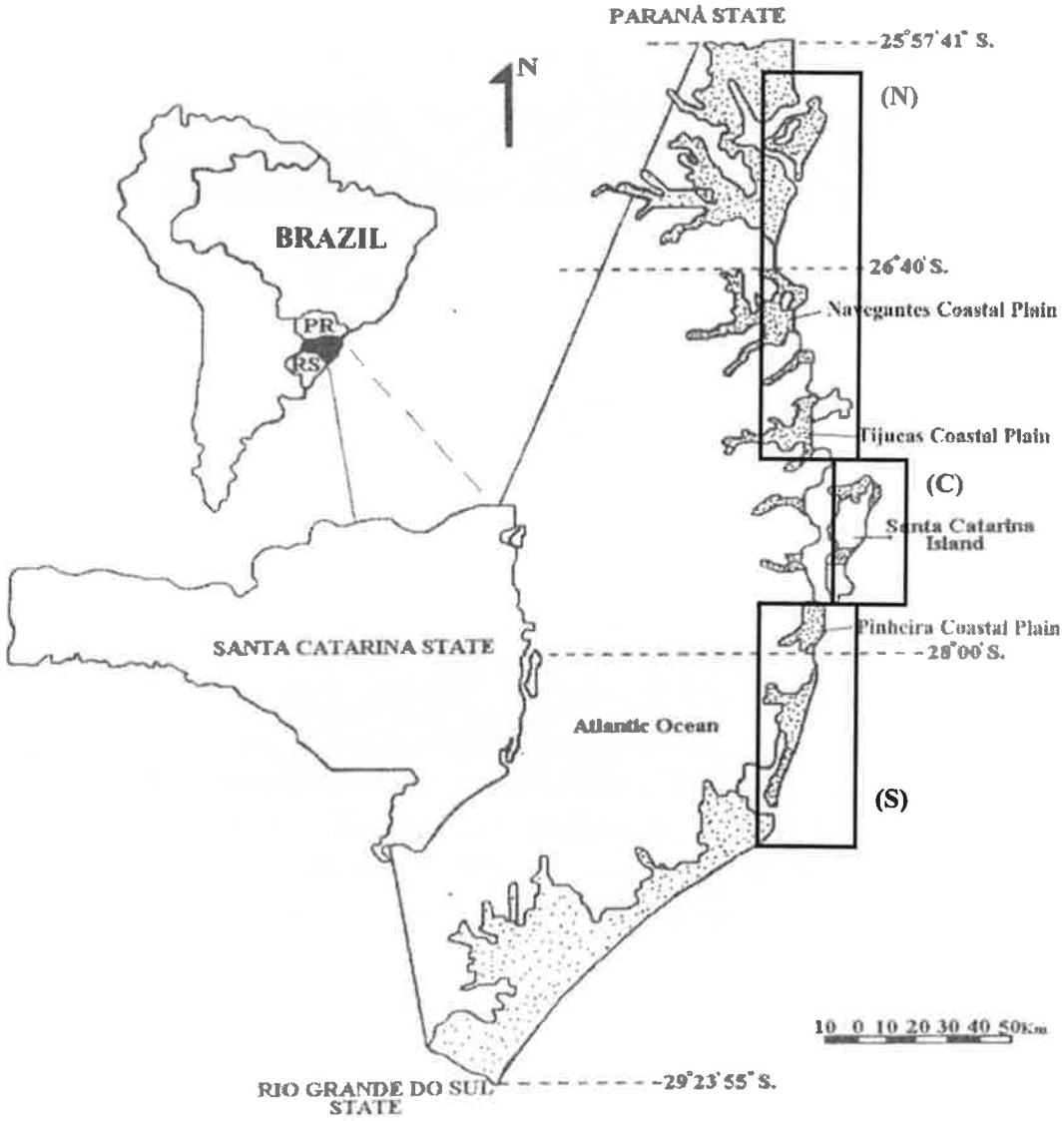

Figure 3.6. Santa Catarina coastline showing three sections of the study area - (N) north, (C) center and (S) south.

3.6. RESULTS

The data showed here is geographically organized from north to south. Aerial photographs used were on 1:12,500 scales to northern sector and, 1:25,000 scales to Florianópolis Island and southern sector. Table 1, 2 and 3 (Appendix II) presents the results of the application of Equation 3.1. Some beaches have double curvature so the simulations were done in both extremities of the beach and are indicated in parentheses as north headland simulations and south headland simulations. In some of the beaches there were also verified double control points and they are indicated in the parentheses as south end controlled by an inner control point, and whole beach, which is controlled by an outer control point. Some of the beaches have control points that shape their curvature on offshore islands; this is also indicated in the parentheses as island control.

3.6.1. Results for all Analyzed Beaches

The overall results are depicted graphically in Figures 3.7. – 3.9. Overall, as shown in Table 3.2, 19% of the analyzed beaches are in static equilibrium, 37% in dynamic equilibrium, and 44% close to static equilibrium. It is also worth noting that there is no regional difference in each category of static, dynamic, and close to static conditions in these three sectors (Table 3.3).

3.6.2. Headland Bay Beaches in Static Equilibrium

Headland bay beaches in static equilibrium have been found at various beach morphodynamic stages and for different bay orientations. For example, Taquaras/Taquarinhas and Flamingo Beaches (Figure 3.10.) on the central north coast

are classified as reflective (*e.g.* Klein and Menezes, 2001, see Chapter 4), Garopaba Beach (central point) and Itapema beach (northern sector) as dissipative (Figure 3.11), and Pantano do Sul Beach as dissipative to intermediate (Figure 3.12). These results, avoid the state of beach stability, based on the parabolic bay shape equation, is independent of other beach classifications, such as morphodynamic stages and beach orientations.

As shown in Figure 3.11, Garopaba Beach (central point) shows an interesting feature, a second (inner) control point, as well as Itapema Beach (see Figure 3.11), never before recognized in the study of bay shape stability. The static equilibrium bay shape has an outer control point that provides almost the entire bay periphery. But, static equilibrium bay shape has also a second (inner) control point that shapes the remaining shoreline further in the curved portion of the bay. This is a result of progressive wave diffraction due to an irregular headland.

Table 3.2. Classification of beach stability versus study sectors, showing the number of beaches in each sector.

	Static	Close to Static	Dynamic	Total
Overall	17	39	34	90
Sector 1	9	18	16	43
Sector 2	3	7	5	15
Sector 3	5	14	13	32

Table 3.3. Percentage of occurrence in the state of beach stability within each sector.

	% Static	% Close to Static	% Dynamic	Mean
Sector 1	21	42	37	19
Sector 2	20	47	33	44
Sector 3	15	45	40	37

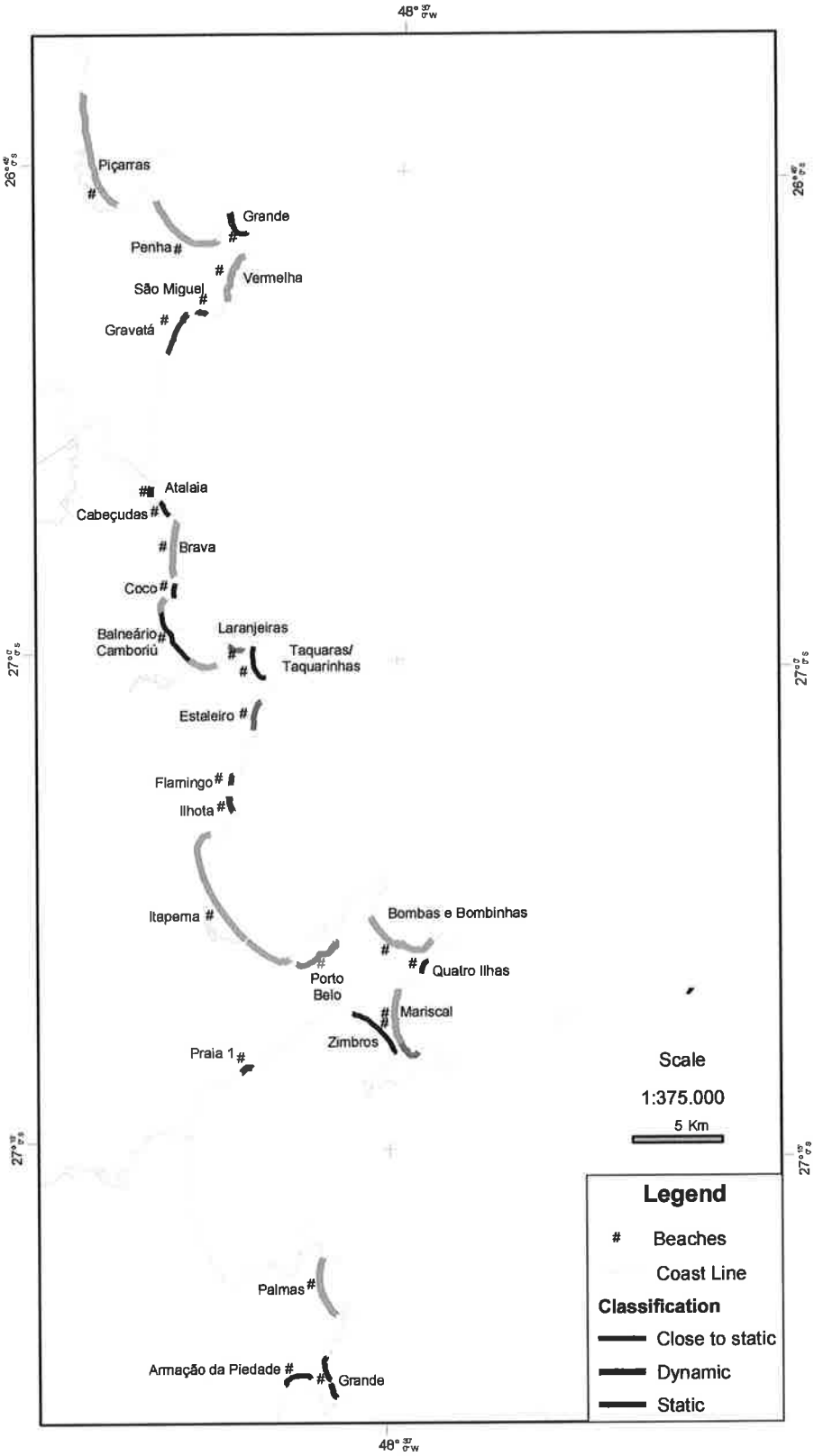

Figure 3.7. Stability of bay beaches in sector 1, the northern coast of Santa Catarina.

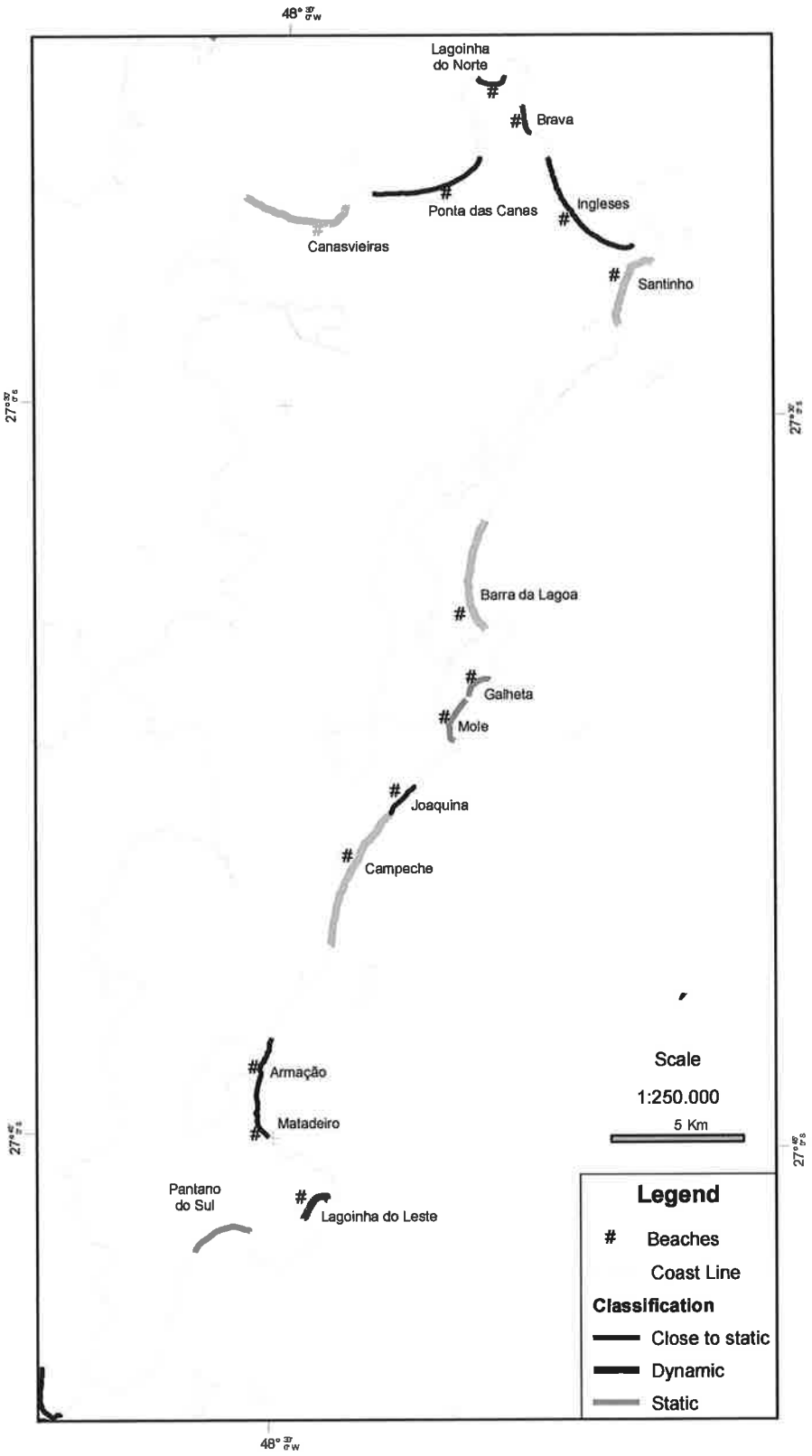

Figure 3.8. Stability of bay beaches in sector 2, in Florianópolis Island and central Santa Catarina coast.

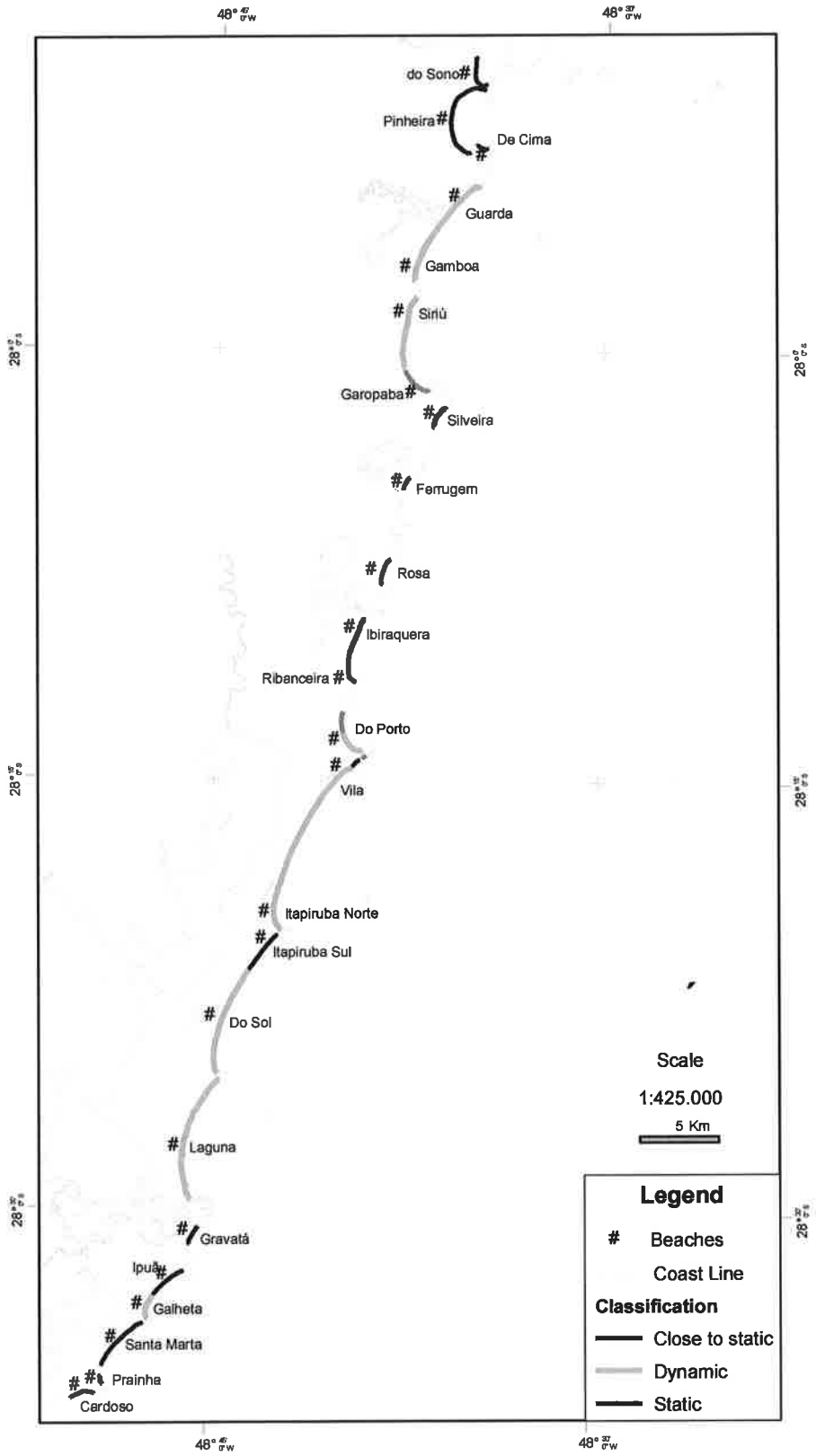

Figure 3.9. Stability of bay beaches in sector 3, in the southern coast of Santa Catarina.

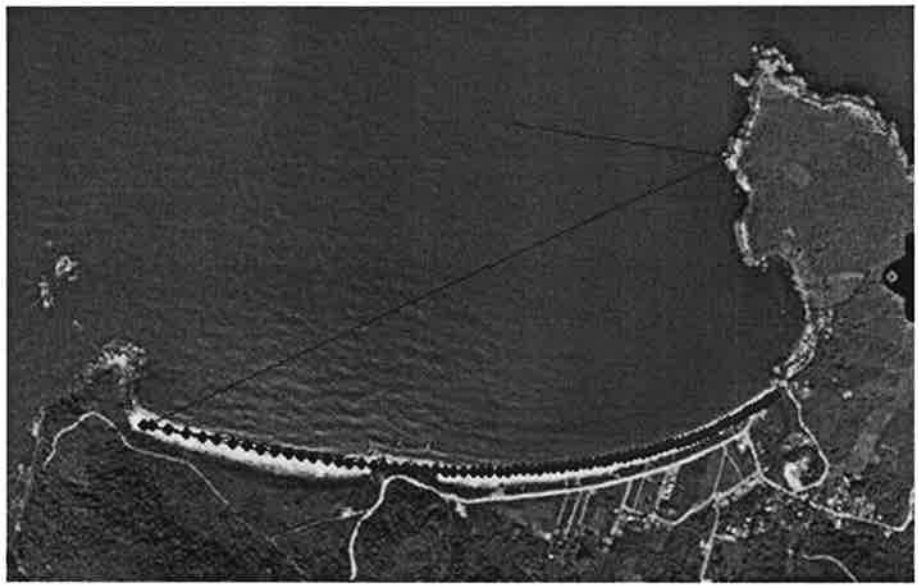

a)

b)

Figure 3.10. Parabolic bay shape equation fit for **(a)** Taquaras/Taqurinhas Beach (β = 34°) and **(b)** Flamingo Beach (up coast; β = 33°), a reflective exposed beach. Black dots = planform.

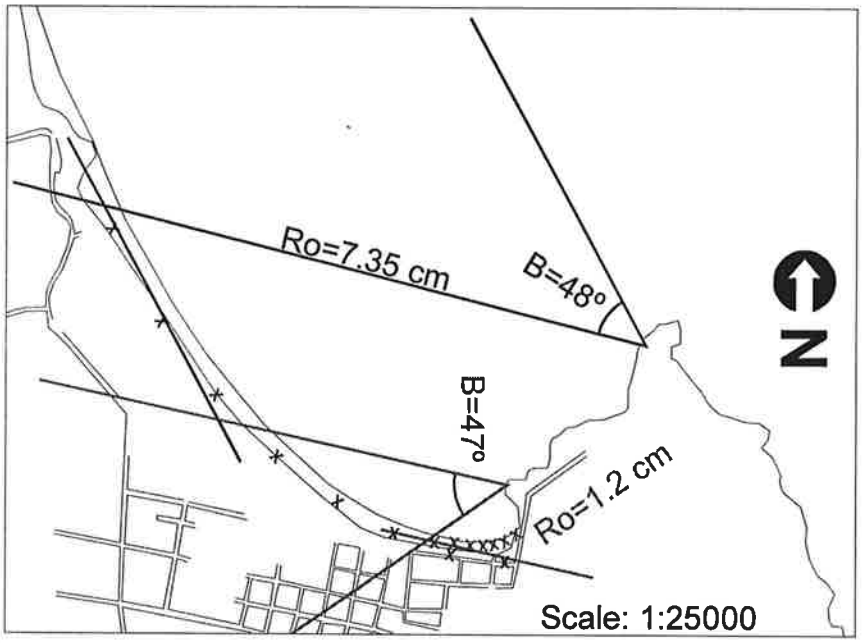

a)

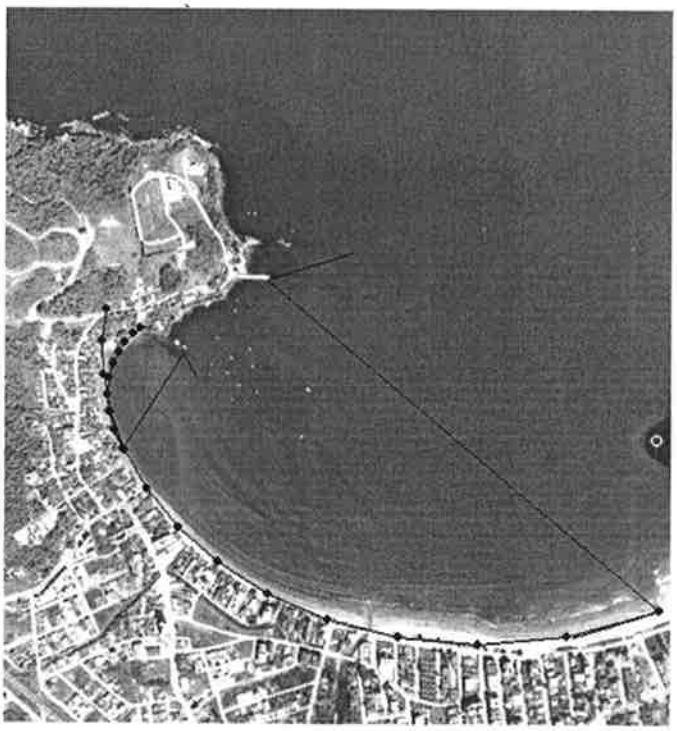

b)

Figure 3.11. (a) Stability of Garopaba Beach (central point), the shape of the curve predicted by the model compared to the measured shoreline configurations indicates the static equilibrium stage of this beach. There are two visible control points, the outer control point, and the inner control point. **(b)** Bay beach with primary and secondary diffraction points (Itapema Beach).

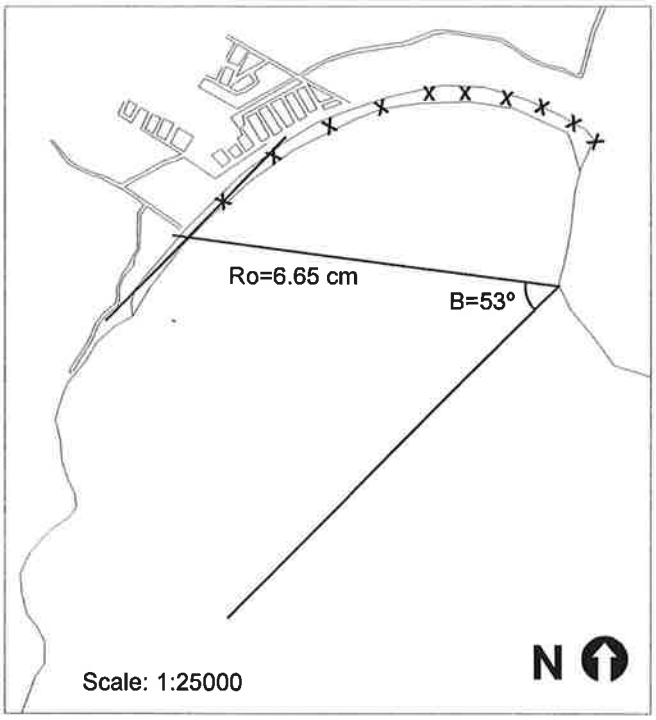

Figure 3.12. Static bay shape for Pantano do Sul beach, an intermediate beach.

3.6.3. Headland Bay Beaches in Dynamic Equilibrium

An example of headland bay beach in dynamic equilibrium is the southern end of Balneário Camboriú Beach (Figure 3.13). The dynamic equilibrium of southern end of Balneário Camboriú Beach can be an influence of river sediment input, which is responsible for maintaining the shoreline position in the past. In the year 1950, the Camboriú River was dammed for water supply, this certainly reduced sediment supply to the beach, thus causing coastal erosion (Abreu *et al.*, 2003). The landward limit of erosion in this case may be estimated by the parabolic bay shape equation, which simulates the planform of a bay in static equilibrium, under the condition of null sediment supply to the beach.

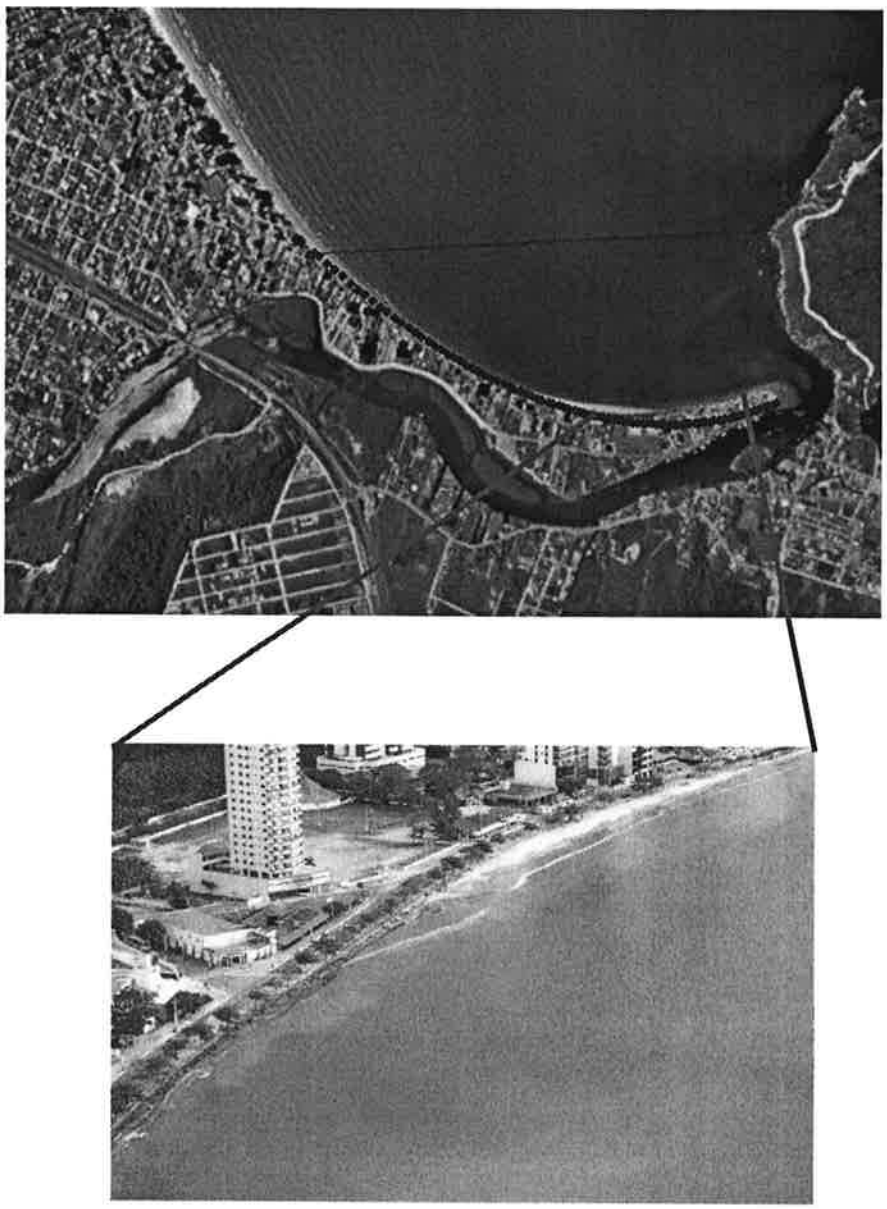

(a)

(b)

Figure 3.13. **(a)** Parabolic bay shape for the southern end of Balneario Camboriu Beach. Black dots indicate the planform of the bay in static equilibrium, $\beta = 40°$. Original scale 1:12,500; **(b)** Overview of erosion problems and beach nourishment project to mitigate the erosion.

Another example of dynamic equilibrium is Piçarras Beach (Figure 3.14). The beach shoreline in this case is landward of its static equilibrium. Recently (summer of 1998/1999) a beach nourishment project was developed at this beach.

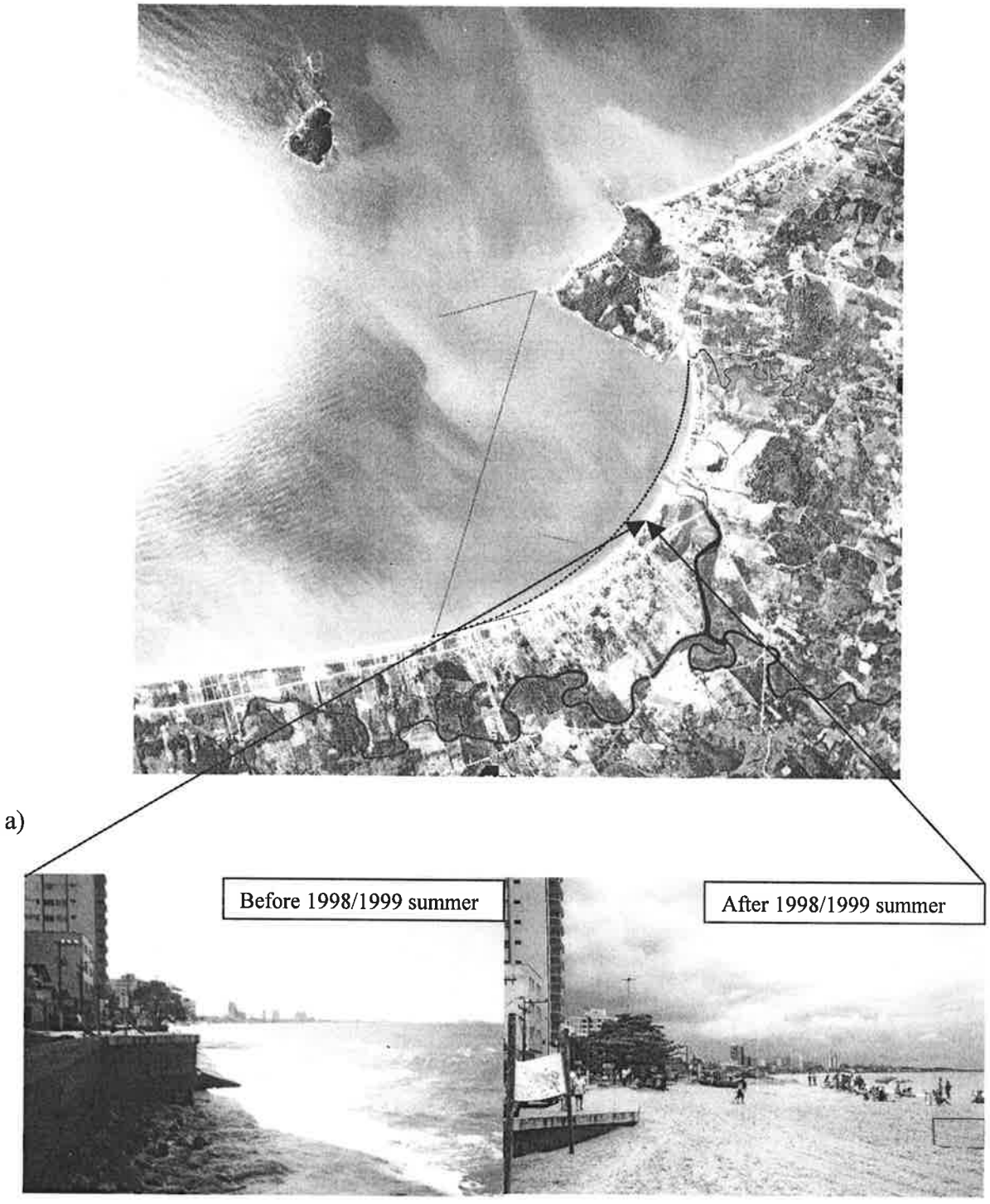

Figure 3.14. **(a)** Parabolic bay shape for Piçarras Beach (β = 58°); **(b)** Overview of erosion problem and beach nourishment project developed in the summer 1998/1999.

Other examples of dynamic equilibrium are Pontas das Canas and Canasvieiras Beaches in Santa Catarina Island (Figure 3.15). The beach shorelines in these cases are seaward of its static equilibrium (southern sector). This may be due to sediment supply bypassed across the headlands. Diehl (1997) reported an increase of Daniela Spit as a result of a net littoral drift from exposed beaches of Santa Catarina Island (east coast) to a protected beach inside the North Bay (northwest coast). In figure 3.15 it is also possible to observe a spit development in Ponta das Canas.

Natural headland bypassing of sediment occurred in many bay beaches in Santa Catarina, especially in southern areas (sectors 1 and 2) where there is sediment exchange between bay beaches (see Figures 3.8 and 3.9), due to continuity of sediment path under the action of the prevailing swell from SE. However, in sector 1 (see Figure 3.7.) in the northern part of the Santa Catarina coastline this phenomena of headland bypassing is absent, because neighboring beaches presenting contrasting sediment characteristics (Klein *et al.*, 2003, see Chapter 6).

3.6.4. Headland Bay Beaches Close to Static Equilibrium

Headland bay beaches in Santa Catarina are also identified as *close to static equilibrium* because their planforms almost perfectly match the parabolic bay shape, as defined by Equation 3.1. However, upon further verification using aerial footages and field trips, it shows that these bays have characteristics of dynamic equilibrium bays, such as sediment supply from rivers, existence of longshore sediment transport, and natural headland sand bypassing. As seen in Figure 3.16, Ingleses Beach is an example of close to static equilibrium. Nowadays, the sediment budget at this beach is negative

since the aeolian headland sand bypass has been partially interrupted by the urbanization, and the available beach sediment is being reworked by the waves.

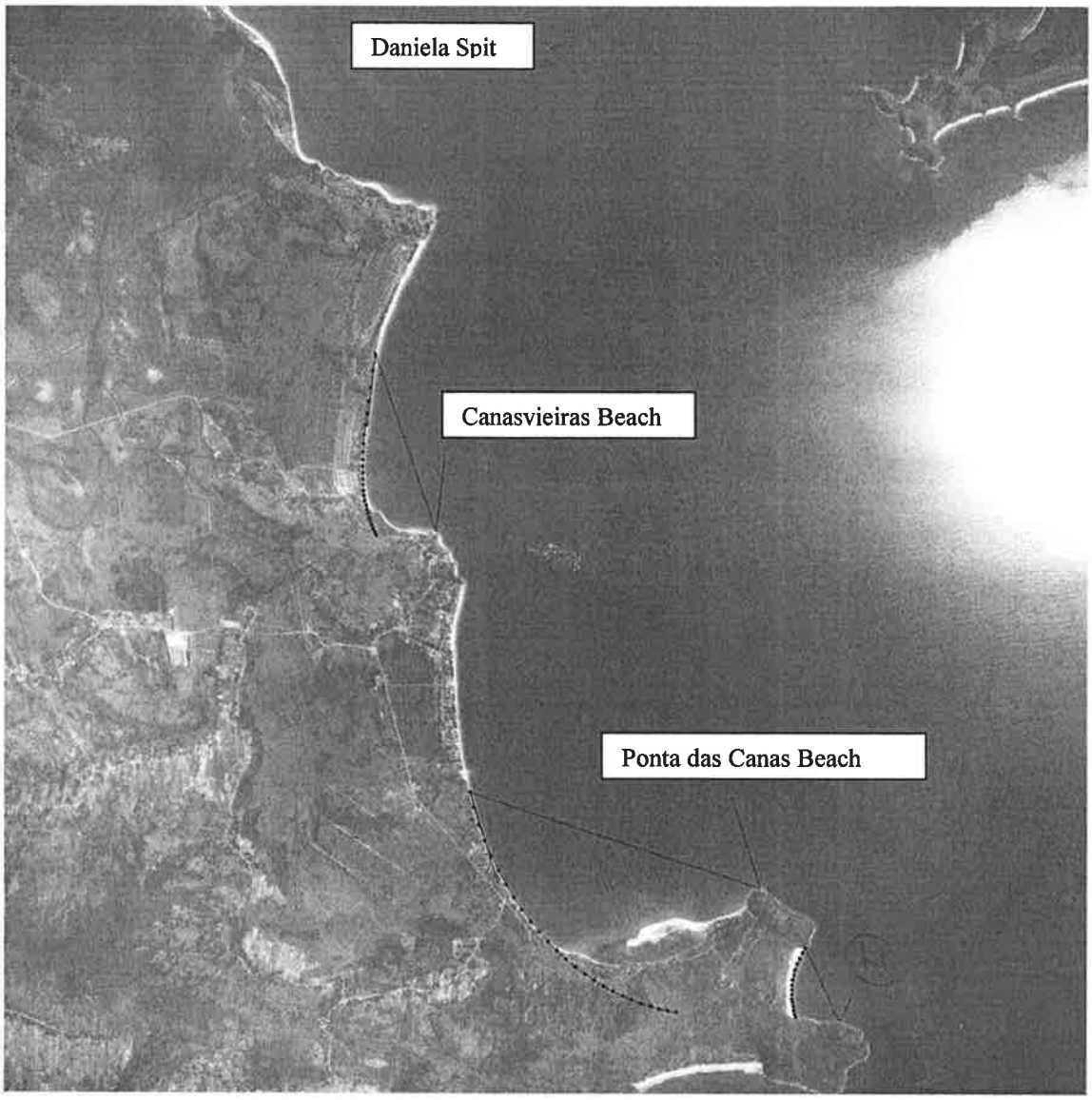

Figure 3.15. Parabolic bay shape for Canasvieiras Beach (β = 26°) and Ponta das Canas Beach (β = 54°). Black dots indicate the planform of the beach in dynamic to close equilibrium.

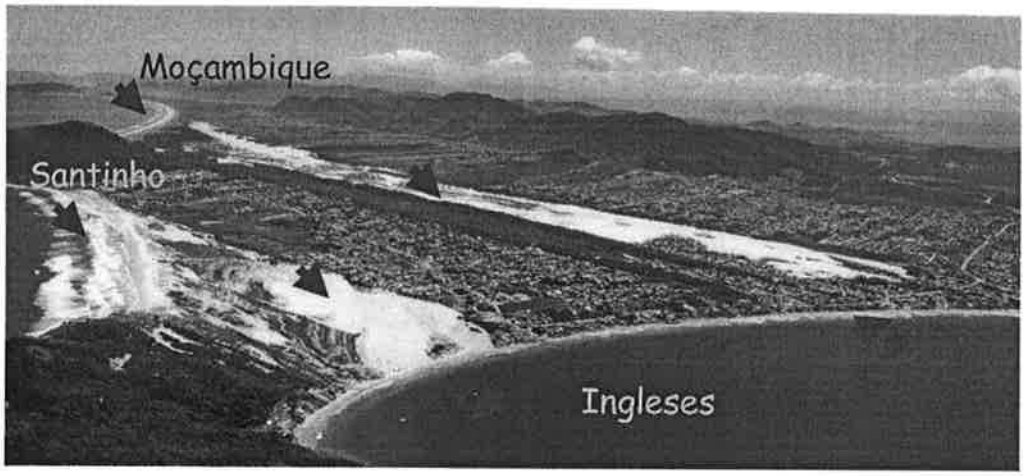

a)

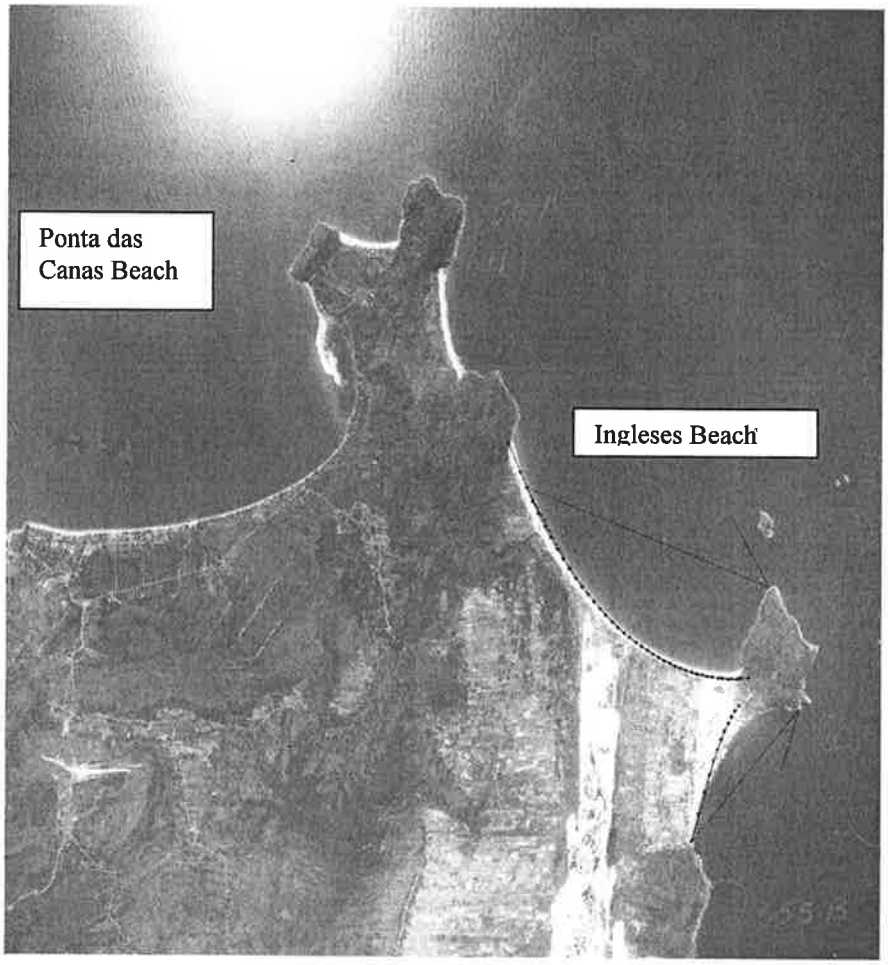

b)

Figure 3.16. (a) Overview of urbanization at Ingleses Beach. **(b)** Parabolic bay shape for Ingleses Beach (β = 39°). Black dots indicate the close to static equilibrium planform, which fits almost perfectly the actual shoreline planform.

Another argument, *i.e.* limitation of method, that can be used to explain this difference between the bay beach periphery found in the aerial photographs and maps and model result (Equation 3.1), is that the scales of the aerial photographs and maps used might have misled the judgment. It is thus necessary to use an aerial photograph or map with a suitable scale, in order to accurately identify the planform shape.

3.6.5. Tombolos and Salients

Zimbros-Mariscal Tombolo: It is located on East-West side of Arvoredo Island, a large island about 40 km SE of Itajai, or about 15 km NE from Tijucas in Santa Catarina (see Figure 3.17). Zimbros Beach is well sheltered behind the island, while Morrinhos Beach is relatively sheltered from the SE swell but exposed to the locally generated wind waves from NE. In the other hand Mariscal is an exposed beach.

For Zimbros Beach, the upcoast control point is Ponta da Baixada, where wave diffraction starts (diffraction point). First, a downcoast tangent near Zimbros was selected, with control line length R_β recorded and the reference obliquity β measured at 68°. The static bay shape was then plotted on the map (see Figure 3.17), and the beach was found to be close to static equilibrium, because the model almost coincided with the map bay periphery. Double checking was performed by relocating a downcoast tangent at Morrinhos, rendering the same β but different R_β. The same condition of "close to static equilibrium" was determined.

A similar approach was applied to test the stability of Mariscal Beach, first with "Ponta do Morcegão" as the upcoast control point (diffraction point), and then another

point for double-checking. Both produced identical curves that are landward of the map bay periphery, *i.e.* this beach is in dynamic equilibrium.

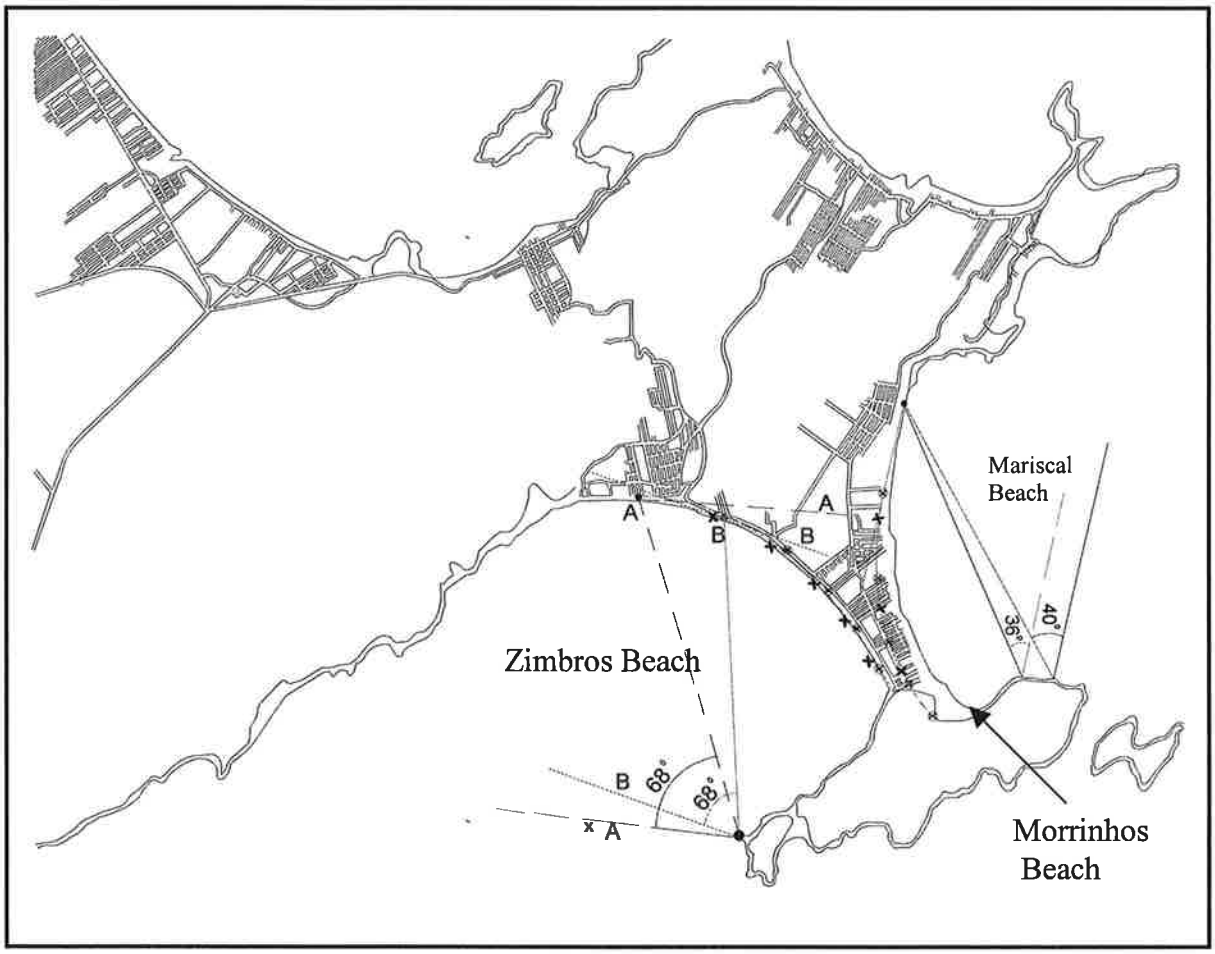

Figure 3.17. Stability of Zimbros and Mariscal beaches, showing static bay shapes using parabolic bay shape equation. Black cross = planform.

Santa Marta Tombolo: An example of parabolic equation to fit a Tombolo is shown in Figure 3.18 for Galheta and Santa Marta beaches, both located in Santa Marta Cape, Laguna municipality. These two beaches resulted from a linkage of a rocky outcrop with the mainland, forming a tombolo. Santa Marta Beach is classified as very

close to static equilibrium, while Galheta Beach to the north, is in dynamic equilibrium, according to the parabolic model, because the bay periphery is seaward from the shape defined by the Equation 3.1.

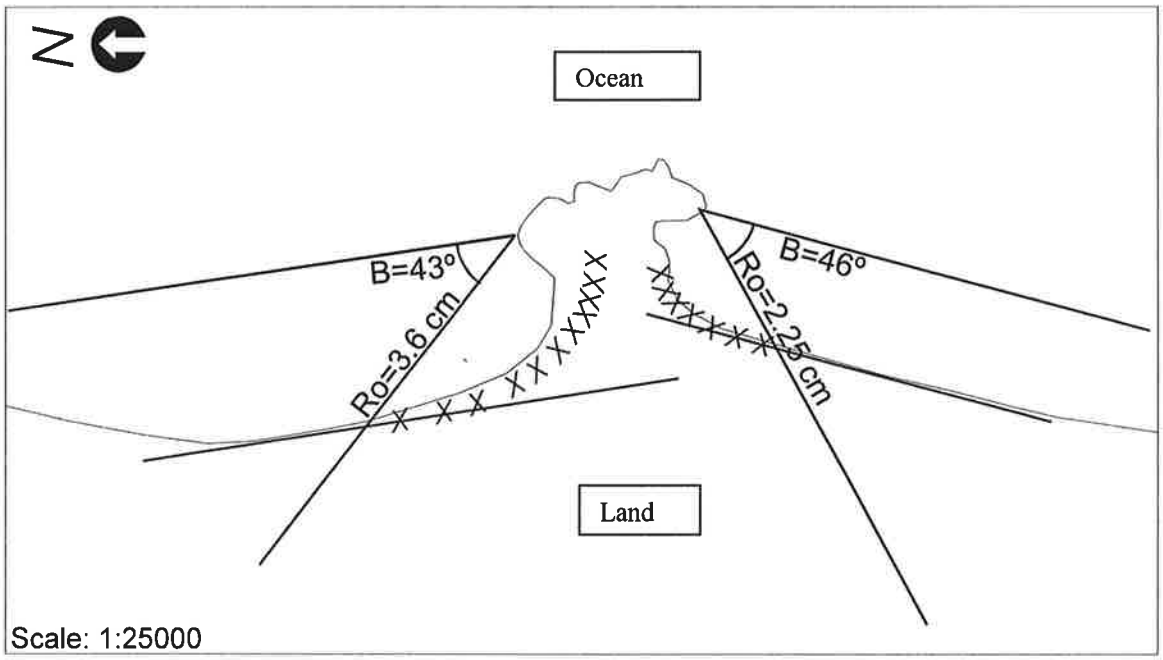

Figure 3.18. Parabolic bay shape fit for the tombolo located at Santa Marta (right side) and Galheta beaches (left side). Black crosses = planform.

Navegantes salient: Initially, three different points of wave diffraction on the island located near Gravatá Beach (Navegantes) were selected, taking an β equal to 40° for each point. For all three diffraction points, the results demonstrated that the formed salient is in dynamic to close to static equilibrium, with a notable progression of the coastline estimated by the model in relation to the current coastline in the case A and B (Figure 3.19a). However, by applying the model with different angles β (β_1 = 58° and β_2 = 28°), the position of coastline obtained is closer to static equilibrium, but landward of the actual coastline. This beach suffers erosive process nowadays.

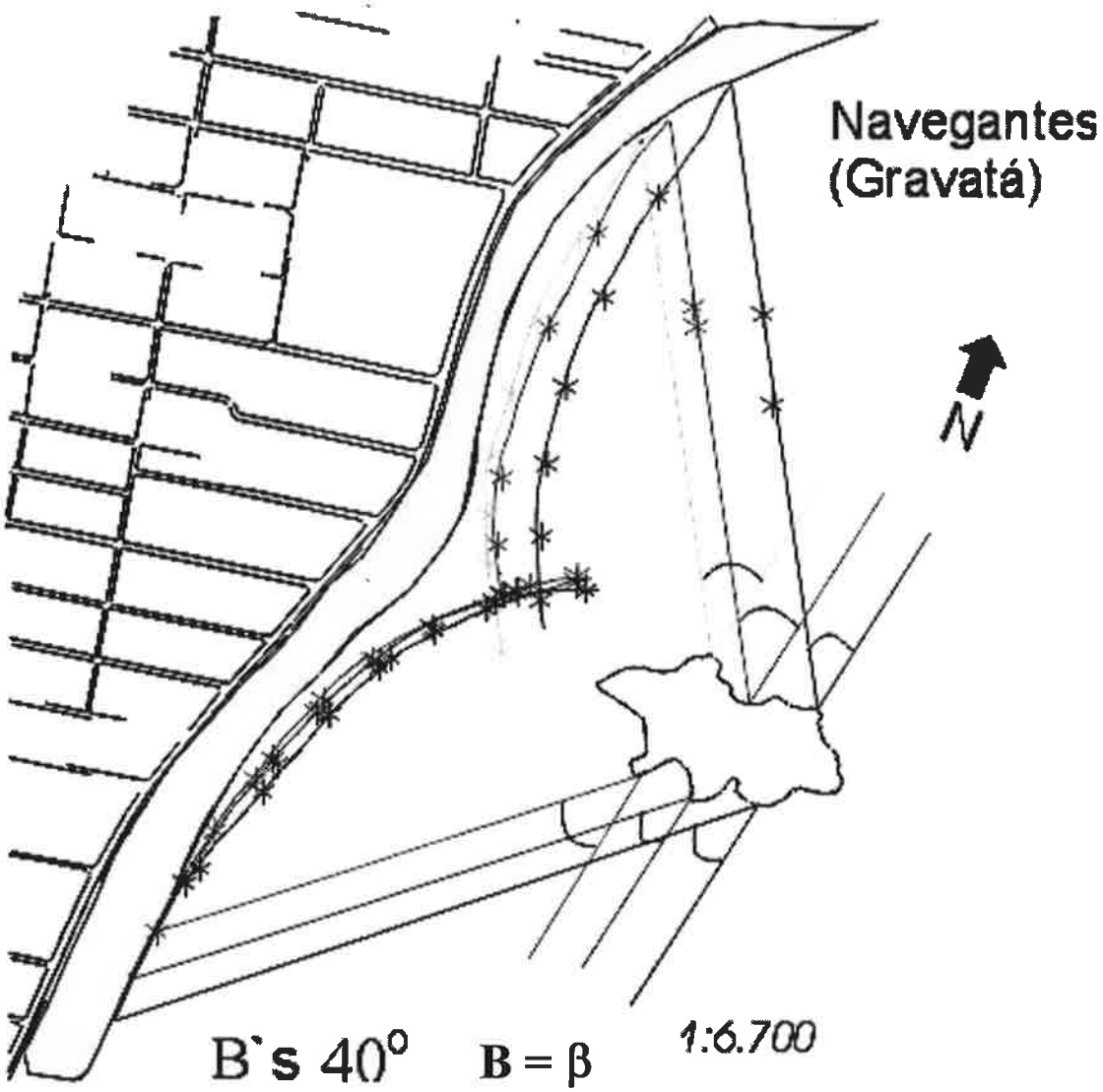

a)

Figure 3.19. Salient on Gravatá Beach, Navegantes. (a) Simulation for three different diffraction points, taking β equal to 40°.

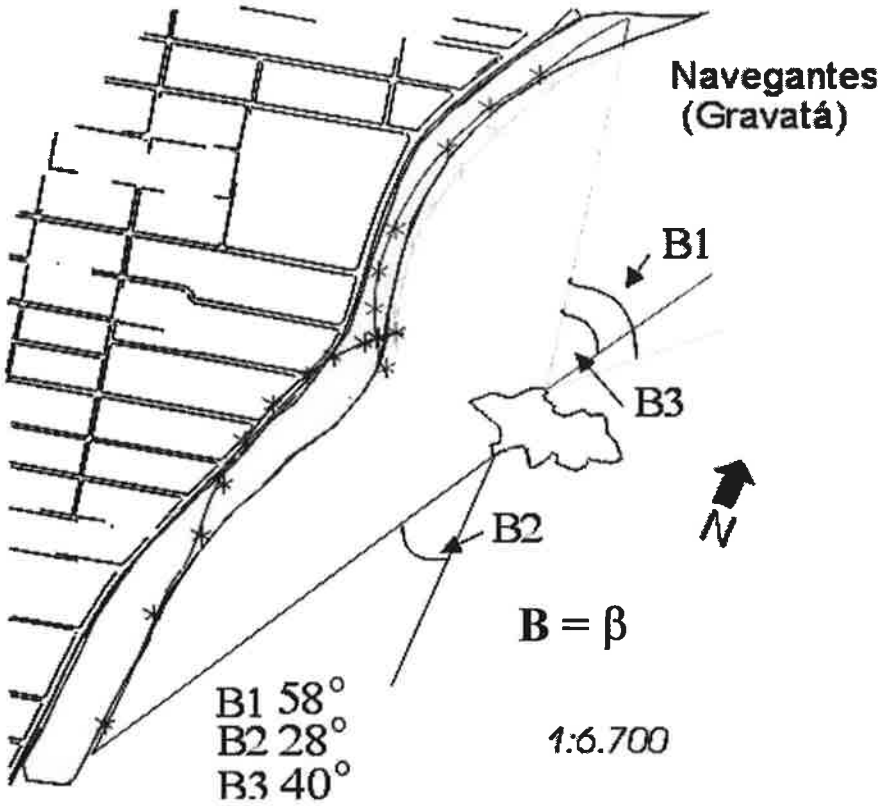

Figure 3.19. (Continuation) Salient on Gravatá Beach, Navegantes. (b) simulation for three different β (58°, 28° and 40°).

Barra do Ibiraquera salient: Figure 3.20 displays the asymmetric salient planform in the Lee of Batuba Island, noth of Imbituba Port in Santa Catariana. Due to the limited dimension of the island inshore-parallel direction, salient planform on either side of the island is produced. The smaller embayed beach in the north is the Luz Beach and the large one in the south is Barra de Ibiraquera Beach. Upon applying the parabolic bay shape equation, both beaches are found to be in static or close to static equilibrium.

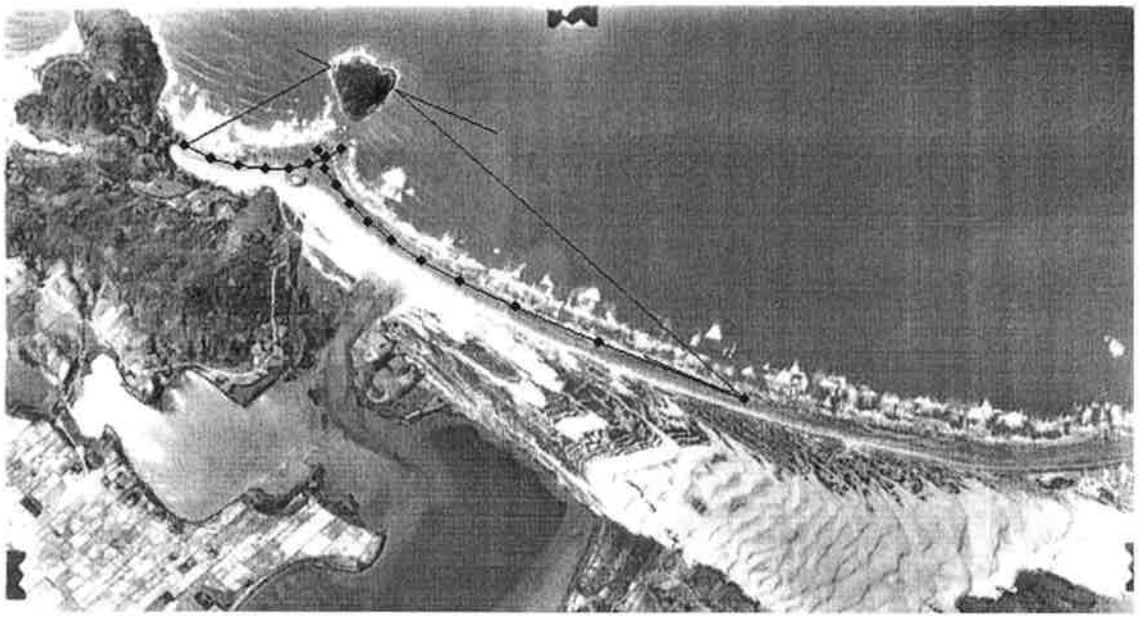

Figure 3.20. Barra de Ibiraquera salient display the asymmetric salient planform in static or close to static equilibrium. Black cross = planform.

Navegantes tombolo: For this feature, two different angles were necessary, because the beach is divided in two sections (Figure 3.21). Two salients delimit the first section, one on each side of the obstacle, while the second salients comprises the areas apart from these salients. Initially, β equal to 40° was proposed, as suggested by Hsu and Silvester (1990). The resultant coastline is very close to the current position of the coastline (see Figure 3.21), with a static equilibrium. However, in the second section, from which angles β were obtained starting from the straighter portion of the beach (β = 23° and 24°), the current coastline protruded in comparison with the simulated coastline (see Figure 3.21).

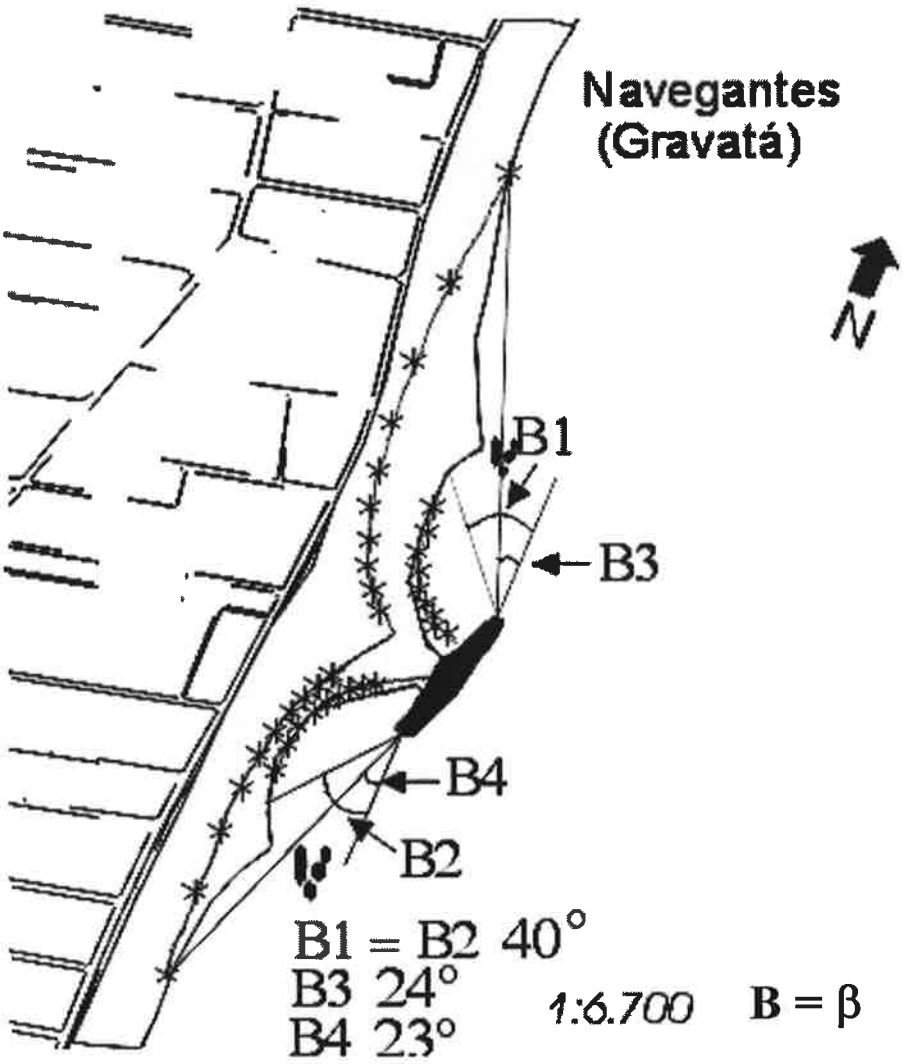

Figure 3.21. Navegantes tombolo, the simulation was performed for three different β angles (40°, 24° and 23°).

Central Beach - Balneário Camboriú salient: The parabolic equation is applied taking β equal to 40°. The result demonstrated that the formed salient on the central beach is in dynamic equilibrium. A notable regression of the coastline is shown in relation to the position suggested by the model (Figure 3.22).

However, by using different angles β, a line closer to the current coastline is obtained. These angles are 68° and 71° (β_3 and β_4 respectively) (see Figure 3.22). The angles found were close to the angles β obtained by Klein *et al.* (2003) for the same feature (73° and 74° respectively). The difference in scales between the studies is highlighted. Klein *et al.* (2003) used aerial photographs on a scale of 1:12,500 and the present work used a digitalized map on a scale of 1:3,000. This difference in scale directly influences the refinement of coastline estimated by the Equation 3.1.

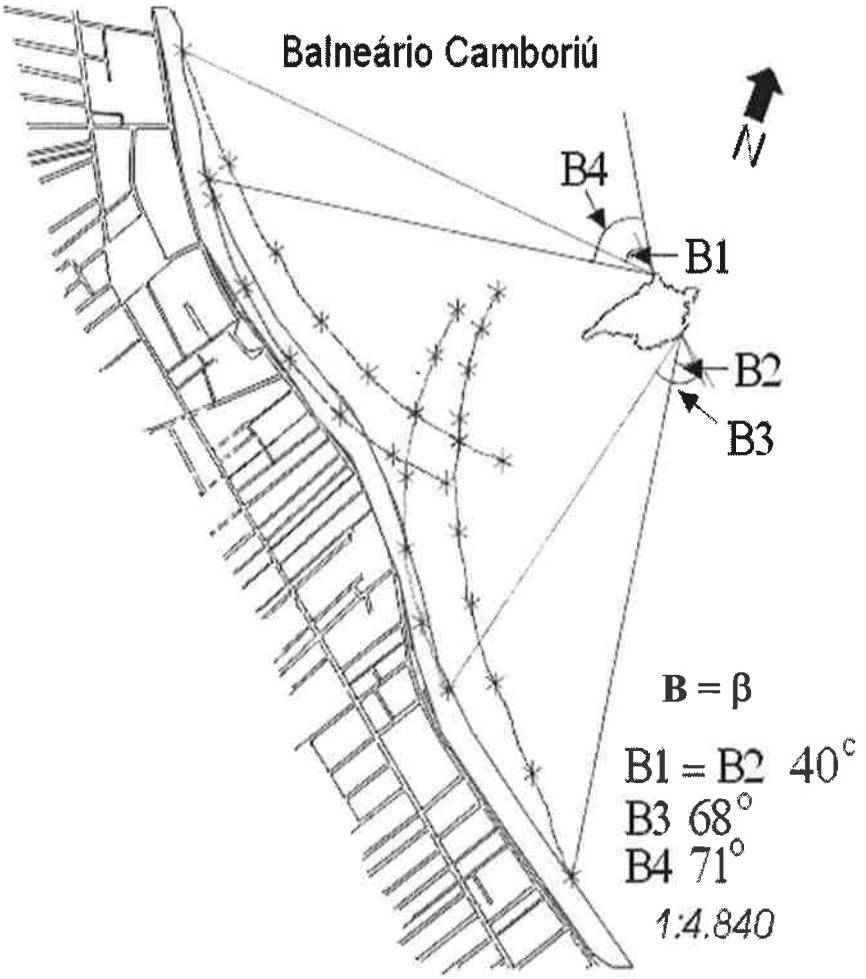

Figure 3.22. Salients of the central beach atf Balneário Camboriú. The simulation used three different β angles (40°, 68° and 71°).

3.6.6. Parabolic Equation Applied to a Harbor Design

In the year 1930th, an offshore breakwater was built at Porto Beach (see Figure 3.23) in Imbituba municipality with the objective of producing calm waters for the Imbituba port. The tip of this breakwater has become an upper control point (diffraction point) for a potential change in the beach coastline to be formed in its lee, with beach accretion joining the downcoast headland and accompanying by erosion further downcoast. As a consequence, engineering applications, such as groins and dredging, had been applied in order to block littoral drift towards the port area and to maintain a deep channel for navigation. The parabolic model was applied for the Porto Beach to simulate the beach situation before and after the breakwater construction. The parabolic model has proven useful to predict the accretion process at this port.

3.6.7. Indentation Ratio

The indentation ratio a/R_β versus reference wave obliquity angle β has been suggested by Silvester and Hsu (1993, 1997) as a second check for the stability of headland bay beaches. They also indicated that the accuracy of this simple approach required further refinement using field data. Based on the results of a/R_β versus β for the bay beaches in Santa Catarina state (see Table 3.2.), a linear regression was applied to bay beaches in all types of equilibrium condition, but with data scattering (Figure 3.24). The results are similar for all types of equilibrium consequently no difference is defined.

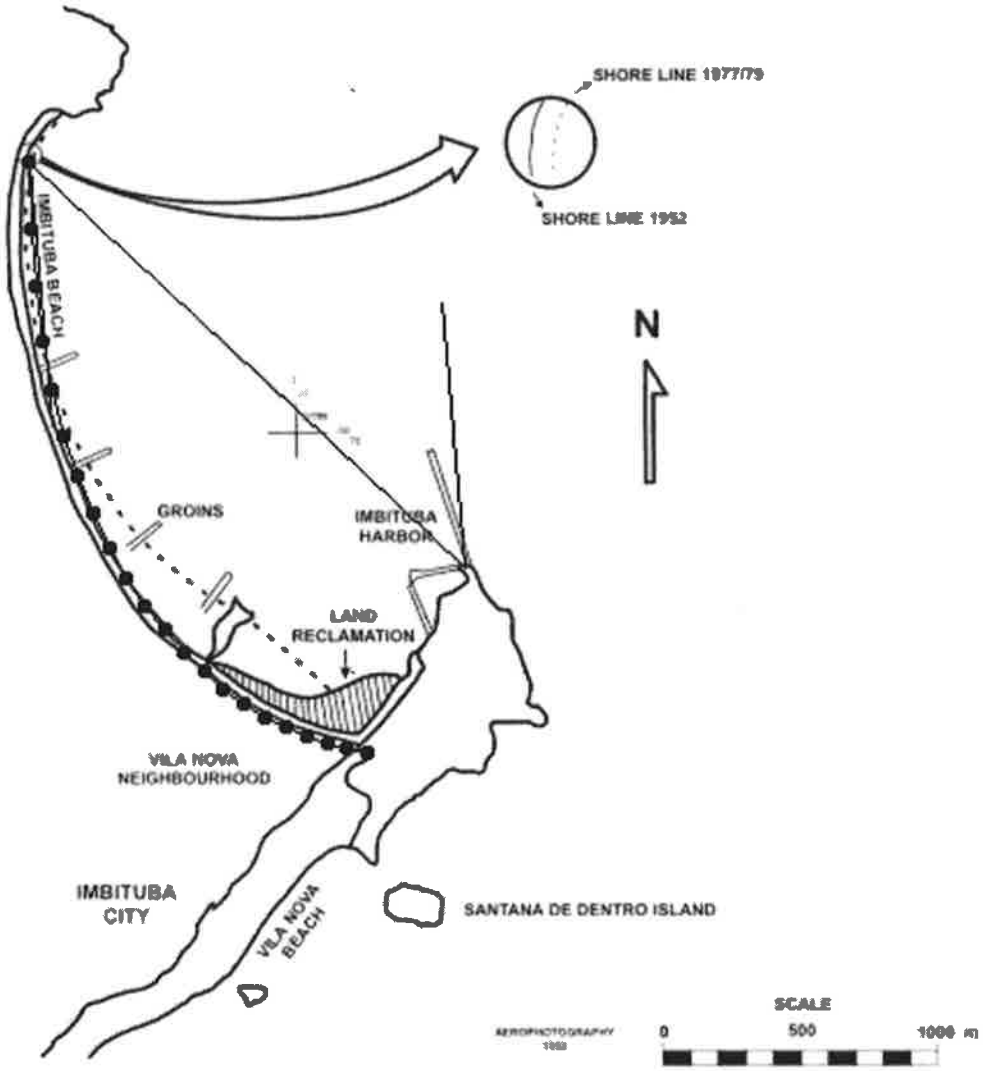

Figure 3.23. (a) Parabolic model applied for the Porto Beach, Imbituba, showing a close to static equlibrium before the breakwater construction ($\beta = 42^{o}$). Black dots = planform.

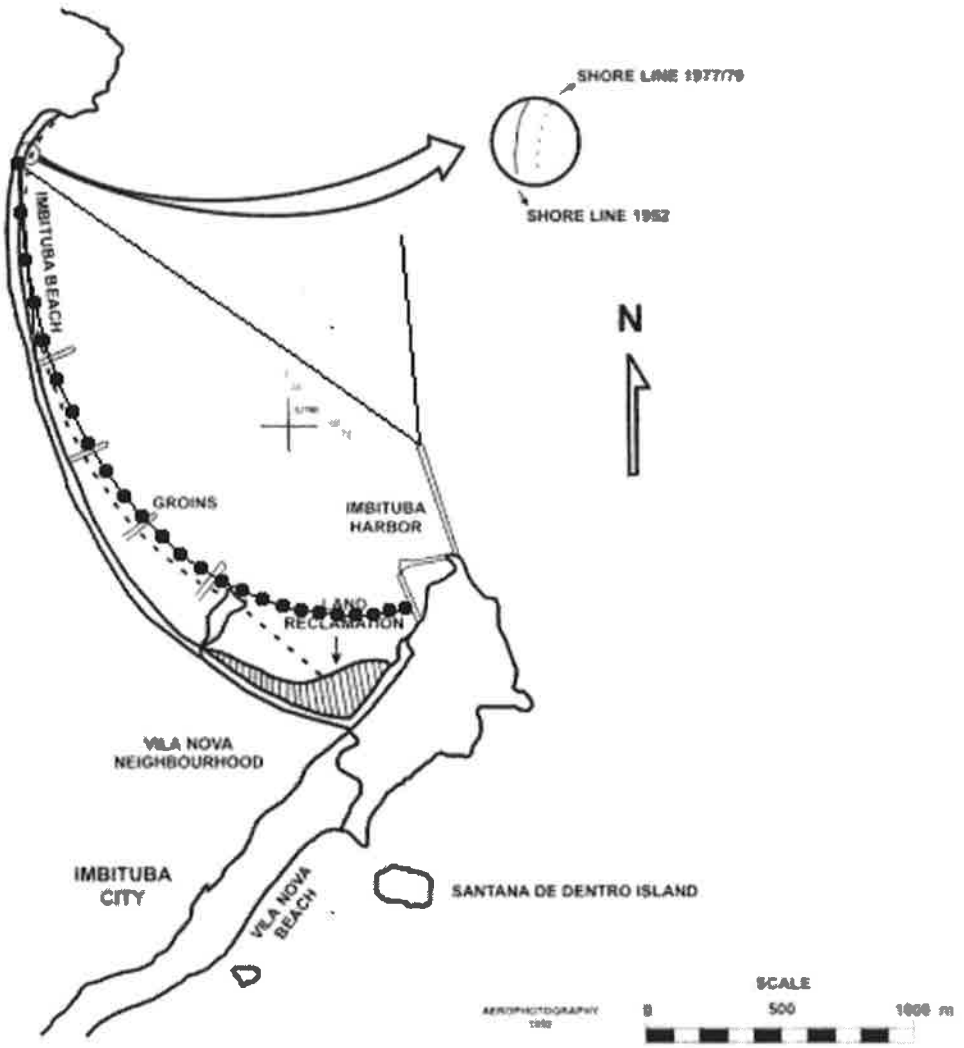

Figure 3.23. (Continuation) **b)** Parabolic model applied for the Porto Beach, Imbituba, showing a dynamic equlibrium beach after the breakwater construction ($\beta = 50^{o}$). The parabolic model has proven useful to predict the accretion experienced at this location. Black dots = planform.

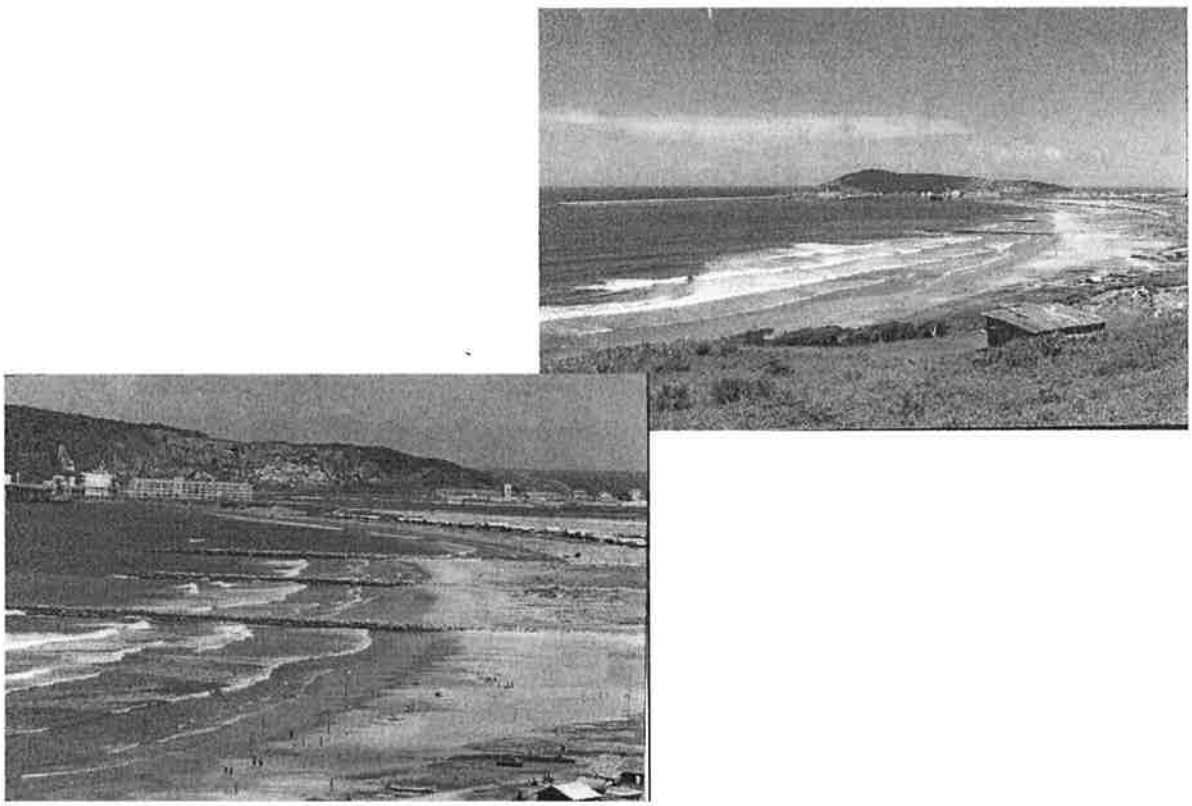

Figure 3.23. (Continuation) c) Overview of Porto Beach, Imbituba, showing the beach after the groins and breakwater construction

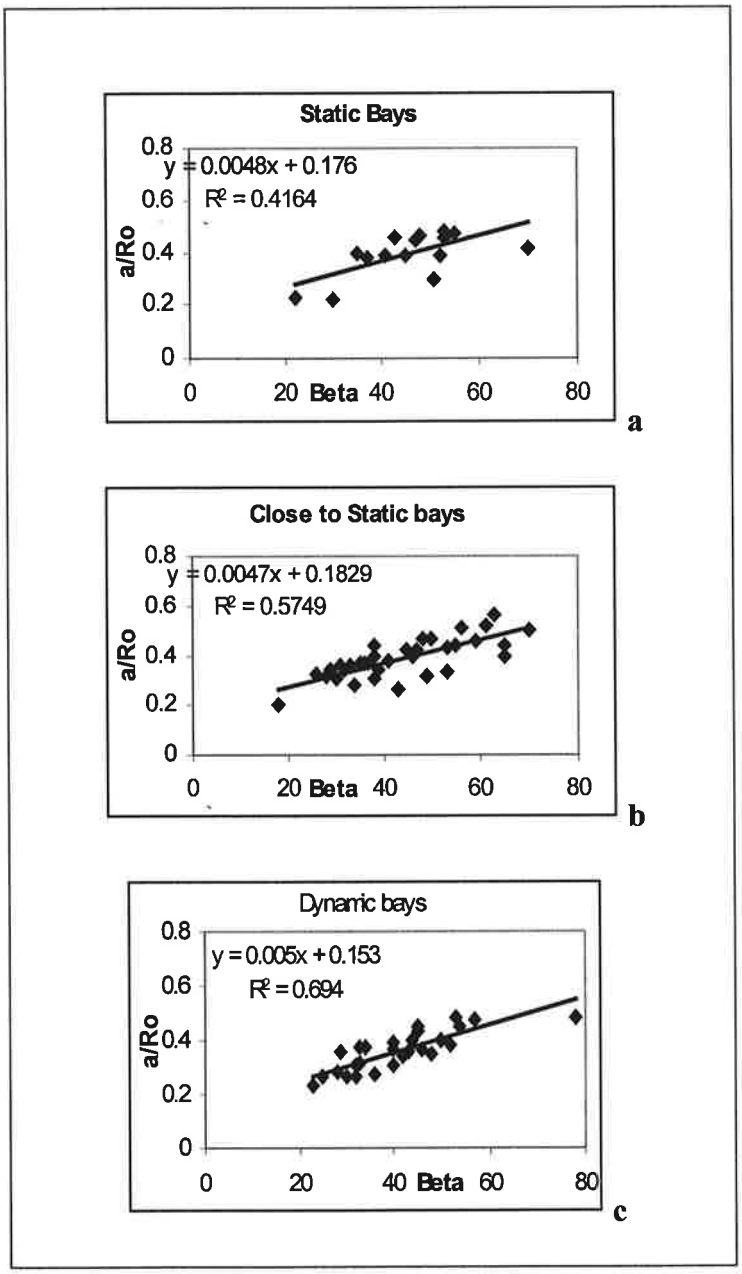

Figure 3.24. Indentation ratio a/R_β versus β for bay beaches in static (a), close to static (b), and dynamic equilibrium (c).

3.7. SUMMARY

(1) The parabolic bay shape equation fits the geometrical shape of headland bay beach, in static equilibrium, with the input of wave direction and the wave diffraction point, *i.e* it is not purely geometrical and the physical insight of wave action exist; consequently it would be possible to predict the environmental impact as the diffraction point changes from its original location by for example the introduction of a man-made structure (*e.g.*, Imbituba Port).

(2) Some technicality arose while applying the parabolic bay shape equation, for example, on the location of both the upcoast and downcoast control points, and the downcoast tangent. Occasionally, it may be difficult to define the diffraction point (*i.e.*, the upcoast control point) from an aerial photograph, especially when the tip of diffraction point is hidden (submerged) or with extensive shallow region in the lee of the compared headland. The determination of the wave crest line, defined to be in the same orientation as the tangent at downcoast, is another issue affecting the accuracy of the prediction. With some experience, a smooth waterline can be drawn from the irregular shoreline, caused by the existence of a shoal offshore or irregularity in bottom bathymetry.

(3) The parabolic bay shape equation (Hsu and Evans, 1989; Silvester and Hsu, 1993, 1997) has proven to be a convenient and practical tool for studying the stability of the headland-bay beaches in Santa Catarina state. Most erosion sites along the State coastline, such as at Piçarras Beach, Southern of

Balneário Camboriú Beach and Canasvieiras Beach, have been identified in dynamic equilibrium, which are vulnerable to human activities causing the imbalance of sediment budget from various sources. Despite the landward limit at the downcoast beach cannot be accurately defined at present, the general trend of the accretion and erosion can be predicted by the parabolic bay shape equation.

(4) Most bay beaches in static equilibrium in Santa Catarina are small and confined within headlands. They do not receive sediment supply from rivers and littoral drift. There are some exceptions, as some beaches that were previously found to have no littoral drift and sediment supply are in the category of dynamical equilibrium. Further investigation is recommended to find out the hidden sources, which may have contributed to the stability of this type of beach.

(5) The state of beach stability, is dependent on other beach classifications, such as morphodynamic stages and beach orientations.

(6) A possibility of using a second (inner) control point, is here recognized to fit bay shape stability. This is a result of progressive wave diffraction at an irregular headland.

(7) It has been experienced from this study compared with Klein *et al.* (2003), that the scale of the aerial photographs and maps used affect the accuracy of the result of the parabolic bay shape model application. In some cases the same beach considered to be very close to static equilibrium in the map on a 1: 50,000 scale, became dynamic equilibrium on a 1:12,500 scale. For coastal management and engineering applications, it is therefore suggested

that the large the scale of a map or aerial photographs used, the better and more accurate for the parabolic model applications. It is also necessary define a qualitative way to considerer the difference between the stages (static, close and dynamic).

(8) It should be emphasized that parabolic model is an efficient tool for determining the planform assumed by the salients and tombolos, when the angle β is variable.

(9) The parabolic bay shape model has shown to be suitable for coastal engineering applications. It can be applied to estimate the impact of coastal structures in the Imbituba Port. Consequently, this method is also beneficial for planning the dimensions and orientation of groins and breakwaters, in order to mitigate the potential beach erosion downcoast, as well as the sedimentation in the harbour.

(10) The indentation ratio a/R_β versus β has shown to have some deficit in becoming an alternative method for assessing the stability of bay beaches, not to mention its accuracy. Incorrect conclusion may be reached if only the indentation ratios are used, instead of plotting the entire bay periphery.

CHAPTER FOUR

Beach Morphodynamics and Profile Sequence for a Headland Bay Coast

Unless referred to otherwise, the contents of this thesis are the results of original research carried out by the author

Some of the results have been published in:

KLEIN, A H.F and MENEZES, J.T de, 2001. Beach Morphodynamics and Profile Sequence for a Headland Bay Coast. *Journal of Coastal Research*, 17 (3), 812-835.

4.1. INTRODUCTION

Global studies of oceanic sandy beaches require many variables responsible to understand the processes and its morphodynamic behaviour. Short (1999) suggests five major parameters: tidal range, wave height, wave period, grain size and beach length/embaymentisation which are incorporated into seven equations that can be used to describe the major features of beach systems. These equations include, among others, beach type, beach slope, number of bars and embaymentisation parameter. However, further studies on different sandy coasts, especially those presenting headland and bay geomorphology, are necessary for developing a global model (Short and Masselink, 1999), owing to the range of exposure to different wave and tidal conditions. In this case, the range of alongshore beach morphology (beach profile sequence) is a result of distance from headland, shape of bay, wave obliquity, indentation ratio, longshore grain size distribution and nearshore slope. The purpose of this chapter is to elucidate a beach profile sequence for the coastal zone of an east coast swell environment with headlands and bay geomorphology.

The study area is located on the central-north coast of the State of Santa Catarina between 26°30' S and 27°20' S (sectors 3 and 4), located on the coastal macro-compartment of the Crystalline Scarps (Muehe, 1998), (Figure 4.1). The beaches present a multitude of environmental settings due to their geographical orientation, level of exposure to incident waves and sediment distribution. Generally, the beaches are relatively sheltered from more energetic southerly waves as most of them are located between headlands that modify incident waves to varying degrees.

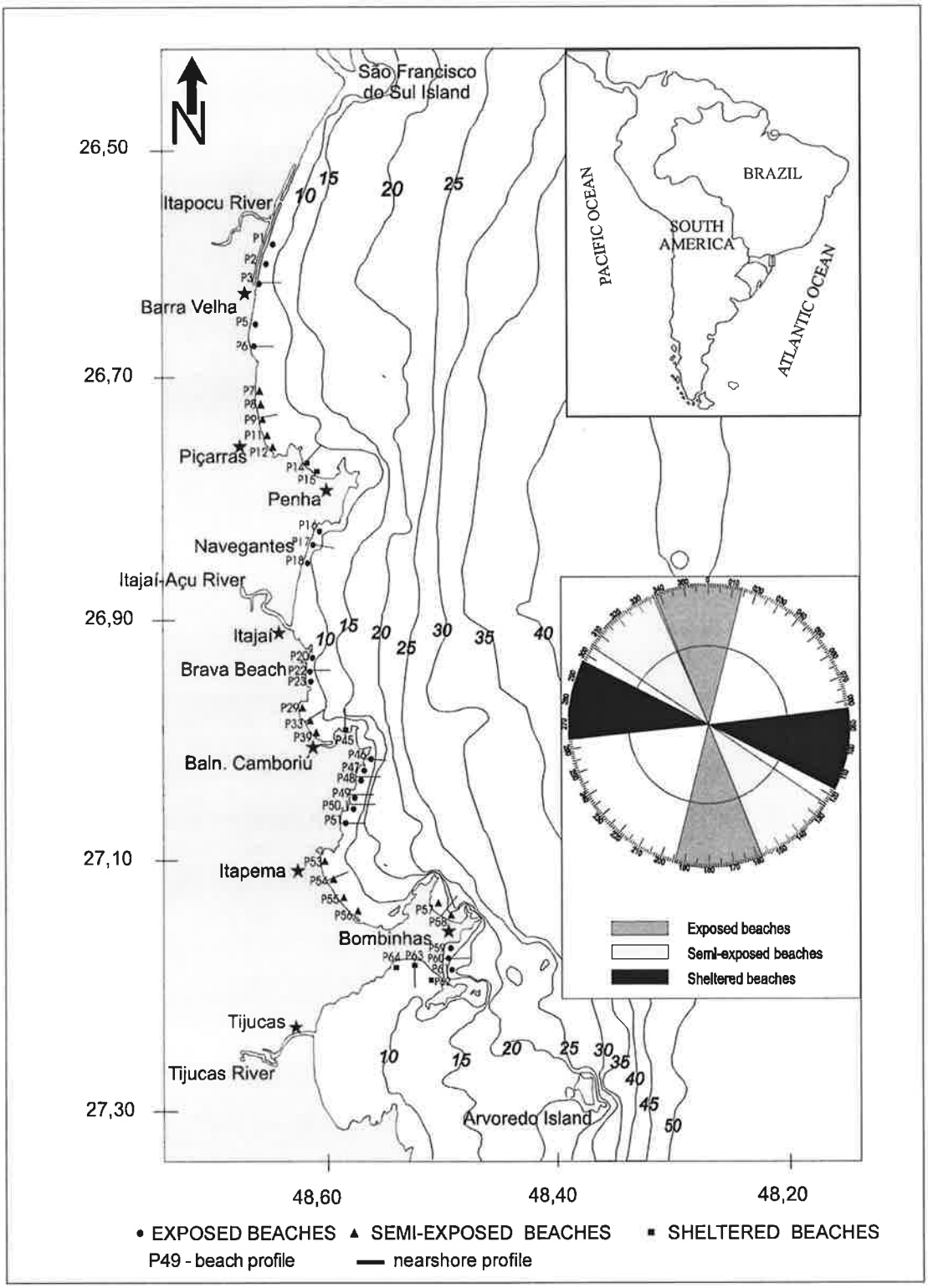

Figure 4.1. Map of the study area showing beach profile and shoreface measurement program conducted on the Central-North coast of the State of Santa Catarina, Brazil, between January 1994 and February 1996 (depth is in meters). Note the beach classification in relation to the wave exposition and beach orientation in relation to the north.

4.2. SAMPLING AND ANALYSES

4.2.1. Beach Exposure - Indentation Ratio and Identification of Predominant Wave Direction (β)

The method employed in this study is presented in Figure 4.2 and 4.3. The ratio of bay indentation (*a*) to headland spacing (R_β) is a result of the obliquity of the dominant wave crests to the headland alignment (β) (Silvester and Hsu, 1997). The obliquity of the dominant wave crest to the headland bay beach is defined as the angle between the shoreline of the downdrift section of the bay and the headland alignment. As seen in the inset of Figure 4.3., the highest indentation (a) is measured normal from the control line (R_β) to the point of largest retreat of the shoreline (Silvester and Hsu, 1997). This is obtained by drawing a tangent parallel to the control line, which is asymptotic to the beach (Silvester and Hsu, 1997). Figure 4.3. shows the relationship between a/R_β and β. This information was obtained by aerial photo interpretation on 1:12,500 scale from years 1995, and charts on a 1:50,000 scale.

4.2.2. Beach Exposure - Degree of Headland Impact

The degree of impact of end effects or embaymentisation is predicted using the nondimensional embayment scaling parameter (δ') (Short and Masselink, 1999). When deepwater waves enter an embayment with a given width (C_l), between headlands, the wave energy will be redistributed along the embayment shoreline (S_l), such as:

$$\delta' = S_l^2 / \underline{k}\, C_l\, H_b \qquad (4.1.)$$

Where $\underline{k}$ is the surf zone slope and H_b is the height of breaking waves. The embayment shoreline (S_l) can be obtained by aerial photo interpretation. Cellular circulation occurs

when δ'is lower than 8, transitional circulation for δ' between 8 and 20, and normal circulation for δ' greater than 20.

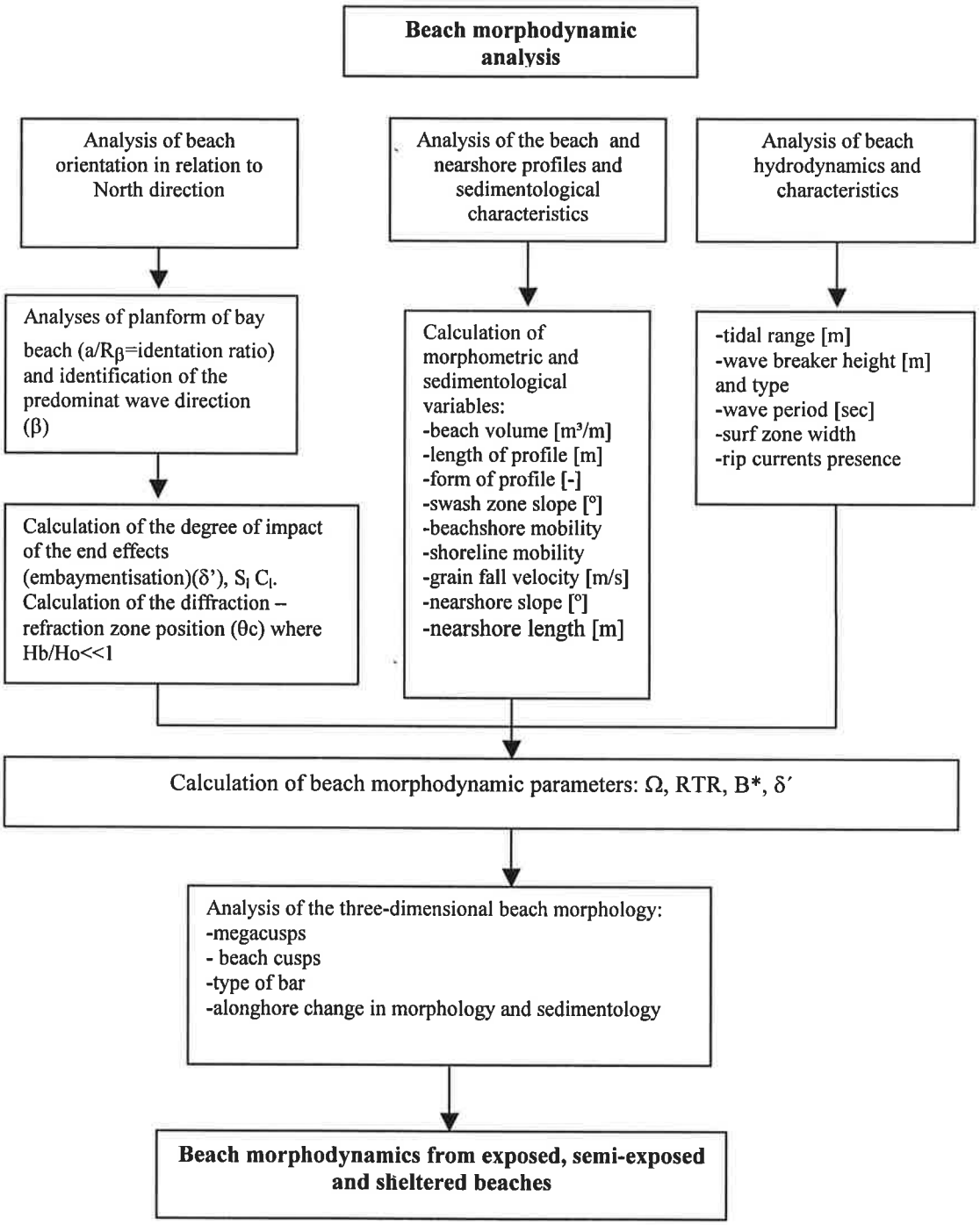

Figure 4.2. Overall methodology employed in this study.

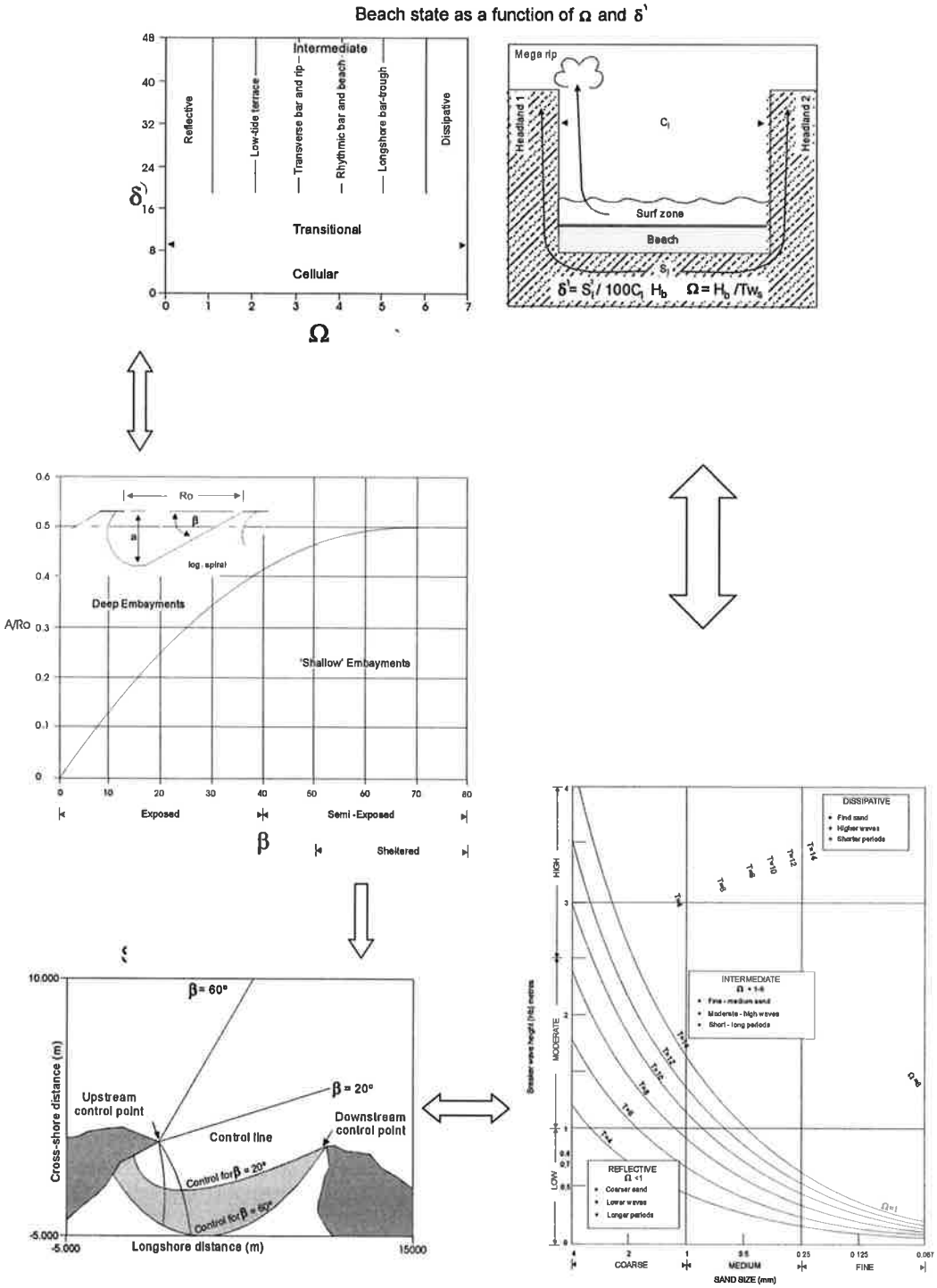

Figure 4.3. Classification of beach state - indentation ratio, embayment scaling parameters, omega, breaker wave height and sand size (after Silvester and Hsu, 1993; 1997; Short, 1999; Short and Masselink, 1999).

4.2.3. Beach and Nearshore Profiles

Between January 1994 and February 1996, a beach-profile measurement program was conducted on the central-north coast of the State of Santa Catarina (see Figure 4.1.). In total, 64 beach profiles were obtained and 32 were monitored almost monthly with a levelling instrument, as proposed by Birkemeier (1981). The beach profiles were evaluated by the Interactive Survey Reduction Program, ISRP (Birkemeier, 1985). In total, 1164 profiles were obtained; and all of them were made one meter equidistant between successive points by linear interpolation between the data points, using the LOD_EQUI program (Bresters and Reijngoud, 1996).

From the profiles, the following morphometric variables were calculated: subaerial beach volume (V) [m^3/m]; subaerial beach width (L) [m]; and subaerial dimensionless beach shape (F) [-] (Figure 4.4.). The x-axis extends seawards, and the y-axis extends vertically upwards. The origin of the co-ordinates is located at mean sea level at a fixed reference point. The morphological variables are computed using the landward boundary (x1) and the seaward boundary (x2) as recommended by Temme *et al.* (1997). The landward boundary (x1) is constant per profile. The locations of these points were determined using the profile envelopes as shown in Figure 4.4.

The profile-envelope is defined by the maximum and minimum height at each cross-shore distance. In these profile envelopes the points without morphological changes can be identified (essentially zero). The location of x1 is chosen so that this part of the profile is not included in the analysis. The seaward boundary, the location of the mean sea level (x2) is used in all cases, as a consequence, only the subaerial parts of the profile change are analysed (mobile subaerial zone). The beach volume (V) is defined as the cross-sectional area within the boundaries x1 and x2 per unit length of the shoreline (Sonu and van Beek, 1971). The beach width (L) is defined as the

distance between the boundaries x1 and x2. The shape of the mobile beach is defined as $Q/L.h_{max}$, where h_{max} is the maximum height of the profile. This parameter describes the form of the profile. High values (about 0.7) can be related to a convex profile and low values (about 0.3) to a concave form. A linear beach profile is represented by a value of 0.5 (Fucella and Dolan, 1996).

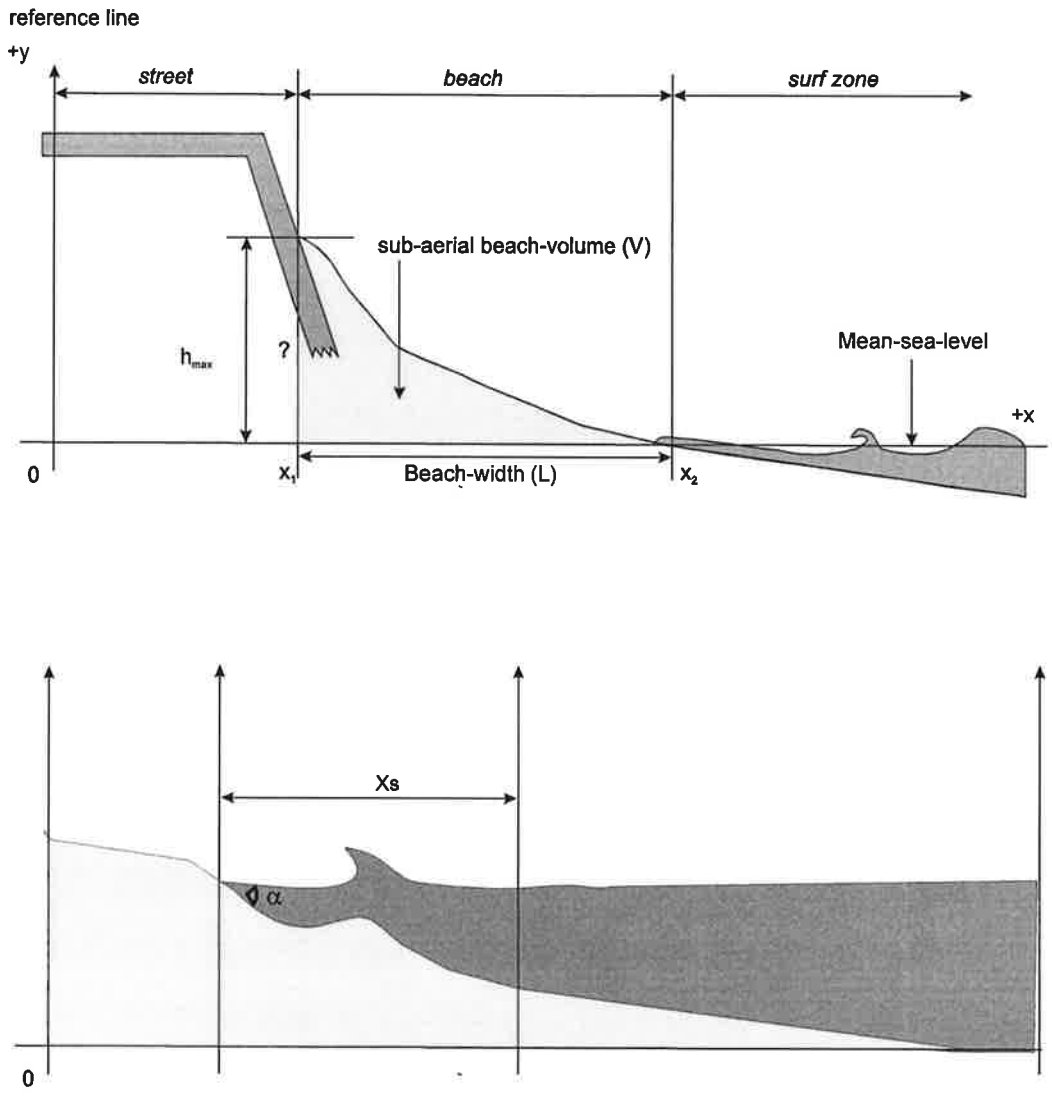

Figure 4.4. (a) Morphometric variables calculated from beach profiles (subaerial beach volume (V) [m³/m]; subaerial beach width (L) [m]; and subaerial dimensionless beach shape (F) [-];(b) wide of surf zone (χ_s)[m].

Seventeen (17) perpendicular bathymetric profiles between 2 and 10 meters were obtained in order to define the length (χs) and the slope of the nearshore study area (see Figure 4.1. and 4.4.). The depth was obtained with an ELAC –recorder and the position by triangulation methodology.

4.2.4. Beach Type and Number of Bars

Beach type and number of bars were obtained by relative tidal range (RTR), dimensionless fall velocity (Ω), empirical dimensionless fall velocity (Ω_t) and bar parameter (B*).

The parameterisation of tidal effects was proposed by (Masselink, 1993). This author found that a useful parameter (relative tidal range – RTR) to quantify tidal effects was:

$$RTR = TR/H_b \qquad (4.2.)$$

Where TR is the spring tidal range. When RTR < 3 the beach is classified as a wave dominated type, a mixed wave-tide beach type for 3 < RTR < 7, and a tidal dominated beach (sand flat) for RTR > 15.

The parameterisation of wave dominated beach type was obtained by the dimensionless fall velocity parameter (Gourlay, 1968; Dean, 1973) adopted for natural beaches by Wright and Short (1984):

$$\Omega = H_b/(W_s\, T) \qquad (4.3.)$$

Where W_s is sediment fall velocity and T^1 is wave period.

The authors related that when Ω<1, beaches tend to be reflective (steep, barless), becoming dissipative when Ω>6, they tend to be flat and multibarred, and in an intermediate state between the two end members (one or two bars) for 1<Ω<5. The

role of the three parameters H_b,T and W_s (grain size) in influencing the beach types is illustrated in Figure 4.3., which shows the sensitivity to each parameter according to Short (1999). Increasing H_b and decreasing T and W_s, favour dissipative beaches, while decreasing H_b and increasing T and W_s, favours reflective beaches with intermediate beaches lying in between (Short, 1999).

The empirical dimensionless fall velocity parameter was obtained by relating the declivity of the beach face (tanβ) with the dimensionless fall velocity parameter, since both vary according to the characteristics of the waves (H_b, T) and of the sediment (W_s). Kriebel *et al.* (1991) and Masselink (1993) analysing Sunamura's data (1984) proposed: $\tan\beta = 0.15\ \Omega^{-0.5}$. Realising that tanβ is a function of Ω, we substituted the values proposed by Wright and Short (1984) with the purpose of determining the theoretical limit value of declivity for the extreme morphodynamic stages (Table 4.1.). Klein (1997) proposed:

$$\Omega_t = 0.0225/\tan\beta^2 \qquad (4.4.)$$

Table 4.2. shows the relationship between Ω and Ω_t for the beaches in the study area.

Finally, the occurrence numbers of nearshore bars was obtained with the bar number equation (B*) (Short and Aagaard, 1993):

$$B^* = \chi_s / g.\tan\beta\ T_i^2 \qquad (4.5.)$$

and confirmed by aerial photo interpretation. This equation indicates that the number of bars in a microtidal environment, increases as the nearshore slope (tanβ), and/or the period of wave during storm $(T_i)^2$ decreases, and the nearshore length (χ_s) increases. If $B^* < 20$, the beach does not exhibit bars. For B* between 20 and 50 the beach exhibits

[1] The wave climete was obtained by visual observation.
[2] The storm wave period was obtained from ALVES (1996)

one bar, between 50 and 100 there are two bars, between 100 and 400 there are three bars, and for B*>400 there are 4 or more bars.

Table 4.1. Theoretical limit values of declivity of the beach face for the morphodynamic stages (Klein, 1997).

Stages	Ω limit	tanβ limit
Dissipative	$\Omega > 6$	$\tan\beta < 0.061$ (3.5°)
Intermediate	$1 < \Omega < 6$	$0.61 < \tan\beta < 0.15$
Reflective	$\Omega < 1$	$\tan\beta > 0.15$ (8.5°)

4.3. BEACH PLANFORM AND MORPHODYNAMIC CHARACTERISTICS

The parameters used to describe the beach planform and beach morphodynamic characteristics are presented in Table 4.2.

The ratio of bay indentation (a) to headland spacing (R_β) is a function of the obliquity of the dominant wave crest to the headland alignment (β) (Silvester and Hsu, 1997) and the degree of the beach wave exposure is also a function of these two variables. Large wave obliquity results in a larger indentation and smaller wave exposure, whilst exposed beaches exhibit a small indentation ratio (between 0.28 and 0.39) and small obliquity (less than 40°)(Figure 4.5.). Generally, semi-exposed beaches have a variable indentation ratio (between 0.37 and 0.49) and the wave obliquity between 40° – 62°, but with northwest-southeast orientation. Sheltered beaches exhibit a variable indentation ratio (> 0.38) and greater wave obliquity (>50°) with east-west orientation. However, all beaches have a nondimensional embayment scaling parameter (δ') greater than 20 (normal circulation) (see Table 4.2.).

Figure 4.6. and 4.7. shows the beach classification of dissipative, intermediate to reflective, based on wave breaker height (H_b), sand grain diameter and beach slope.

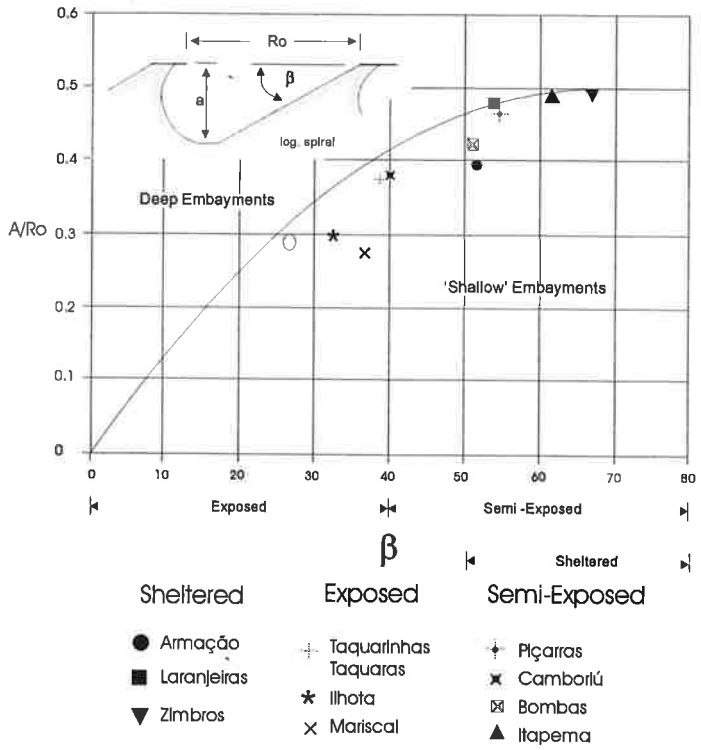

Figure 4.5. Indentation ratio versus angle of wave direction for beaches on the Central-North coast of the State of Santa Catarina, Brazil

4.3.1. Exposed Beaches

Several beaches in the study area are classified as exposed, such as: Itajuba, Taquarinhas, Taquaras, Estaleiro, Estaleirinho, Barra Velha, Brava, Ilhota, Navegantes and Mariscal (see Figure 4.5., 4.6. and 4.7. and Table 4.2.). They have north-south orientation (see Figure 4.1.) and are wave-dominated beaches (RTR < 3), low energy, and can be divided into reflective, intermediate and dissipative (multiple bars). The role of the parameters H_b, T and W_s (grain size) influencing the beach type is illustrated in Figure 4.6., showing the sensitivity of these parameters (Short, 1999). Sediment size and waves control the beach shape and dynamics. Fine sand produces a lower slope (1° to 3°) on the swash zone and a wider surf zone (≈100m) with potential high mobile sand, whilst medium to coarse sand beaches have a steeper slope (5° to 10°) and a narrower surf zone (< 50m).

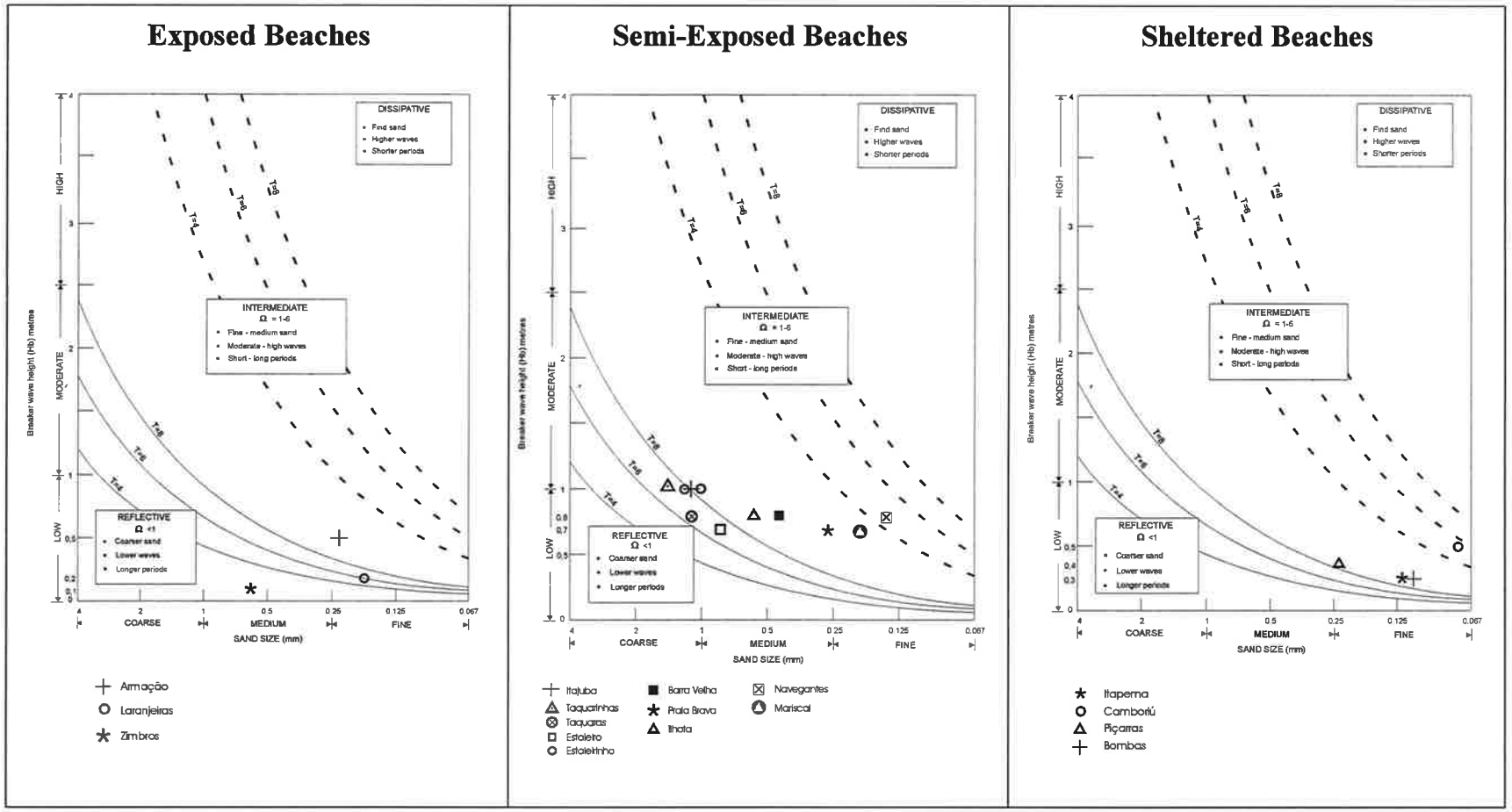

Figure 4.6. Beach classification based on breaker height and sand size for beaches of the Central-North coast of the State of Santa Catarina, Brazil.

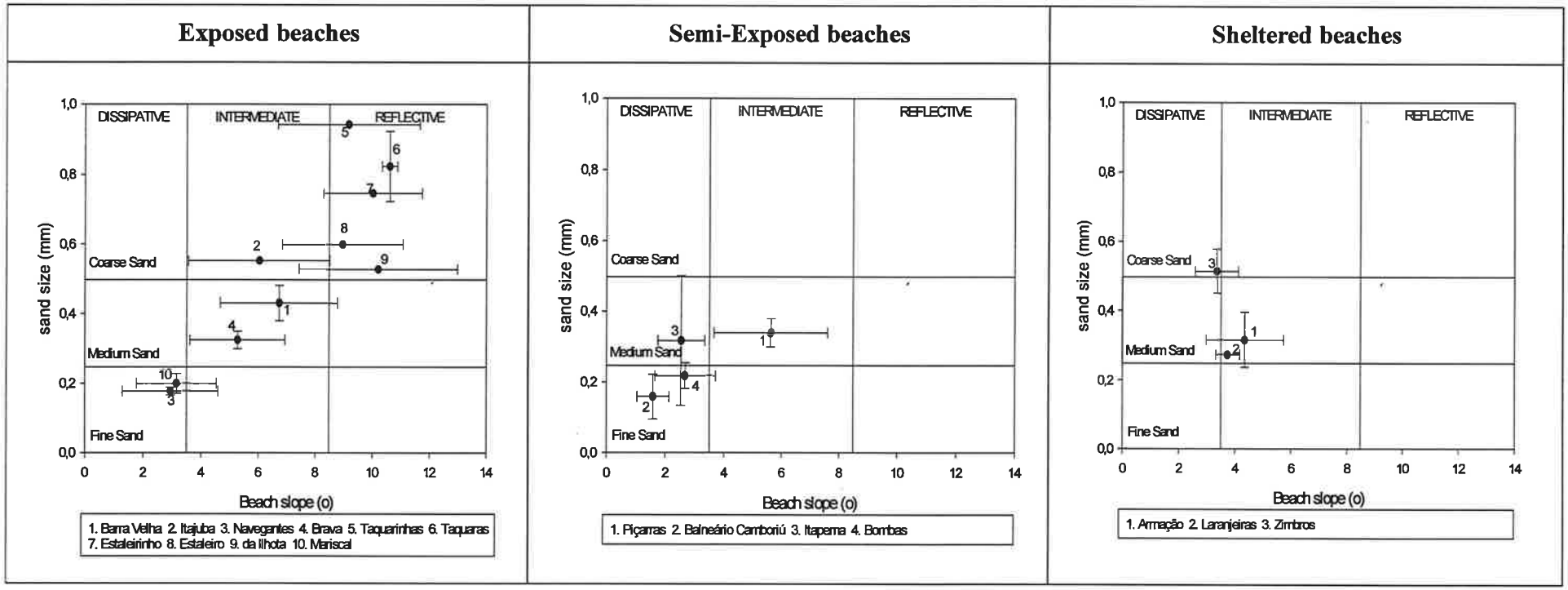

Figure 4.7. Grain size versus beach face slope for different beach types (exposed, semi-exposed and sheltered) for beaches on the Central-North coast of the State of Santa Catarina, Brazil.

Traditionally, wave height has been directly and positively correlated with beach sediment size (King, 1973; Bascom, 1951). However, the exposed and sheltered beaches from the study area do not show an obvious relation positively between grain size and wave height (see Table 4.2. and Figure 4.6. and 4.7.; and Chapter 6). There is a correlation between type of beach and grain size mainly for exposed and semi-exposed beaches (at exposed areas). Reflective beaches are composed by coarse sands (0.59mm-0.94mm) and dissipative beaches are composed by fine sands (0.20mm). Medium sands (0.30mm-0.45mm) defined intermediate beaches.

Short (1979), Wright and Short (1984) and more recently Short (1999), indicate that high-energy beaches can be composed by fine sand through coarse sediments (see Figure 4.6.). Short and Ni (1997) found that there was no correlation between wave height and sediment size; if anything the higher energy beaches have finer sand. This relation indicates that in headland bay beaches the average sand size is inherited from geological source and can be not selected by the prevailing waves (Short, 1999; Klein *et al.*, 1999; Miot da Silva *et al.*, 2000; see Chapter 6).

Beach type can be more directly associated with geological inheritance through its influence on sediment source and type. In the study area reflective beaches have coarser sediments resulting from reworking of older deposits (fan deltas or old barrier islands systems) (Figure 4.8a.). Dissipative beaches are associated with foredune ridges with fine sediment input (sand) through a river influx (Figure 4.8c.) and intermediate beaches are placed where medium sand reworked from old barrier islands (Pleistocenic deposits) and river sediment input occurs (Figure 4.8b.). There is a relationship between nearshore slope and the types of exposed beach. Reflective

beaches normally present steeper nearshore slope (1:40) than that intermediate and dissipative beaches (between 1:100 and 1:300).

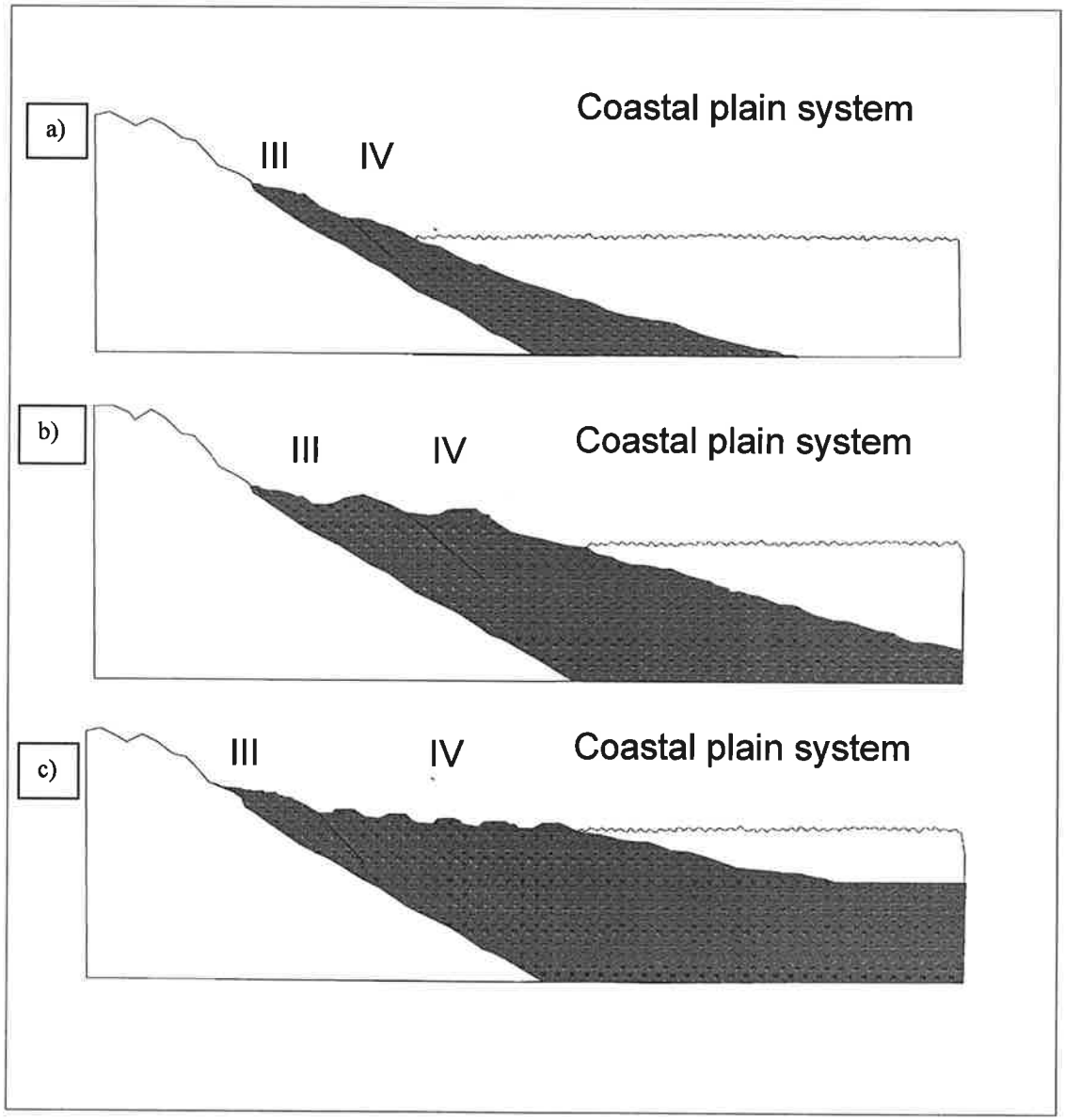

Figure 4.8. Relation between type of beach and coastal plain system for exposed beaches (a) Reflective beaches; (b) dissipative beaches; and (c) intermediate. (not to scale). Pleistocene sediments (III); Holocene sediments (IV).

4.3.1.1. Reflective Beaches Characteristics

The beaches of Itajuba, Taquarinhas, Taquaras, Estaleiro and Estaleirinho are classified as exposed reflective beaches (see Table 4.2.). Principal beach characteristics observed at Taquarinhas during the time of study are presented in Figure 4.9., as a representative example from exposed reflective beaches.

The general characteristics for all exposed reflective beaches during the study period were: backshore with one or two well developed berms; no frontal dunes; the width of the surf-zone between 10 and 30 meters; the wave breaker type are surging (unbroken) and collapsing between 0.7 to 1 meters in height; wave periods between 7 and 8 seconds; swash zone slope between 7 and 10 degrees; spacing of beach cusps between 10 and 35 meters; well developed beach step composed of coarse material (sand, rocks fragments and shells); beach scarp between 1.5 and 2 meters as a result of the storms actions; converging swash together with the beach cusps; swash zone with coarse to very coarse sand; nearshore zone with a slope between 1:20 and 1:40; average subaerial beach volume between 52 to 77 m^3/m, with a variation coefficient between 16 and 27%; average beach width between 29 and 37 meters, with variation coefficient between 14 and 25%; dimensionless fall velocity - Ω - parameter between 1.22 and 1.57; empirical dimensionless fall velocity between 0.67 and 2.19; and bar parameter between 2 and 17.

The exposed reflective sand beaches exhibited a large subaerial volume. Figure 4.9 shows the beach profile envelope and the subaerial volume and length change during the study time (e.g. Taquarinhas). It exhibits a cyclic change in volume and length. During storm period this beach presented a scarp and a terrace. No bars are present due to a greater nearshore slope (1:40). At Itajuba beach, nearshore slope was

about 1:300, much smaller than at other beaches, but with the same morphodynamic and morphometric characteristics as the other reflective beaches discussed in this study (see Table 4.2). In this case the grain size is the most important parameter to define the reflective stage.

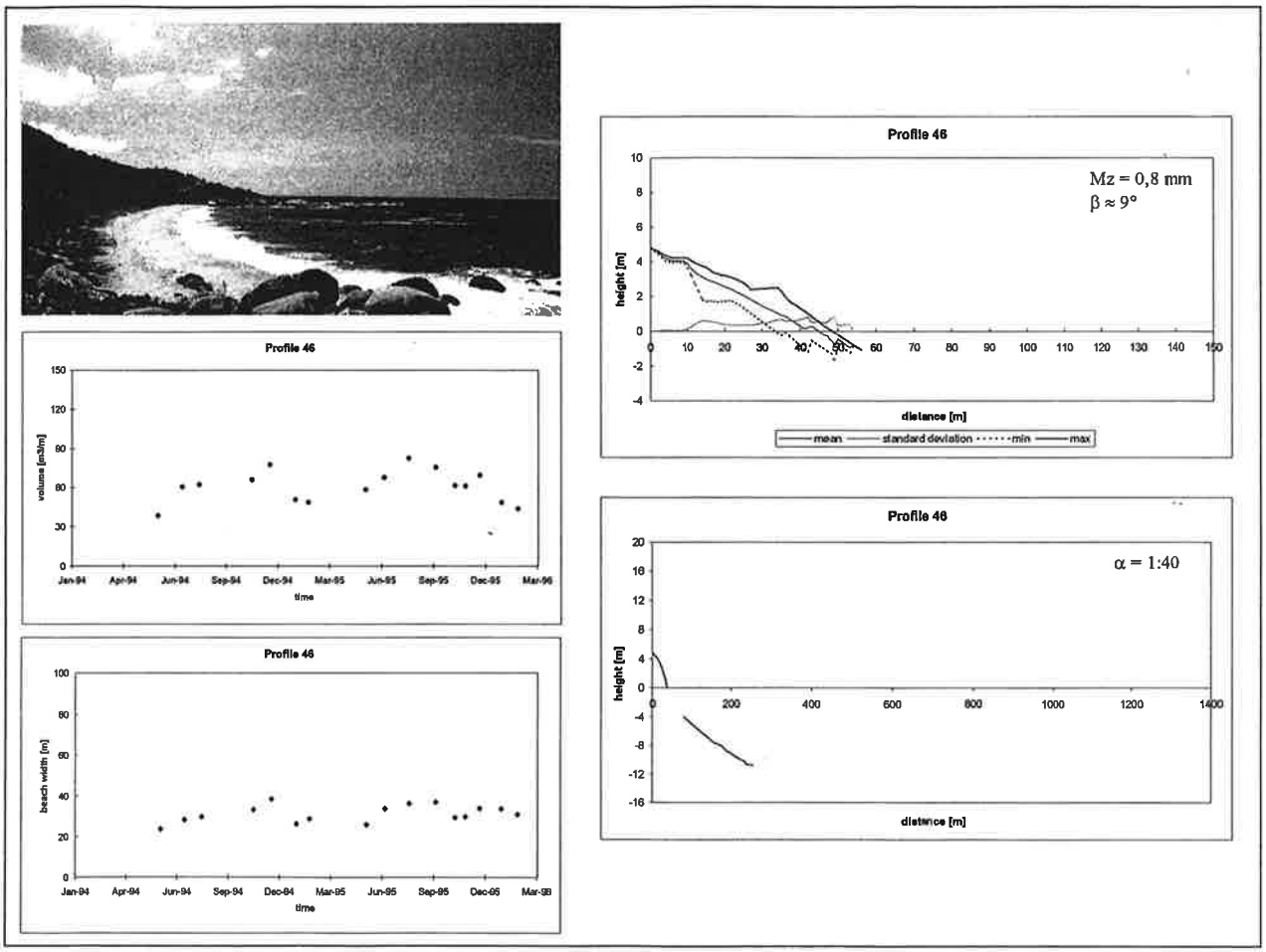

Figure 4.9. Principal beach characteristics observed at an exposed reflective beach during the study period (Taquarinhas beach). Note the narrow surf-swash zone.

4.3.1.2 Intermediate Beaches Characteristics

Three beaches are classified as exposed intermediate beaches in the study area: Barra Velha, Brava and Ilhota Beaches (see Table 4.2.). Figure 4.10 shows the principal characteristics observed at Barra Velha beach.

The beaches mentioned above presented similar characteristics during the study period. The backshore exhibited occasionally one well developed berm (mainly on Brava beach); well developed frontal dunes (Barra Velha); wide surf zone between 35 and 68 m; plunging and spilling breakers with heights between 0.7 to 0.8 m and wave period of 7 to 8.5 seconds; longshore bar and trough system, rhythmic and transverse bars; swash zone with slope between 5 and 10 degrees; spacing of the beach cusps range from 10 to 30 m and megacusps from 140 to 200 m; strong rip currents with a similar spacing; swash zone composed by medium sand; nearshore slope between 1:100 and 1:250; average subaerial volume from 16 to 37 m^3/m with variation coefficient from 15 to 63%; average beach width between 14 and 25 m with variation coefficient from 22 to 33%; dimensionless fall velocity – Ω - between 2.04 and 2.83; empirical dimensionless fall velocity between 0.82 a 3.06; bar parameter change from 15 to 41.

The bar type varied according to the beach as seen in the aerial photographs obtained in November, 1995 (Figure 4.11.). Barra Velha beach showed rhythmic and transverse bars. Brava beach had also longshore intercalated bars with bar parameter smaller than 20 (see Table 4.2.). Ilhota beach exhibited intercalated bars parallel to the coast. This variation was due to different morphodynamic stages.

Normally, the intermediate beaches are composed of medium sand (0.30mm-0.45mm) with gentle nearshore slope (1:100-1:200) (see Table 4.2.). The coastal plain

presents barrier island (barrier beaches and island bar) system (Barra Velha and Brava).

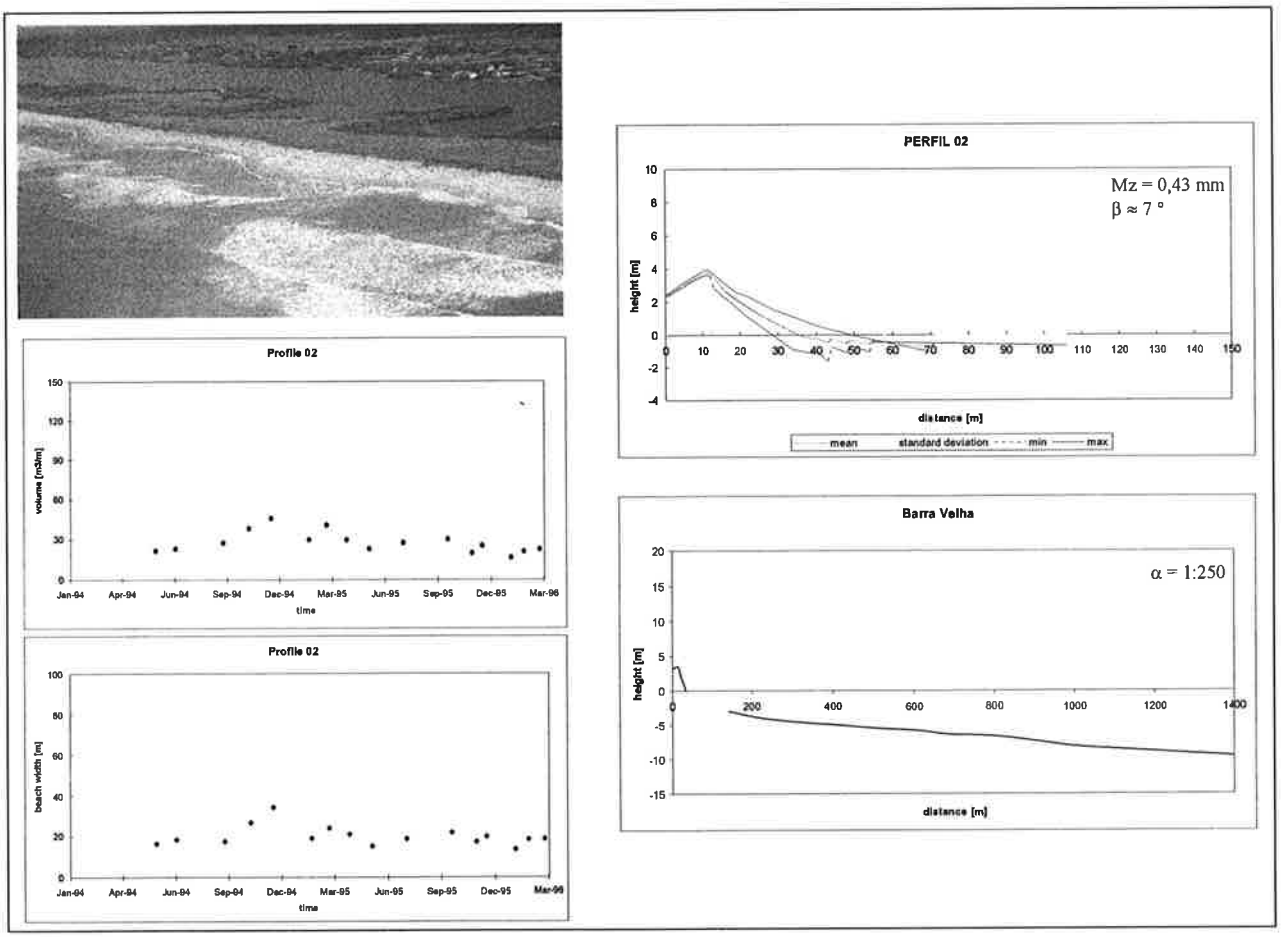

Figure 4.10. Principal beach characteristics observed at an intermediate beach during the study period (Barra Velha beach). Note the rhythmic shoreline (megacusps) and well developed rip channels.

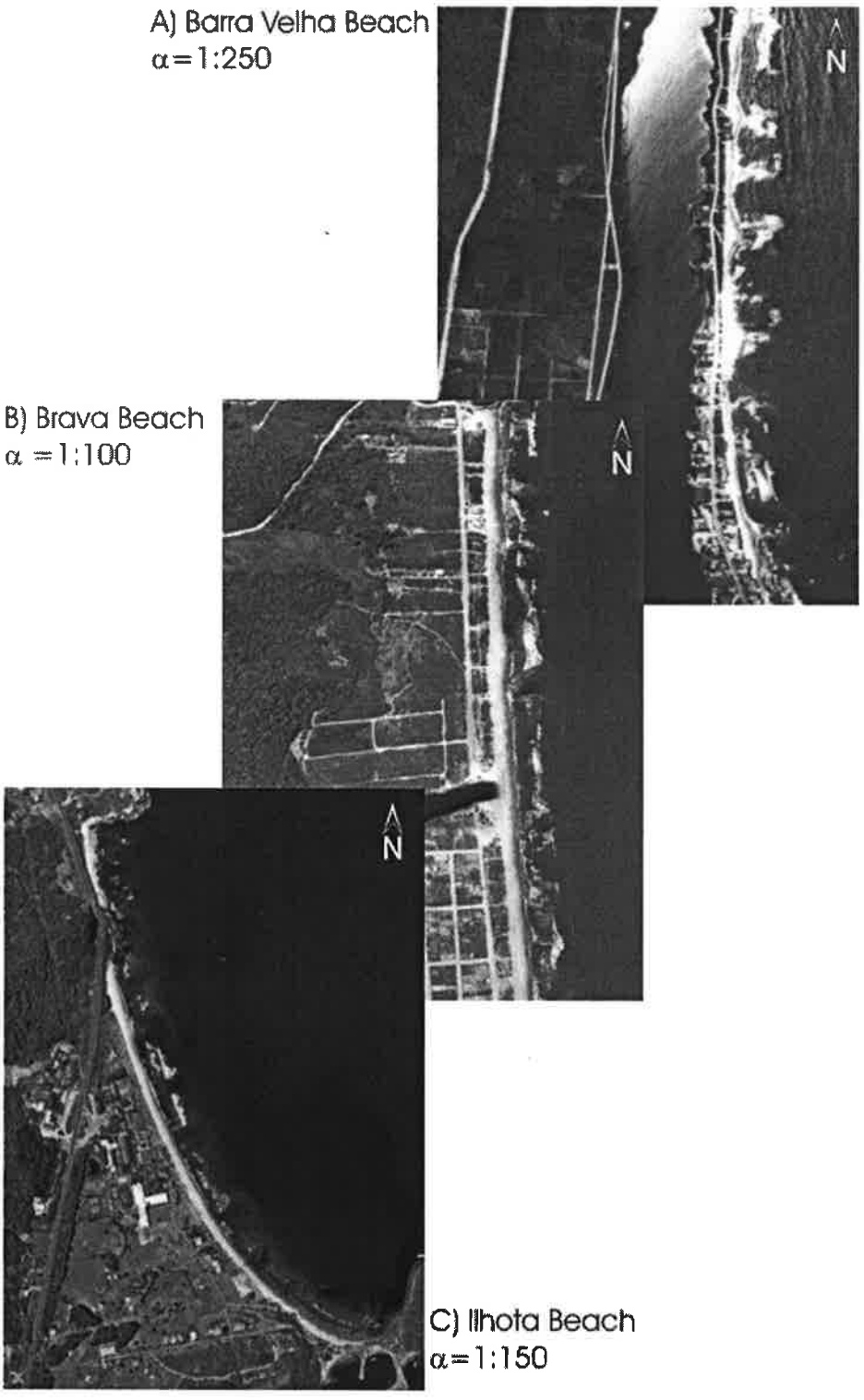

Figure 4.11. Intermediate beaches with different bar morphology: (a) Barra Velha beach; (b) Brava beach and (c) Ilhota beach (original scale 1:12,500).

4.3.1.3 Dissipative Beaches Characteristics

Navegantes and Mariscal are classified as exposed dissipative beaches. The sediment size at Navegantes beach is finer than that at Mariscal beach and the nearshore slope is smaller (see Table 4.2.). Figure 4.12. exhibits the main beach characteristics observed at an dissipative stage for Navegantes beach.

During the study period the following conditions were observed in dissipative beaches: very well developed frontal dunes (mainly Navegantes) with parallel scarp after storms; a surf zone width between 54 and 83 m; a plunging and spilling wave breaker; a wave height between 0.5 and 0.8 m and a period of 8 to 9 seconds; one bar (Mariscal) and multiple bar system (Navegantes with 2 bars); a beach face with an average slope of 3 degrees; spacing of the cusps between 15 and 24 m and megacusps between 165 and 300 m; stationary strong megarip currents; a beach face composed of fine sand (0.17 mm); a nearshore slope of 1:70 (Mariscal) and of 1:200 (Navegantes); an average subaerial beach between 26 and 39 m^3/m with a variation coefficient from 14 to 40%; an average beach width between 32 and 39 m with a variation coefficient from 10 to 24%; a dimensionless fall velocity between 4.23 and 7.68; a empirical dimensionless fall velocity between 15 and 21.5; and a bar parameter between 20 and 75.

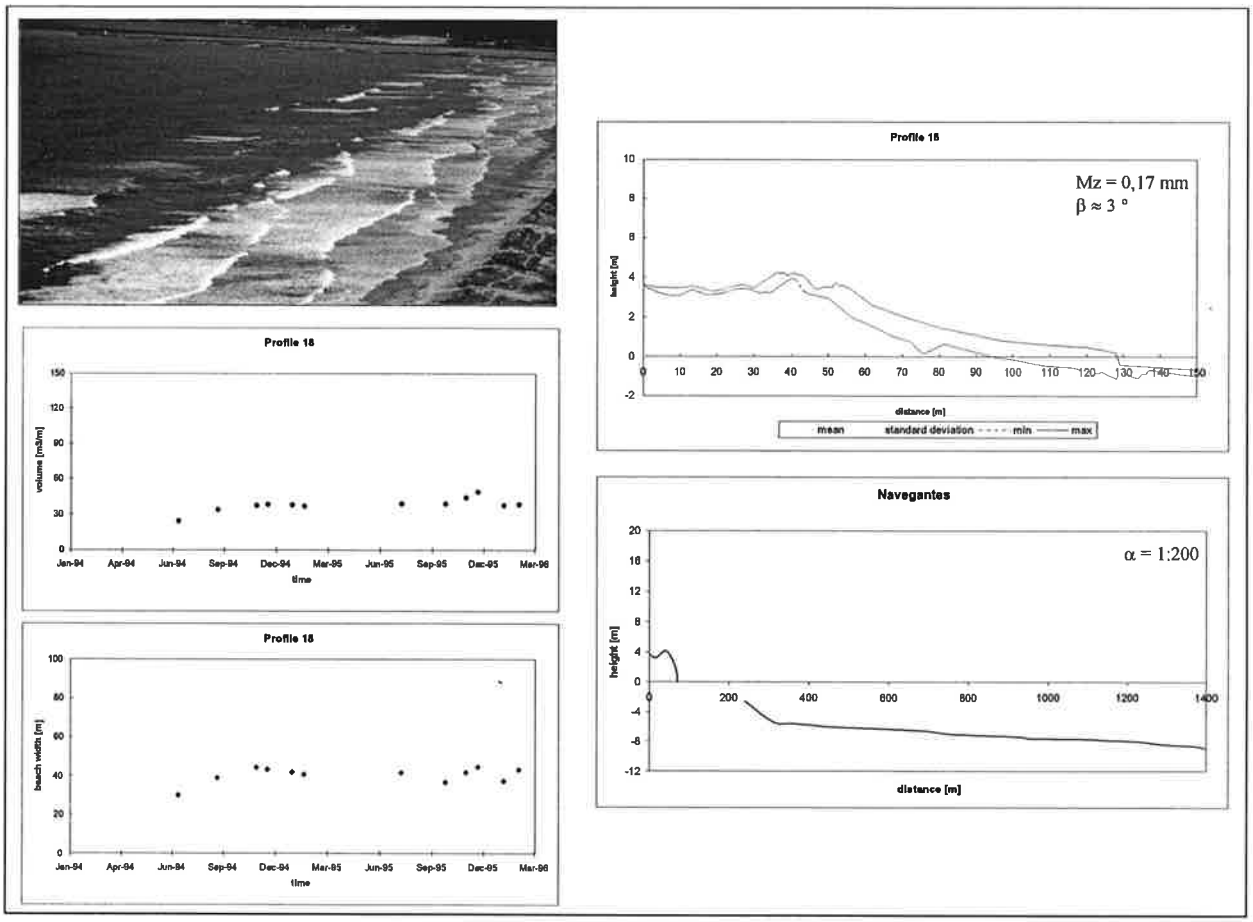

Figure 4.12. Principal beach characteristics observed at a dissipative beach, during the study period (Navegantes beach). Note the wide low slope surf zone and tow bars.

The Navegantes beach presents a multiple-bar system, which can be observed in the aerial photo (Figure 4.13. and Table 4.2.). This system is a response to the gentle nearshore slope formed in this case by Itajai river sediment supply during the Quaternary period (Abreu, 1998). This area is backed by a very well developed coastal plain comprising Holocene foredune ridges (Caruso and Araujo, 1999). The alongshore variation in the bar form at this beach is a function of longshore ranges in nearshore slope and consequently wave breaker (see Figure 4.1.).

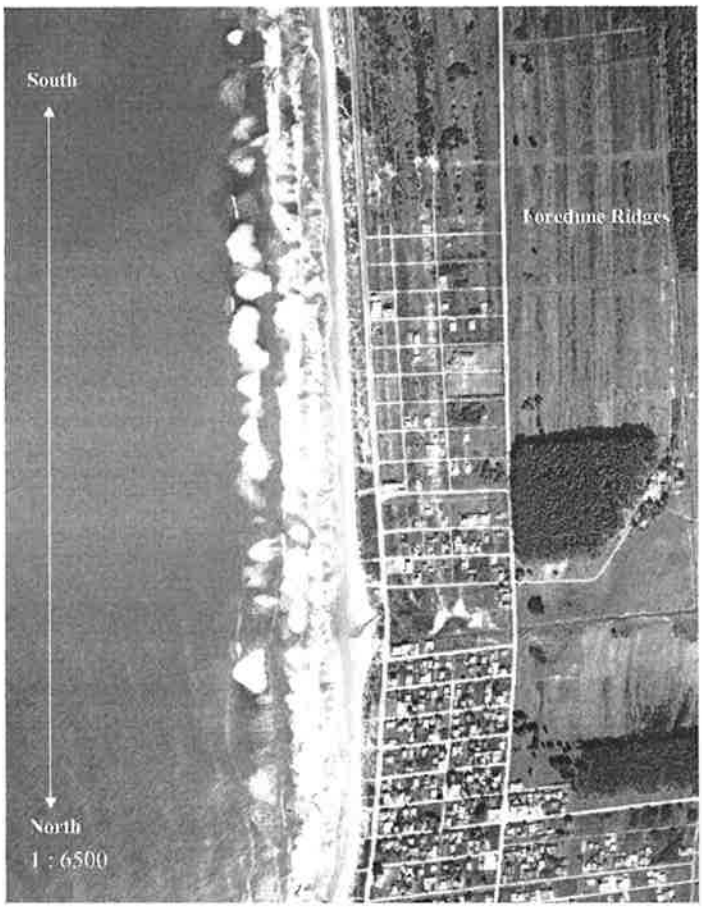

Figure 4.13. Multiple bars system of Navegantes beach (Original scale 1:12,500). Note the foredune ridge system on the coastal plain.

4.3.2. Semi-Exposed Beaches

The beaches partially exposed to southerly waves are: Piçarras, Balneário Camboriú, Itapema (see Table 4.2. and Figures 4.14., 4.15. and 4.16.) and Bombas. They have Northwest –Southeast orientation (see Figure 4.1.). Additionally, the Tijucas mud flat is introduced in this analysis to assess the influence of the sediment source (river input) in the coastal type.

volume [m3/ml]

Fi

volume [m3/ml]

Fi

The semi-exposed beaches exhibit similar characteristics (see Table 4.2.). Their plan form is a result of the distance between headlands and wave obliquity (Silvester and Hsu, 1997). Generally there is an alonghore morphological variation (see Figure 4.14. to 4.16.) that is a result from longhore variation in beach dynamics. The northern part of the beaches bay are more exposed (e.g profiles 7,8 and 9 – Picarras and 24, 25, 26, 27 and 29 - Balneário Camboriú– Figures 4.14. and 4.16.) while the southern portions of the bays are increasingly sheltered (profiles 11, 12 at Picarras and 37, 38, 39 at Balneário Camboriú). The plots of volume change also show that beach dynamics diminishes to the south in response to the lower waves. A large diffraction zone behind the southern headlands occurs. Hoefel (1998), Klein et al. (1997) and Temme *et al.* (1997) present similar results for Piçarras and Balneário Camboriú beaches, respectively. Rea and Komar (1975) and Leblond (1979) confirmed the important role of refraction and diffraction in the determination of the shape of embayed beaches with numerical models.

In Itapema the beach morphology and volume variation is relatively larger in the central area due to the presence of two diffraction areas at both ends of the beach (e.g. profile 53; Figure 4.16.). However, the variations in these parameters at Itapema beach are smaller than at other semi-exposed beaches.

Wave energy is low in the diffraction zone behind the southern headland, where the wave action is mild, therefore the relative tidal range (RTR) should be larger (Figure 4.17.). The larger the relative tidal range is, the more important tidal effects become in respect to wave effects. The concept of a relative rather than absolute tidal range provides an effective scaling for the mutual effects of waves and tides (Hayes, 1979; Davies and Hayes, 1984; Masselink, 1993; Masselink and Turner, 1999). The morphodynamics of microtidal sheltered zones, in an estuarine and bay beach, can be

in many aspects similar to that of a macrotidal beach (Masselink and Turner, 1999), since the difference in tidal range is compensated by the variation in wave-energy (Nordstrom and Jackson, 1990; Short, *per. com.*). In this type of area the relationships between wave obliquity, indentation ratio, grain size distribution (source) and relative tidal range are very important for the three-dimensional beach morphodynamics and profile sequence.

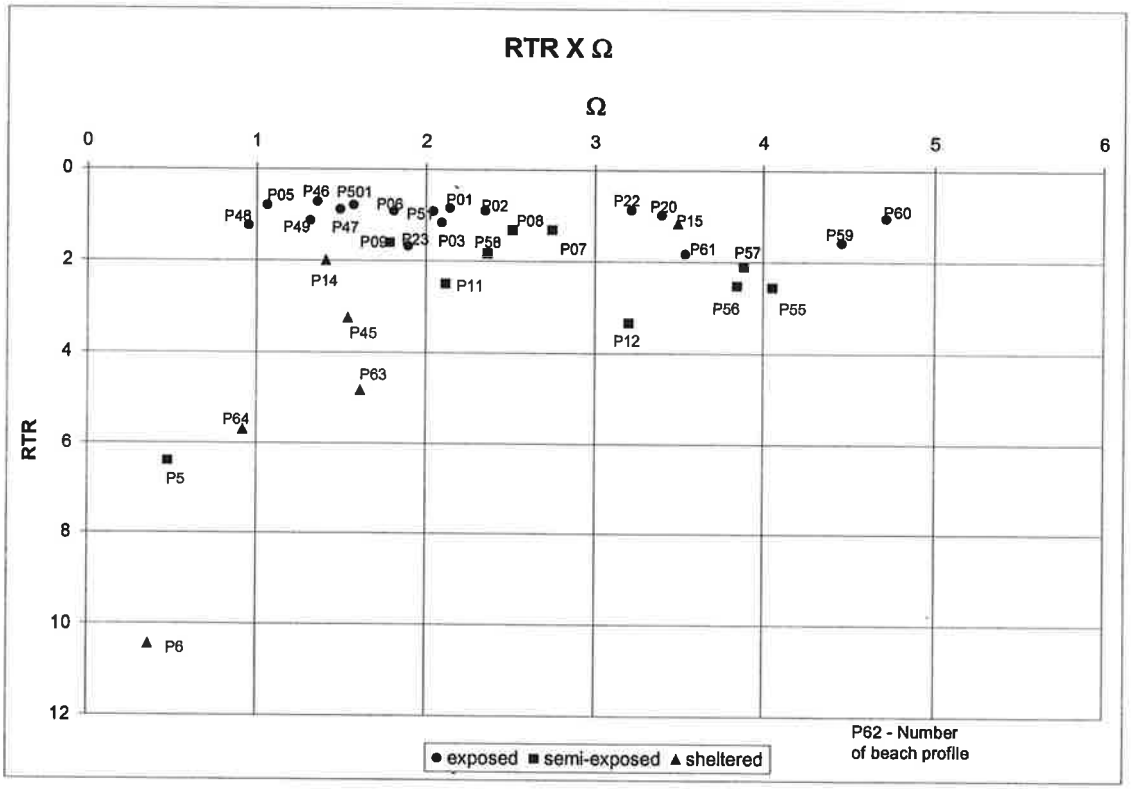

Figure 4.17. Parameter Ω versus relative tidal range for beaches during study period.

For a bay with large indentation ratio and fine sediment a flat beach develops near the headlands, occasionally sand with mud co-exists in this zone (swash zone and nearshore), due to milder waves and sediment input from a river (e.g. Balneário Camboriú beach). In this case, the sheltered zone must be classified as a mixed energy

enviroment (Hayes, 1979) and the length and volume of the beach change from the sheltered to the exposed zone (see Figure 4.14. to 4.16.). With wave increasing, more sediment deposition in the form of berm or bar takes place. Frontal dunes can also be developed in order to dissipate the wave energy during extreme events (beach buffer system).

Embayments can range from tidal flats to high-energy beaches depending on the level of the waves versus tidal energy. An extreme example in the study area is given at the river mouth in Tijucas Bay (Figure 4.18). The combination of fine sediment input (*mud*) from Tijucas River, low wave energy (sheltered zone) and gentle nearshore slope (1:400) results in a subaerial beach (ridge) with coarse sediment (*chenier* deposits), deposited during episodic periods (Caruso and Araujo, 1997; Schettini and Klein, 1997). Also present is a tidal flat with mud ridges in the intertidal and supratidal zone. The resultant coastal plain is composed of *cheniers* complex (Caruso and Araujo, 1997). At other semi-exposed beaches, the coastal plains are composed of Quaternary foredune ridges (Balneário Camboriú and Itapema) due to the sea level change during the Quaternary period (Caruso and Araujo, 1997; Caruso *et al.*, 2000a,b; Caruso and Araujo, 1999) and sediment input from rivers.

The principal beach characteristics of semi-exposed beaches observed during the study period were: backshore area with one berm (exposed zone); surf zone width between 5 and 110 m (sheltered to exposed zone); plunging and spilling wave breaker type; wave breaker height between 0.1 and 0.5 m and period between 6 and 8 seconds; beach face slope between 3 and 5 degrees; length of beach cusps range from 10 to 28 m; rip currents presented on the exposed zone; grain size range between fine and coarse sand; nearshore slope range from 1:35 (Bombas) to 1:550 (Itapema); average

subaerial volume between 20 and 36 m^3/m with deviation of 9% to 23%; average beach width between 17 and 40 m with deviation of the 8% and 32%; dimensionless fall velocity between – Ω – 2.4 and 10; empirical dimensionless fall velocity between 3.8 and 38; bar number parameter between 3 and 19; and relative tidal range between 1.66 (exposed) and 3.32 (sheltered area) (see Figures 4.14., 4.15. and 4.16.).

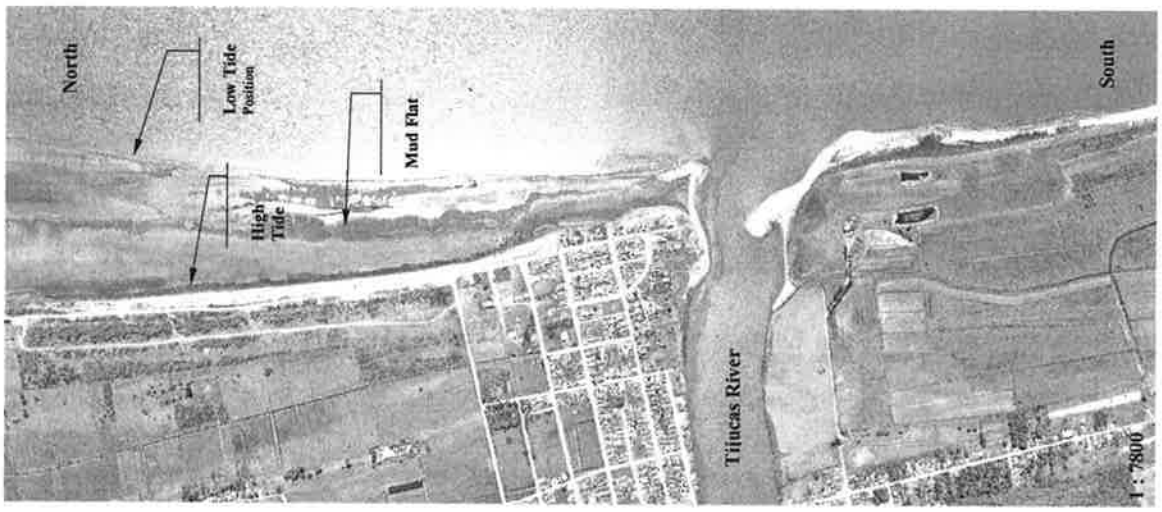

Figure 4.18. The tidal flat and mud ridge at the river mouth in Tijucas Bay.

The morphodynamic stage of the semi-exposed beaches therefore ranges from dissipative/low tide terrace to reflective. Piçarras beach shows a reflective modal stage (convex to linear beach profile with medium sand) in the north area (exposed) and dissipative/low tide terrace (concave and flat beaches profile with fine sand) in the south area (sheltered). Balneário Camboriú and Itapema Beaches exhibit dissipative or low tide terrace morphodynamic stage, mainly in the summer, with a barless beach profile varying from concave to linear. During lower low tide period a small seepage face occurs mainly on the foreshore zone from Balneário Camboriú beach. In this

beach during the summer time a ridge and runnel system in low swash zone (low tide) and rip currents occurs (Hoefel and Klein, 1998a,b) due to lowest sea level.

4.3.3 Sheltered Beaches

Armação, Laranjeiras and Zimbros beaches are classified as sheltered beaches. They have west – east orientation (see Figure 4.1.). The volume changes in these beaches are very small when compared with exposed and semi-exposed beaches (Figure 4.19.). This happens as a result of constant wave climate in this type of beaches. Similar results for Santa Catarina Island area are presented by Diehl (1997).

The sheltered beaches during the studied period had the following beach characteristics: surf zone width between 5 and 15 m; plunging and spilling wave breakers; wave breaker height between 0.1 and 0.5 m and period of 3.5 and 8 seconds; beach face slope range from 3 and 4 degrees; 10 m beach cusps length; grain size range from fine to coarse sand; nearshore slope range from 1:50 and 1:400; average beach volume between 18 and 36 m^3/m with deviation between 6% and 21%; average beach length between 22 and 32 meters with deviation from 4% and 15%; dimensionless fall velocity between 1.44 and 2.45; empirical dimensionless fall velocity between 3.83 and 7.43; bar parameter from 5 to 10; and relative tidal range between 1.59 and 6.98.

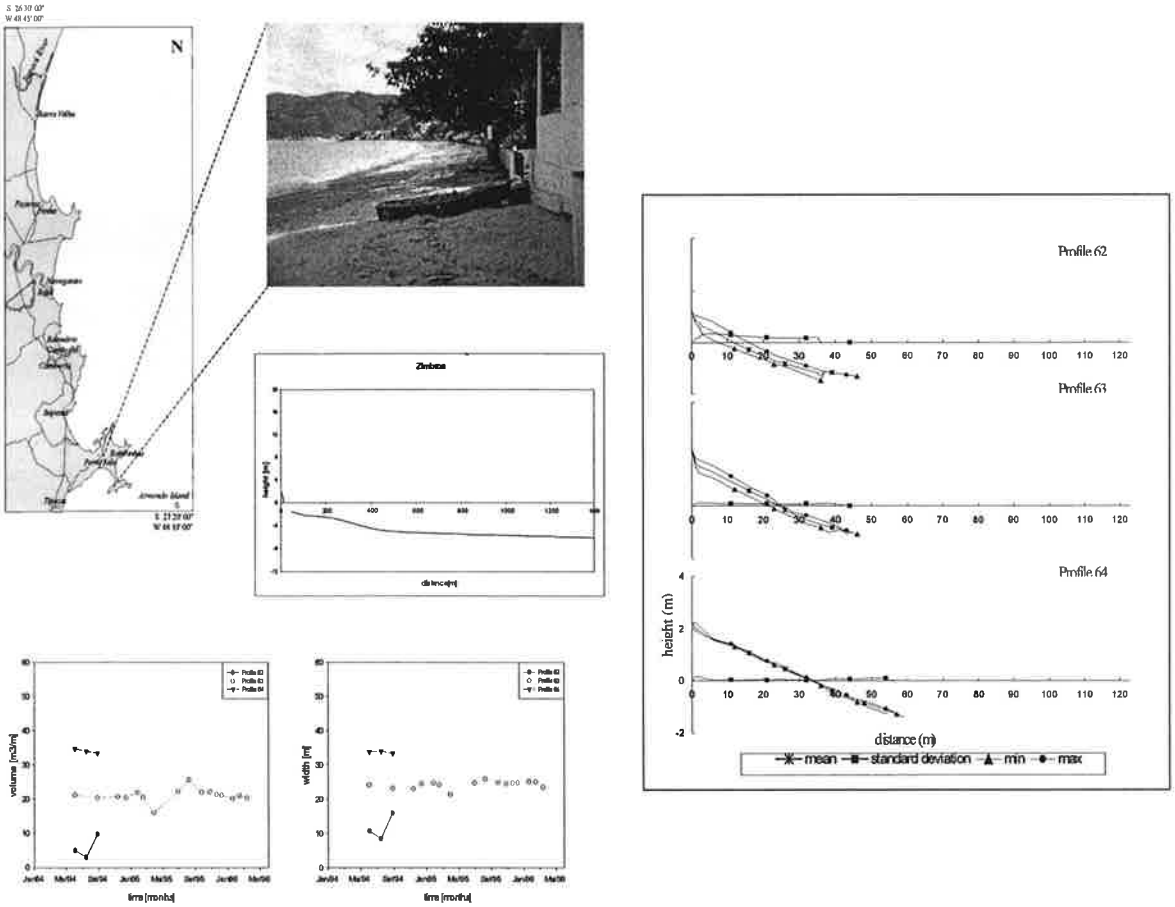

Figure 4.19. Principal beach characteristics observed in a sheltered beach stage (Zimbros beach), during the study period.

The larger the relative tide range , the more important are the tidal effects relative to wave effects or water level change (see Figure 4.17.). The morphodynamics of microtidal estuarine/sheltered beaches are in many aspects similar to that of macrotidal beaches (Masselink and Turner, 1999), since the difference in tidal range is compensated by the variation in wave-energy (Nordstrom and Jackson, 1990; Makaske and Augustinus, 1998). The shorter wave periods detected at Zimbros beach are a result from its geographical position. Generally, the waves were generated by local winds. This beaches can only be classified in relation to its morphology (profile

shape). Hegge *et al.* (1996) proposed seven (7) different morphologies for sheltered beaches in the Australian coast. They suggested a relation between concave profile and dissipative conditions and convex profile and reflective beach type. However, the results presented here show that it is difficult to include sheltered beaches in the morphodynamic classification proposed by Wright and Short (1984) and Short (1999) using the dynamic approach (see *e.g.* Omega (Ω) in Table 4.2.). These types of beaches are in the low limit between wave and tidal dominated environments and a small change in wave height results in a modification from the wave to tidal domain or vice –versa and also in the omega parameter (Short, *per. com.*). For this beach type, the source of sediment and consequently grain size, define the beach shape and slope (concave or convex). In direction to a more universal classification will be necessary intrudes the shape of beach in the parameters. The results shows that for sheltered beaches the empirical Omega are more realistic (see Table 4.2. and Figure 4.6. to compare). In this case the surf scaling parameter should give a better morphodynamic beach classification, since it is a descriptive equation of the state of the waves and beach gradient (Short, 1999). A non-dimensional parameter to define the morphology should also be introduced to compare the wave and tidal environment beaches at the same scale (Eliot, *per com.*).

4.4. BEACH PROFILE SEQUENCE MODEL

Based on the description for the major types of beach state, the average values for each beach parameters can be summarised. This is presented in Table 4.3. and Figure 4.20.. Table 4.3. provides the general morphodynamic and morphometric characteristics of the headland bay beaches in microtidal-east coast swell environment

with a wide shelf. Figure 4.20. shows a model sequence of beach profiles or alonghore morphology variation and the types of beaches associated with headland bay beaches in east-coast swell environment. Beach type and mobility is a function of distance between headlands, bay shape, wave exposure, grain size (source), nearshore slope and relative tidal range.

Two types of reflective beaches can be observed. In exposed areas, they have large quantities of subaerial sediment and high mobility, due to the change in wave climate and consequent beach erosion and accretion.

During storm events, scarps form up to 2 m high and the sediment deposits in the form of a terrace, since the nearshore beach slope is too steep to form bar systems (1:20 to 1:40). A bar system occurs only occasionally on Itajuba beach (nearshore slope 1:300). These reflective beaches exhibit a convex to linear profile with one or two berms composed of coarse sand. Normally, steep slope with coarse sediments and well-developed beach cusps are present.

The reflective beaches in semi-protect and sheltered beaches are stable as described by Short (1979) and Short (1999), since the wave climate range is smaller in the shadow zone (result of diffraction zone and more interaction with gentle slope). The beaches have medium to coarse sand, and exhibit convex to linear profile, with smaller sediment volume. Frontal dunes are not present.

Intermediate conditions are more frequent on exposed beaches with medium sand. They contain only one nearshore bar that can be longitudinal, transverse or rhythmic, and the mobile subaerial volume and its changes are less than on the reflective beaches because the wave energy is dissipated mainly on the bar (beach buffer system).

Table 4.3. General morphodynamic characteristics of headland bay beaches.

Characteristics	Exposed Reflective	Exposed Intermediary	Exposed Dissipative	Semi-exposed	Sheltered
Relative Tidal Range (RTR)	0.9	1	1.2	2.25	3.9
Wave break height	0.9	0.8	0.7	0.4	0.3
Wave period	7.6	7.7	8.5	7	5.8
Approximately Surfe Zone Width	10-30	35-68	54-83	5-110	5-15
Wave breaking type	Colapsing/ Surging	Plunging/ Spilling	Spilling Plunging	Spilling Plunging	Spilling Plunging Surging
Rip currents	Present	Strong	Strong and stacionary	Presents (change)	Absent
Bars	Absent	1	1 to 3	Absent (change)	Absent
Beach slope	7-10°	5-10°	3°	3-5°	3-4°
Inner Shelf Slope/Nearshore Slope	1:88	1:166	1:135	1:255	1:183
Beach form	Convex to Linear	Convex to Linear	Concave to Linear	Change	change
Cusps length	15-30	10-30	14-24	10-28	10
Megacuss length	Absent	140-200	165-300	Absent	Absent
Foreshore grain size	Coarse sand	Medium sand	Fine Sand	Fine to coarse sand	Fine to coarse sand
Ws (cm/s)	12	6	2	2.73	5
Frontal Dunes	Absent	Presents	Presents	Absent (change)	Absent (change)
Omega parameter	0.60	2.4	6	4.79	1.8
Theoretical Omega	1.3	2.2	18.3	19.2	5.4
Average mobile beach length	32	21	36	28	27
Standard deviation from average mobile beach length	3	6	5	10	5
Average mobile subaerial beach volume	60	26	29	29	26
Standard deviation from average mobile subaerial beach volume	10	11	8	8	9

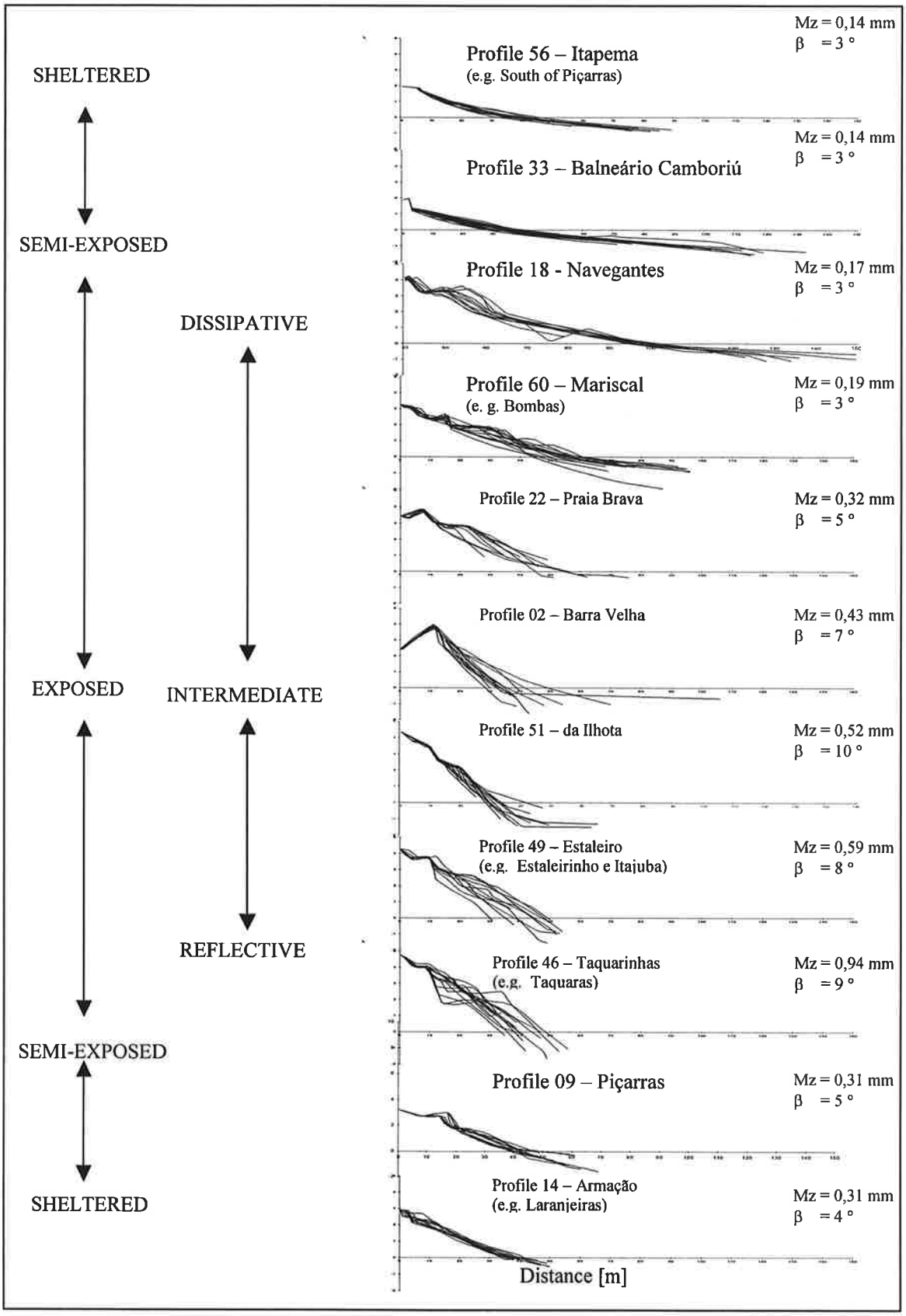

Figure 4.20. The model sequence of beach profiles and beach types for headland bay beach morphology, in east coast east coast swell environmental. The figure shows examples of beaches from central north of Santa Catarina State, Brazil.

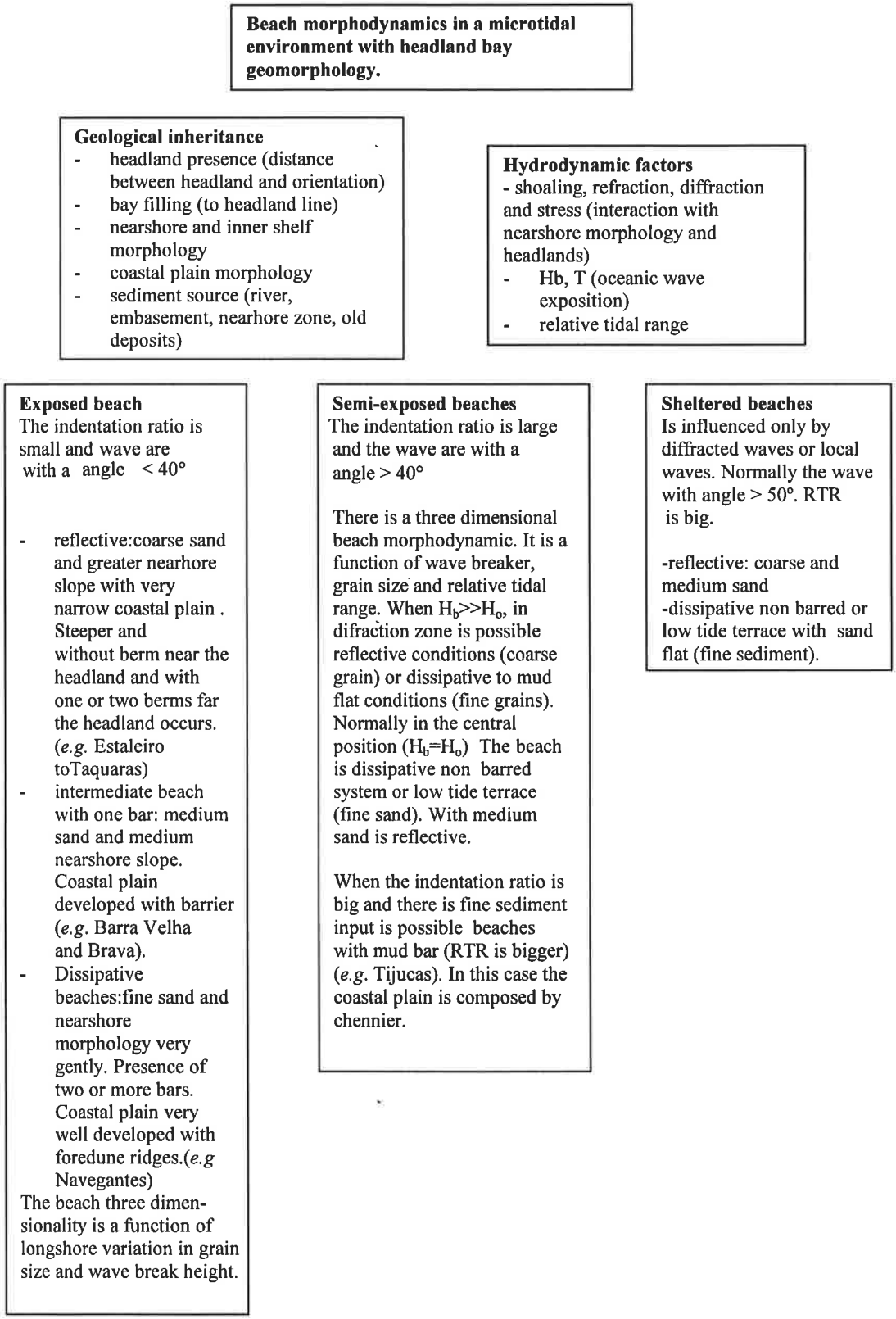

Figure 4.21. Beach morphodynamic parameters for beach classification in a microtidal environment with headland bay beach morphology, based on geological inheritance and hydrodynamic factors

After breaking at the bar, waves reform and break again with less energy in the swash zone. Strong rip currents occur and these are responsible for local rip embayment erosion as reported by Short (1999). The beach profile is linear and with short to well developed frontal dunes formed mainly by overwash processes, e.g. Barra Velha (Klein *et al.*, 1999).

The dissipative beaches occur in the three types of exposure. In exposed areas, they are well developed, composed by fine to very fine sand, with two (2) or more bars and well-developed frontal dune. The surf zone is up to hundreds of meters wide. During storms parallel scarps in the dunes can be developed as also described by Short (1999).

The beach profile is linear and the subaerial volume change is small. In the semi-exposed areas no bars in the surf zone are present and the profile is from concave to linear with fine sand composition, whilst a low tide terrace with small swash bar in the low tide position can occur during summer. Rip currents are present in the exposed zone. Normally, the swash zone presents backwash ripple morphology similar exposed to dissipative beaches. These characteristics are representative of an ultradissipative beach, but in minor scale of size than tidal dominated beach classification proposed by Short and Masselink (1999).

In sheltered areas, beaches are composed by fine to very fine sand and the profiles are concave, with narrow beaches and the nearshore zones are composed of very fine sand with mud. Normally, the nearshore slope is smaller than in reflective conditions.

The final type of profile not represented by the model, is a intertidal zone with mud bars with subaerial coarse deposits, which is a result of the combination of fine sediment input (river), very slow nearshore slope and sheltered conditions.

4.5. SUMMARY

Beach morphodynamics in a microtidal environment with headland bay geomorphology can be classified with the morphodynamic and morphometric parameters highlighted in Figure 4.21. They are a function of: 1) Geological inheritance (distance between headland and orientation; nearshore and inner shelf morphology; coastal plain morphology; sediment source); and 2) Hydrodynamic factors (Hb, T, oceanic wave exposition and relative tidal range).

For a coast with headland bays, the alongshore range in beach geomorphology is a function of headland distance, bay shape, wave obliquity, indentation ratio, grain size distribution and nearshore slope. Both models presented by Short (1999, pg.8) and Carter (1988, pg. 214) are possibly dependent on geological inheritance and hydrodynamic characteristics of the study area.

The beaches are classified as: (1) exposed, (2) semi-exposed or (3) sheltered. In the exposed beaches, the indentation ratio is small and waves approach the coast parallel. They can be divided into three types: Firstly, (a) reflective beach, occurs with coarse sand and steep nearshore slope with a very narrow coastal plain. Steep backshore without berm near the headland or with one or two berms far the headland can also occur (Estaleiro to Taquaras). This type of beach is present when the bedrock is exposed at the coast.

Secondly (b) intermediate beach have one bar with medium sand and medium nearshore slope. Coastal plain developed with barrier island (Barra Velha and Brava). And thirdly, (c) dissipative beaches have fine sand and gentle nearshore morphology with the presence of two or more bars. The coastal plain is very well developed with foredune ridges (Navegantes). The three dimensionality of these beaches is a function of longshore variation in grain size and wave breaker height.

In semi-exposed beaches the indentation ratio is larger and the wave obliquity is usually greater than 40°. A three-dimensional beach morphodynamics is presented and it is a function of wave breaker height and grain size and relative tidal range. When $H_b << H_o$, the diffraction zone may be in reflective condition with coarse grain or dissipative/low tide terrace to sand-mud flat condition with fine grains. Normally, in the central position ($H_b \geq H_o$) the beach is dissipative without bars or low tidal terrace (fine sand), but reflective with medium sand. When the indentation ratio is larger and with fine sediment input from rivers, beach and mud flat with mud ridges (RTR is larger - eg. Tijucas) are possible. In this case, the coastal plain is composed by *chenier* systems.

Only diffracted waves or locally-generated waves influence sheltered beaches. Usually, waves approach the beach with angle greater than 50°. RTR is larger (>2). Again, they can be divided into: (a) reflective mode with medium to coarse sand with convex to linear profile and (b) dissipative mode non-barred or low tide terrace (fine sediment) with concave to linear profile.

The present sequential beach profile model is a first approximation. Studies in other areas with the same geographical characteristics and better wave data (wave rider) are necessary to provide more information and the model validation. The present model can be applied to define the type of coastline uses and, when combined with the parabolic model from Silvester and Hsu (1997), it can be used to make better nourishment and coastline design projects for this type of coastline.

CHAPTER FIVE

Beach Rotation Phenomena on Headland Bay Beach

Unless referred to otherwise, the contents of this thesis are the results of original research carried out by the author

Some of the results have been published in:

KLEIN, A.H.F; BENEDET FILHO., L. and SCHUMACHER, D.H., 2002. Short - Term Beach Rotation Processes in Distinct Headland Bay Beach Systems. *Journal of Coastal Research*, 18(3), 442-458.

5.1. INTRODUCTION

Seasonal longshore and cross-shore sediment transport takes place in headland bay beaches simultaneously. While the cross-shore component is responsible for interactions between the subaerial beach and submerged bars, longshore transport is responsible for rotation of beach planforms, as shown diagrammatically in Figure 5.1. Beach rotation processes are common associated with headland bay beaches. According to Short and Masselink (1999), beach rotation refers to a change in direction in alongshore-sand transport between opposite extremities of headland bay beaches. These alternations of sand transport directions are attributed to periodic or long-term changes in wave climate, mainly in wave direction.

A beach rotation phenomenon occurs over a range of time scales, incurring in large variation and movement of the coastline without net gain or loss of sediment in the compartment or cell. However, this process was only well understood for an intermediate beach stage by Short *et al.* (1995, 2000). These authors, analyzing twenty years of data, and discovered a rotation cycle between 3 and 8 years. The rate of change is related to the size of bay, wave period and the magnitude of wave directional change. Farias *et al.* (1985) and Bittencourt *et al.* (1987) in Brazil and Masselink and Pattiaratchi (2001) in Australia reported the same phenomena of beach rotation in short-term scale (one to two years), without considering the type of beach morphology.

The purpose of this chapter is to explain morphological changes in headland bay beach, with emphasis on the short-term beach rotation processes, elucidating how it is affected in planform by the degree of beach curvature, and by morphodynamic characteristics of the beach systems.

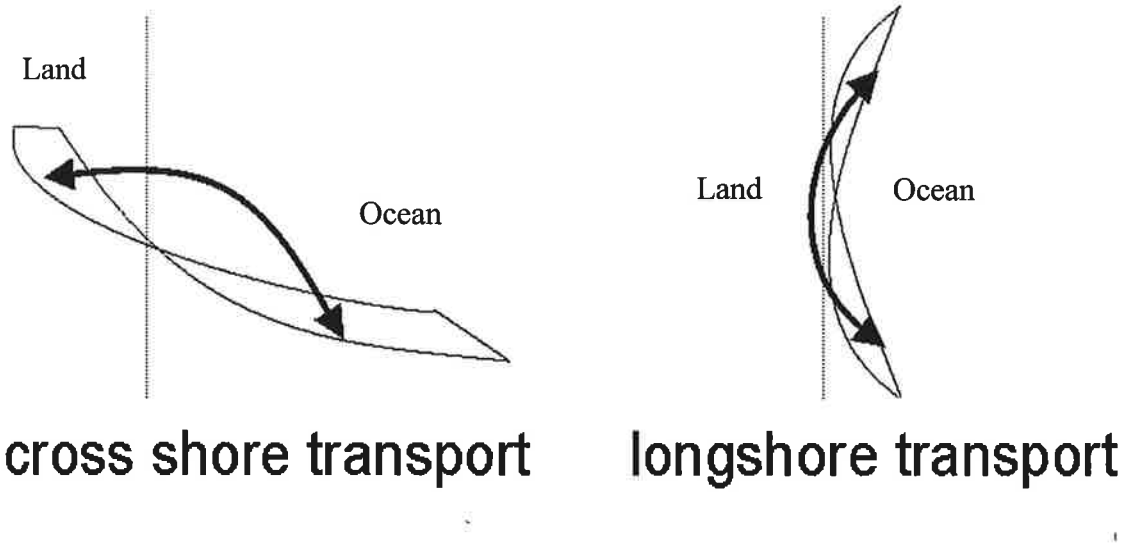

Figure 5.1. Cross-shore and longshore transport components in headland bay beaches and their resultant interactions. The diagram on the right represents the rotation of the beach planform as a result of shifts in longshore drift direction at headland bay beaches (modified from Verhagen, 2000).

5.2. ENVIRONMENTAL SETTING

Three beaches were monitored in the present study, Brava, Balneário Camboriú, and Taquaras/Taquarinhas. Those beaches are located in the central-north coast of Santa Catarina between 26°30' S and 27°20' S (Figure 5.2), in the coastal macro-compartment of the Crystalline Scarps (Muehe, 1998), sector 3.

Balneário Camboriú is a headland bay beach in the form of a broad arc that is delimited by two rocky outcrops with a central salient. The salient results from the diffraction of incident waves when they meet das Cabras Island. The shoreline is 5840 m long, with a average dry beach width of 17 m, and a general NW-SE orientation. The northern portion of the beach is exposed to waves from the SE, but its southern sector is more sheltered. This dissipative beach is composed of fine sand (0.16 mm), and shows

wavelength of beach cusps between 15 and 20 m (Temme *et al.*, 1997; Menezes, 1999; Benedet Filho *et al.*, 2000; Miot da Silva *et al.*, 2000, Klein and Menezes, 2001).

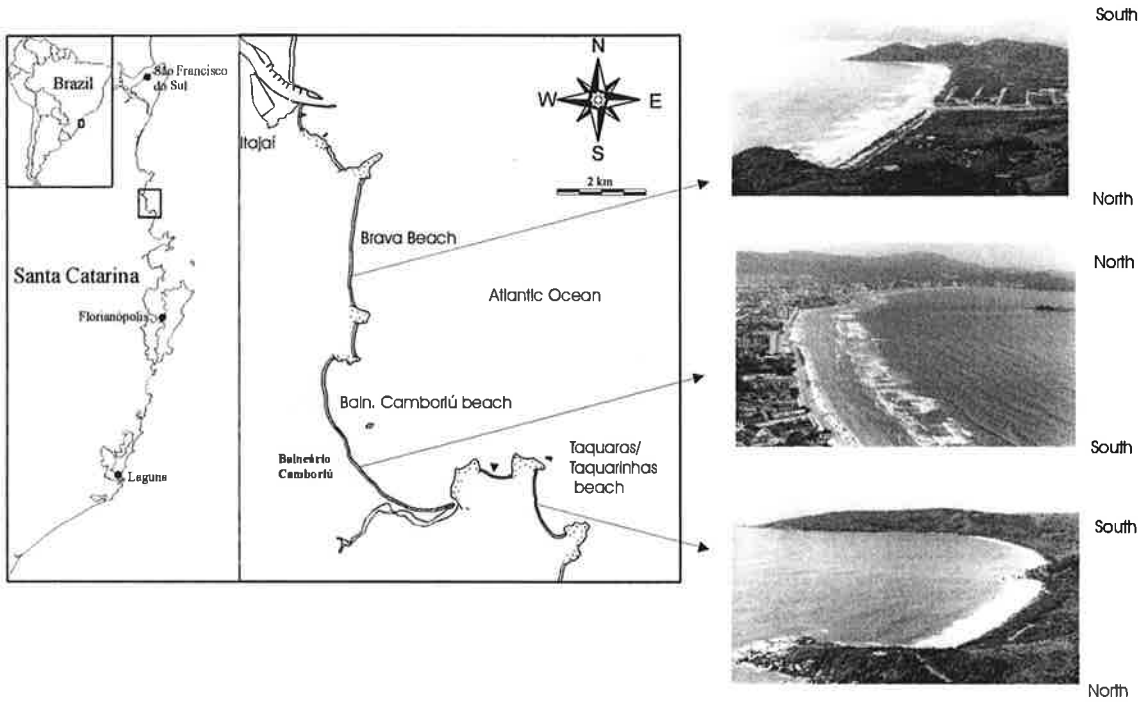

Figure 5.2. Study area and oblique aerial photos showing Balneário Camboriu, Brava, and Taquaras/Taquarinhas beaches.

Brava Beach is a headland bay beach with little curvature between the rocky outcrops. The shoreline is 2650 m long, with an average dry beach width of 34 m, N-S orientation, and is exposed to waves from the SE. This intermediate beach is composed by medium sand (0.32mm), has submerged bars, 25 to 30 m long beach cusps, and megacusps wave length spaced about 160 m between horn. Strong rip currents are also present (Hoefel and Klein, 1998; Dafferner *et al.*, 2002).

Taquaras/Taquarinhas Beach is divided by a rocky outcrop that extends about 10 m offshore, located in the northern sector of the beach arc. For this study these beaches

are considered to be part of the same beach system, as they belong to the same beach arc and the outcrop does not interrupt the continuity of the shoreline. They have also similar sedimentary characteristics (Miot da Silva *et al.*, 2000) and sediment exchanges (Benedet Filho *et al.*, 2000). This beach system has a parabolic planform, with a curved zone, a transitional zone, and a straight end. The shoreline is 1570 m long, with an average dry beach width of 27 m (Menezes, 1999). This reflective beach is composed by coarse sand (0.90 mm), has a N-S orientation, and is exposed to the waves from the SE quadrant. Morphologic characteristics include beach cusps wave length between 30 to 35 m, and there are no submerged bars (Menezes, 1999; Benedet Filho *et al.*, 2000; Klein and Menezes, 2001).

5.3. SAMPLING AND ANALYSIS

5.3.1. Point of Greater Indentation and Indentation Ratio

The following parameters were estimated from aerial photos from 1978 (1:25,000 scale) and from 1995 (1:12,500 scale): control line (R_β), predominant wave direction (β), and greater indentation (a), following the methodology proposed by Hsu and Evans (1989), Silvester and Hsu (1993) (see Figure 5.3). Two basic parameters in their method are the reference wave obliquity β and *control line* length R_β (Figure 5.3). Variable β is a reference angle of wave obliquity or that between the incident wave crest (assumed linear) and the *control line*, which is the line joining the upcoast diffraction point to the near straight downcoast beach (see Figure 5.3).

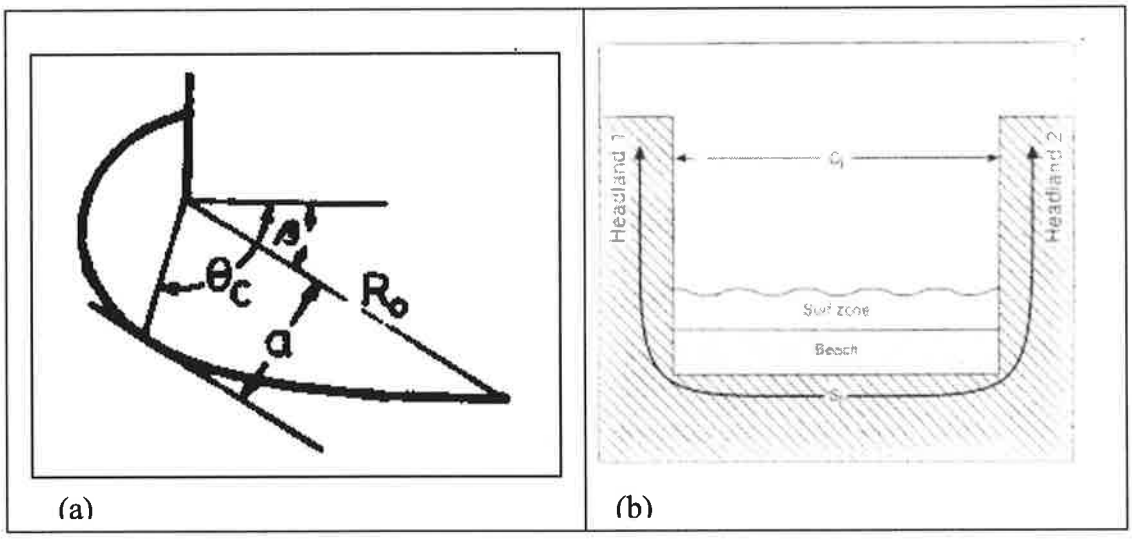

Figure 5.3. (a) Illustration of the "a" and R_β parameters according to Silvester and Hsu (1993), and (b) the CL and SL parameters according to Short and Masselink (1999).

The greater indentation is drawn normal from the control line to the point of more pronounced retreat of the bay shoreline. The point between the downdrift headland and the greater indentation is the shadow zone of the bay, protected from the direct attack of the incident waves. The indentation ratio (a/R_β) indicates the degree of curvature of the headland bay beach.

5.3.2. Relation Between Embayment Width (CL) and the Length of the Embayment Shoreline (SL)

To measure the shoreline curvature (deepness of the bay), and make further comparisons with the indentation ratio from Silvester and Hsu (1993), and with the morphological changes observed at the headland bay beaches, the relation between the shoreline length and the embayment width (SL/CL) is used. The parameters SL and CL

(illustrated in Figure 5.3) were derived from the nondimensional embayment scaling parameter (δ') described by Short and Masselink (1999).

5.3.3. Beach Profile Measurements

Balneário Camboriu Beach profiles were obtained between January 1994 and February 1996. Eighteen profiles were monitored monthly along the beach shoreline, six profiles were chosen for the present chapter. The profiles were monitored with a leveling instrument (Leika) as proposed by Birkemeier (1981) and evaluated by the Interactive Survey Reduction Program (ISRP) (Birkemeier, 1985).

At Brava and Taquaras/Taquarinhas beaches, profiles were obtained between January and November 2000. Five profiles were monitored at Brava Beach and six profiles at Taquaras/Taquarinhas Beach; a total of 17 surveys were conducted. The profiles were obtained using an electronic theodolite, as proposed by Borges (1977), which consists of profile measurement using trigonometry. Beach profile surveys were carried out every fifteen days.

A scheme of the beach profile envelope is shown in Figure 4.4a (Chapter 4). As described in Chapter 4, the x-axis extends seawards and the y-axis extends vertically upwards. The origin of the co-ordinates is located at mean sea level at a fixed reference point. The morphological variables are computed using the landward boundary (X1) and the seaward boundary (X2) as recommended by Temme *et al.* (1997). The landward boundary (X1) is constant per profile. The locations of these points were determined using the profile envelopes shown in Figure 5.4. The location of X1 is chosen so that this part of the profile is not included in the analysis. The seaward boundary, the location of mean sea level (X2) is used in all cases; as a consequence, only the subaerial

parts of the profile change are analyzed (mobile subaerial zone). The beach volume (V) is defined as the cross-sectional area within the boundaries X1 and X2 per unit length of the shoreline (Sonu and van Beek, 1971). The width of the beach (L) is defined as the distance between the boundaries X1 and X2.

Simple linear correlation tests were made between the beach volume and beach width variations for different profiles on the same beach. Correlations were considered to be significant when $p<0.05$. The correlation tests were conducted to check for positive or negative correlation between the variations of beach width and beach volume in the profiles located on opposite ends of the headland bay beaches. Period fluctuations less than one month were filtered using moving average with the interval of two surveys, and anomalies were calculated in an effort to enhance the graphic visualization of the beach volume and width fluctuations.

5.3.4. Visual Wave Estimations

Visual wave observations were made almost daily on the northern end of Brava Beach from January to November 2000. The visual wave estimations were made using the methodology adapted from the sea sentinels project (Melo, 1 993). The following wave parameters were collected:

1) Wave direction was obtained from the top of the headland, from the direction of propagation of wave trains in deep water, relative to the coastline orientation, which was obtained from nautical charts.
2) Wave breaker height was visually estimated in 0.5 m intervals as the difference between wave crest and trough.

3) Wave period was estimated using a chronometer, as the interval of time elapsed between the passage of two consecutive wave crests past a fixed point such as boats, surfers floating, or fixed structures. The procedure is repeated three or four times for calculations of an average.

Simultaneously to visual wave observations in daily wave forecast models were recorded from the following Internet sites: www.atlasul.inpe.br and www.fnmoc.navy.mil. These model images were used to visualize the fetch of the incident waves, as well the predominant direction of wave propagation in the offshore zone.

There were a total of 238 daily wave observations. Wave height was represented in a temporal series to visualize the peaks of greater wave height. The wave period was divided in five frequency classes of occurrence. Wave direction data were divided into three main directions of approach, and their monthly frequency of occurrence were calculated to detect shifts in predominant wave direction throughout the year.

5.4. RESULTS AND DISCUSSION

5.4.1. Beach Planform Measurements and their Relation with Profile Mobility

Figure 5.4 shows the planform of monitored beaches with their respective control line (R_β) and indentation (a), accompanied by profile variations in the sheltered zone and volume variations in exposed and sheltered zones plotted together. Indentation ratios (a/R_β) and the values of Sl/Cl are shown in Table 5.1. The more indented beaches, Balneário Camboriú and Taquaras/Taquarinhas show a/R_β values on the order of 0.4 and 0.39, respectively, whereas less indented Brava Beach shows a value of 0.26.

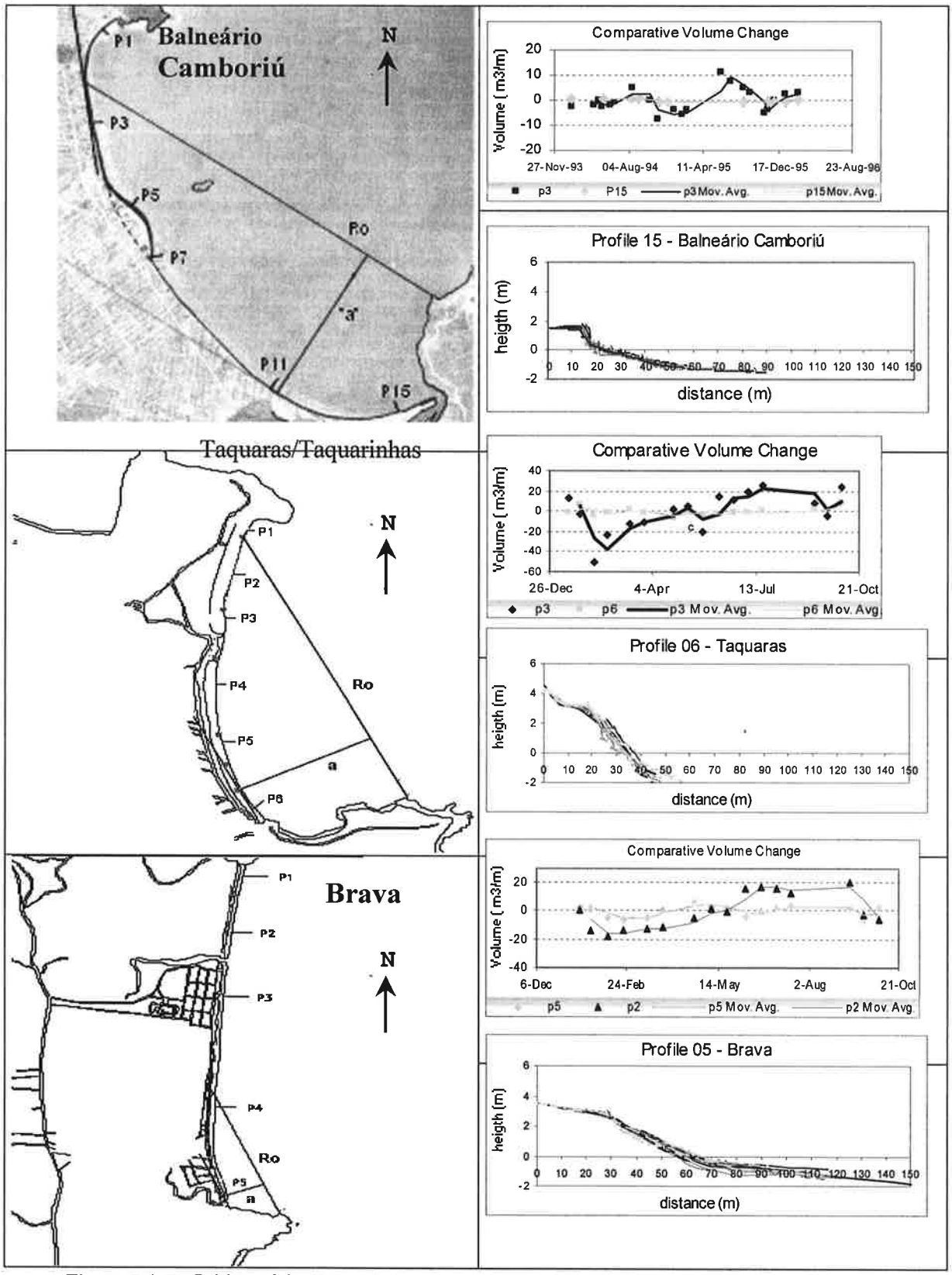

Figure 5.4. Definition of the largest indention point, definition of "a" and R_β, beach volume fluctuations at profiles with bigger and smaller mobility, and less mobile profile for each beach monitored. Extracted from aerials at a 1:25,000 scale (Balneário Camboriu), and at a 1:12,500 scale (Taquaras/Taquarinhas and Brava beaches).

Table 5.1. Relations a/R_β and SL/CL in the monitored beaches.

Beach	a/R_β	SL/CL
Balneário Camboriú	0.40	1.82
Brava	0.26	1.18
Taquaras/Taquarinhas	0.39	1.86

Figure 5.4 shows discrepancies in volume variations between the sheltered and exposed zones at Balneário Camboriú and Taquaras/Taquarinhas beaches, and a more similar behavior at Brava Beach. While at Taquaras/Taquarinhas Beach, in the exposed profile, three volume variations on the order of 77 m^3/m were measured, the sheltered Profile 6 showed volume variation on the order of $15m^3/m$ during the whole period. At Balneário Camboriú, the maximum volume variation measured was 19 m^3/m for the exposed Profile 3. At the sheltered Profile 15, maximum measured variation was on the order of 1.7 m^3/m. At Brava Beach, this difference was less pronounced with maximum beach volume variation on the order of 38.2 m^3/m at Profile 2, compared to 14.9 m^3/m in Profile 5.

Based on these results, a relationship between beach profile mobility (variations of beach width and volume throughout the year) and the curvature of headland bay beaches is evidenced. Profiles located between the point of greater indentation and the downdrift headland, had smaller mobility in the headland bay beaches monitored. Examples are Profiles 11 and 15 at Balneário Camboriú, Profile 6 in Taquaras and Profile 5 at Brava Beach (see Figure 5.4). Highly curved beaches, those with an indentation ratio around 0.40 or SL/CL around 1.8, experience greater headland influence on profile mobility and have a well defined shadow zone. Beaches with less

curvature, smaller indentation ratio (around 0.20) and smaller SL/CL (around 1.18), experience less headland impact on profile mobility and have a small, poorly defined shadow zone.

Southeastern waves have major influence on the planform of these beaches, as previously described by Klein and Menezes (2001). Consequently, the greatest impact of headlands on beach planform and profile mobility occurs toward the south end of each beach.

As a result of different degrees of curvature and different orientation, these beaches were classified in relation to their degree of exposure to southeast swells (e.g. Menezes and Klein, 1997; Menezes, 1999; Klein and Menezes, 2000, 2001). These researchers classified the beach of Balneário Camboriú as semi-exposed and the beaches of Taquaras/Taquarinhas and Brava as exposed.

The relation between shoreline length and embayment width (SL/CL) showed results similar to those obtained with the indentation ratio (a/R_β) (see Table 5.1). However, the relation SL/CL provides no definition of a transition point of greater curvature on the bay shoreline.

As the curvature of a headland bay beach increases, the portion protected from direct attack by incident waves (shadow zone) increases. As a result, greater variations of morphodynamic parameters such as profile mobility, beach volume and width, and wave breaker height along the headland bay beach shoreline is observed in highly curved beaches. In these beaches, the exposed straight end experiences greater profile mobility, larger breaker height, and greater fluctuations of beach volume and width values compared to sheltered sections of the beach. On the other hand, as the curvature of a headland bay beach decreases and it assumes a straight planform, it tends to have a

smaller shadow zone, and the fluctuations in beach volume and width will have similar magnitudes along the headland bay beach shoreline.

5.4.2. Wave Observations

Wave data resulting from the 276 observations conducted between January and October 2000 are presented in Figures 5.5 and 5.6. Wave breaker height, and wave periods is shown in Figure 6a and b, respectively. During the monitored period, average breaker height was 0.8 m. During three storm events wave heights were above 1.8 m (Figure 6a). Predominant classes of wave period was 7 to 9 seconds (43% of the observations), followed by 9 to 11 second waves (34% of the occurrences) (Figure 6b).

Predominant wave direction was S/SE (49% of the occurrences), followed by N/NE waves (34% of the occurrences) (Figure 7a). Shifts in predominant wave direction occurred during the year of 2000 (Figure 7b and 7c). March and April, S/SE waves were predominant (58% of the occurrences), while during September and October N/NE waves predominated (62% of the occurrences) (Figures 7b and 7c). These changes in wave direction influence the behavior of the headland bay beaches.

5.4.3. Short Term Beach Rotation Process

In response to changes in wave direction, fluctuations of beach volume and width can be out of phase between opposite ends, due to beach rotation. Headlands are physical obstacles to the littoral drift. Beaches in this study showed out of phase behavior, at different scales, showing distinct patterns according to their particular morphodynamic characteristics. The following examples briefly illustrate the behavior of the three beaches.

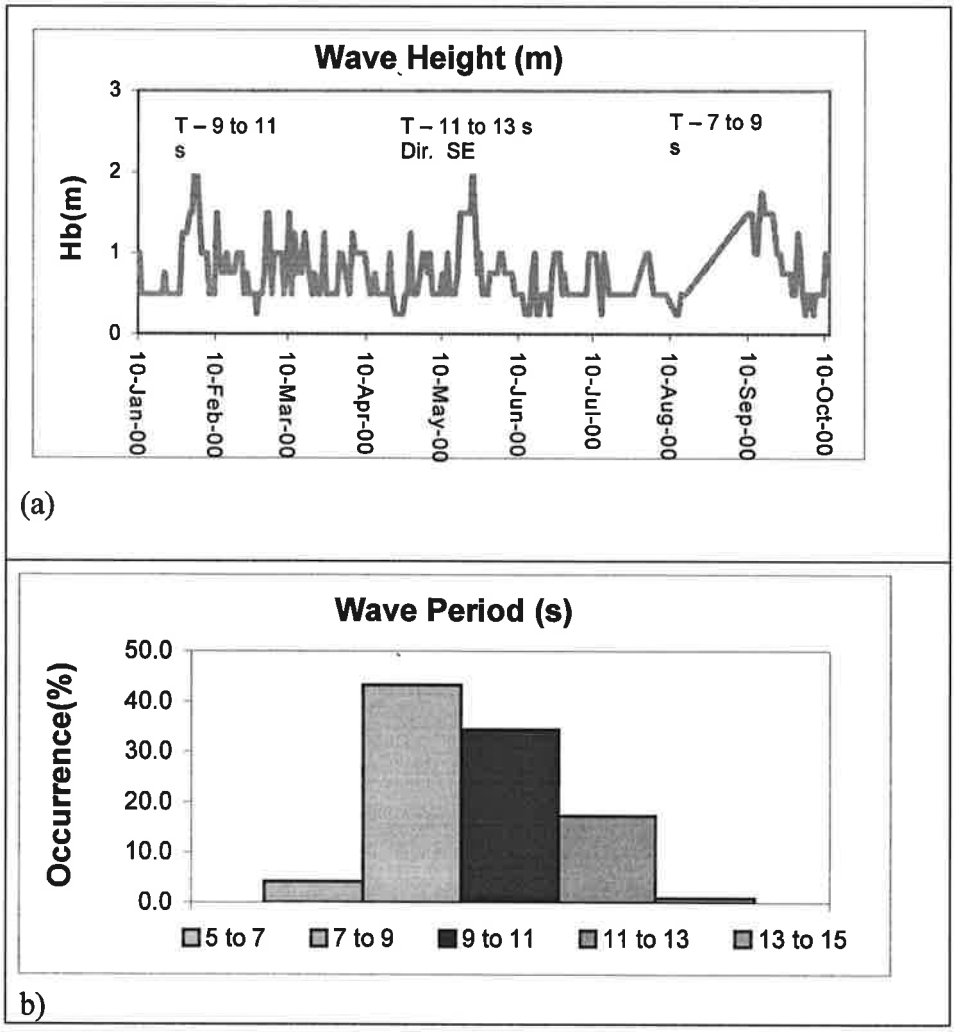

Figure 5.5. Wave data resulting from the 276 observations conducted between January and October 2000. (a) Temporal series of wave breaker height (Hb), (b) wave period intervals of predominant occurrence.

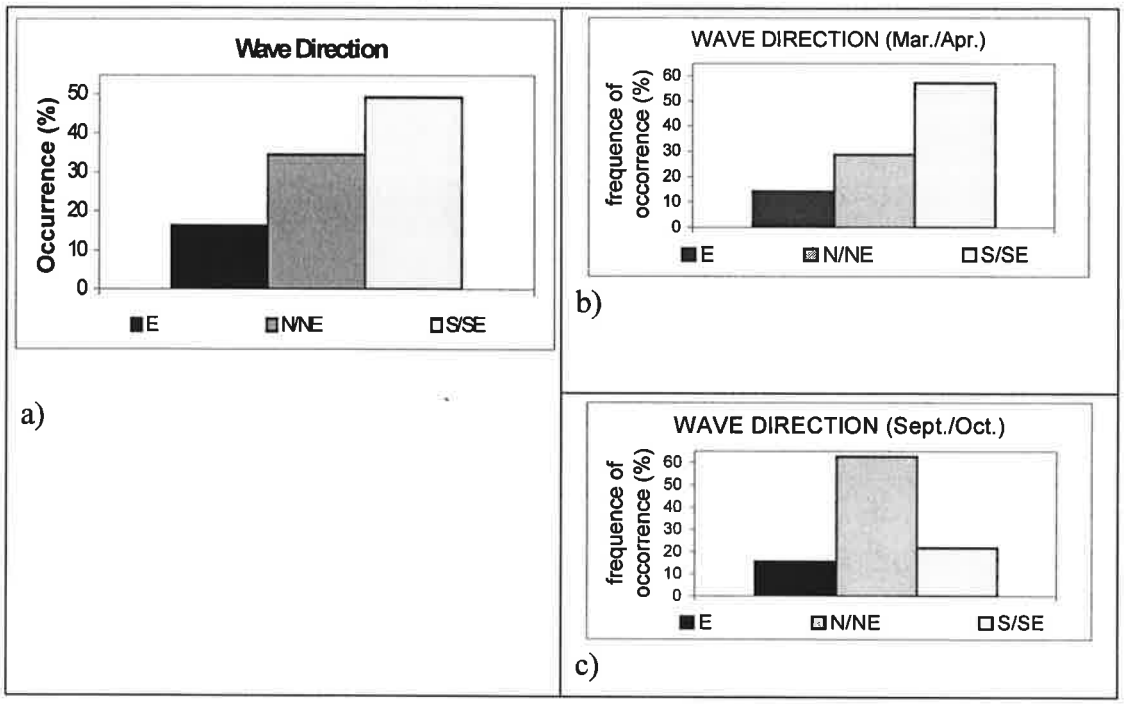

Figure 5.6. Predominant wave direction during the monitoring period (a) and during March/April (b) and October/September (7c).

5.4.3.1. Taquaras/Taquarinhas Beach

Beach volume variation in different sections of the beach is presented in Figure 5.7. This figure shows, starting from the top left, beach volume variations in Profiles 1 and 5 during the period shown. Note the opposite trends between these two profiles, while Profile 1 is eroding Profile 5 is accreting, and vice versa. Profile 1 is located at the northern end of the beach, while Profile 5 is located at the southern end of the beach (see Figure 5.4). The opposite behavior between these two profiles results from changes in wave direction, as illustrated in the top right diagram. Simple linear correlation between volume variations in different profiles are shown in the table (right bottom); similar variations of Profiles 2 and 3 in the central north section of the beach is shown in the left bottom diagram.

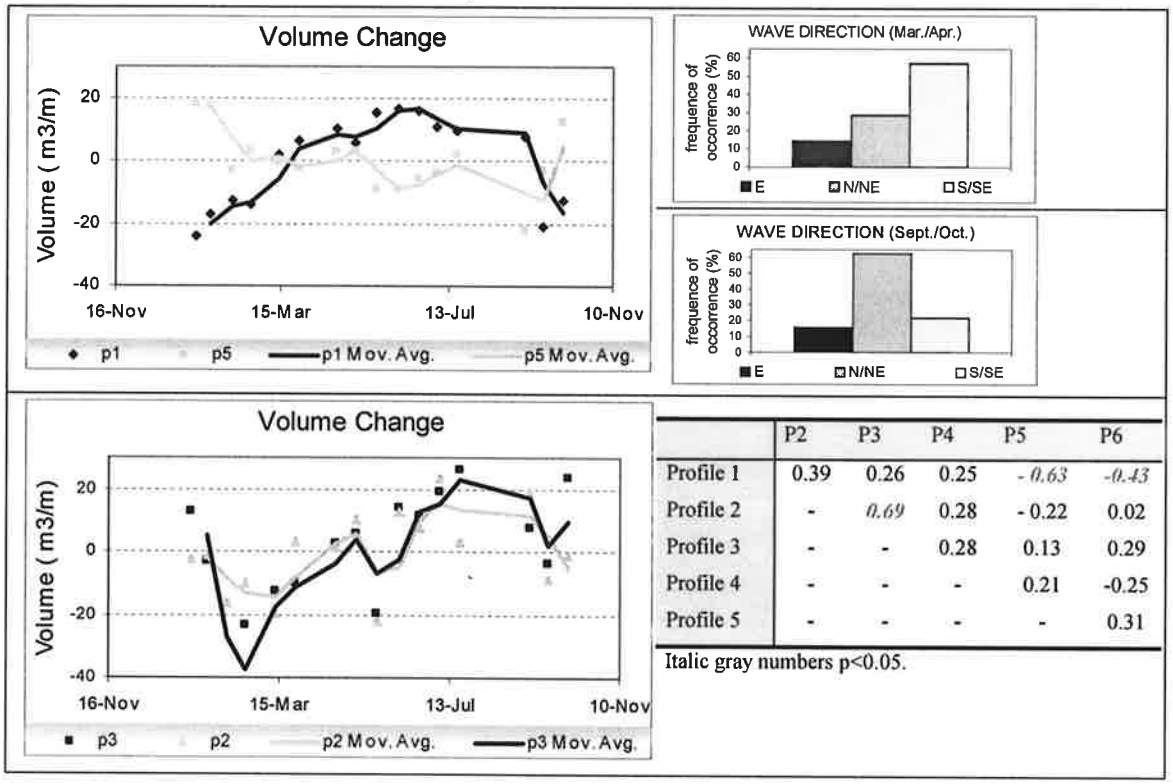

	P2	P3	P4	P5	P6
Profile 1	0.39	0.26	0.25	*-0.63*	*-0.43*
Profile 2	-	*0.69*	0.28	-0.22	0.02
Profile 3	-	-	0.28	0.13	0.29
Profile 4	-	-	-	0.21	-0.25
Profile 5	-	-	-	-	0.31

Italic gray numbers $p<0.05$.

Figure 5.7. Inverse beach volume changes between Profiles 1 and 6, similar volume variation between Profiles 2 and 3, and correlation coefficients between all profiles at Taquaras/Taquarinhas Beach. Predominant wave directions are shown for the months March and April, and September and October.

The periods of accretion on the northern extremity correlated significantly ($p<0.05$) with periods of erosion on the southern extremity and vice-versa (see Figure 5.7). In other words, the variations between opposite ends are out-of-phase. It was observed that between January and June while Profile 1, located on the northern extremity of the beach eroded, Profile 5 (in the south) accreted. From July to beginning of September, two inverse cycles occurred almost monthly, and in September/October while Profile 1 experienced great erosion, profile 5 accreted (see Figure 5.7).

Profiles in the central portion of the beach did not correlate significant with beach extremities. However, there is a general trend of similar behavior between

Profiles 1, 2 and 3 (see Figure 5.7). Periods of erosion in the northern extremity of the beach were related to the previous occurrence of east/northeast waves as during September and October of 2000. Periods of erosion in the southern extremity were related to previous occurrences of south/southeast waves similat to what happened during May/June (see Figure 5.7), and described by Benedet Filho *et al.* (2000).

The out of phase variations between opposite ends observed at Taquaras/Taquarinhas Beach suggests an apparent rotation of the beach planform, and this rotation might be a response of changes in predominant wave direction. According to field data, Taquaras/Taquarinhas Beach exhibited a behavior similar to the one described by the theoretical model presented in Figure 5.8. In this beach, erosive events in one extremity imply in sediment being transported and redistributed to another sector of the beach. It shall return to its original location when predominant wave direction changes.

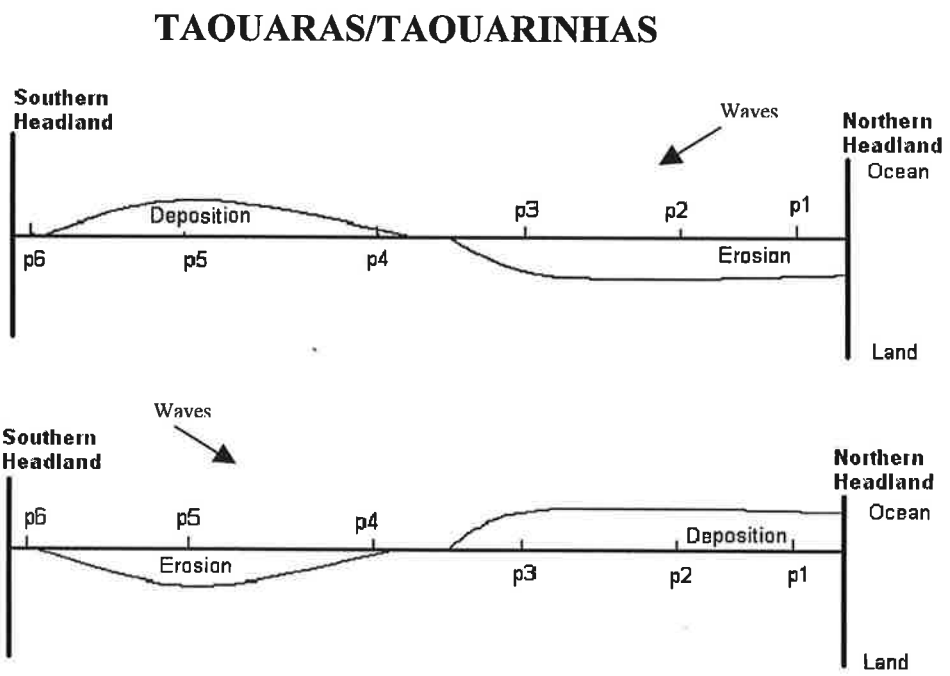

Figure 5.8. Schematic diagram representing the general trend of sediment removal at Taquaras/Taquarinhas Beach.

5.4.3.2. Brava Beach

Figure 5.9 shows the main results for Brava Beach. The top two diagrams, show variations in beach volume for Profiles 1, 2 and 3. The middle diagram shows variations for Profiles 5 and 4. The bottom figure shows correlation coefficients between the volume variations in all profiles. At this beach out-of-phase variations of beach volume between opposite ends were not observed.

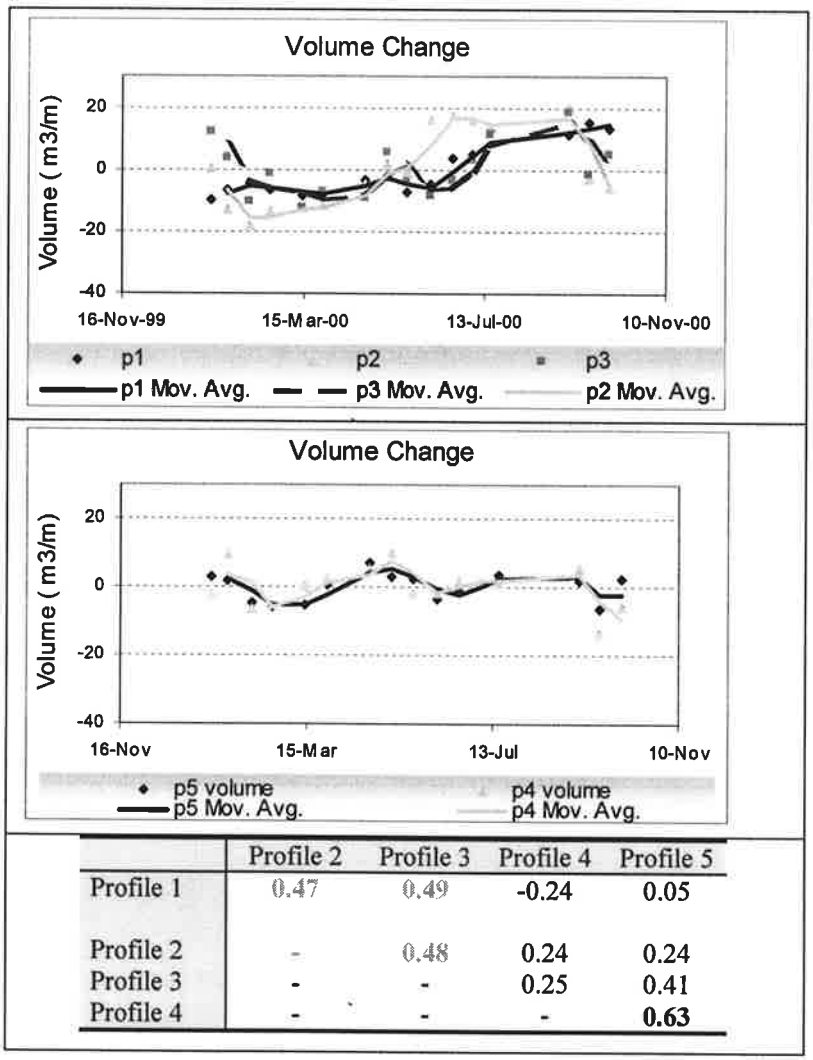

	Profile 2	Profile 3	Profile 4	Profile 5
Profile 1	0.47	0.49	-0.24	0.05
Profile 2	-	0.48	0.24	0.24
Profile 3	-	-	0.25	0.41
Profile 4	-	-	-	**0.63**

Figure 5.9. Similar volume variations between profiles 1, 2, and 3 and between profiles 4 and 5 at Brava Beach, representing the two compartments of this beach, and correlation coeficients between these profiles. Values between the profiles cited above are significant with $p<0.05$.

Positive correlations between profiles located in the north and central sectors of the beach (1, 2 and 3), and between profiles of the southern end of the beach (4 and 5) were verified. However, no correlation between these two compartments was observed. This suggests a division of the beach in two sectors with different behaviors, the central north sector represented by Profiles 1, 2 and 3, and the southern sectors being represented by Profiles 4 and 5 (Figure 5.9).

During the same period of monitoring, the occurrence of short term beach rotation processes at Taquaras/Taquarinhas Beach was verified, but no evident rotation occurred at Brava Beach. It is thus necessary to consider the different characteristics of these two particular beach systems. Taquaras/Taquarinhas is a reflective beach without submerged bars, and rip currents. On the other side, Brava Beach is an intermediate beach with remarkable characteristics such as mobile submerged bars and strong rip currents. Inverse patterns of erosion and accretion between opposite ends at Brava Beach might be occurring, but were not detected by the current analysis, as underwater measurements of bar migration were not performed. Another important factor that has to be considered is that the northern headland of Brava Beach does not totally block the littoral drift. In events where breaker height observed exceeded 1.5 m, the breaker line extended about 20 m offshore of the headland. Headland bypassing occurs in this case and the sediments are transported to the neighboring beach, instead of accumulating against the northern headland.

The occurrence of strong rip currents can also represent a very important mechanism of sediment transport (Short, 1999). The profiles monitored in this type of beach can manifest some erosion, and this erosion may not be directly related to high waves or the incidence of oblique waves. Rather, some of these erosive events may be

directly related to the occurrence of strong rips in front of, or in the adjacent areas of the monitored beach profiles (Figure 5.10). According to Short (1999), rip currents are responsible for the transport of beach sediments offshore.

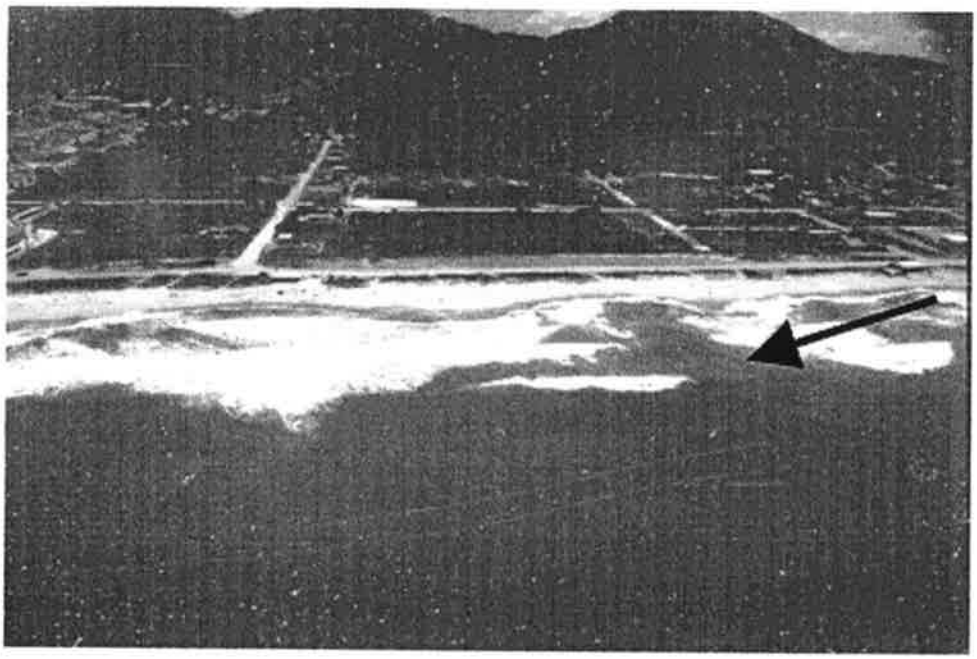

Figure 5.10. Rip current channel located between Profiles 4 and 3 at Brava beach.

The data obtained in the present study for Brava Beach demonstrate similar behavior to that in the model proposed in Figure 5.11. As observed at this beach, during erosive events the whole beach erodes, but with different magnitudes. Smaller magnitudes of profile mobility were verified in the southern extremity, and greater magnitude was verified in the central and northern extremity. The same behavior is observed in depositional periods. The occurrence of erosive or depositional trends at Brava Beach did not show a clear relation with the wave direction, as observed in Taquaras/Taquarinhas Beach (see Figure 5.9).

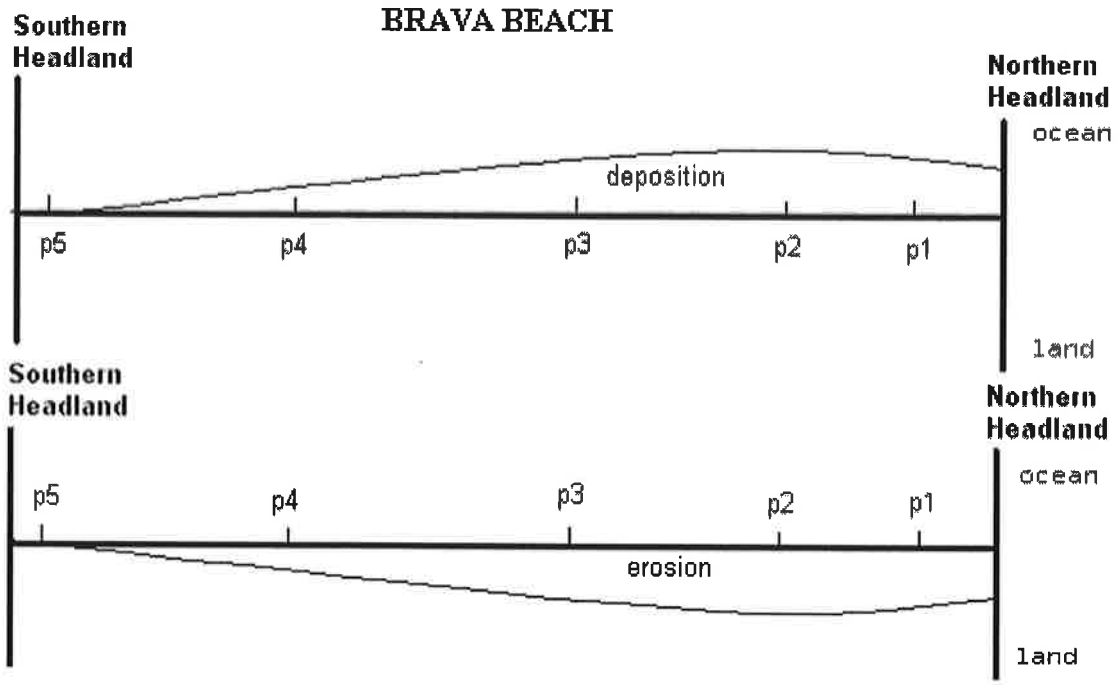

Figure 5.11. Schematic diagram representing the general pattern of sediment removal at Brava Beach, where depositional and erosive events occur simultaneously along the beach but with different magnitudes.

5.4.3.3. Balneário Camboriú Beach

The beach of Balneário Camboriú is divided in two large sectors, which form two distinct beaches with distinct behavior. Those two sectors are divided by a salient formed adjacent to das Cabras Island (see Figure 5.4 and 5.12)

Figure 5.12 summarizes the main results for Balneário Camboriú beach. Clockwise from the top left, it is shown that: (1) the beach planform with the profile measurement locations, on the top right (2) the variations of beach volume for the profiles on the southern section; and on the bottom right (3) volume variations for the northern section. At the bottom left, simple linear correlation between the profiles is presented.

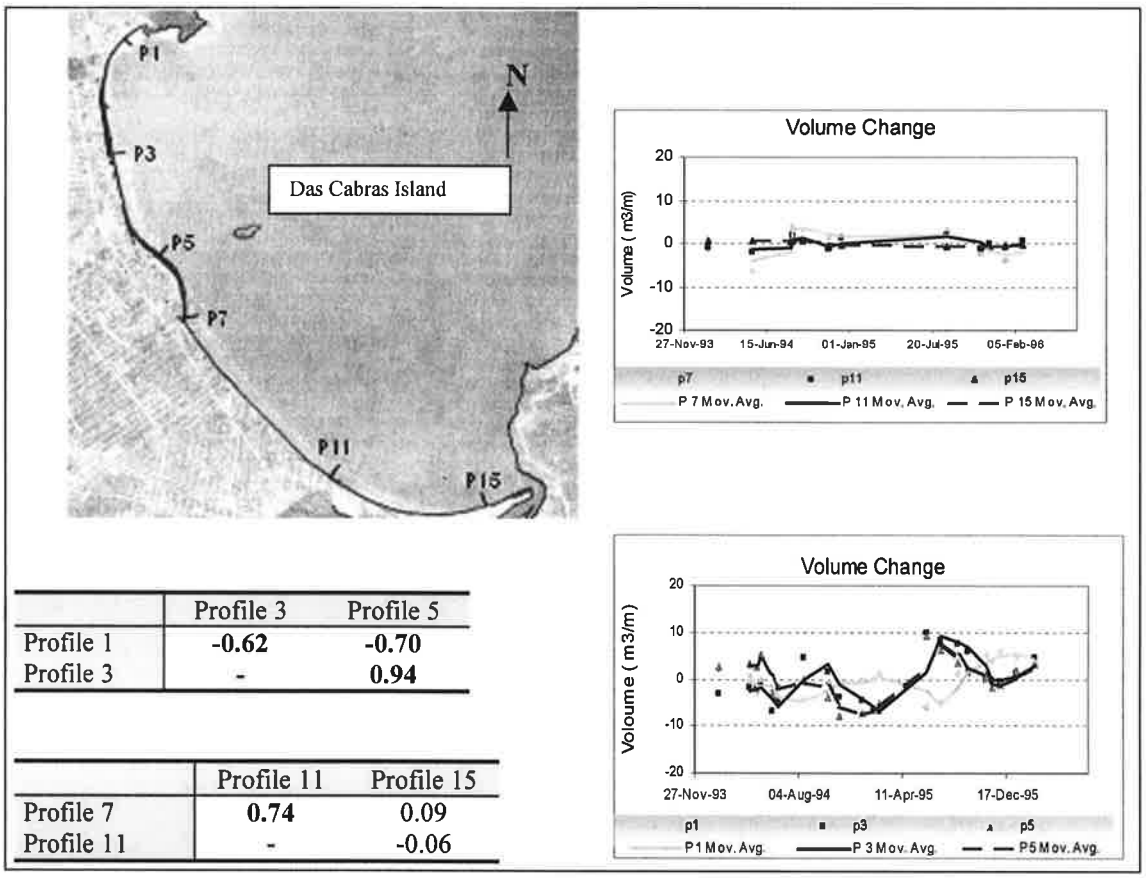

	Profile 3	Profile 5
Profile 1	**-0.62**	**-0.70**
Profile 3	-	**0.94**

	Profile 11	Profile 15
Profile 7	**0.74**	0.09
Profile 11	-	-0.06

Figure 5.12. Beach volume variations at the sheltered (Profiles 7, 11 and 15) and exposed (Profiles 1, 3 and 5) sectors of Balneário Camboriu and overview of the profile locations. The table shown correlation coefficients between these profiles where values in bold indicate $P<0.05$.

Southward of the salient, the area represented by Profiles 15, 11 and 07 in the beach shadow zone, variations of beach volume and width were minimal when compared to the exposed northern sector (see Figure 5.12), and with the other monitored beaches. As previously shown by Temme *et al.* (1997) and Klein and Menezes (2001) this is caused by the strong influence that the southern headland and das Cabras Island have on this sector of the beach. As a consequence, this zone is protected from the direct incidence of the most energetic southeast swells. Thus, the waves do not have the same capability for moving the sediments around.

The northern sector of the salient, represented by Profiles 1, 3 and 5, is directly exposed to waves from various directions and consequently they experience greater mobility and larger morphologic variability.

Profiles 3 and 5 exhibit similar behavior, while Profile 1 presents opposite behaviour (see Figure 5.12). From these results, it is inferred that in this sector of the beach, inverse patterns of erosion and accretion between opposite ends are occurring. The depositional periods at the north extremity (Profile 1) correlated with erosive events in the central and southern extremity (Profiles 3 and 5) and vice-versa, indicating an apparent rotation of the beach planform. However, while beach rotation was well defined in 1995 to beginning of 1996; it was not so clear in 1994 (see Figure 5.12), enforcing the need for long term monitoring programs. Unfortunately, there are no wave data in these years that could make possible an association with the beach behavior observed. The beach rotation observed 1995 to beginning of 1996 occurred in cycles of about 3 to 4 months (see Figure 5.12).

The data acquired for this beach are summarized in Figure 5.13. In the southern protected sector, minimal sediment removal was observed while in the northern sector out-of-phase variations of beach volume and width occurred between extremities. As a main result of these analyses, it was found that the different extremities and the different sectors of the headland bay beaches did not respond in the same way to higher energy wave events. There was no defined seasonality in beach volume and width fluctuations, rather each section of the beach has its own behavior. Other examples of this behavior in the literature are verified in Masselink and Pattiaratchi (2001). These authors attributed the morphological variations observed in the Perth beaches, Western Australia, to a seasonal variation in the littoral drift direction, which for the Perth area,

is toward north in the summer and south in the winter. These authors verified that beaches located south of coastal structures or headlands have their width increased during summer, while beaches located north of coastal structures/headlands experienced erosion in the same period, and the inverse is true for the winter period.

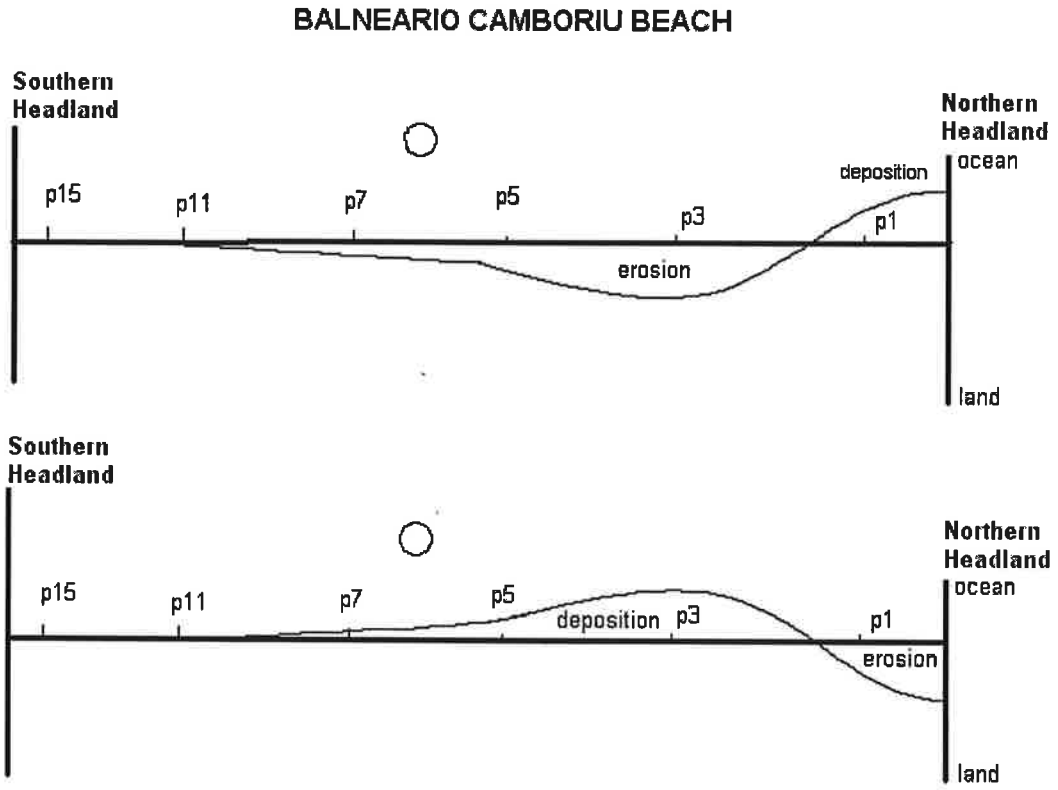

Figure 5.13. Schematic diagram representing the general trend of sediment removal at Balneário Camboriu beach, where depositional and erosive events occurs out of phase in the northern sector, and the southern sheltered sector presents minimal sediment removal.

5.4.4. Comparison of the Magnitude of Short Term Beach Rotation Processes within Different Beach Types

Measured beach profile variations at the exposed section of each of the beaches monitored are observed in Figure 5.14. Profile mobility was greatest on the reflective exposed beach of Taquaras/Taquarinhas, followed by Brava Beach, an intermediate exposed beach, and smallest on the dissipative semi-exposed beach of Balneário Camboriú.

Like profile mobility, short-term beach rotation processes can differ significantly between dissipative, reflective, and intermediate beaches, and as well between beaches with different degrees of curvature and exposure to the incident waves. In this study, short-term beach rotation processes on the subaerial beach were more easily detected in exposed reflective beaches (*e.g.* Taquaras/Taquarinhas). In this case, the absence of submerged bars dissipates wave energy directly on the beach slope, which in turn leads to greater profile mobility and removal of larger amounts of sediment in the subaerial beach. As a result, the occurrence of oblique waves on these kind of beach systems causes sediment exchange between its ends. In other words, beach rotation where the sediment eroded from one extremity of the beach is deposited at the opposite extremity.

In exposed intermediate beaches (*e.g.* Brava Beach), the occurrence of hydrodynamic features like strong rip currents, cellular circulation, and morphologic features such as mobile submerged bars, and the small size of the northern headland may lead to different beach behavior. These phenomena blocked the occurrence of, or made undetectable by the present methods, short-term beach rotation. In this type of beach, long term monitoring of the subaerial and submerged part of the beach, and of the northern neighboring beach are necessary in order to better understand its temporal

and spatial variations. Short *et al.* (2000) identifed beach rotation in a intermediate type beach, which is of 3.6 km long in the Sydney area (Narraben Beach), with cycles of rotation ranging from 3 to 8 years.

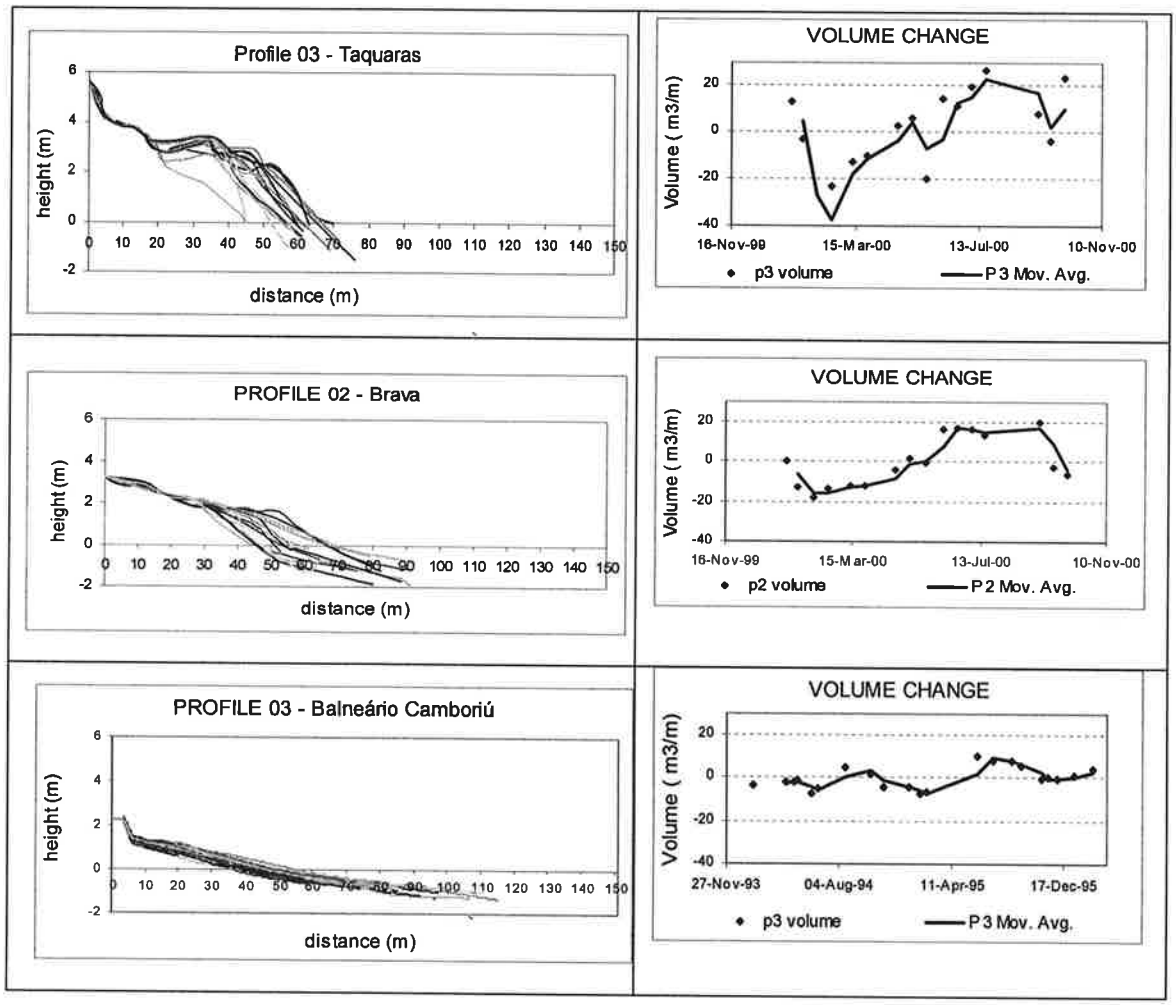

Figure 5.14. Beach profile envelopes with greater mobility, and volume variations for: the reflective beach of Taquaras/Taquarinhas, the intermediate beach of Brava Beach, and the dissipative beach of Balneário Camboriú.

In exposed dissipative beaches (*e.g.* Balneário Camboriú northern sector), beach rotation is seen from the out-of-phase variation of beach volume and beach width between opposite ends. This rotation presented a three to four months cycle. However,

sediment removal was of smaller magnitude than at the reflective beach (Taquaras/Taquarinhas). Balneário Camboriú results also demonstrated that beach rotation processes show interannual variability, which requires long term monitoring. The results did not show any clear trend of erosion or deposition. Rather, the fluctuations observed were beach responses to high wave events, where sediment is not lost from the system, but redistributed to other sectors of the beach, in accordance to the direction of wave incidence. Klein *et al.* (*in press*), and Miot da Silva *et al.* (2000), studying the pattern of sediment distribution at these beaches, identified distinct sediment characteristics. They emphasize that no sediment exchange between these beaches is occurring.

5.4.5. Relation Between the Amplitude of Beach Rotation and the Headland Bay Beach Length

Cowell *et al.* (1996) proposed for the amplitude of beach rotation in Headland bay beaches, the following relation:

$$Ax=0.0139L \qquad (5.1)$$

Where Ax is the amplitude of rotation in meters, and L in the shoreline length. According to this relation, the beach of Taquaras/Taquarinhas would show an rotation amplitude of 22 m, and the northern sector of Balneário Camboriú would experience an rotation amplitude of 28 m. Comparison of amplitude values for rotation observed in the field, versus those predicted by the relation above are available in Table 5.2.

A simple linear regression using the data of Cowell *et al.* (1996) and data from this work (see Figure 5.15) resulted in an relation similar to the one predicted by these authors, supporting the idea of a relation between the amplitude of beach rotation and

the beach length. However, this relation is influenced by other parameters besides beach length, and at this state-of-the-art there is not enough data to definitely validate such a relation.

Table 5.2. Beach shoreline length, amplitude of beach rotation predicted according to Cowell *et al.* (1996) and the amplitude of beach rotation observed in field during the period of monitoring.

Beach	L(m)	Ax(m) (predicted)	Ax(m) (observed)
Balneário Camboriú (north sector)	2050	28	21
Taquaras/Taquarinhas	1582	22	22

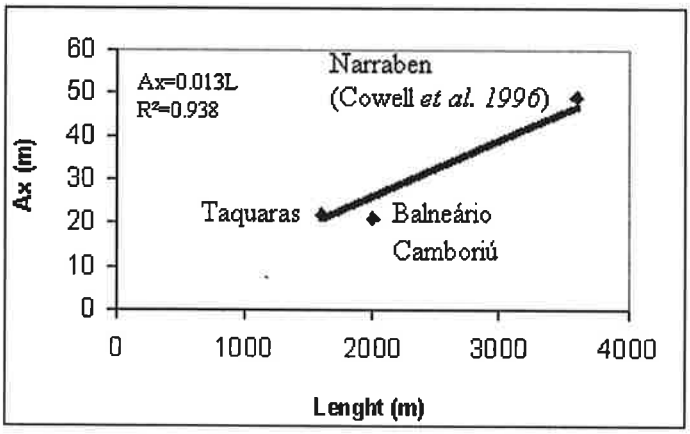

Figure 5.15. Simple linear regression with the values of amplitude of beach rotation observed plotted against the beach shoreline length. Values from the present study and from Cowell *et al.* (1996) were used.

Long term detailed studies of beach rotation processes in beach systems with distinct degrees of curvature and distinct morphodynamic characteristics are necessary. These would lead to a more realistic relation that could predict the amplitude of beach rotation in headland bay beaches. As demonstrated in this study, other factors such as beach type, beach curvature and its exposure to the incident waves have a direct

influence on the profile mobility and magnitude of sediment removal. It is then expected that these factors will influence in the amplitude of beach rotation in different headland bay beach systems.

5.5. SUMMARY

The headland bay beaches studied in Santa Catarina, Brazil exhibited different patterns of sediment removal as a function of the following parameters:

(1) Degree of curvature of the beach: This can be measured by the indentation ratio or by the SL/CL ratio. In highly curved beaches, there is a well-developed shadow zone and a range of morphodynamic conditions, from a sheltered low energy beach adjacent to the downdrift headland to a high energy exposed beach on the straight end of the headland bay beach. The less curved beaches instead, tend to show a more uniform behavior, since they are directly exposed to incident waves. The parameters a/Ro and SL/CL show similar results, but the SL/CL parameter does not provide the point of greater indentation of the beach, which would be a hypothetical limit of the shadow zone.

(2) Occurrence of submerged bars, rip currents, and cellular circulation: These factors play an important role in determining the morphodynamic behavior of the studied beach systems, as they directly impact magnitudes of sediment exchanges on the subaerial and submerged portion of the beach.

(3) Shoreline length also influences the amplitude of beach rotation and the time that the whole beach takes to readjust to new wave conditions.

(4) Beach Type: Short-term beach rotation processes were evident in the exposed reflective beach at Taquaras/Taquarinhas, and on the exposed dissipative

northern sector of Balneário Camboriú. The process probably occurs on other headland bay beaches along the Santa Catarina coastline, in response to waves from varying angles of incidence.

(5) Previous studies of beach rotation phenomena as developed by Short *et al.* (2000), detected a pivotal point with minimal variation, about which the beach rotates. In this study no pivotal point was detected, but rather a transitional zone.

Cycles of erosion and deposition in different sectors of the beach were detected during the same study period, suggesting complex behavior of headland bay beaches. In order to analyze temporal cycles of sediment mobility in headland bay beaches, it is necessary to monitor several profiles along the beach. If only one profile on the headland bay beach is monitored, observed beach behavior would not be representative of the whole headland bay beach. As demonstrated in this study, when one sector of the headland bay beach is eroding, another sector might be accreting, stable, or eroding at different rates. In this way, headland bay beaches require spatio-temporal analysis, in order to properly understand its behavioral trends. Headlands interrupt littoral drift and block approaching incident waves, therefore influencing on the morphodynamic behavior of the beach.

The mechanisms of headland bay beach response to wave angle should not be limited to cross-shore analysis, which typically shows sediment exchange between submerged bars and the subaerial beach, as a function of fluctuations in wave energy. The mechanism needs to be analyzed both cross-shore and alongshore, as a function of fluctuations in wave energy and direction, especially when there are oblique high-energy waves and longshore drift that is interrupted by headlands.

CHAPTER SIX

Beach Sediment Distribution for a Headland Bay Coast

Unless referred to otherwise, the contents of this thesis are the results of original research carried out by the author

Some of the results have been published in:

KLEIN, A.H.F; MIOT DA SILVA, G.; FERREIRA, Ó., and DIAS, J.A., 2004 (*in press*). Beach Sediment Distribution for a Headland Bay Coast. *Journal of Coastal Research*.

6.1. INTRODUCTION

The study of textural variations of beach sediments, alongshore and cross-shore and in terms of spatial and temporal distribution patterns, greatly improve the understanding of geological and dynamic processes that take place in sandy beaches. Previous studies recognized a positive relationship between wave height (or wave energy) and grain size distribution (e.g. Bascom, 1951). Bascom (1951), in his classic studies on California Coast, specially on Halfmoon Bay concluded that the grain size increase with the increase of wave energy and when the degree of protection decreases. In the exposed area of Halfmoon Bay the grain size is bigger than in the protect area behind the headland (changing from 0.17 mm to 0.65 mm). However, Nordstrom (1977) after studying exposed and sheltered beaches at Hook Spit, USA, observed that the grain size did not vary with changing wave height. This author suggested that the provenience (source of sediments) is the most important factor defining grain size on beaches. More recently, Short and Ni (1997) and Short (1999) agree with Nordstrom (1977) observations and concluded that provenience defines grain size distribution on beaches.

The purpose of this chapter is to present sediment distribution patterns for headland and bay coastal types, along the central-northern coast of Santa Catarina State, in southern Brazil. The main goal is to define if grain size distributions mainly depends on the source of sediments or on the hydrodynamics (wave energy).

6.2. ENVIRONMENTAL SETTING

The study area is the central-north coastline of the Santa Catarina State, between Itapocu (26.50°S and 48.60°W) and Tijucas (27.30°S and 48.60°W) river mouths (sector 3)(Figure 6.1). This area is bedrock – controlled embayed coastline - with Pre-Cambrian

crystalline rock outcrops interrupting the Quaternary coastal plain continuity. Headland-bay beaches can be identified in this region (see Figure 2.2, Chapter 2, page 28).

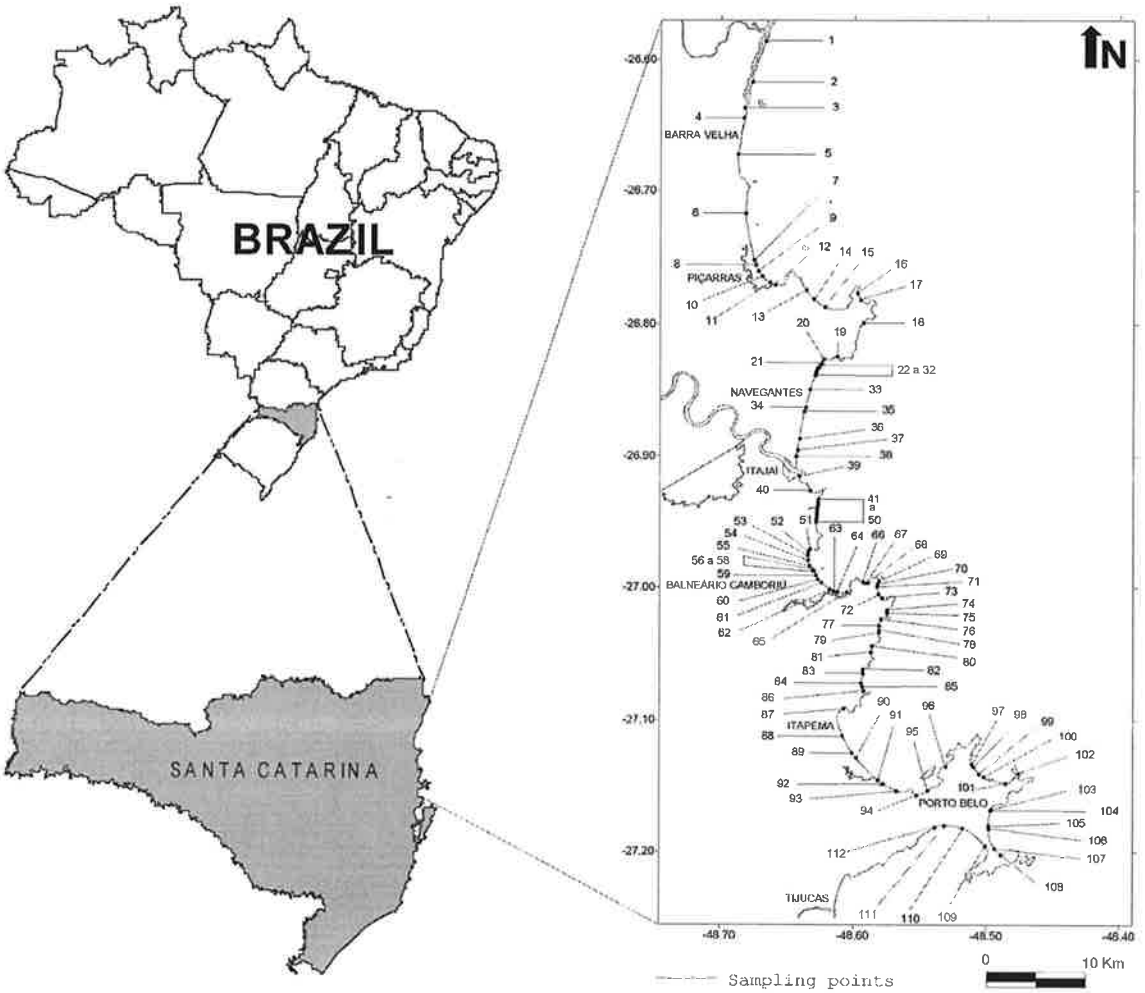

Figure 6.1. Location of the study area at the central-north coastline of the Santa Catarina State, between Itàpocu (26.50°S and 48.60°W) and Tijucas (27.30°S and 48.60°W) river mouths and location of the sediment samples collected.

The rivers that drain the coastal plain are part of the drainage system of "Vertente Atlantica", where the Itajaí Basin is dominant, with approximately 15,000 km^2 of drainage area (Santa Catarina - SEDUMA, 1997) (see Figure 2.3, page 34). The Itapocu River's hydrographic basin has a drainage area of 2,930 km^2, located at the northern part of the study area. Caruso *et al.* (2000) mention that this river drains a

metamorphic rocks area, constituted by gneisses and other lithologies, contributing with sandy sediments to fluvial bedload. The hydrographic basin of Tijucas' river also drains metamorphic rocks, composed of schists and phyllite, contributing with fine sands to the fluvial transport (Caruso and Araújo, 1997; Schettini and Klein, 1997). This hydrographic basin is located in the south of the study area; with a drainage area of 2,240 km^2 (Santa Catarina – SEDUMA, 1997).

Even though there are no quantitative mineralogical studies in the region that define source areas for sediment dispersal patterns, Gianini (1993), Caruso *et al.* (2000) and Klein and Menezes (2001) suggest that basement rocks constitute sedimentary provenience of sediments that are deposited in the coastal plain.

The coastal deposits originated at Quaternary sea level high stands (Caruso *et al.*, 1997; Caruso *et al.*, 2000; Angulo and Lessa, 1997), include bay barrier systems, beaches linked to basement rocks, beach and foredune ridges, spits and "chenier" plains (Caruso and Araujo, 1997, 2000; Klein and Menezes, 2001).

Martins *et al.* (1970) have shown that the beach grain size in general increased from Santa Catarina Island to Barra Velha beach. These authors also defined that the beach sediments are mainly composed by two populations: one from a first sedimentary cycle, represented by coarse sand, and another formed by fine sand being the source the reworked of old coastal plain systems (polycycle sediments).

The inner continental shelf is narrow (30 to 45 km) and has water depths between 2 and 50m (Muehe, 1998; Abreu, 1998). There is a variability of nearshore slopes, as a result of basement and sediment deposition (Abreu, 1998; Klein *et al.*, 1999; Klein and Menezes, 2001). Near the river mouths and bays the nearshore slope is low (1:200), while it tends to be steeper (1:40) in regions where the basement rock outcrops is near the coast (Muehe, 1998; Abreu, 1998; Klein *et al.*, 1999; Klein and Menezes,

2001). According to Corrêa (1980) and Abreu (1998) the inner continental shelf mainly presents a sandy texture, with biodetritic gravel in some areas. Abreu (1998) shows that fine sediments are dominant mainly near the mouth of estuaries, as a result of the present contribution of rivers.

Waves arriving from east and southeast dominate the local wave climate, while the most energetic waves are from south-southeast (Alves, 1996). The littoral drift in southern Brazil is predominantly northward, generated by the southeasterly waves. Local littoral drift reversion in headland-bay beaches can be identified. The mean tidal range is 0.8 meters, with a maximum of 1.2 meters. Storm surges can raise water levels to around one meter (1.0) above the astronomical tide (Truccolo, 1998).

6.3. SAMPLING AND ANALYSIS

6.3.1. Sediment Sampling

Figure 6.1 shows 112 sites where 555 samples were collected during different surveys. These sediment samples were obtained from beach profiles at 28 beaches (Table 6.1). The purpose of sample collection at different points of the coast and at different time was:

a) **Sampling for spatial analysis**: In July, 1994, 112 samples were collected on the midpoint of the beachface, in the first 20 cm below surface to avoid the recently reworked sediments in an effort to characterize alongshore sediment distribution patterns between the beaches. Additionally 392 samples were obtained between May 1994 and March 1996 at different times to analyse longshore grain size variation.

b) **Sampling for time series analysis variation:** sampling were conducted in the first 5 cm below surface at different times (15, 17 and 19 surveys,

between May 1994 and March 1996, on Navegantes, Barra Velha and Taquaras beaches respectively). Samples were taken in the midpoint of the beachface, in fixed profiles with known coordinates, allowing repeated sampling.

Table 6.1. Beaches and points where samples were undertaken and surveys number.

Beach	Points	Samples number(spatial)	Samples number(temporal)
Barra Velha	1 to 4	1 to 51	1 to 51
Itajuba	5 and 6	52 to 71	52 to 71
Piçarras/Alegre	7 to 12	72 to 163	72 to 163
Armação	13 to 15	164 to 186	
Grande	16 and 17	187 to 189	
São Miguel	18	190	
Vermelha	19	191	
Gravatá/Navegantes	20 to 38	192 to 239	193 to 202, 215 to 225, 227 to 230
Atalaia	39	240	
Cabeçudas	40	241	
Brava	41 to 50	242 to 279	
Balneário Camboriú	51 to 65	280 to 375	
Laranjeiras	66 to 68	376 to 395	
Taquaras/Taquarinhas	69 to 73	396 to 441	397 to 439
Pinho	74 and 75	442 to 444	
Estaleiro	76 to 79	445 to 463	
Estaleirinho	80 and 81	464 to 483	
Mata Camboriú	82 and 83	484 to 486	
Ilhota	84 to 86	487 to 511	
Itapema	87 to 93	512 to 557	
Porto Belo	94 to 96	558 to 561	
Bombas	97 to 100	562 to 584	
Bombinhas	101	585	
Retiro dos Padres	102	586	
Mariscal	103 to 108	587 to 621	
Canto Grande	109	622 to 625	
Zimbros	110 to 112	626 to 631	

6.3.2. Measurement Methods

Soluble salts in the samples were removed by washing in the laboratory. Samples were then dried, and quartered into sub-samples of 30 to 40 gr. to obtain a representative sample of the sediment to be analysed. The samples were sieved for

approximately 15 minutes using screen battery of $\frac{1}{4}$ phi (ϕ) to obtain the frequency size distribution. The phi notation (ϕ), of Krumbein (1934), was used to describe the size, which is the negative logarithm to the base two of the particle diameter (d) in millimeters (Equation 6.1):

$$\phi = -\log_2 \frac{d(mm)}{1mm} \tag{6.1}$$

The weight of each grain size class was obtained and the Analisador Granulométrico (Moraes and Griep, 1985) - software ANGRA - was used to determine grain size parameters. This software uses the graphic measures, as proposed by Folk and Ward (1957) and reviewed by Folk (1966). To define the central tendency was used the Graphic Mean, given by Equation 6.2:

$$Mz = \frac{\phi 16 + \phi 50 + \phi 84}{3} \tag{6.2}$$

Were ϕ 16, ϕ 50 and ϕ 84 represents the 16, 50 and 84 percentiles.

The grain size classes according to the Wentworth (1922) scale of very fine sand (4.0 ϕ to 3.0 ϕ), fine sand (3.0 ϕ to 2.0 ϕ), medium sand (2.0 ϕ to 1.0 ϕ) and coarse sand (1.0 ϕ to 0.0 ϕ) were used.

The Inclusive Graphic Standard Deviations was used, given by Equation 3:

$$\tau_I = \frac{\phi 84 + \phi 16}{4} + \frac{\phi 95 + \phi 5}{6.6} \tag{3}$$

Were ϕ 95 and ϕ 5 represent the 95 and 5 Percentiles.

Results from Equation 3 indicate the sorting level of sediments, where: τ_I <0.35ϕ is very well sorted; between 0.35ϕ and 0.5ϕ is well sorted; between 0.5ϕ and 0.71ϕ is moderately well sorted; between 0.71ϕ and 1.0ϕ is moderately sorted;

between 1.0ϕ and 2.0ϕ is poorly sorted; between 2.0ϕ and 4.0ϕ is very poorly sorted and $\tau_I > 4.0\phi$ is extremely poorly sorted.

The studies of the statistical parameters of beachface samples, used for spatial analysis of sediment distribution, were based on average values for all surveys, i.e. average of Graphic Mean (Mz) and Inclusive Graphic Standard Deviations (τ_I) from 555 samples. To analyze temporal changes of beachface sediments, Graphic Mean (Mz) values were used from each survey. However, the sampling method in July, 1994, was different (20 cm) from the others (5 cm). These data was used to complement the time series analyses.

Values for beachface slope was obtained with clinometers, and visual wave height and period are average values obtained for all surveys.

6.4. RESULTS AND DISCUSSION

6.4.1. Longshore Grain Size Distributions versus Morphodynamic Beach Type

Figure 6.2 shows the average of mean (Mz) grain size distribution on the beachface. Three sediment types can be differentiated at the study area:

- **Sediment Type 1** - designates the grain size between 2.0 and 3.5 ϕ (0.1 to 0.2 mm), fine to very fine sand. Represents the finest sands in the study area, comprising 33% of the samples. It includes the beaches of Alegre, Armação, Vermelha, São Miguel, Gravatá, Navegantes, Atalaia, north of Brava, Balneário Camboriú, Laranjeiras, south of Itapema, Meia Praia, Perequê, Porto Belo, Bombas, Bombinhas, Mariscal, Canto Grande and Conceição.

- **Sediment Type 2** - is characterized by grain size 1.0 and 2.0 ϕ (0.2 to 0.5 mm), medium sand, has 38% of the total number of collected samples. It is observed at the following beaches: Barra Velha, Piçarras, Armação, Praia Grande, São Miguel, Cabeçudas, Brava, Laranjeiras, Estaleiro, Ilhota, Itapema, Porto Belo, Araçá, Retiro dos Padres, Mariscal, Canto Grande and Zimbros.
- **Sediment Type 3**, grain size between 0.0 and 1.0 ϕ (0.5 to 1.0 mm), coarse sand. Represents 27% of the samples collected on the beachface. This sediment type is found in the north of the study area on Barra Velha and Itajuba beaches, and in the south part of the study area Taquaras, Taquarinhas, Pinho, Estaleiro, Estaleirinho, Mata Camboriú, and Ilhota beaches.

Figure 6.3 shows the distribution of the standard deviation for grain size on mid beachface positions. Sorting levels range between well sorted and moderately well sorted; only two points are poorly sorted (points 65 and 94, Balneário Camboriú and Porto Belo beaches, respectively).

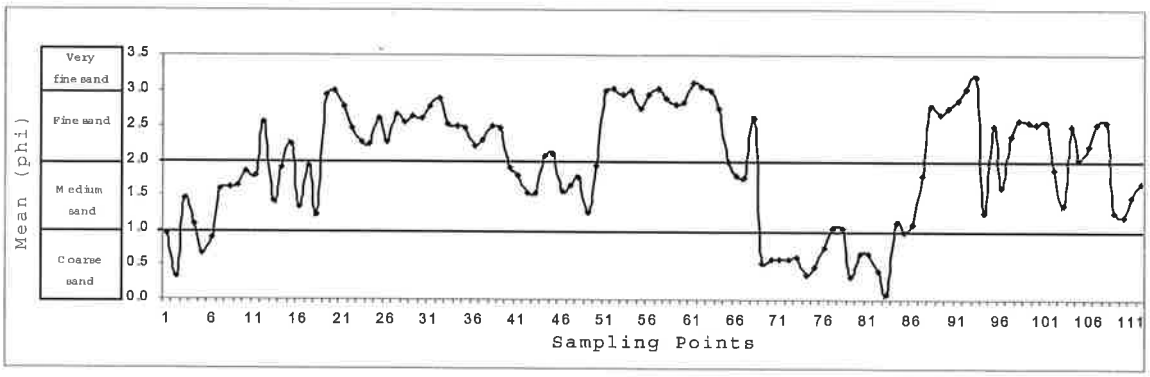

Figure 6.2. Alonghore distribution of average mean (Mz) grain size at the beachface.

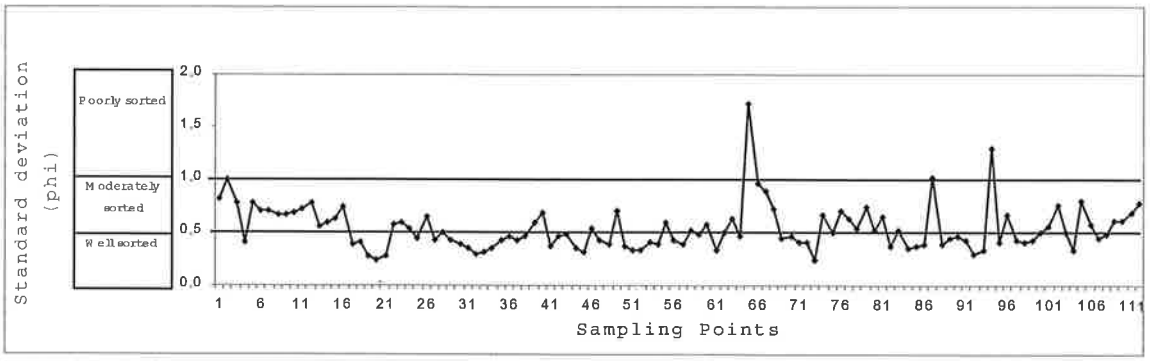

Figure 6.3. Distribution of grain size standard deviation on mid beachface positions.

Despite the poor correlation between mean grain size and standard deviation (Figure 6.4), and consequently sediment type, there is a tendency for fine sands (Type 1) to be better sorted than coarse sands (Type 3).

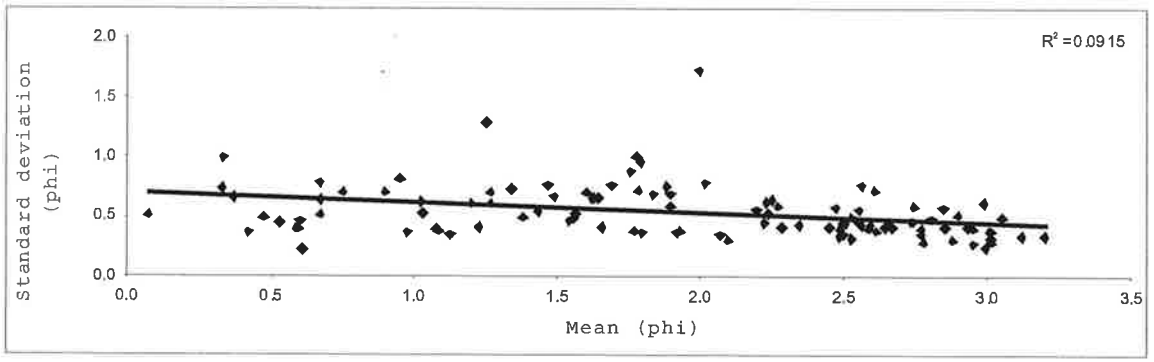

Figure 6.4. Mean grain size versus standard deviation.

Studies regarding grain size distribution on beaches (Bryant, 1982; Wright and Short, 1984; Short, 1994, 1999; Short and Ni, 1997 and Klein and Menezes, 2001) shown that reflective beaches - beach face slope higher than 8.5° - contain Type 3 sediment (coarse sand); the intermediate beaches contain sediment from all types (1,2 and 3); and dissipative beaches are composed by Type 1 sediment (fine sand).

Southern beaches of Santa Catarina coast are in front a large coastal plain systems, which were responsible to introduces policyclic fine sands to beach deposits (Martins *et al.*, 1968). On northern and central-northern beaches, increased grain size variability and sand size (medium to coarse sands) is due to outcrops of basement rock near the coast (Martins *et al.* 1970; 1972; Klein and Menezes, 2001; Miot da Silva *et al.*, 2000 and 2003).

Medium and coarse sands (Types 2 and 3) from intermediate and reflective beaches are associated with beaches that are placed on small coastal plains or over rocky outcrops; often originated from the reworking of alluvial fans, barrier islands or river inputs (Miot da Silva, 2003; Klein and Menezes, 2001). This can be mainly identified in the samples between 68 and 86 (Taquarinhas to Estaleiro beaches) where the beach sediment is a result of a close source of sediments (rework of alluvial fans) (see Figure 6.2).

Fine grained sands (Type 1) on dissipative beaches are associated with fluvial supply and to well developed coastal plain systems (foredunes ridges systems) (Klein and Menezes, 2001).

Beaches show morphodynamic state variability due to sedimentary characteristics. Finer sediments, for example, tend to produce dissipative beaches and coarser sediments tend to be associated with reflective beaches, for a given constant wave height. According to Short (1999), the grain size (with the wave height) controls beach shape and its dynamics. Similar waves on beaches composed by fine, medium or coarse-grained sediments interact to produce different beach types.

The results for the study area also show that occurrence of distinct sediment grain size distribution patterns in nearly beaches indicates that littoral transport of

sediments is restricted to discrete beach systems, with no exchange of sediments or mixture of grain size populations among different cells (see Figure 6.2).

6.4.2. Beachface Slope and Mean Grain Size

Beaches in the study area have a steeper beachface when composed by coarse sand, and a smoother profile when composed of fine sands (Figure 6.5). The highest value of beachface slope (11.5°) in the study area occurs on Taquarinhas Beach, a reflective beach (Type 3). The lowest value (0.9°) is associated with a dissipative state on Balneário Camboriú Beach (Type 1). Beaches composed of sediment Type 2 are intermediate (Figure 6.5).

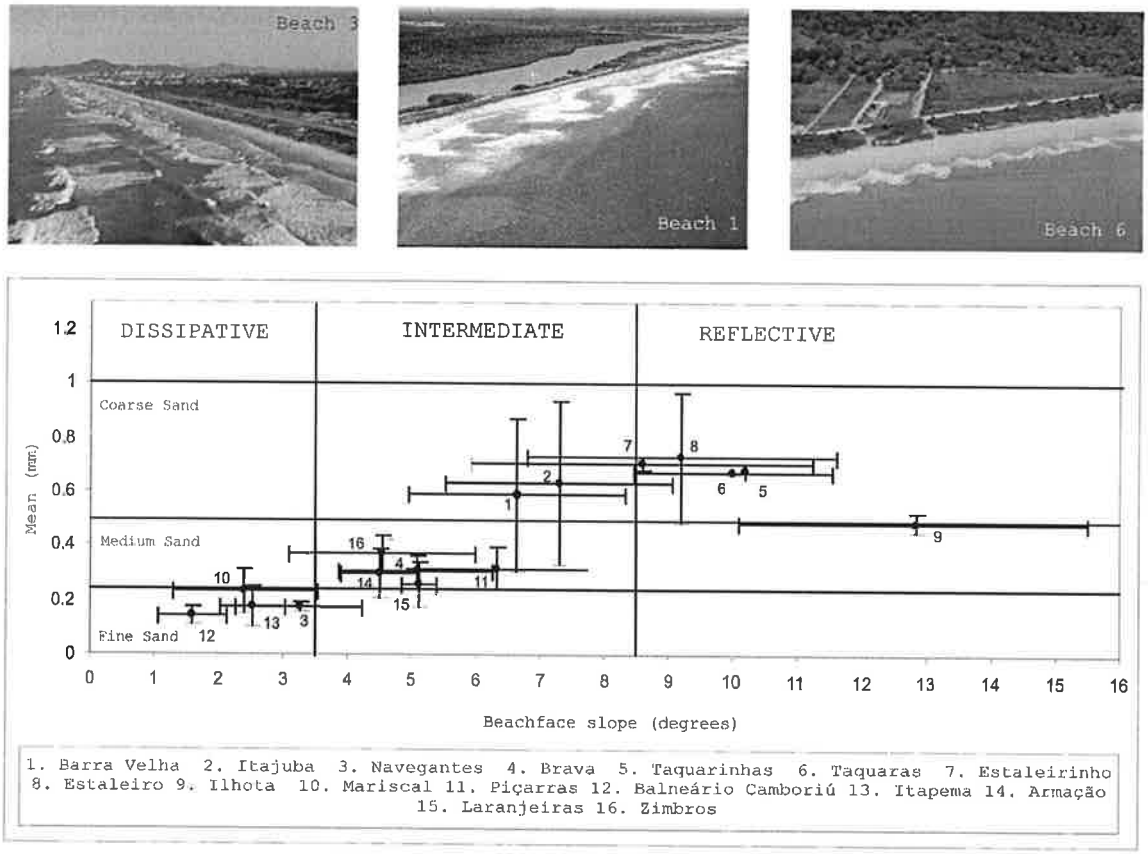

Figure 6.5. Relationship between sedimentary grain size and slope of the beachface indicates the importance of morphodynamic stages and energy level.

This relationship between sedimentary grain size and slope of the beachface indicates the importance of morphodynamic stages and consequently energy level. Bascom (1951) studied forty (40) sandy beaches on the U.S.A. east coast and found similar results; flatter beaches are composed by fine sands while steeper beaches are composed by coarse sands. This sediment-morphologic relationship is mentioned by others such as Johnson (1956), Shepard (1963), Wiegel (1964), McLean and Kirk (1969), Krumbein and Graybill (1965), Dubois (1972, 1989), King (1972), and Finkelstein (1981).

6.4.3. Wave Height and Grain Size

Figure 6.6 shows the distribution of grain size and wave height in the study area for each beach type. There is no obvious relationship between the wave height and grain size. Figure 6.7 shows the longshore distribution of grain size and wave height in the study area. In general, longshore grain-size variations do not show clear agreement with changes in wave height. The longshore wave height variations are related to the degree of beach exposure. It is important also consider that it is more easy define the height of wave break in reflective beaches than in a large dissipative surf zone. The results presented here agree with Nordstrom's (1977) observations that grain sizes of beach sediments that are exposed to different wave energies do not show variation in grain size. This author attributes his results to provenance and beachface processes, and not to wave characteristics. If a coastline is supplied with fine sands, wave height is not important and coarse sands will not be found on this coast. Similarly, if a coastline is supplied with coarse sands, it is not important how low the wave height is, because fine sands will not occur there (Folk, 1968). Only the beachface slope will change in boths cases. Short and Ni (1997) also suggested that there is no relationship between wave

height and grain size, noting that for 471 New South Wales beaches (65% of the total number of NSW beach systems) grain sizes are not selected by waves.

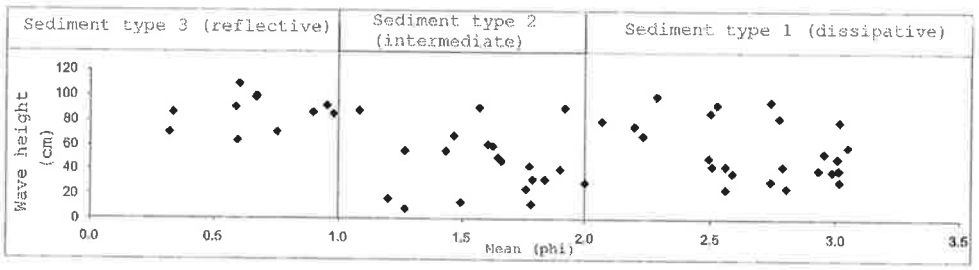

Figure 6.6. Wave height versus mean grain size.

At headland bay beaches without present sediment supply (*e.g.* Armação Beach), alongshore grain size grading can develop in response to selection by variations in wave energy as proposed by Bascom (1951). Navegantes Beach, for example, can not develop longshore grading since the Itajaí-Açu river provides fine grained sediments to this beach and other size classes are simply not available. On the other hand Itapocu river supplied coarse sand to the coastal zone, this reflect in a coarse beach as find in Barra Velha. The reworking of alluvial fan during the Holocene made coarse sediments available to form beaches between Taquarinhas and Plaza.

Curray (1964) suggests results between grain size and wave energy should be analised in terms of budget between processes of sediments input (provenience) and the distribution process (*e.g.* wave action). According to Emery (1968), when there is an important source of sediment to coastal zone, the effectiveness of wave process in the distribution of sediment, decreases proportionally.

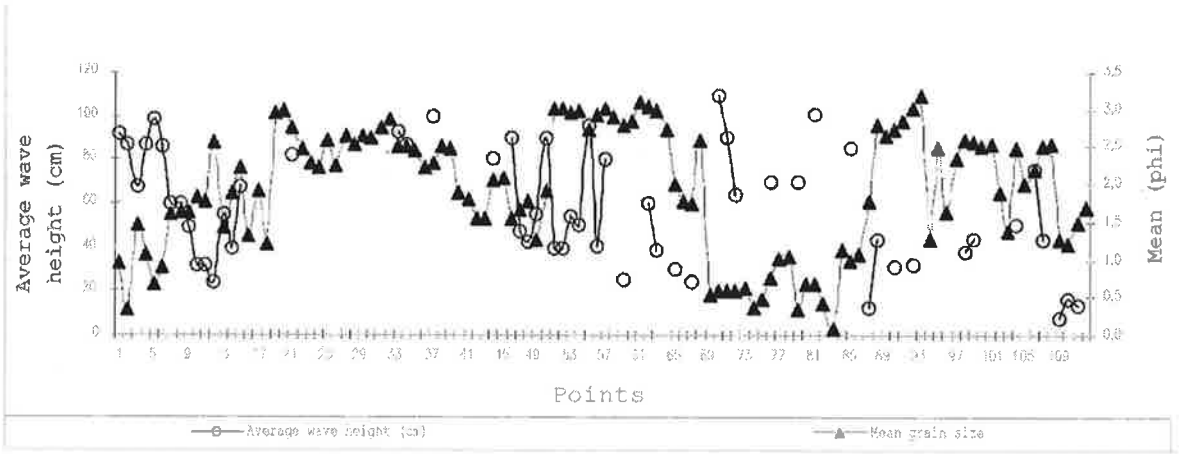

Figure 6.7. Longshore distribution of grain size (o) and wave height (▲) in the study area.

6.4.4. Relation Between Grain Size, Beachface Slope and Wave Height

Figure 6.8 shows the poor relationship between average beachface slope and the ratio between wave height and mean grain size (Hb/Mz) for the beaches in the study area.

It is possible to infer that as the beachface slope decreases, the ratio between wave height and mean grain size (Hb/Mz) increases due to the existence of higher waves and fine-grained sediments.

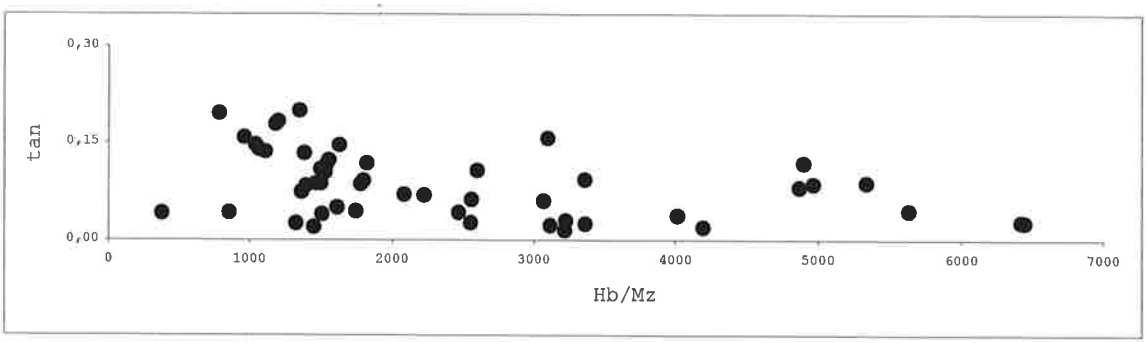

Figure 6.8. Relationship between average beachface slope and the ratio between wave height and mean grain size (Hb/Mz) for the beaches of the study area.

Komar (1976, 1998) in a review about beach face slope concluded that there are several variables that affect the slope of the beach face (*e.g.*: grain size and sorting of sediments, wave energy between storm and swell profile, wave period, water table interaction, tidal cycle). But he pointed out that the most important variable is the grain size of the beach sediment, with coarse-grained beaches having steeper beach slopes. Added to this is the effect of the wave energy level: for a given grain size, higher energies (wave heights) produce lower beach slopes as also proposed by King (1972) and in Sunamura (1984) review. King (1972) obtained an empirical equation for predicting the beach face slope. Her equation shows the positive dependence on the grain size, but it indicates that an increase in the wave energy (height) will result in a decrease in the slope. However, Komar (1976, 1998) and recently Ferreira (1998) finalize their review suggesting that because there are a number of variables involved in the process, quantitative predictions of beach slopes are still remote.

6.4.5. Grain Size Time Series Variation

Navegantes, Barra Velha and Taquaras beaches, which represent different morphodynamic beach types, were studied to assess grain size variations through time. Mean grain size (Mz) and wave height (Hb) data were obtained from a higher number of surveys (15, 17 and 19 surveys respectively), and therefore their analysis allows for a more informed discussion on grain size variation in time.

Navegantes, a dissipative beach composed by Type 1 sediment, shows a low variability of grain size (circa 0.5 ϕ) with time, compared to Barra Velha, an intermediate beach, with large variations of grain size (circa 2.0 ϕ) (Figure 6.9). At

Taquaras, a reflective beach composed by coarse sand (Type 3 sediment), grain size variations through time were less than 0.9 Ø.

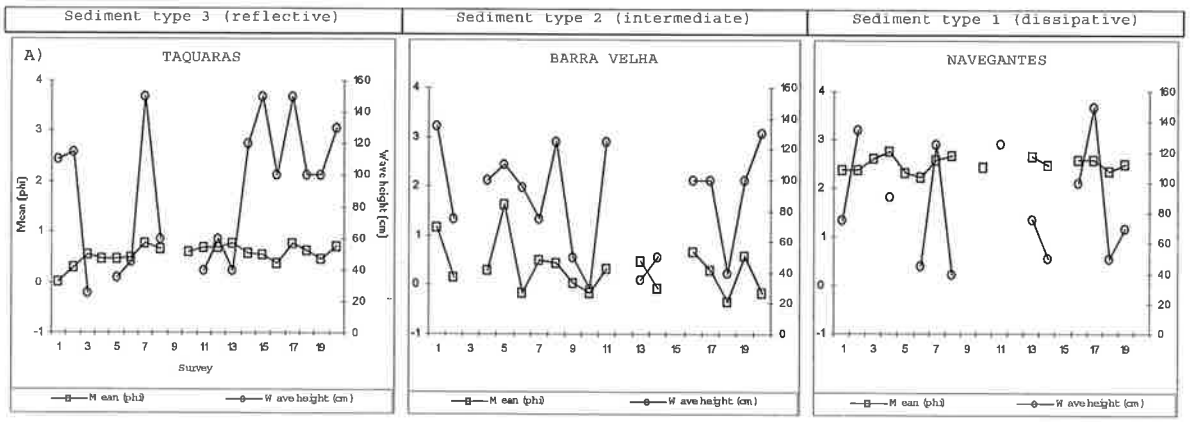

Figure 6.9. Grain size variations through time for different beach morphodynamic stages.

These grain size results suggest that intermediate beaches are more dynamic in space and in time than dissipative or reflective beaches as defined in the classic beach models from Wright and Short (1984), when there are available source of sediments. The dynamics of this beach type is due to the presence of alternating bars and rip currents that promote a continuous variation in beach morphology. Dissipative beaches tend to have stable grain-size distributions in time. Beach stability is promoted by low slope gradient, which makes them less susceptible to changes induced by dissipation in wave energy across a wide surf zone, before reaching the beach.

6.5. SUMMARY

The analyses of sediment distribution patterns for headland and bay coastal types, along the central-northern coast of Santa Catarina State, in southern Brazil show that:

(1) Three grain size types are identified in the study area. The Type 1 represents sediments that have a mean (Mz) grain size between 2.0 ϕ and 3.5 ϕ (0.1 to 0.2 mm, fine to very fine sand). Type 2 is characterized by medium grain size (1 ϕ to 2 ϕ and 0.2 mm – 0.5 mm). Type 3 is characterized by grain sizes between 0.0 ϕ and 1.0 ϕ (0.5 to 1.0 mm, coarse sand). Even though there is an incipient relationship between mean grain sizes and sorting, there is a tendency for fine grained sediments (between 2.0 ϕ and 3.5 ϕ) to be better sorted than coarse sands (between 0.0 ϕ and 1.0 ϕ).

(2) There is a relationship between grain size and morphodynamic beach type. Dissipative beaches are composed of fine sediments (Type 1) if compared to reflective beaches, which are composed by coarse grain sizes (Type 3). Intermediate beaches comprise all grain sizes.

(3) There are different grain size types on the adjacent beaches studied, indicating that circulation patterns are restricted to each beach, without sediment exchanges among different cells along headland-bay beaches coasts.

(4) The beachface slope is positively related to grain size and consequently morphodynamic beach type as proposed in the literature since 60 years. Dissipative beaches, comprisal by fine sands have flatter beachface slopes while reflective beaches, composed of coarse grain sizes, have steeper beachface slopes.

(5) There is no obvious relationship between average wave height and mean grain size (Mz), indicating the importance of sediment provenance to characterize the distribution patterns of sediments in the study area.

(6) Dissipative beaches show greater grain size stability over time due to the low declivity of the beachface, which makes them more resistant to coastal processes. Reflective and intermediary exposed beaches are more dynamic.

In sandy coastal areas, with exposed beaches and with a single source of sediments, the action of the waves (alongshore variation) and the selection imposed by the source make that variation could exist (gradation) in the sedimentary characteristics. This can also happen in beaches of bays sufficiently long and exposed. In coastal areas with bay beaches associated to different sedimentary sources general gradation should not exist relatively to the energy exhibition, for larger relative importance of the source. The gradation will only be able to exist inside of each beach and only if they are long and with different exposure to the waves.

CHAPTER SEVEN

General Conclusions

7.1. GENERAL CONCLUSIONS

This thesis contributed to increase the understanding of headland-bay beach morphology and sedimentology in an east coast swell environment with headlands and bay-beach geomorphology at a Large Scale Coastal Behaviour approach.

The main limitations of this work include the absence of offshore wave record, field experiments to define wave refraction and diffraction/attenuation, and wave shape behind headlands. This study was mainly a coastal geomorphologic approach. More dynamic studies are required to improve knowledge on the processes of this type of coasts.

The following general conclusions of this thesis were obtained:

(1) The parabolic bay shape equation (Hsu and Evans, 1989; Silvester and Hsu, 1993, 1997) has proven to be a convenient and practical tool for studying the stability of the headland-bay beaches, tombolos, and salients in Santa Catarina. Moreno and Kraus (1999) showed that a parabolic model defines very well the beach planform. Some technicalities arose while applying the parabolic bay shape equation, for example, on the definition of the location of upcoast and downcoast control points, and the downcoast tangent. Occasionally, it may be difficult to define the diffraction point (*i.e.* the upcoast control point) from aerial photographs, especially when the tip is hidden (submerged) or with extensive shallow regions in the lee of the headland. The determination of the wave crest line, assumed to be in the same orientation as the tangent downcoast, is another issue affecting the accuracy of the prediction. With some experience, a smooth waterline can be drawn from the irregular shoreline, caused by the existence of a shoal offshore or irregularity in bottom bathymetry.

(2) The analysis of a two-years beach profile-monitoring program showed that beach morphodynamics and sequence profiles for a bay-headland coast in a microtidal environment are a function of geological inheritance (distance between headland and orientation; nearshore and inner shelf morphology; coastal plain morphology; sediment source), and hydrodynamic factors (Hb, T, oceanic wave exposition and relative tidal range). The variation of beach type and surf zone morphodynamics (reflective to dissipative) are mainly a function of the degree of embaymentization (defined by wave exposure and beach sheltering) and sediment source. The presented sequential beach profile model is thus a first approximation. Studies in other areas with the same geographical characteristics are necessary to provide more information and the model validation.

(3) The longshore beach profile monitoring program in three different morphodynamic types of beach exhibited different patterns of sediment removal as a function of the degree of beach curvature. In highly curved beaches, there is a well-developed shadow zone and a range of morphodynamic conditions, from a sheltered low-energy beach adjacent to the downdrift headland to a high-energy exposed beach on the straight end of the headland bay beach. The less curved beaches instead, tend to show more uniform behavior since they are directly exposed to incident waves. Submerged bars, rip currents, and cellular circulation are present. Shoreline length also influences the amplitude of beach rotation. Short-term beach rotation processes were evident in the exposed reflective and dissipative beach. In this study a pivotal point of sediment exchange was not detect, but rather a transitional zone. The absence of wave records and monitoring surf zone morphology were the main problems

concerning this topic. The beach rotation model and proposed relationship must be extended to other areas to provide more information and validation.

(4) Approximately five hundred samples were used in this study to show that there is no obviously relationship between average wave height and mean grain size (Mz), showing the importance of sediment source to characterize the sedimentary distribution patterns in the study area. In terms of a temporal analysis, dissipative beaches have greater grain size stability due to the low declivity of the beachface, which make them resistant to wave processes. Reflective and intermediary beaches are more dynamic. The different beach grain-size types can be used to indicate that circulation patterns are restricted to each beach, which does not allow sediment changes between different cells for a headland bay beach coast.

The main aim of this study was related with research and pure science. However, some practical approaches can be defined (*e.g* beach nourishment projects, harbours) in a headland bay beach: (1) The parabolic model can be used to define the shape of the beach (planform) after the introduction of breakwater/groins. It can also be used to define the surface area to be nourished when the beach is not in equilibrium (*i.e.* erosion). (2) Understand the rotation process and determine whether there is an exchange in sediment type and consequently beach morphodynamics can be used to make better nourishment projects designs.

This thesis increases the knowledge on beach morphology and sedimentology on a headland bay coast, but there is still much work to be done in beach morphodynamic research.

REFERENCES

ABREU, J.G.N. 1998. *Contribuição a sedimentologia da plataforma continental interna de Santa Catarina entre a Foz do Rio Tijucas e Itapocu.* Dissertação de Mestrado. Universidade Federal Fluminense. Instituto de Geociências. Depto. de Geologia. Curso de Pós-Graduação em Geologia e Geofísica Marinha. 64 p. (unpublished).

ABREU, J.G.N., PEZZUTO, P.R., RESGALLA JR., C., MENEZES, J.T. and VINTÉM, G., 2003. Impacto ambiental e modificações texturais dos sedimentos provocadas pela alimentação artificial da praia de Balneário Camboriú (SC). *IX Congresso Brasileiro da Associação Brasileira de Estudos do Quaternário*, ABEQUA, Recife, PE, p 199.

ABREU DE CASTILHO, J.A., 1995. *Estudo evolutivo, sedimentológico e morfodinâmico da parai de Armação, Ilha de Santa Catarina, Florianópolis, SC.* Dissertação de Mestrado, Geografia, UFSC, Florianópolis. 134p. (Unpublished).

ALVES, J.H.G.M. 1996. *Refração do espectro de ondas oceânicas em águas rasas: Aplicações à região costeira de São Francisco do Sul, SC.* Dissertação de Mestrado, Engenharia Ambiental, UFSC, Florianópolis. 89p. (unpublished).

ANGULO, R.J. and LESSA, G., 1997. The Brazilian sea level curves: a critical review with emphasis on the curves from the Paranagua and Cananeia regions. *Marine Geology*, 140, 141-166.

ARAUJO, C.E.S., FRANCO, D., MELO, E. and PIMENTA, F., 2003. Wave regime characteristics of the southern Brazilian coast. *In*: *Proceedings of the Sixth International Conference on coastal and Port Engineering in Developing Countries*, COPEDEC VI, Colombo, Sri Lanka, Paper no. 097; pp 15. (published in CD, no pages).

BASCOM, W.N., 1951. The relationship between sand-size and beach face slope. *Transactions of the American Geophysical Union*, 32, 866-874.

BENEDET FILHO, L., KLEIN, A.H.F., SCHUMACHER, D.H. and MENEZES, J.T., 2000. Beach rotation process in distinct morphodynamic beach types: a preliminary analysis. *In* Klein *et al* (2000) (*Eds*), *Anais do Simpósio Brasileiro Sobre Praias Arenosas: morfodinâmica, ecologia, usos, risco e gestão*. Ed. UNIVALI, Itajai. 178-179 p.

BIRD, E.C.F., 1996. *Beach Management.* John Wiley & Sons Ltd, Baffins Lane, Chichester, England, 281pp.

BIRKEMEIER, W. A. 1981. *Fast accurate two-person beach survey. Coastal Engineering Technical Aid.* U.S. Army Engineer Waterways Experiment Station. Coastal Engineering Research Center, Vicksburg, Mississipi. 81-11 p

BIRKEMEIER, W. A. 1984. Time scales of nearshore profile change. *Proc. 19th Coastal Eng. Conf.*, ASCE, New York, pp. 1507-1521.

BIRKEMEIER, W. A. 1985. *A user's Guide to ISRP: The Interactive Survey Reduction Program.* Instruction Report CERC-84-1. U.S. Army Engineer Waterways Experiment Station. Coastal Engineering Research Center, Vicksburg, Misiissipi. 38 p.

BIGARELLA, J.J., 1972. Eolian environments - their characteristics, recognition and importance. *In*: RIGBY, J.K. and HAMBLIN, W.K. (eds.) *Recognition of ancient sedimentary environments. Soc. Econ. Paleontologists and Mineralogists*, Spec. Publication, 16:12-62.

BIGARELLA, J.J., 1975. Lagoa dune field (State of Santa Catarina, Brazil), a model of eolian and pluvial activity. International Symposium on the Quaternary, *Boletim Paranaense de Geosciences*, p. 133-167.

BITTENCOURT, A.C.S.P., FARIAS, F.F., and ZANINI JR., A., 1987. Reflexo das variações morfodinâmicas praiais nas características texturais dso sedimento da praia da Armação, Slavador, Bahia. *Revista Brasileira de Geosciências* (São Paulo), 17(3), 276-282.

BITTENCOURT, A.C.S.P., DOMINGUEZ, J.M.L. and USSAMI, N., 1999. Flexure as a tectonic control on the large scale geomorphic characteristics of the eastern Brazil coastal zone. *Journal of Coastal Research*, 15 (2), 505-519.

BORGES, A.C., 1977. *Topografia aplicada à Engenharia Civil.* São Paulo: Edgard Blucher, Vol. 1, 187p.

BRANDER, R.W. 1999a. Field observations on the morphodynamic evolution of a low-energy rip current system. *Marine Geology*, 157, 199-217.

BRANDER, R.W. 1999b. Sediment transport in low-energy rip current systems. *Journal of Coastal Research*, 15(3), 839-849.

BRANDER, R.W. and SHORT, A.D., 2000. Mofphodynamics of a large-scale rip current system at Muriwai Beach, New Zealand. Marine Geology, 165, 27-39.

BRESTERS, B. and REIJNGOUD, T. 1996. *Practical use of advanced computer technolgy in the NOURTEC-project.* Part 8: The LOD_EQUI package. Internal report Utrecht University - The Netherlands.

BRYANT, E., 1982. Behavior of grain size characteristics on reflective and dissipative foreshores, Broken Bay, Australia. *Journal of Sedimentary Petrology*, 52, 431-450.

CALLIARI, L.J. 1994. Cross-shore and longhshore sediment size distribution on Southern Currituck Spit, North Carolina: Implications for beach differentiation. *Journal of Coastal Research*, 10 (2), 360-373.

CARTER, R.W., 1988. *Coastal Environments: Na Introduction to the Physical, Ecological and Cultural Systems of Coastlines.* Academic Press, London, England, 617p.

CARUSO JR, F. and ARAÚJO, S.A 1997. A planície de cheniers da Baía de Tijucas, litoral de Santa Catarina. *In: Anais da X Semana Nacional de Oceanografia*. Itajaí. 40-43.

CARUSO JR, F. and ARAÚJO, S.A 1999. Mapa geológico da folha de Itajaí, Santa Catarina. *VII Congresso da ABEQUA*, Porto Seguro – Bahia. 03-09 de Outubro. Vii Abequa_zcp025.pdf.

CARUSO JR, F. and ARAÚJO, S.A., 2000. Ambientes de Sedimentação Costeira da Região Centro-Norte de Santa Catarina e seu Relacionamento com a Geologia regional. *In*: KLEIN, A.H.F. (*eds.*), *Simpósio Brasileiro sobre Praias Arenosas: morfodinâmica, ecologia, usos, risco e gestão*. Itajaí, Santa Catarina, pp. 202-203.

CARUSO JR, F., BITTENCOURT, M. F. and ARAÚJO, S. A., 1997. Contribuição à geologia da região de Itapema, Porto Belo e Bombinhas (SC): Características das rochas

neoproterozóicas e dos ambientes deposicionais cenozóicos. Itajaí . *In*: Anais da X Semana Nacional de Oceanografia, Itajaí, p.48-50.

CARUSO JR, F., KREBS, A., J., WILDNER, W., ARAÚJO, S.A, DIEHL, F.L., FRASSON, H. and CARMO, V.B., 2000. Mapa Geológico da Folha Camboriú-SC, Escala 1:50.000. *In*: KLEIN, A.H.F. (*eds.*), *Simpósio Brasileiro sobre Praias Arenosas: morfodinâmica, ecologia, usos, risco e gestão*. Itajaí, Santa Catarina, pp. 192-194.

CARVALHO, J.L.B, KLEIN, A.H.F, SCHETTINI, C.A.F. and JABOR, P.M., 1996. Marés meteorológicas em Santa Catarina: Influência do vento na determinação de parâmetros de projeto para obras costeiras. In: *Proceedings III Simpósio sobre Oceanografia*, São Paulo, p 380.

CERF – COASTAL ENGINEERING RESEARCH CENTER, 2002. Coastal Engineering Manual (on line). Washington, DC: US Army Corps of Engineers.

CORRÊA, I.,C.,S., 1980. Distribuição dos Sedimentos Modernos da Plataforma Continental entre São Paulo e Santa Catarina. Pesquisas, 13, 109-141.

COWELL, P.J. and THOM, B.G., 1994. Morphodynamics of coastal evolution. *In*: CARTER, R.W.G. and WOODROFFE, C.D. (*eds*), *Coastal Evolution: Late Quaternary Shoreline Morphodynamics*. Cambridge University Press, Cambridge, 33-86.

COWELL, P.J., ZENG, T.: HENNECKE, W., and THOM, B., 1996. Regional Predictions of Climate change Impacts. *Proceedings of the Australian Coastal Management Conference* (Genelg), pp 185-193.

CPTEC/INPE, 2001. *La Niña*. Relatório elaborado pelo CPTEC/INPE em 05 de Agosto de 1998. Available on home-page: http://www.cptec.inpe.br.

CRUZ, O., 1993. *Estudo geomorfológico de áreas costeiras da Ilha de Santa Catarina e do continente circunvizinho (municípios de Florianópolis, São José, Palhoça, Bigauçu e Governador Celso Ramos)*. Florianópolis, UFSC. Relatório Técnico Final de Pesquisa para o CNpq. (unpublished).

CRUZ, O., 1998. *A Ilha de Santa Catarina e o continente próximo: Um estudo de geomorfologia costeira*. Florianópolis, UFSC. 280 p.

CURRAY, J.R., 1964. Transgressions and regressions. In: Donald J.P. Swift and H.D. Palmer (Eds) Coastal Sedimentation. Dowden, Hutchinson & Ross Inc. S troudsburg Pennsylvania. P 97-125.

DAFFERNER, G., KLEIN, A.H.F., SCHUMACKER, D., ANDRADE, A.C. 2002. Correntes de retorno: uma análise preliminar de caracterísiticas morfodinâmicas. In: *Anais do XLI Congresso Brasileiro de Geologia – A Geologia e o Homem*, João Pessoa, p 86.

DAVIES, R.A and HAYES, M.O 1984. What is a wave-dominated coast? *Marine Geology*, 60: 313-329.

DEAN, R.G. 1973. Heuristic models of sand transport in the surf zone. *Proceeding of First Australian Coastal Engineering Conference*, Sydney. Institute Engineers Australia, 208-214.

DEAN, R.G., and DALRYMPLE, R.A., 2002. Coastal Processes with Engineering Applications. Cambridge University Press, 475 pp.

DEAN, R.G. and MAURMEYER, E.M., 1977. Predictability of characteristics of two embayments. Proceedings of Coastal Sediments'77, American Society of Civil engineers, 848-866.

DIEHL, F.L., 1997. *Aspectos geoevolutivos, morfodinâmicos e ambientais do Pontal da Daniela, Ilha de Santa Catarina, Brasil.* Dissertação de Mestrado, Geografia, UFSC, Florianópolis, 128 p. (Unpublished).

DHN, 1 994. *R oteiro C osta S ul: d o C abo F rio a o A rroio Chuí, Lagoas dos Patos e Mirim.* Diretoria de Hidrografia e Navegação, Rio de Janeiros. 282 pp.

DOMINGUEZ, J.M.L., BITTENCOURT, A.C.S.P., LEAO, Z.M.A.N. and AZEVEDO, A.E.G., 1990. Geology of the coastal Quaternary deposits of the State of Pernambuco, *Rev. Bras. Geoc.*, 20, 208-215.

DUBOIS, R.N. 1972. Inverse relation between foreshore slope and mean grain size as a function of the heavy mineral -content. Geol. Soc. Am. Bull., 83:871-876.

DUBOIS, R.N., 1989. Seasonal variation of mid-foreshore sediments at a Delaware beach. Sedimentary Geology, 61, 37-47.

EMERY, K.O., 1968. Relict sediments on continental shelves of word. *The American Association of Petroleum Geologists Bulletin*, Vol 52, No. 3, p 445-464.

EMERY, K.O. and KUHN, G.G., 1982. Sea cliffs: their processes, profiles and classification. *Geological Society of America, Bulletin* 93, 644-654.

EVERTS, C.H., 1983. Shoreline changes downcoast of a littoral barrier. *Proceedings of Coastal Structures'83*, American Society of Civil Engineers, v.1, 673-689.

FARIAS, F.F., BITTENCOURT, A.C.S.P., ZANINI JR., A., and DOMINGUES, J.M.L., 1985. Variações temporais e espaciais na dinâmica de sedimentação da praia da Armação – Salvador/BA. *Revista Brasileira de Geociências* (São Paulo), 15 (1) 48-54.

FERREIRA, Ó., 1998. Morfodinâmica de praias expostas: Aplicação ao sector costeiro Aveiro-Cabo Mondego. Tese de Doutoramento, Universidade do Algarve, 337p.

FINKELSTEIN, K., 1982. Morphological variations and sediment transport in crenulate-bay beaches, Kodiak Island, Alaska. *Marine Geology*, 47: 261-281.

FOLK, R.L. and WARD, W.C., 1957. Brazos River Bar: A Study in the Significance of Grain Size Parameters. Journ. Sediment. Petrol., 27(1), 3-26.

FOLK, R.L., 1966. A Review of Grain-Size Paramters. Sedimentology, 6: 73-93.

FOLK, R.L., 1968. Petrology of Sedimentary Rocks. Austin, Texas: Hemphill's, 169 p.

FUCELLA, J. E and DOLAN, R. 1996. Magnitude of subaerial beach disturbance during Northeast storms. *Journal of Coastal Research*, 12, 420-429.

GAN, M.A., 1992. *Ciclogêneses e ciclones sobre a América do Sul*. Tese de doutorado, Instituto Nacional de Pesquisas Espaciais, São José dos Campos. pp

GARCIA, C.A.E., 1996. Environment and Biota of the Pattos Lagoon Estuary: Hydrographic Chartacteristics. *In*: Seeliger, U., Odebrecht, C. and Castello. J.P. (eds). *Subtropical Convergence Environments: The Coast and Sea in the Southwestern Atlantic.* Springer-Verlag, Berlim, Heidelberg, Germany. p 18-20.

GIANINI, P.C.F., 1993. *Sistemas Deposicionais no Quaternário Costeiros entre Jaguaruna e Imbituba.* Tese de Doutorado, Geologia Sedimentar. Curso de Pós-Graduação em Geologia Sedimentar, Universidade de São Paulo, São Paulo. 277p.

GONZALEZ, M. and MEDINA, R., 1999. Equilibrium shoreline response behind a single offshore breakwater. *Proceedings of Coastal Sediment'99*, American Society of civil Engineers, v. 1, 844-859.

GONZALEZ, M. and MEDINA, R., 2001. On the application of static equilibrium bay formations to natural and man-made beaches. *Coastal Engineering*, 43 (3-4): 209-225.

GOURLAY, M.R. 1968. *Beach and Dune Erosion Tests*. Delft Hydarulics Laboratory, Report No. M935/M936.

HALLIGAN, G.H., 1906. Sand movement on the New South Wales coast. *Proceeding of the Limnology Society of New South Wales*, 31, 619-640.

HARDAWAY, C.S. and GUUN, J.R., 1999. Chesapeake Bay: Design and early performance of three headland breakwater systems. *Proceedings of Coastal Sediments'99*, American Society of Civil Engineers, v.1, 828-843.

HAYES, M.O., 1979. Barrier island morphology as a function of tidal and wave regime. In: LEATHERMAN, S.P. (ed.). *Barrier Islands*. Academic Press, New York, 1-27.

HEGGE, B., ELIOT, I. and HSU, J. 1996. Sheltered sandy beaches of southwestern Australia. *Journal of Coastal Research*, Fort Lauderdale, 12(33):748-760.

HOEFEL, F. G 1998. *Diagnostico da erosao costeira na praia de Picarras, Santa Catarina*. Dissertacao de Mestrado. Programa de Pos-graducao de Engenharia da Universidade federal do Rio de Janeiro, 86p. (unpublished)

HOEFEL, F. G. and KLEIN, A.H.F., 1998a. Beach safety issue at oceanic beaches of central northern coast of Santa Catarina, Brazil: Magnitude and nature. *In*: FINKL, CW. (ed), *ICS'98 Proceedings*, Fort Lauderdale, Florida. *Journal of Coastal Research*, Special Issue, 26 (2), 87-93.

HOEFEL, F. G. and KLEIN, A.H.F., 1998b. Environmental and social decision factors of beach safety in the Central Northern coast of Santa Catarina, Brazil. *Notas Técnicas da FACIMAR*, 2, 155-165.

HOGBEN, N. and LUMB, F.E., 1967. *Ocean Waves Statistics*. National Physical Laboratory. Ministry of Technologie, London. 263 p.

HOGBEN, N., DA CUNHA, L.F. and OLLIVER, H.N., 1986. *Global Waves Statistics*. British Maritime Technology Limited, pub. Unwin Brothers Ltd., London.

HOM-MA, M. and SONU, C.J., 1962. Rhythmic pattern of longhore bars related with sediment characteristics. Proc. 8th Coastal Eng. Conf., ASCE, New York, pp. 248-278.

HORN FILHO, N.O., ABREU DE CASTILHOS, J., GRÉ, J.C.R. and DIEHL, F.L., 1994. The coastal Pleistocene of Santa Catarina State, southern Brazil. *In*: RABASSA, J. (*ed.*), Symposium and Field meeting "The Termination of the Pleistocene in South America", Tierra del Fuego. Quaternay of South America and Antarctic Peninsula, Rotterdam, v:10.

HSU, J.R.C. and EVANS, C., 1989. Parabolic bay shapes and applications. *Proceedings of the Institute of Civil Engineers*, Part 2, 87, 557-570.

HSU, J.R.C. and SILVESTER, R., 1990. Accretion behind single offshore breakwaters. Journal of Waterway, Port, Coastal and Ocean Engineering, American Society of Civil Engineers, 116(3):362-380.

HSU, J.R.C. and SILVESTER, R., 1996. Stabilizing beaches downcoast of harbor extension. *Proceedings of the 25th International Conference on Coastal Engineering*, American Society of Civil Engineers, v.4, 3986-3999.

HSU, J.R.C., UDA, T. and SILVESTER, R., 1993. Beaches downcoast of harbours in bays. *Coastal Engineering*, 19(1,2): 163-181.

HSU, J.R.C., UDA, T. and SILVESTER, R., 2000. Shoreline protection methods – Japanese experience. *In*: HERBICH, J.B. (Ed.), Handbook of Coastal Engineering. McGraw-Hill, New York, pp. 9.1-9.77.

HSU, J.R.C., KLEIN, A.H.F., BENEDET, L., RAABE, A., and TSAI, C.P., 2004. Static equilibrium bay beach for coastal management and protection. (*in preparation*)

HUNTLEY, D.A and SHORT, A.D., 1992. On the spacing between observed rip currents. *Coastal Engineering*, 17, 211-225.

INMAN, D.L. and NORDSTROM, C.E., 1971. On the tectonic and morphologic classification of coasts. *Journal of Geology*, 79, 1-21.

INPH, 2000. *Estudo para o engordamento da praia de Camboriú, SC.* Instituto de Pesquisas Hidroviárias, Divisão de Engenharia Hidráulica – DIENGH, Rio de Janeiro. INPH 28/2000, Camboriú 900/91. 55p.

JICA, 1990. *Feasibility study on the Flood Control Project in the Lower Itajaí River Basin*. Final Report, Supporting Report: Japan International Cooperation Agency.

JOHNSON, J. W., 1956. Dynamics of nearshore sediment movement. *Bull. Am. Soc. Petrol. Geologists*, 40 (9), 2211-2232.

KING, C.A.M., 1972. *Beaches and Coasts*. 2nd ed. London: Edward Arnold, 570p.

KLEIN, A.H.F., 1997. Regional Climate. *In*: Seeliger, U., Odebrecht, C. and Castello. J.P. (eds). *Subtropical Convergence Environments: The Coast and Sea in the Southwestern Atlantic.* Springer-Verlag, Berlim, Heidelberg, Germany. p 5-7.

KLEIN, A.H.F. 1997. Um método indireto para a determinação do estágio morfodinâmico de praias oceânicas arenosas. *Anais, VI Congresso da Associação Brasileira de Estudos do Quaternário*, Curitiba, ABEQUA. 76-78.

KLEIN, A.H.F and MENEZES, J.T. 2000. Beach Morphodynamics and profile sequence for headland bay coast. *In* Klein *et al* (2000) (*Eds*), *Anais do Simpósio Brasileiro Sobre Praias Arenosas: morfodinâmica, ecologia, usos, risco e gestão*. Ed. UNIVALI, Itajai. 97-98 p.

KLEIN, A.H.F. and MENEZES, J.T., 2001. Beach morphodynamics and profile sequence for a headland bay coast. *Journal of Coastal Research*, 17 (4), 812-835.

KLEIN, A .H.F, MENEZES, J.T. and ABREU, J.G.N 1999. Morfodinâmica das praias do litoral centro-norte de Santa Catarina. *Anais: VII Congresso da ABEQUA. Porto Seguro*. Viiabequa_zcp035.pdf

KLEIN, A.H.F., ADRIANI JR, N., and MENEZES, J.T., 2002. Shoreline salients and tombolos on the Santa Catarina coast (Brazil): Description and analysis of the morphological relationships. *Journal of Coastal Research*, SI (36), 425-440.

KLEIN, A.H.F., BENEDET FILHO, L. and HSU, J.R.C., 2003a. Stability of headland bay beaches in Santa Catarina: a case study. *In*: KLEIN, A.H.F., FINKL, C.W., RÖRIG, L.R., SANTANA, G.G., DIEHL, F.L. and CALLIARI, L.J. (eds), *Journal of Coastal Research*, Special Issue 35, Proceedings of the Brazilian Symposium on Sandy Beaches: Morphodynamics, Ecology, Uses, Hazards and Management, 151-166.

KLEIN, A.H.F., BENEDET, L., and SCHUMACHER, D.H., 2002. Short-term beach rotation processes in distinct headland bay beach systems. Journal of Coastal Research, 18(3), 442-458.

KLEIN, A.H.F., VARGAS, A., RAABE, A.L.A., and HSU, J.R.C, 2003b. Visual assessment of bayed beach stability using computer software. *Computer and Geosciences*, 29, 1249-1257.

KLEIN, A.H.F., TEMME, B., MENEZES, J.T., DIEHL, F.L., CARVALHO, J.L.B and JABOR, P.M., 1997. Comportamento morfológico de uma praia semi-protegida: Balneário Camboriú, SC. *Anais, VI Congresso da Associação Brasileira de Estudos do Quaternário*, Curitiba, PR. pp.82-84.

KLEIN, A.H.F, MOCELLIM, O., MENEZES, J.T., BERIBILI, M., VINTÉM, G., DAFFERNER, G., DIEHL, F.L., SPERB, R.M. and SANTANA, G. (*in press*). Beach safety management in the coast of Santa Catarina, southern Brazil. *Zeitchirift Geomorlogie.*

KLEIN, A.H.F., MIOT DA SILVA, G., FERREIRA, Ó. and DIAS, J.A. (*in press*). Beach sediment distribution for a headland bay coast. *Journal of Coastal Research.*

KOMAR, P.D., 1976. *Beach Processes and Sedimentation.* Prentice-Hall, Inc., New Jersey, 429 pp.

KOMAR, P.D., 1998. *Beach Processes and Sedimentation.* Second edition. Prentice-Hall, Inc., New Jersey, 544 p.

KRIEBEL, D.L., KRAUS, N.C. and LARSON, M. 1991. Engineering methods for predicting beach profile response. *Coastal Sediments'91.* ASCE, New York, 557-571.

KRUMBEIN, W.C., 1934. Size frequency distribution of sediments. Journal of Sedimentary Petrology, 4, 65-77.

KRUMBEIN, W.C., 1944. Shore processes and beach characteristics. *Technical Memorandum N° 3*, Beach Erosion Board, U.S. Army Corps Engineers, 47p.

KRUMBEIN, W.C, and GRAYBILL, F.A., 1965. An introduction to statistical models in geology. McGAW-HILL, New York, 574 pp.

LARSON, M. and KRAUS, N.C, 1989. SBEACH: numerical model for simulating storm-induced beach change, Report1: empirical foundation and model development. Tech. Rep. CERC – 89-9. U.S. Army Eng., Waterways Expt. Stn., Coastal Eng. Res. Center, Vicksburg, MS.

LARSON, M. and KRAUS, N.C, 1994. Temporal and spatial scales of beach profile change, Duck, North Carolina. *Marine Geology* , 117, 75-94.

LARSON, M. and KRAUS, N.C, 1995. Prediction of cross-shore sediment transport at different spatial and temporal scales. *Marine Geology*, 126, 111-127.

LEBLOND, P.H., 1972. On the formation of spiral beaches. *Proceedings of the 13th International Conference on Coastal Engineering*, American society of Civil Engineers, v.2, 1331-1345.

LEBLOND, P.H., 1979. An explanation of the logarithmic spiral plan shape of headland-bay beaches. *Journal Sedimentary Petrology*, 49(4), 1093-1100.

LEAL, P.C., 1999. *Sistema praial Moçambique – Barra da Lagoa, Ilha de Santa Catarina, SC, Brasil: Aspectos morfológicos, morfodinâmicos, sedimentológicos e ambientais.* Dissertação de Mestrado, Geografia, UFSC, Florianópolis. 125 p (unpublished).

LIANG, G. and SEYMOUR, R.J. 1991. Complex principal component analysis of wave-like sand motions. Proc. Coastal Sediments'91, ASCE, New york, pp 2175-2186.

LIPPMAN, T.C. and HOLMAN, R.A., 1990. The spatial and temporal variability of sand bar morphology. *Journal of Geophisical Research*, 95(C7), 11,575-11,590.

MAKASKE, B. and AUGUSTINUS, G.E.F, 1998. Morphologic changes of a micro-tidal, low wave energy beach face during a spring-neap tide cycle, Rhône-Delta, France. *Journal of Coastal Research*, 14(2): 632-645.

MARTIN, L., SUGUIO, K. and FLEXOR, J.M., 1979. Le Quaternaire marin of littoral bresilien entre Cananeia (SP) et Barra de Guaratiba (RJ). *International Symposium on Coastal Evolution in the Quaternary*, Sao Paulo, p. 296-331.

MARTIN, L., SUGUIO, K. and FLEXOR, J.M., 1984. Informações adicionais fornecidas pelos sambaquis na reconstrução de paleolinhas de praia quaternária: exemplo da costa do Brasil. *Rev. Pre-Historia*, Univ. Sao Paulo, 6, 128-147.

MARTIN, L., DOMINGUEZ, J.M.L. and BITTENCOURT, A.C.S.P., 2003. Fluctuating Holocene sea levels in eastern and southeastern Brazil: Evidence from multiple fossil and geometric indicators. *Journal of Coastal Research*, 19 (1), 101-124.

MARTINS, L.R., EICHIER, B.B., PODOLSKI, V.M. 1968. Propriedades texturias dos sedimentos litorâneos de Santa Catarina. I. Areias de praias, trecho Mampituba-Araranguá. *Iheringia*. Série Geologia, Pôrto Alegre, 2:41-53.

MARTINS, L.R., GAMERMANN, N., SCHEIBE, L.F. and TEIXEIRA, V.H., 1970. Sedimentologia da Ilha de Santa Catarina: I – Areias praiais. *Publicação Especial No. 18, Escola de Geologia*. Porto Alegre, 18: 1-55.

MARTINS, L.R., JOST, H., VILLWOCK, J.A., and MARTINS, I.R. 1972. Misturas populacionais e efetividade de energia ambiental. *Pesquisas*, 1: 13-24.

MARTINO, E., MORENO, L. and KRAUS, N.C., 2003. Engineering guidance for the use of bayed-beach formulations. *Proceedings of Coastal Sediments '03, American Society of Civil Engineers*. pp

MASSELINK, G., 1993. Simulating the effects of tides on beach morphodynamics. *Journal of Coastal Research*, Special Isssue 15, 180-197.

MASSELINK, G. and TURNER, I.L. 1999. The effect of tide on beach morphodynamics. *In* SHORT, A.D. *Ed.* (1999). Handbook of Beach and Shoreface Morphodynamics – John Wiley & Sons Ltda, Baffins Lane, Chichester, 204-229 p.

MASSELINK, G. and PATTIARATCHI, C.B., 2001. Seasonal changes in beach morphology along the sheltered coast of Perth, western Australia. *Marine Geology*, 172, 243-263.

MCLEAN, R.F., and KIRK, R.M., 1969. Relationship between grains size, size-sorting, and foreshore slope on mixed sand-shingle beaches. *N.Z.J. Geol. And Geophys.*, 12: 138-155.

MELO, E., 1993. The sea sentinel project: wathing waves in Brazil. In: 8th Symposium on Coastal and Ocean Management, July 19.

MELO, E. and ALVES, J.H.G.M., 1993. A note on the arrival of long traveled swell at the Brazilain Coast. *Proc. X Simposio Brasiliero de Recursos Hídricos*, ABRH, Bramado, RS, 5: 362-369. (Esta errado e em protugues).

MELO, E., PIMENTA, F.M., MENDES, D.A.R., HAMMES, G.R., ARAÚJO, C.E.S., FRANCO, D., ALVES, J.H.G.M., BARLETTA, R.C., SOUTO, A.M., CASTELÃO, G., PEREIRA, N.C. and BRANCO, F.V., 2003. A real time, on-line coastal information program in Brazil. *In*: *Proceedings of the Sixth International Conference on coastal and Port Engineering in Developing Countries*, COPEDEC VI, Colombo, Sri Lanka, Paper no. 104; pp 14. (published in CD, no pages).

MENEZES, J.T., 1999. *Aspectos morfodinâmicos das praias do litoral centro-norte catarinense.* Curso de Oceanografia, Universidade do Vale do Itajaí, Itajaí. Monografia de conclusão de Curso. 130p (unpublished).

MENEZES, J. T. and KLEIN, A. H. F. 1997. Variações morfológicas das praias do litoral centro-norte do Estado de Santa Catarina: resultados preliminares. *Anais, X Semana Nacional de Oceanografia*. Itajai. 58-60.

MIOT DA SILVA, G., 2003. Efeito do estado de equilíbrio em planta na sedimentologia de praias desenvolvidas entre promontórios. Dissertação de Mestrado em Geociências, Programa de Pós-graguação em Geociências, Universidade Federal do Rio Grande do Sul, Porto Alegre (unplished).

MIOT DA SILVA, G., KLEIN, A.H.F. and LAFIN, N.A., 2000. Longshore Grain Size Distribution in headland-bays coasts: preliminary results. *In*: KLEIN, A.H.F. (eds.), *Simpósio Brasileiro sobre Praias Arenosas: morfodinâmica, ecologia, usos, risco e gestão*. Itajaí, Santa Catarina, pp. 208-210.

MIOT DA SILVA, G., KLEIN, A.H.F. and ALMEIDA, L.E.S B. 2003. Estudo do padrão de distribuição de sedimentos em praias de enseada. *Anais do IX Congresso da Associação Brasileira de Estudos do Quaternário*, Recife. p73.

MORAES, G.N. and GRIEP, G.H., 1985. ANGRA, um analisador granulométrico para micros. *Proceedings of II Encontro Brasileiro de Oceanólogos*. Rio Grande, RS.

MORENO, L.J. and KRAUS, N.C., 1999. Equilibrium shape of headland-bay beaches for engineering design. *In*: *Proceedings of Coastal Sediments'99*, Vol. 1. American society of Civil Engineers, New York, pp. 860-875.

MUEHE, D., 1998. O litoral brasileiro e sua compartimentação. In: Cunha, S.B. and Guerra, A.J.T (eds). *Geomorfologia do Brasil*. Capitulo 7. Rio de Janeiro. Editora Bertrand Brasil S.A., pp 273-349.

NOBRE, C.A., CAVALCANTI, I.F.A., GAN, M.A., NOBRE, P.A., KAYANO, M.T., RAO, V.B., BONATTI, J.P., SATYAMURTI, P., UVO, C.B. and COHEN, J.C., 1986. Aspectos da climatologia dinâmica do Brasil. *Climanálise N° Especial*. 65p.

NORDSTROM, K.F., 1977. The use of grain size statistics to distinguish between high and moderate energy beach environments. *Journal of Sedimentary Petrology*, 47(3), 1287-1294.

NORDSTROM, K.F., 1981. Differences in grain size distributions with shoreline positions in a spit environment. *Northeast. Geol.*, 3, 252-258.

NORDSTROM, K.F. and JACKSON, N. L. 1990. Migration of swash zone step and microtopographic during tidal cycles on na estuarine beach, Delaware Bay, New Jersey, U.S.A . *Marine Geology*, 92, 147-154.

OLIVEIRA, I.B.M., TEIXEIRA, A.T. and DO VALE, A.D., 2000. West coast of Portugal (Espinho): a comparison between project predictions and reality. *Proceedings of the 27th International Conference on Coastal Engineering*, American Society of Civil Engineers, v. 4, 3552-3565.

PAPPS, D. and PRIESTLEY, S., 2003. Project Manukau: coastal restoration using crenulated beaches. *Australian Conference on Coasts & Ports 2003*, Paper No. 119.

PETTIJOHN, F.J. and RIDGE, J.D., 1932. A textural variation series of beach sands from Cedar Point, Ohio: *Journal of Sedimentary Petrology*, 2, 76-88.

PIRAZZOLI, P., 1991. *World Atlas of Holocene sea-level changes*. New York: Elsevier, Oceanography Series, 58, 1-300.

PIRAZZOLI, P., 1996. *Sea-Level Changes: The Last 20,000 Years*. John Wiley, Chichester, England. 378 p.

PHILLIPS, J.D., 1985. Headland-bay beaches revisited: an example from Sandy Hook, New Jersey. *Marine Geology*, 65, 21-31.

REA, C.C. and KOMAR, P.D., 1975. Computer simulation of a hooked beach shoreline configuration. *Journal Sedimentary Petrology*, 45, 866-872.

RODRIGUEZ, D.E.M.G., 1995. Morfologia de Playas en Equilibrio: Planta y Perfil. Escuela Técnica superior de Ingenieros de Caminos, Canales y Puertos, Universidad de Cantabria, Santander, Espanha. 350 p.

SANTA CATARINA - GAPLAN, 1986. *Atlas de Santa Catarina*. Florianópolis. 173p.

SANTA CATARINA - SEDUMA, 1997. *Bacias Hidrográficas do Estado de Santa Catarina: diagnóstico geral*. Florianópolis, 163p.

SANTOS, C.R., 1995. *Inter-relação entre a dinâmica da vegetação pioneira e os padrões morfo-sedimentológicos sazonais da Praia de Joaquina, Ilha de Santa Catarina, Brasil*. Dissertação de Mestrado, Geografia, UFSC, Florianópolis. 207 p. (unpublished).

SCHETTINI, C.A.F, CARVALHO, J.L.B. and JABOR, P. 1996. Comparative hydrology and suspended matter distribution of four estuaries in Santa Catarina State – southern Brazil. *In*: *Proceedings, Workshop on Comparative Studies of Temperate Coast Estuaries*. Bahia Blanca.

SCHETTINI, C.A .F and KLEIN, A .H.F 1997. Processos costeiros e dinâmica estuarina: um modelo para o estuário do rio Itapocu, Santa Catarina. *VI Congresso da ABEQUA*, Curitiba, 127-131.

SHEIBE, L.F.A., 1986. A geologia de Santa Catarina – Sinópse provisória. *GeoSul*, N° 1, 7-38.

SHEPARD, F.P., 1963. Submarine geology. 2sd ed. Harper & Row, New York, 557 pp.

SHORT, A.D., 1979. Three-dimensional beach-stage model. *Journal of Geology*, 87, 553-571.

SHORT, A.D., 1983 . Sediments and structures in beach-nearshore environments, southeast Australia. *In* : MCLACHLAN, A. and ERASMUS, T. (eds). *Sandy Beaches as Ecosystems*, Junk, The Hague, England., 145-155.

SHORT, A.D., 1984a. Temporal change in beach type resulting from a change in grain size. *Search*, 15, 228-230.

SHORT, A.D., 1984b. Beach and nearshore facies, southern Australia. *Marine Geology*, 60, 261-282.

SHORT, A.D., 1985. Rip current type, spacing and persistence, Narrabeen Beach, Australia. *Marine Geology*, 65, 47-71.

SHORT, A.D., 1986. Sandy shore facies in southeast Australia. *In*: FRANKEL, E., KEENE, J.B. WALTHO, A.E. (eds). *Recent Sediments in Eastern Australia*. NSW Division, Geological Society of Australia, 87-100.

SHORT, A.D., 1994. Sediment characteristics of the New South Wales coast and implications for beach type and stratigraphy. *Proceedings of 14th International Sedimentological Congress*, Recife, Brazil, D-74.

SHORT, A.D, 1999 (*ed*). *Handbook of Beach and Shoreface Morphodynamics*. Wiley, New York, 379pp.

SHORT, A.D, 2002. Large scale behaviour of topographically-bound beaches. *International Conference Coastal Engineering*. Cardiff, American society Civil Engineers, 3778 – 3890.

SHORT A.D. and AAGAARD, T. 1993. Single and multi-bar beach change models. *Journal of Coastal Research*, SI 15, p. 141-157.

SHORT, A.D., and BRANDER, R.W., 1999. Regional variations in rip density. *Journal of Coastal Research*, 15(3), 813-822.

SHORT, A.D., and HOGAN, C.L. 1994. Rip currents and beach hazards, their impact on public safety and implications for coastal management. *In*: FINKL, C.W. (ed). *Coastal Hazards. Journal of Coastal Research*, Special Issue 12, 197-209.

SHORT, A.D. and MASSELINK, G., 1999. Embayed and structurally controlled beaches. *In*: SHORT, A.D. (Ed.), *Handbook of Beach and Shoreface Morphodynamics*. Wiley, New York, pp. 230-249.

SHORT, A. and NI, M., 1997. Regional and systematic controls on New South Wales beach characteristics. *Institute of Australians Geographers and New Zealand Geographers Society Zoint Conference,* Hobart, 143.

SHORT, A.D., COWELL, P.J., CADEE, M., HALL, W., and VAN DIJK, B., 1995. Beach rotation and possible relation to southern oscilation. *In*: AUNG, T.H. (ed), *Ocean Atmosphere Pacific Conference*, National Tidal Facility, Adelaide: pp. 329-334.

SHORT, A.D., TREMBANIS, A.C. and TURNER, I. L., 2000. Beach oscillation, rotation, and the Southern Oscilation, Narraben Beach, Australia. *Proceedings International Conference on Coastal Engineering* (Sydney).

SILVESTER, R., 1960. Stabilization of sedimentary coastlines. *Nature*, 188, 467-469.

SILVESTER, R., 1970. Development of crenulate shape bays to equilibrium. *J. Waterways and Harbors Division*, American Society of Civil Engineers, 96 (WW2): 275-287.

SILVESTER, R. 1974. Coastal Engineering, Elsevier Amsterdam, 2 vols.

SILVESTER, R. and HO, S.K., 1972. Use of crenulate shape bays to stabilize coasts. *In*: *Proceedings of the International Conference on Coastal Engineering*, Vol. 2, American Society of Civil Engineers, New York, pp. 1394-1406.

SILVESTER, R. and HSU, J.R.C., 1993. *Coastal Stabilization: Innovative Concepts*. Prentice-Hall, Englewood Cliffs, N.J, 578pp.

SILVESTER, R. and HSU, J.R.C., 1997. *Coastal Stabilization*. Advanced Series on Ocean Engineering, Vol. 14, World Scientific, Singapore, 578pp. (Reprint of SILVESTER and HSU, 1993).

SILVESTER, R., TSUCHIYA, Y. and SHIBANO, T., 1980. Zeta bays, pocket beaches and headland control. *Proceedings of the 17th International Conference on Coastal Engineering*, Vol. 2, American Society of Civil Engineers, New York, pp. 1306-1319.

SONU, C. J. and VAN BEEK, J. L. 1971. Systematic beach changes on the outer banks, North Carolina. *Journal of Geology*, (74) 3: 247-268.

SMITH, G.G., DUNKLEY, E. and SOLTAU, C., 2000. Shoreline response to harbour developments in Table Bay. Proceedings of the 27th International Conference on Coastal Engineering, American society of Civil Engineers, v.3, 2822-2835.

SONU, C.J., 1973. Three-dimensional beach changes. *Journal of Geology*, 81, 42-64.

SUGUIO, K., MARTIN, L. and FLEXOR, J.M., 1980. Sea-level fluctuations during the past 6,000 years along the coast of the State of Sao Paulo, Brazil. *In*: MORNER, M.A. (ed.) *Earth Rheology, Isostasy and Eustasy*. New York: Wiley, p. 471-486.

SUNAMURA, T., 1984. Quantitative predictions of beach-face slope. Geological Society of American bulletin, 95, 242-245.

TALJAARD, J.L., 1972. Synoptic meteorology of the southern hemisphere. *In*: NEWTON, C.W. (ed). *Meteorology of the southern hemisphere*. Bonston (Am. Meteorol. Soc.). *Meteorology Monographs*, 13(35), 139-213.

TAN, S-K. and CHIEW, Y-M., 1994. Analysis of bayed beaches in static equilibrium. *Journal of Waterway, Port, Coastal and Ocean Engineering*, American Society of Civil Engineers, 120 (2), 145-153.

TEMME, B, KLEIN, AHF, CARVALHO, J.L.B and DIEHL, F.L. 1997 Morphologic behaviour of the beach of Balneario Camboriu: preliminar results. *Notas Técnicas da FACIMAR*, 1,49-65.

TORRONTEGUY, M.C., 2002. *Sistema Joaquina-Morro das Pedras e praias adjacentes da costa leste da Ilha de Santa Catarina: Aspectos morfodinâmicos, sedimentológicos e fatores condicionantes*. Dissertação de Mestrado, Geografia, UFSC, Florianópolis. 158 p. (Unpublished).

TRUCCOLO, E.C., 1998. *Maré meteorológica e forçantes atmosféricas locais em São Francisco do Sul, SC.* Dissertação Mestrado, Engenharia Ambiental, Programa de Pós-Graduação em Engenharia Ambiental, UFSC, Florianópolis, 100p. (Unpublished).

TRUCCOLO, E.C., FRANCO, D. and SCHETTINI, C.A.F., 2002. Coastal sea level variability due to meteorological forcing in the Northern Coast of Santa catarina, Brazil: Observations. *In*: *Proceeding Littoral 2002 , The Changing coast, EUROCOAST/EUCC*, Porto, Portugal, p 219-223.

UDA, T., M. SERIZAWA, T. SAN-NAMI, and K. FURUIKE, 2002. Shoreline changes of a pocket beach caused by elongation of harbor breakwater and their prediction. *Transactions, Japanese Geomorphological Union*, 23 (3): 395-413.

VERHAGEN, H.J., 2000. Sea Breeze. *Proceedings of the 2nd International Conference on Port development and Coastal Environment around the Black Sea, Bulgaria (Varna)*.

YASSO, W.E., 1965. Plan geometry of headland bay beaches. *Journal of Geology*, 73, 702-714.

YBERT, J.P., BISSA, W.M., CATHARINO, E.L.M. and KUTNER, M., 2003. Environmental and sea-level variations on the southeastern Brazilian coast during the Late Holocene with comments on prehistoric human occupation. *Palaeogeography, Palaeoclimatology, Palaeoecology*, 189, 11-24.

ZENKOVICH, V.P., 1967. Processes of Coastal Development. Ed: Steers, J.A.. Trans: Fry, D.G. Edinburgh, Oliver & Boyd. 500 p.

VAN RIJN, L.C., 1998. Principles of Coastal Morphology. Amsterdam: Aqua Publications.

WEESAKUL, S., 1999. Erosion control of downcoast area of ports in Thailand using parabolic bay shape. *Proceedings of Coastal Sediments '99*, American society of Civil Engineers, v. 1, 876-884.

WENTWORTH, C.K., 1922. A scale of grade and class terms for clastic sediments. *Journal of Geology*, 30, 377-392.

WIEGEL, R.L., 1964. Oceanographical Engineering. Prentice-Hall, Englewood Cliffs. N.J., 532 pp.

WONG, P.P., 1981. Beach evolution between headland breakwaters. *Shore and Beach*, 49(3): 3-12.

WRIGHT, L.D. and SHORT, A.D., 1984. Morphodynamics variability of surf zones and beaches: a synthesis. *Marine geology*, 56, 93-118.

WRIGHT, L.D. and THOM, B.G., 1977. Coastal depositional landforms, a morphodynamic approach. Progress in Physical Geography, 1, 412-459.

WRIGHT, L.D., CHAPPELL, J., THOM, B.G., BRADSHAW, M.P. and COWELL, P., 1979. Morphodynamics of reflective and dissipative beach and inshore systems, southern Australia. *Marine Geology*, 32, 105-140.

APPENDIX I

Data for 90 simulations- Santa Catarina Beaches

Table 1. Data for 35 simulations for northern sector of Santa Catarina.

BEACH	β(degree)	Rβ(cm)	a(cm)	Equilibrium
Armação da Piedade (south headland)	53	6.55	2.8	close to static
Armação da Pied. (north headland)	45	5.7	2.4	close to static
Praia Grande 1	52	2.6	1	static
Praia Grande 2	28	1.9	0.6	close to static
Praia Grande 3	31	5.8	2.1	close to static
Palmas (south headland)	52	5.45	4.3	dynamic
Praia 1	45	1.8	0.7	static
Zimbros	70	30.6	15.3	close to static
Mariscal (south end)	65	7.4		Static
Mariscal (whole beach)	38	18.5	5.8	Dynamic
Quatro Ilhas (south headland)	33	4.2	1.5	close to static
Quatro Ilhas (north headland)	39	3.5	1.2	close to static
Bombinhas (south end)	62	12.3	6.4	dynamic
Bombas/bombinhas (whole beach)	67	16.35	6.95	dynamic
Portobelo (w/o the groin)	49	5.4	2	close to static
Portobelo (new Ro is the groin)	30	1.6	0.35	static
Portobelo (north end)	53	1.1	0.5	static
Portobelo (island control)	67	10.5		dynamic
Itapema (south headland)	57	60.9	29.1	dynamic
Itapema (north headland)	29	22.3	7.9	static
Ilhota	33	7.4	2.3	dynamic
Flamingo	33	5.7	2.2	static
Estaleiro	47	6.3	2.8	static
Taquaras/Taquarinhas	34	13.1	5.15	static
Laranjeiras	55	5.3	2.52	static
Balneario Camboriu (south headland)	40	16.2	5.9	dynamic
Balneario Camboriu (island control to south)	73	6.8		close to static
Balneario Camboriu (island control to north)	74	7.4		close to static
Balneario Camboriu (north headland)	44	7.5	2.98	dynamic
Praia do Coco (south end)	26	3.1	1	close to static
Praia Brava (south end)	30	6.8	1.8	Dynamic
Cabecudas	65	8.5	3.4	close to static
Praia do Atalaia	39	2.05	0.7	close to static
Atalaia (man made control point)	78	7.25	3.5	Dynamic
Gravatá (north headland)	56	4.35	2.2	close to static
Gravatá (island control to south)	36	6.5	2.4	close to static
Gravatá (island control to north)	61	4.65	2.4	close to static
São Miguel	53	4.6	2.2	static
Vermelha	45	3.7	1.6	dynamic
Grande (whole beach)	49	9.8		dynamic
Grande (south end)	59	6.6	3	close to static
Penha (south end)	57	5.1	1.8	dynamic
Penha (whole beach)	50	23.1	9.2	dynamic
Piçarras	58	18.5	13.85	dynamic

Table 2. Data for the 15 simulations for beaches on Florianopolis Island.

BEACH	B(degrees)	Ro(cm)	a(cm)	Equilibrium
Canasvieiras	26	8.7	2.5	Dynamic
Ponta das Canas	54	15.1	6.6	Dynamic
Lagoinha do norte	50	3.2	1.5	close to static
Brava	32	5	1.7	close to static
Ingleses	39	10.4	4.4	close to static
Santinho	28	7.25	2.05	Dynamic
Barra da Lagoa	33	14.3	4.5	Dynamic
Gallheta	43	2.4	1.1	Static
Mole	22	1.9	0.43	Static
Joaca	18	3.9	0.8	close to static
Campeche	34	14.95	5.65	Dynamic
Armação	29	7.3	2.5	close to static
Matadeiro	65	3.9	1.7	close to static
Lagoinha do leste	46	4.6	1.7	Dynamic
Pantano do Sul	53	6.65	3.2	Static

Table 3. Data for 33 simulations in southern sector of Santa Catarina.

BEACH	β(degree)	Rβ(cm)	a(cm)	Equilibrium
Do Sonho	50	4.7	2.2	close to static
Pinheira (north headland)	63	7.7	4.35	close to static
Pinheira (south headland)	49	4.1	1.3	close to static
De cima	41	2.1	0.8	close to static
Guarda	25	4.5	1.2	dynamic
Gamboa	23	5.2	1.2	dynamic
Siriú	45	8	3.6	dynamic
Garopaba (whole beach)	48	7.35	3.3	close to static
Garopaba (south end)	48	1.3	0.6	Static
Silveira (north headland)	36	2.9	0.8	dynamic
Silveira (south headland)	32	2.95	0.9	dynamic
Ferrugem (north headland)	35	1.1	0.41	close to static
Ferrugem (south headland)	34	1.35	0.38	close to static
Rosa (north headland)	35	2.8	1.1	Static
Rosa (south headland)	43	4.6	1.22	close to static
Ibiraquera	53	3.6	1.2	close to static
Ibiraquera	33	7	2.6	dynamic
Ribanceira	23	0.7	2	dynamic
Do porto (north headland)	37	2.4	0.9	Static
Do porto (man made control)	62	5.8		dynamic
Vila (north headland)	70	1.7	0.7	Static
Vila (island control to north)	70	3.2		close to static
Vila (island control to south)	40	6.7	2.6	dynamic
Itapiruba norte	48	6	2.1	dynamic
Itapiruba sul	38	2.5	1.1	close to static
Do sol	32	4.15	1.1	dynamic
Laguna (man made control point)	42	12	4.1	dynamic
Gravatá	48	2	0.93	close to static
Ipuã	37	2.1	0.78	close to static
Galheta	43	3.6	1.3	dynamic
Santa Marta	46	2.25	0.9	close to static
Prainha	51	1.2	0.35	Static
Cardoso	38	2.3	0.7	close to static

APPENDIX II

Software for Stability Assessment of Headland-Bay Beaches

http://www.cttmar.univali.br/~meppe

Unless referred to otherwise, the contents of this thesis are the results of original research carried out by the author.

Some of the results have been published in:

VARGAS, A.; RAABE, A.L.A e KLEIN, A.H.F., 2002. Software Educacional para Auxílio na Aplicação e Aprendizegem do Modelo Parabólico de Praias de Enseada. *Revista Brasileira de Geomorfologia*, 3(1), 11-20.

KLEIN, A.H.F., VARGAS, A., RAABE, A.L.A., and HSU, J.R.C, 2003. Visual assessment of bayed beach stability using computer software. *Computer and Geosciences*, 29, 1249-1257.

Introduction

Current applications of the parabolic model require hand calculation of theoretical shoreline positions and manual tracing of the results on a map or aerial photography. The process, though straightforward, is repetitive and tedious, especially when comparing the results among several different options. However, this process could be improved with the aid of software for computational processing and graphic display. This justifies the creation of a software package to simulate this application herein referred to as "Model for Equilibrium Planform of Bay Beaches" (MEPBAY). The results of its implementation are in a graphic form, which makes the learning and application of this theme a much enjoyable experience.

Manual application of the parabolic model

In manual application of the parabolic model (Hsu and Evans, 1989), map, topographical chart, vertical aerial photograph, or satellite image of a bay beach may be used to obtain the main variables for the model (β and R_o). The usual procedure is described in the following sections.

1) Choosing a control line R_o: A line is drawn connecting the upcoast wave diffraction point to an appropriate point on the straight section downcoast (see Figure 1). This gives in a straight line R_o (see Figure 2). Physically, a large physical obstacle at the upcoast alters the initial pattern of offshore waves that propagates toward the beach, and the downcoast control point may be considered as the limiting position that may be influenced by the incoming waves through diffraction process.

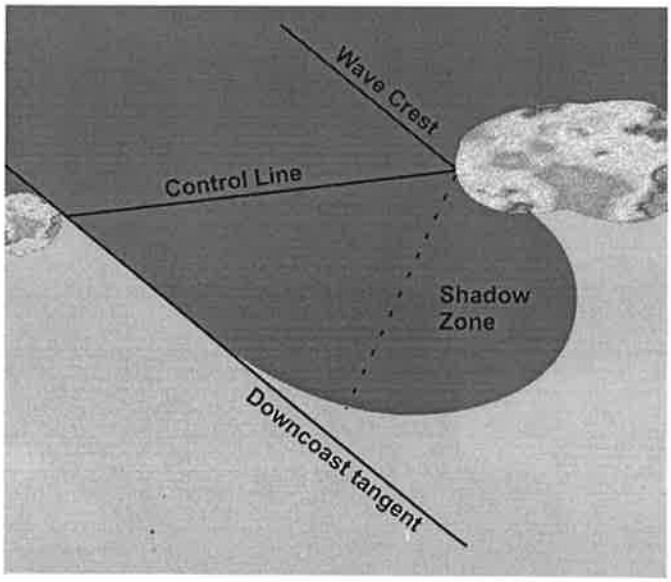

Figure 1. Principal components of a headland bay beach.

2) Determining the predominant wave direction from reference wave angle β: From the downcoast control point, a tangent may be drawn. This may be taken as the wave crest line, which is perpendicular to the incoming waves to the bay beach. A short line segment parallel to the tangent at downcoast is then drawn from the wave diffraction point (see Figure 1 and 3). The angle forms between this line segment and the control line R_o is denoted as β, which represents the reference wave angle for the bay beach under consideration.

3) Calculating ray lengths R_n: Staring from $\theta = \beta$ at downcoast boundary, rays R_n with angle θ in constant intervals (see Figure 2) of 10 degrees are calculated using Equation 3.1 (Chapter 3), until a maximum of 150 or 180 degrees. The pairs of (R_n, θ) calculated represent the shoreline position radiating out from the upcoast diffraction point for a hypothetical bay shape in static equilibrium.

4) Sketching shoreline planform in static equilibrium: Joining the (R_n, θ) points calculated finally produces the planform in static equilibrium. The same process may be repeated for other sets of β and R_o, which represent several engineering or management options due to different conditions of

the man-made structure that may alter the position of the upcoast control point on an existing bay beach.

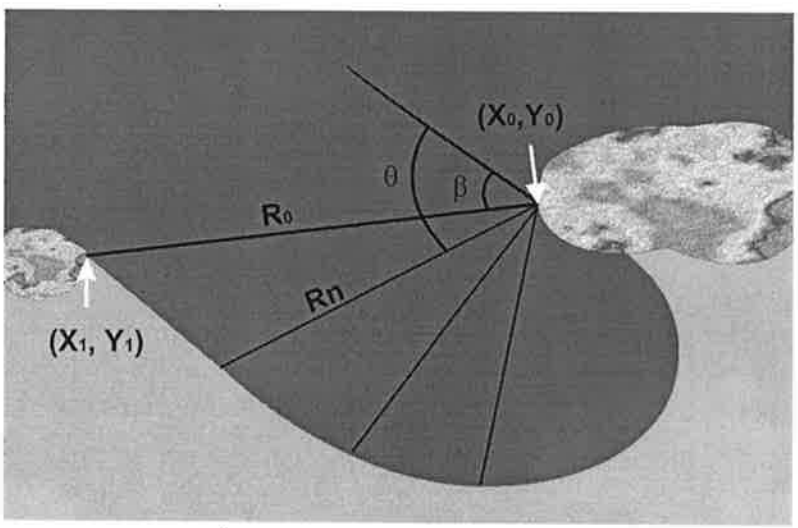

Figure 2. Definition sketch of the parabolic model given by Hsu and Evans (1989).

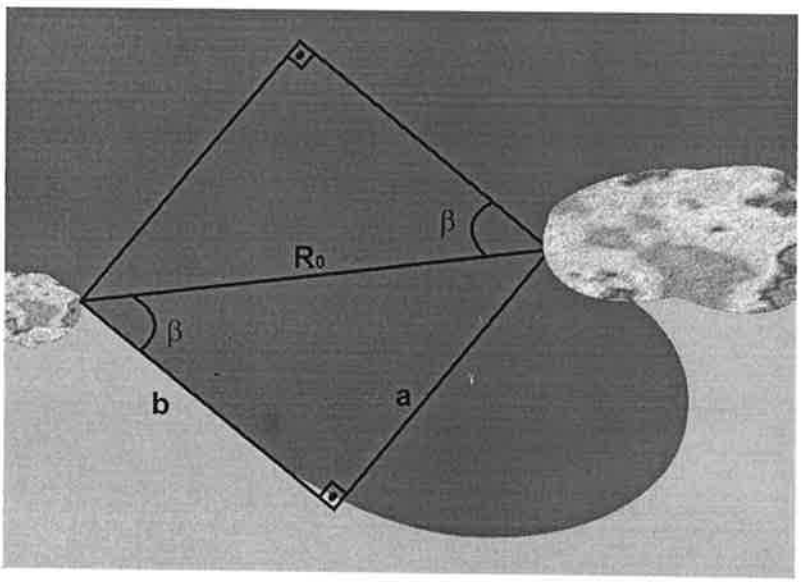

Figure 3. Definition of reference wave angle β.

Together with the existing bay beach, the new planform predicted using Equation 3.1 might be traced on the screen. The user may then examine the beach stability by comparing the nearness of the existing shoreline to the one predicted in static equilibrium. Should they coincide with each other or very close, it indicates that the existing beach is in or close to static equilibrium. If the existing one departs from the predicted one, the beach is said to be in dynamic equilibrium, in which shoreline changes may occur as sediment budgets vary from other sources. However, should wave approaching direction varies seasonally, alternative beach planform has to be considered.

The process described above, though seeming straightforward, is in fact repetitive and laborious. In order to make the process more agile and less difficult, software is proposed to apply the parabolic model for testing the stability of a headland-bay beach. The main objective of developing software of this kind is (1) to provide a user with a friendly environment in applying the parabolic model, and (2) to help a user arrive at an optimum design from several different options.

Computational implementation

Utilities resources of a modern computer are used for the manipulation of graphic images, after applying the MEPBAY to simulate beach changes and to display the computed results using the parabolic model (Hsu and Evans, 1989). The application of these resources is described in the following sections.

Defining control line R_o

The first step of the routine is to search and define the *control line* (R_o) on the display unit. The length of R_o, in Equation 3.1 (chapter 3), is the distance between two points in the plan (Boulos

and Camargo, 1987). In the present case, these are the upcoast and downcoast control points, located at (X_o, Y_o) and (X_1, Y_1), respectively (see Figure. 2). The downcoast control point is an arbitrary point on the straight section downcoast. The distance between them is then given by Equation (1):

$$d^2 = (X_1 - X_0)^2 + (Y_1 - Y_0)^2 \quad (1)$$

where,

d is the length (in units of screen) of the control line R_o.

X_0 is the x-coordinate of the upcoast control point where R_o begins.

Y_0 is the y-coordinate of the upcoast control point where R_o begins.

X_1 is the x-coordinate of the downcoast control point where R_o finishes.

Y_1 is the y-coordinate of the downcoast control point where R_o finishes.

Calculation of wave reference angle β

After choosing R_o, the next step is to define the direction of the predominant wave. However, rather than using the invisible wave direction, the visible wave crest line is used instead, from which the reference wave angle β is defined. As seen in Figure 3, the direction of the predominant wave is drawn perpendicular to the tangent downcoast, i.e., the wave crest line at the wave diffraction point upcoast. A right-handed triangle is then constructed.

With the values on the three sides of the triangle, the *control line* R_o, the line for the predominant wave direction and the downcoast tangent (Figure 3), the law of the cosines is used to obtain $\cos\beta$ (Boulos and Camargo, 1987), giving by Equation (2):

$$\cos\beta = \frac{|a|^2 - |b|^2 - |c|^2}{2|b||c|} \tag{2}$$

Where,

$\cos\beta$ is the cosine of the reference wave angle β.

a is the length along the downcoast tangent.

b is the length in the direction of predominant wave.

c is the length of *control line* R_o.

To find the true value of β, the function "arcCos" in the "Object Pascal" language is used (Cantù, 2000). The function returns the value of β in radians, which is then converted into degrees.

Application of parabolic model

Substituting the values of R_o and β into the empirical equation of the parabolic model (Equation 1) renders ray R_n for each θ specified. The calculated values of R_n, corresponding to the range of θ from β to 150° or 180°, are stored in a vector form with the corresponding θ specified. While performing the iteration of calculating R_n for each θ, under a specific wave reference angle β, values of the coefficients C_1, C_2 and C_3 used are also stored in a two-dimensional array. The C values as a function of angle β is given in Table 3.1 (Chapter 3).

The algorithm that demonstrates the application of Equation 1 to find the theoretical shoreline location R_n for a bay beach in static equilibrium is depicted in Table 1.

4.1 Visualization of a predicted static bay shape

After obtaining the values of R_n for all the rays to the points on the whole bay periphery, it becomes necessary to location them onto the screen, in other words, to know where they should appear exactly.

A computer screen works similar to a plan of Cartesian coordinate system. As shown in Figure 4, the global origin (0,0), i.e., the initial zero point, is at the top left corner of the screen, with the x-axis (length) positive to the right, and the y-axis (height) positive pointing downwards. In this manner, to find the point drawn on the screen with local coordinates (X, Y), translocation of the coordinates is required, that is, to transport the initial zero to the point of local origin (0,0) at the point of wave diffraction (upcoast control point of the beach). Polar coordinates are then used to implement all the R_n lines calculated to determine the X and Y coordinates for the end point for each pair of (R_n, θ) by $X = R_n\cos\alpha$ and $Y = R_n\sin\alpha$ (Figure 4), with translation and proper subtractions or additions (Anton, 2000).

Table 2. Algorithm for the evaluation of radii R_n, based on Equation 1.

```
Beginning
        limit of increment of the angle = 150;
        // the increment limit receives the value 150 //
        increment = 10;
        // the value of the increment of the angle θ it receives the value 10 //
        cont := 1;
        // it begins the accountant with 1;
        θ = 0;
        // the begins θ with the value 0, for to 1.ª iteration //
        While (θ <= it limits of increment of the angle) it does
```

```
// repetition structure //
Beginning
    Rn [cont] = (C[β,1] + C [β, 2] * β/ (+ C[β,3] * (β/ θ)²) * R0;
    // accomplishment of the operation //
    θ = (θ+increment);
     cont = cont+1;
    // after each iteration,  is added to θ the value of the increment and the cont the
value 1 //
 end; / / end of the repetition structure / /
end;        // end of the algorithm //
```

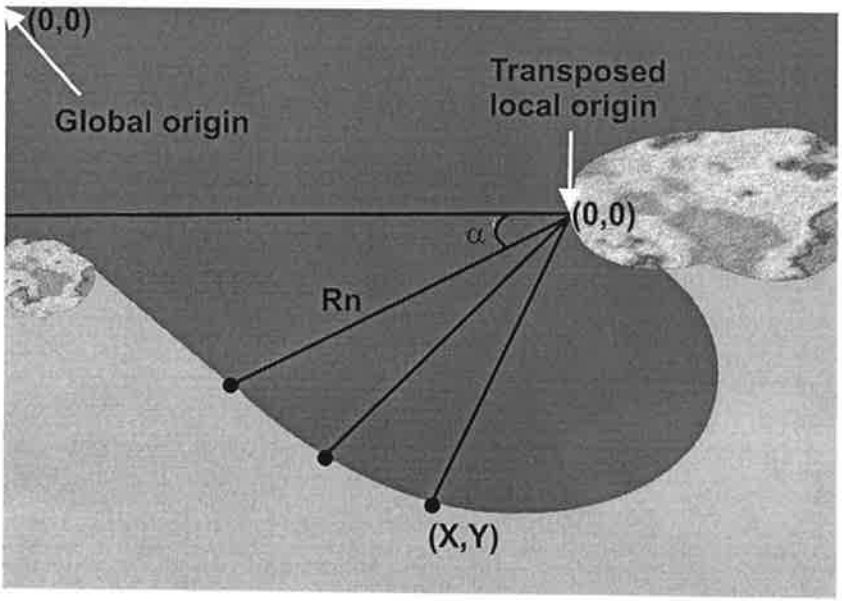

Figure 4. Shoreline locations on a theoretical planform of a bay beach in static equilibrium.

The construction and application of MEPBAY software

Starting from the planform (files in the Raster format) of a headland bay beach on an aerial photography or map, the proposed software package offers an interface that allows the user to indicate the relevant points on the beach and to trace the complete bay periphery in static equilibrium. The software facilitates the experimentation in a very efficient way for the graphic representation of the idealized waterline in static equilibrium, in relation to the control points selected from the display on the screen.

The construction of MEPBAY software

With MEPBAY, the implementation of the parabolic model not only becomes a simple task, due to its efficiency, but also streamlines the physical interpretation for any practical applications. The user will be benefited from the learning process, because the result generated by the software is the consequence of his conscious selection of the control points for a beach under consideration. The user can then analyze the effect of any likely modification to the beach due to the construction of structures for harbors or marinas, due to the changes to the diffraction point. MEPBAY present the graphical output of the existing beach and the theoretical curve in static equilibrium for each application. In this way the user can elaborate various options for a specific problem.

MEPBAY may also motivate user's curiosity from working on various engineering and management applications, due mainly to its simplicity in applying the parabolic model and the graphic visualization of the results.

While working with MEPBAY, the operation follows a set of procedure in the background:

1. The user loads the screen of the computer, through the software, the image of a beach on a map or an aerial photography (see Figure 5), in Raster format (extensions *bmp* or *jpg*),

2. With the beach image on the screen, the options that indicate the disposition of the beach and the promontory in relation to the screen should be selected and defined (including "beach orientation" showing the upward or down direction normal to the sandy beach, etc.),
3. By using the mouse the user then selects three points on the image required for the parabolic model application, these being: (1) the upcoast control point (i.e., the point of wave diffraction, (2) the downcoast control point of the beach (downcoast), and (3) an end point along the tangent to the beach downcoast, hence the normal to the propagation direction of the predominant wave (see Figure 3);
4. The MEPBAY then calculates the wave reference angel β and radii R_n for each increments of angle θ. It also displays the results on the screen, after the user clicks on an option under the "Tools" sub-window to the right of the image of the beach. In the same time, the results are also saved in a raster format and may be printed out later, if requested.

MEPBAY software also presents the values of wave reference angle β, control line length R_o, all R_n with corresponding θ. The most important part is that it draws the predicted static bay shape on the image of the existing beach. The condition of beach stability can then be evaluated, in static (see Figure 5) or dynamic equilibrium (see Figures 6 and 7), depending on the degree of agreement between the existing beach and the predicted static bay shape. Should the existing beach matches well with the predicted, the beach is said to be in static equilibrium, implying the beach would maintain its stability without sediment input from any sources. Otherwise, the beach is in dynamic equilibrium, or may be unstable, should sediment from other sources reduces or diminishes.

Practical applications of MEPBAY

The proposed MEPBAY would be most suitable for project evaluation to determine the optimum design options from several alternatives in which variations in the length, location and orientation of a structure have to be considered. As the condition of a structure varies, the point of wave diffraction changes, for which the MEPBAY software could be employed to perform evaluation and also to display the static bay shape predicted for each case tested. In this manner, the user will gain the maximum benefit from applying the parabolic model, not only having the insight of the physical processes of beach changes, but also achieving the best solution for the work to minimize beach erosion or for coastal management.

MEPBAY can be applied to test the stability of an existing headland-bay beach. Figure 5 shows the use of MEPBAY software for Taquaras-Taquarinhas beach. This beach is located in the central north coast of Santa Catarina state, southern Brazil, and was classified as a reflective beach (Klein and Menezes, 2001). By applying the MEPBAY, it can be observed that the existing beach planform is almost identical to the static bay shape given by the parabolic bay shape equation, Eq. 1. It thus indicates that this beach is close to or in static equilibrium.

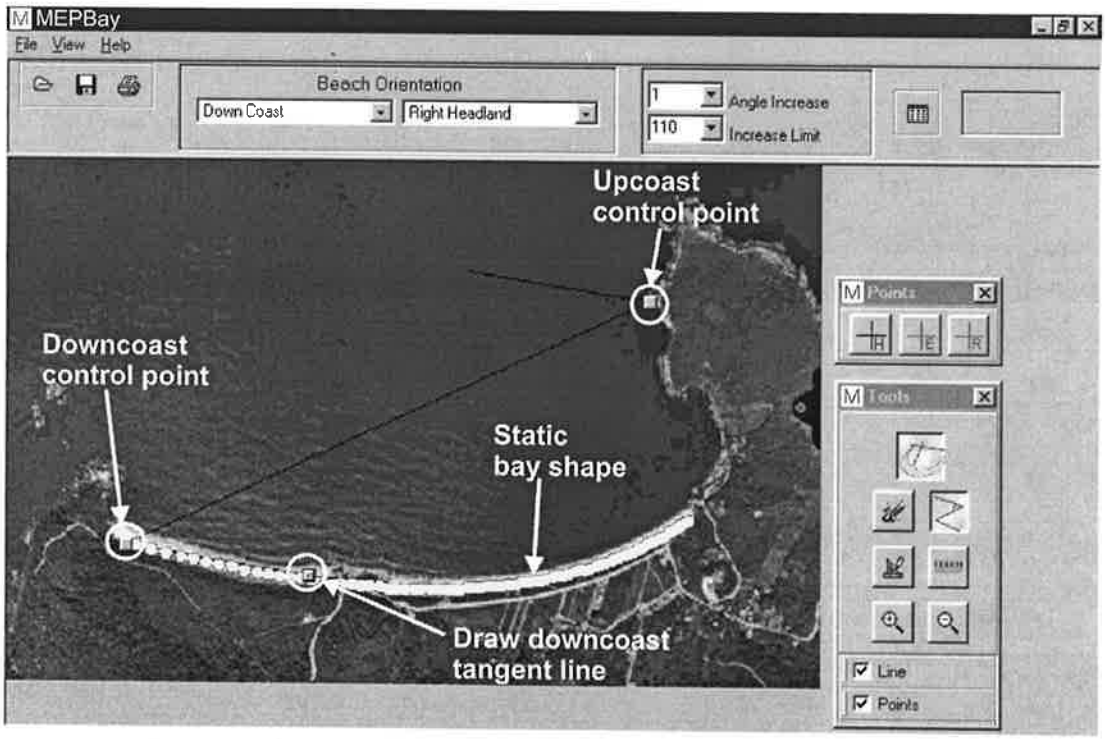

Figure 5. Example illustrating the use of the MEPBAY software to Taquaras-Taquarinhas Beach, State of Santa Catarina in southern Brazil.

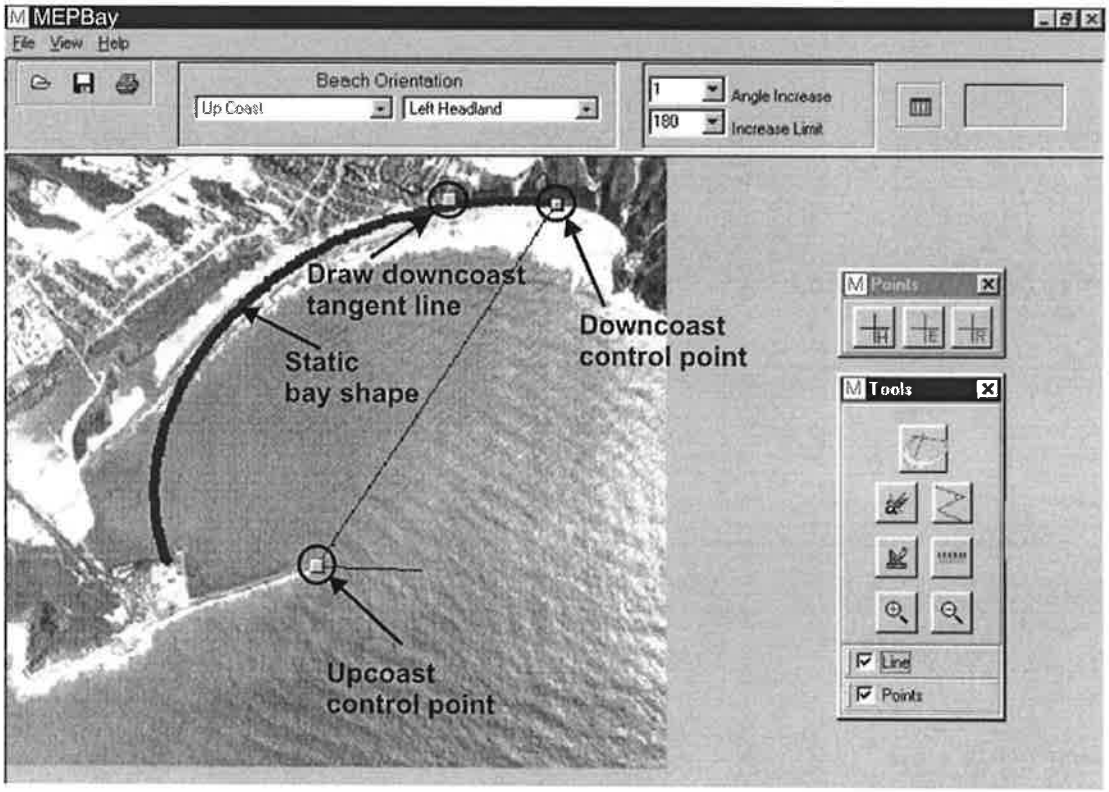

Figure 6. Example illustrating the use of the MEPBAY software to Imbituba Port, State of Santa Catarina in southern Brazil.

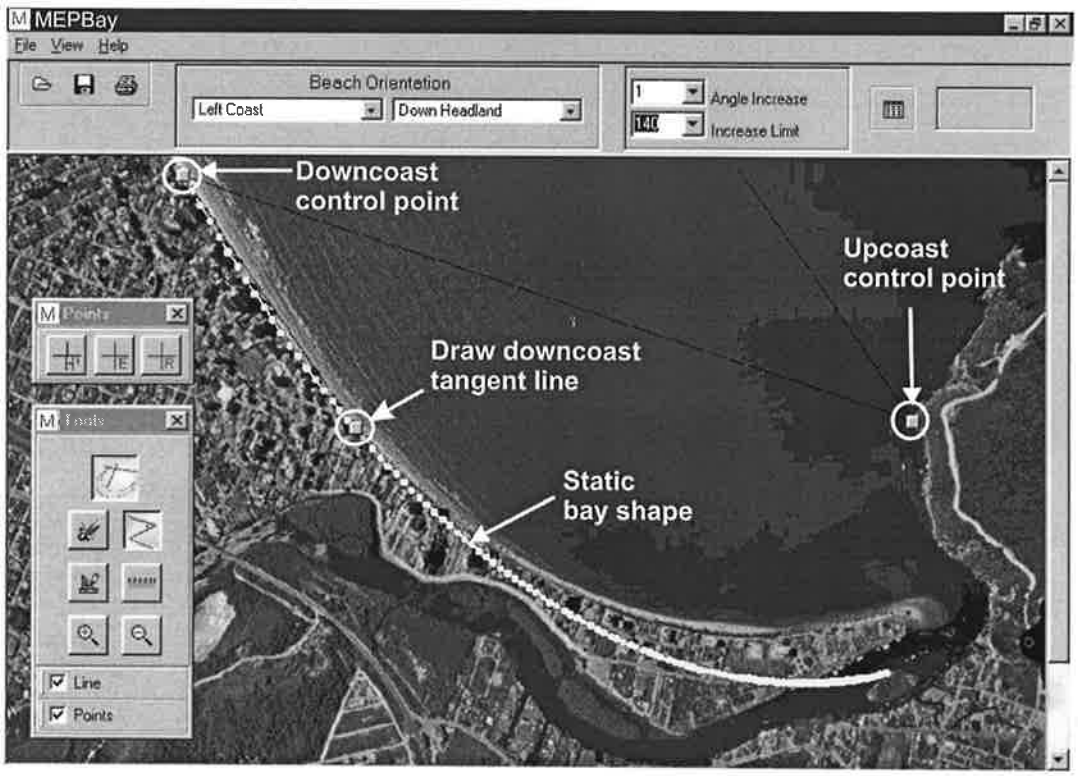

Figure 7. Example illustrating the use of the MEPBAY software to Balneário Camboriú Beach, State of Santa Catarina in southern Brazil.

MEPBAY helps identify the effect of constructing a man-made structure on a bay beach in dynamic equilibrium. As shown in Figure 6, an offshore breakwater was built at Porto Beach in Imbituba municipality, Santa Catarina, Brazil with the objective to produce calm waters for the Imbituba port. The tip of this breakwater has since become an upper control point for a potential salient beach to be formed in its lee, with beach accretion joining the downcoast headland, accompanying by erosion further downcoast. As a consequence, engineering applications, such as groins and dredging, had been applied in order to block littoral drift towards the port area and to maintain a deep channel for navigation. The parabolic model is applied for the port beach to predict the accretion felt at this port. For a similar case elsewhere, it is strongly recommended that stability of the original beach planform be tested first, to see whether it was in static or dynamic equilibrium.

Tests on several options for the combination of the length and orientation of an offshore breakwater may then be followed. These can be processed using MEPBAY.

Figure 7 shows the application of the parabolic bay shape model for the southern end of Balneario Camboriu beach in dynamic equilibrium, where shoreline is maintained seaward of the static bay shape by sediment supplied from a river. The white dots indicate the planform of the bay beach in static equilibrium. If the sediment supply form the river ceases as a result of human interventions along the river (such as catchment/soil conservation or damming the river for various purposes), shoreline would erode back to the static equilibrium planform predicted. Should this occur it might cause undesirable damages to beach facilities, roads, and properties. To safe guard against this environmental damage to the popular tourist resort beach in the future, artificial extension by an engineering means at the existing upcoast control point may be considered. Again, MEPBAY can be used to facilitate this engineering task to convert a beach in dynamic into static equilibrium.

Concluding Remarks

MEPBAY is developed as a tool of aid to help educator and student in the teaching and learning process in coastal management, shore protection and project evaluation related to the uses of sandy beaches. It has the capacity to predict the consequence of installing a coastal structure on a sandy beach, using the parabolic model of Hsu and Evans (1989) for headland-bay beaches in static equilibrium. The developers have no intention to substitute the intelligence of educator and student, but want to contribute to the motivation of the development of such intelligence. Even with the use of the software, the user has to possess the knowledge of coastal geomorphology, to use the model properly, and to verify the theory through practice. To achieve these aims, it is also essential that the students undertake the process with accompaniment of a tutor.

With MEPBAY working to display the results, application of the parabolic model for headland-bay beaches becomes simpler. The learning and evaluation of beach stability, in static or dynamic equilibrium, induced by man-made structures on beaches could become a more efficient and less time consuming process.

More over, the efficiency of applying MEPBAY can be better satisfied by the user to test several different options for a proposed coastal or management project, in which a beach may be affected by the installation of a coastal structure which changes the location of the wave diffraction point to an existing beach.